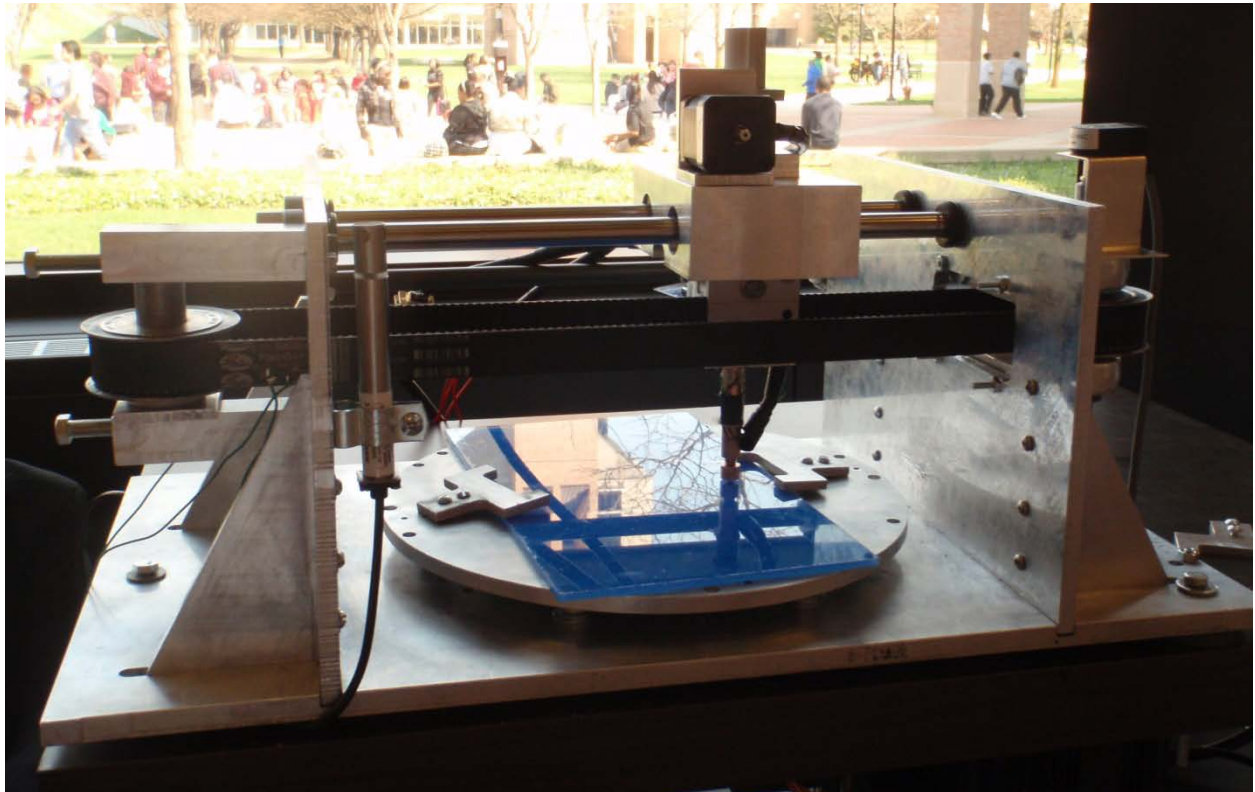


# Multi-Function Tribometer Design

**Sponsor: Professor Gordon Krauss**  
**Advisor: Professor Shorya Awtar**



## Final Report

April 20, 2010

Section 2 – Team 5

Bob Chlum, Kelsey Hanson, Steve Lindsay, Ben Pascoe

ME 450 – Design and Manufacturing III

Winter 2010

University of Michigan

## EXECUTIVE SUMMARY

Professor Gordon Krauss of the University of Michigan Mechanical Engineering Department has challenged our team to design and manufacture a tribometer device. The functionality required for Prof. Krauss' research is not available in any existing commercial products and the lab's budget does not allow for the purchase of any of these devices for modification. The tribometer must perform standard pin-on-disk and linear reciprocating tests in compliance with the ASTM G99 and G133 standards, respectively, as well as tests of complex two dimensional wear paths in order to investigate path dependence of wear. It will test metal, ceramic, and polymer materials in pin, disk, and plate geometries with or without coatings and lubricants. It must test specific ranges of normal loads, and linear and rotational velocities, allow control of temperature and humidity, and measure the resulting lateral force, the contact resistance across the sample interface, and the depth of material wear. A summary of the customer requirements can be found in Table 2 on page 15 of this report.

We have performed benchmarking of commercially available tribometers and relevant patents in order to gain an understanding of the difficulties involved in wear testing. Based upon this research and the customer requirements we have developed specifications for the engineering characteristics of the tribometer that we will optimize to meet those requirements. These engineering specifications can be found in Table 3 on page 16. We have evaluated working principles developed concept designs, and selected and developed "alpha design". Based upon this work we have finalized a product design that will meet the engineering specifications, as well as a reduced cost prototype that may be used for validation purposes and later upgraded to the full final proposed design. These designs do not include an environmental control system, but use an open structure to allow for implementation of a modular chamber at a later date.

The proposed design enables both standard and 2D tests to be performed at speeds of up to 1 m/s under a maximum normal force of 200 N. Normal force is applied between pin and plate samples using a screw driven by a DC stepper motor to lower the pin holder. The pin holder and forcing device are mounted on a linear stage that translates along a sliding rod gantry. This system is driven by a ball screw and dc servo motor to achieve linear reciprocating motion. Rotational motion is achieved through a rotating disk on which the plate sample is mounted using clamps. The plate is driven by a stepper motor and spur gears. Strain gauges mounted to the pin sample enable measurement of frictional and normal force, providing feedback for control of the applied normal force. The drivers for the three motors will be controlled in real time using logic compiled on an Arduino board. Temperature and humidity are measured using a relative humidity sensor and all data is recorded using a LabVIEW-based DAQ.

We have fabricated a proof-of concept prototype modeled after the proposed design with two major exceptions. First, the ball screw system that we proposed for driving the linear stage has been replaced by the timing belt drive used by the previous team. This change was necessary for our prototype because we could not procure a ball screw system within Prof. Krauss's budget. The DC servo motor has been chosen such that it can be used to power a ball screw system should such an upgrade be desired at a later date. The cost to do so will be \$3150. The second major exception to the proposed final design is that for our prototype, we will mount the strain gauges to the pin ourselves. For the final design, we recommend that they be professionally installed to ensure reliability and precision. The total cost to fabricate the prototype was \$2910. We have completed preliminary validation testing of the force measurement and application, linear velocity, and rotational velocity, however due to noise in the DAQ measurements additional testing will be needed once a filter has been installed. The mechanical aspects of the system are sufficient for the sponsor's requirements; however, due to the limited processing power of the Arduino board, an upgrade will be required before all three motor systems may be run at once for the 2D wear path tests.

## Table of Contents

EXECUTIVE SUMMARY .....	2
ABSTRACT.....	9
PROBLEM STATEMENT.....	9
LITERATURE REVIEW .....	9
<i>ASTM Standards</i> .....	10
Pin-on-disk wear testing (ASTM G99):.....	10
Linear reciprocating wear testing (ASTM G133):.....	10
Measuring friction coefficients (ASTM G115): .....	12
Measuring electrical contact resistance (ASTM B539): .....	12
<i>Current Technology</i> .....	12
<i>Proprietary Devices</i> .....	14
<i>Existing Patents</i> .....	15
DEVELOPMENT OF TARGET ENGINEERING SPECIFICATIONS.....	16
<i>Customer Requirements</i> .....	17
<i>Engineering Characteristics</i> .....	18
<i>Specification Targets</i> .....	19
Control parameters:.....	19
Data collection and contact resistance range: .....	19
Sample holding and positioning:.....	20
Physical constraints:.....	20
CONCEPT GENERATION.....	20
<i>Subsystems</i> .....	20
<i>Working Principles</i> .....	21
Motion control system .....	21
Motion generation:.....	21
Transmission and conversion.....	21
Constraint and support: .....	22
Best options:.....	23
Force application system:.....	23
Force actuators: .....	23
Best options:.....	24
Force measurement .....	25
Best option: .....	26
Environmental control system: .....	26
Temperature control:.....	26

Humidity control:.....	27
Best options:.....	27
Data acquisition and control system: .....	27
PC-based software processing: .....	27
FPGA processing: .....	28
Best option: .....	28
Sample holding: .....	28
Pin sample holder.....	28
Plate sample holder:.....	29
Best options:.....	30
<i>Concept Designs</i> .....	30
Tribometer concepts:.....	30
Concept 1: .....	30
Concept 2: .....	31
Concept 3: .....	32
Concept 4: .....	33
Concept 5: .....	34
Environmental control concepts: .....	35
Environmental chamber: .....	35
Concept 1: .....	35
Concept 2: .....	36
Temperature control:.....	36
Humidity Control Concept:.....	37
Evaluation: .....	37
ALPHA DESIGN.....	38
<i>Motion Actuation</i> .....	38
<i>Force Application</i> .....	38
<i>Environmental Chamber and Control</i> .....	39
<i>Control System</i> .....	40
<i>Feedback Sensors</i> .....	40
<i>Sample Holding</i> .....	40
ENGINEERING ANALYSIS.....	41
<i>Motion and Force Application</i> .....	41
<i>Environmental Chamber Engineering Analysis</i> .....	41
<i>Controller / Data Acquisition</i> .....	41
<i>Lateral Force Measurement</i> .....	42

<i>Sample Holders</i> .....	42
ENGINEERING DESIGN PARAMETER ANALYSIS .....	43
<i>Force Application System</i> .....	43
Motor Selection and Gearing: .....	43
<i>Linear Reciprocating Motion System</i> .....	43
Alpha design - Linear servomotor: .....	44
Final design - Ball screw:.....	44
In house construction: .....	44
Prefabricated actuator: .....	44
Final design – DC servo motor: .....	45
Prototype design - Belt drive: .....	46
Belt Tensioner:.....	46
Linear Motor Drive Shaft:.....	47
Prototype design: Linear gantry and stage:.....	47
<i>Rotational Motion System</i> .....	48
Gear selection: .....	48
Rotational motor selection: .....	49
<i>Chassis</i> .....	50
<i>Pin Material Selection and Geometry Analysis</i> .....	50
<i>Sensors and Feedback System</i> .....	51
Controls System: .....	51
Data Acquisition: .....	51
<i>Sample Holding</i> .....	52
FINAL DESIGN DESCRIPTION .....	52
<i>Normal Force Application System</i> .....	52
Gear Constraint .....	53
Bolt Application.....	53
Elasticity .....	53
Pin Constraint.....	54
Wear Depth Measurement .....	54
<i>Linear Motion System</i> .....	54
<i>Rotational Motion System</i> .....	55
<i>Chassis Design</i> .....	56
<i>Force Measurement</i> .....	57
Strain Gage Pin Orientation: .....	58
Strain Gage Selection:.....	60

Analog to Digital Conversion :	60
Pin manufacturing:	61
Cost Analysis:	62
<i>Data Acquisition and Control System</i>	62
<i>Sample Holding</i>	63
Ball sample:	63
Plate sample:	64
<i>Environmental Control</i>	65
Prototype design Explanation	65
<i>Linear Motion System</i>	66
Flexible motor coupling:	66
Belt tensioner:	67
INITIAL FABRICATION PLAN	68
VALIDATION TESTS AND RESULTS	68
<i>Force Measurement Validation and Verification</i>	68
<i>Vertical Force Application</i>	71
<i>Friction Force Measurement</i>	72
<i>Velocity of Linear Stage</i>	72
<i>Rotational Velocity of Disk Sample</i>	72
<i>Position Accuracy Validation</i>	73
DISCUSSION	73
RECOMMENDATIONS	74
<i>Processor Recommendations</i>	<b>Error! Bookmark not defined.</b>
<i>Strain Gauge Recommendations</i>	75
<i>Strain Gauge Signal Conditioning Recommendations</i>	76
<i>Environmental Chamber Recommendations</i>	76
<i>Safety Recommendations</i>	77
<i>Motor Overheating Recommendations</i>	77
<i>Rotational Bearing System Recommendations</i>	77
CONCLUSION	77
ACKNOWLEDGEMENTS	78
REFERENCES	80
TEAM MEMBER BIOS	81
APPENDIX A: DESIGN TOOLS	84
A.1: QFD	84
A.2: Function Diagram	86

<i>A.3: Motion Generation Pugh Chart</i> .....	87
<i>A.4: Motion Transmission Pugh Chart</i> .....	88
<i>A.5: Force Application Pugh Chart</i> .....	89
<i>A.5: Force Application Pugh Chart (Continued)</i> .....	90
<i>A.6: Force Measurement Pugh</i> .....	91
<i>A.7: Data/Control Pugh Chart</i> .....	92
<i>A.8: Plate Sample Holding Pugh Chart</i> .....	93
<i>A.8: Plate Sample Holding Pugh Chart (Continued)</i> .....	94
<i>A.9 Pin Sample Holding Pugh Chart</i> .....	95
<i>A.10: Humidification Pugh Chart</i> .....	96
<i>A.11: Dehumidification Pugh Chart</i> .....	97
<i>A.12: Heating Pugh Chart</i> .....	98
<i>A.13 Cooling Pugh Chart</i> .....	99
<i>A.14: Full Tribometer Concept Pugh Chart</i> .....	100
APPENDIX B: DESCRIPTION OF ENGINEERING CHANGES .....	101
APPENDIX C: DESIGN ANALYSIS ASSIGNMENT .....	103
<i>Chassis Material Selection</i> .....	103
<i>Chassis Sides Mass Production</i> .....	106
<i>Pin Shaft Material Selection</i> .....	107
<i>Pin Shaft Mass Production</i> .....	110
<i>Environmental Performance</i> .....	111
APPENDIX D: MOTOR CONTROL CODE .....	116
Running the Stepper Motors .....	116
Normal Force Motor with Feedback .....	120
Running the DC Motor .....	121
Reading the Optical Encoder .....	123
Running a Linear-Reciprocating Pattern with the DC Motor .....	124
Generating 2D Paths .....	126
APPENDIX E: MICRON INSTRUMENTS DESIGN FOR FORCE MEASUREMENT .....	130
APPENDIX F: STRAIN GAUGE BONDING PROCEDURE .....	132
APPENDIX G: PARAMETER VALIDATION SUPPLEMENTARY INFORMATION .....	141
<i>Figure G.1: Gates Design Pro Flex belt selection criteria and results</i> .....	141
<i>Figure G.2: Nook Industries Ball Screw Specifications</i> .....	142
<i>Figure G.3: Nook Industries ELK 60 Linear Actuator</i> .....	143
<i>Figure G.4: Previous Year's Motor Curves</i> .....	145
APPENDIX H: MANUFACTURING DRAWINGS AND PROCEDURE .....	146

APPENDIX I: FABRICATION DETAILS .....	164
<i>I.1 Manufacturing Plan</i> .....	164
<i>I.2: Detailed Assembly</i> .....	168
APPENDIX J: BILL OF MATERIALS .....	183
APPENDIX K: PROJECT GANNT CHART .....	184



## **ABSTRACT**

Friction and wear properties of many material combinations are becoming increasingly important as engineers look to create more durable and reduced-friction materials. Currently, there is no tribometer which can measure real world complex 2D wear patterns at speeds required by our sponsor.

Because of this, our team has been asked to design a tribometer which will measure friction and wear in complex two-dimensional wear patterns to better model and test real world applications. Key design characteristics will include both closed-loop environmental control and closed-loop normal force application. A successful prototype must have each of the aforementioned functionalities among others.

## **PROBLEM STATEMENT**

The investigation of the wear and friction properties of materials, known as tribology, is often conducted using a device known as a tribometer, which creates relative motion between two contacting test samples. The nature of the friction and material removal induced is quantified and used to predict the behavior of the materials in real world applications. The accuracy with which laboratory test results may be applied to actual applications depends greatly upon the ability to replicate the conditions of the actual application during the test. Wear properties are highly dependent upon kinematic conditions, such as path of travel, normal force at the material interface, and relative velocity of the surfaces, as well as environmental factors, such as temperature and humidity. These parameters must be closely monitored and controlled in order to produce meaningful results. Tribological research in the past has generally been limited to relatively simple test configurations, such as linear reciprocating motion of a pin on a flat plate, or a stationary pin on a rotating disk. However, the wear properties for such simplified wear paths have been found to correlate poorly to the material behavior under the more complicated conditions experienced in actual applications.

Our sponsor, Professor Gordon Krauss of the University of Michigan, requires a tribometer capable of performing standard linear reciprocating and pin-on-disk tests, as well as custom two-dimensional wear path tests under a wide range of environmental and loading conditions for a variety of specimen sizes. Commercially available tribometers tend to be limited to single test configuration, thus requiring the purchase of several devices to meet all of the lab's needs. Those that do provide multiple test configurations are expensive, often include modules for tests that will not be required, and generally lack custom path generation capability. Furthermore, none of the devices can accommodate the range of testing speeds, normal loads and sample sizes required. The objective of this project is therefore to design and prototype a tribometer that will provide the functionality required for Professor Krauss' research at a reduced cost. The device will include systems to control the temperature and humidity of the test environment, secure both planar and pin type test specimens, control the relative motion of the two samples for both standard and custom test configurations, and apply and maintain constant normal force between the specimens. It will also measure and record the normal and lateral forces, relative velocity of the samples to each other, contact resistance across the samples, the temperature and humidity of the test environment, as well as the specimen wear.

## **LITERATURE REVIEW**

In this section we present an overview of tribological testing methods and the standards governing them. We also discuss the current state of tribometer technology, including commercially available devices, proprietary devices in use in private industry, and related patents.

## ASTM Standards

During the literature search, a review was performed of the current American Society for Testing and Materials (ASTM) standards for tribology testing relating to the pin-on-disk and linear reciprocating methods. This section summarizes the finding of that review.

**Pin-on-disk wear testing (ASTM G99):** ASTM standard G99 [1] defines a pin-on-disk wear testing apparatus as one which revolves a sample with a spherically-tipped pin about the center of another sample in the form of a disk (Fig. 1). The pin is held at a constant radius on the disk, such that the wear path is a circle, with the pin traveling through the same track during each revolution.

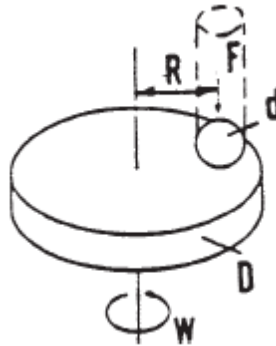


**Figure 1: ASTM schematic of pin-on-disk wear test system [1]**

A force is applied to the pin to push it into the disk during the test. Typical pin on disk systems have a method for measuring both the applied force and the resulting lateral force on the disk, from which a coefficient of friction can be calculated. The apparatus must be constructed such that these lateral forces do not compromise the orientation of the pin. The pin must remain within  $\pm 1^\circ$  of perpendicular relative to the disk.

The apparatus is to have a variable speed motor. This motor must be able to provide a rotational velocity that is constant to within  $\pm 1\%$  of the rated full load motor speed. These tests are typically performed within the range of 60 to 600 RPM. The apparatus is also to have a means of keeping track of the number of revolutions, as well as the ability to terminate the test after a specified number of revolutions.

The ASTM standard reports on a benchmark test conducted to determine the repeatability of the pin-on-disk wear test. The 95% repeatability limit for steel vs. steel ball wear scar diameter was found to be 0.37 mm for within-lab tests and 0.81 mm for between-lab tests.

**Linear reciprocating wear testing (ASTM G133):** ASTM standard G133 [2] defines a linear reciprocating wear testing apparatus as one which slides a sample with a spherically-shaped tip back and forth along a linear path along a flat plate sample. A typical set-up can be seen in Figure 2.

As with the pin-on-disk test, a force is to be applied to the pin sample to push it into the flat sample. Typical apparatuses have a mechanism for measuring the resulting lateral forces, from which the coefficient of friction is calculated.

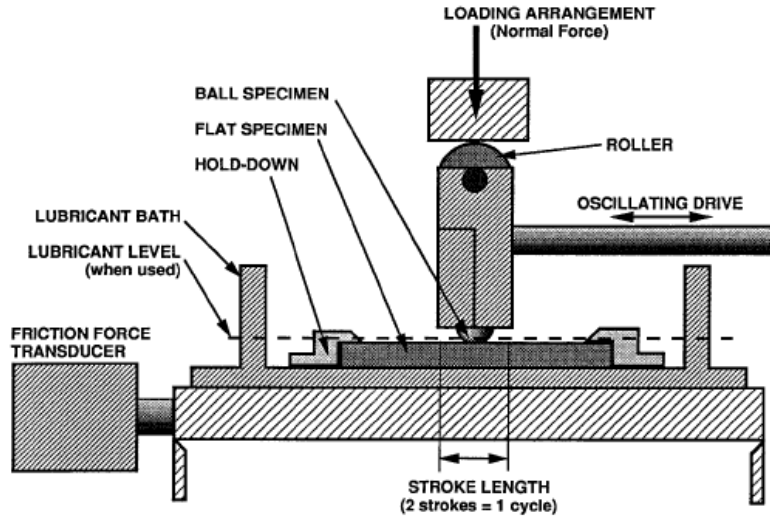


**Figure 2: ASTM schematic of a typical linear reciprocating test apparatus [2]**

The ball specimen is to be driven in a smooth manner. The ASTM standard suggests implementing a drive mechanism which would allow for the ball specimen to follow a reciprocating motion without the need for the drive motor to stop and reverse direction between each stroke. Additionally, the apparatus must be fitted with either a timer or a mechanism to count the number of cycles, such that the test may be automatically terminated after a specified time or number of cycles.

The ASTM standard dictates that the atmospheric conditions under which the test is conducted are accounted for. The relative humidity must be measured to an accuracy of  $\pm 3\%$ . Tests are typically conducted in the range of 40 % to 60 % relative humidity. Temperature must be measured to an accuracy of  $\pm 2^\circ \text{C}$ .

There are two sets of system parameters under which a linear reciprocating test can be considered “in compliance” with the ASTM standards. Those parameters are listed in Table 1.

**Table 1: ASTM-compliant test parameters [2]**

System Parameter	Values	
	Procedure A	Procedure B
Pin tip radius	4.76 mm	4.76 mm
Normal force	25.0 N	200.0 N
Stroke length	10.0 mm	10.0 mm
Oscillating frequency	5.0 Hz	10.0 Hz
Test duration	16 min 40 s	33 min 20 s
Temperature	22° C	150° C
Relative humidity	40 to 60 %	40 to 60 %
Lubrication	None	Fully immersed

The ASTM standard reports on a benchmark test conducted to determine the repeatability of the linear reciprocating wear test. It was found that using Procedure A (Table 1) with samples of silicon nitride sliding on silicon nitride produces within-laboratory variations of  $\pm 34.7\%$  on wear volume and  $\pm 1.8\%$  on coefficient of friction. Between-laboratory variations using Procedure B are reported as  $\pm 48.6\%$  for wear volume and  $\pm 5.29\%$  for coefficient of friction.

**Measuring friction coefficients (ASTM G115):** This ASTM standard [3] lists a few guidelines for devices used to measure the coefficient of friction between sliding objects. Most relevant is the stipulation that any coefficient of friction calculation is only valid if the normal and lateral forces were measured while the two objects were sliding across each other smoothly. If the system experiences stick/slip behavior, the resulting force measurements will not allow for a valid calculation of friction. This stick/slip behavior will be more likely to occur in elastic systems (for example, if the pin in a pin-on-disk system is made from a material with too low of a Young’s modulus). The ASTM standard warns, however, that making a system too rigid (by using a chain drive, for example) will not allow for adequately measuring the breakaway force needed to calculate static friction.

**Measuring electrical contact resistance (ASTM B539):** This ASTM standard [4] provides for finding the contact resistance between two objects. It should be noted that this standard only covers measurements of static conditions. Any measurement made of the resistance between sliding contacts will not be considered to be ASTM compliant.

The ASTM standard details a method of measuring contact resistance using a four-wire system. A four wire system is utilized in order to eliminate the effects of contact resistance between the meter probes and each of the samples. A schematic of the ASTM four-wire measurement circuit can be found in Figure 3, where V represents the voltmeter, I represents the ammeter, and R is resistance measured.

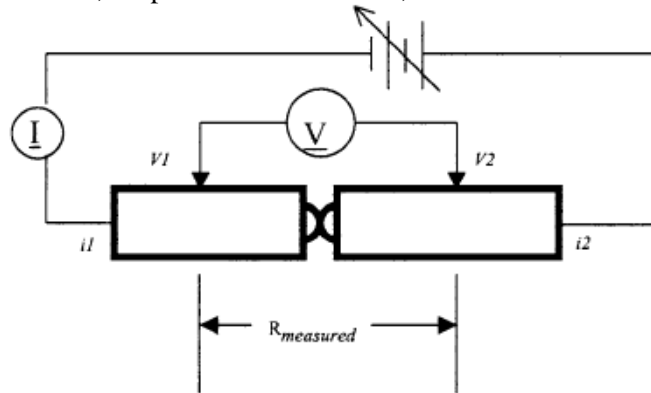


**Figure 3: ASTM schematic diagram of four-wire measurement circuit [4]**

The measurement circuit must utilize a power supply that has the ability to limit the current to 100 mA and the voltage to 20 mV. If a DC power supply is used, it must have the ability to switch the direction of the applied current (this occurs naturally in an AC power supply). The supplied current must be variable and readily adjustable, and must be measured to an accuracy of  $\pm 1\%$  of the measured value. The voltmeter must be able to measure the voltage to an accuracy of  $\pm 1\%$  of the measured value. The resistance is to be calculated using Equation 1, where  $R$  is the resistance in ohms,  $E_f$  is the forward voltage drop in volts,  $E_r$  is the reverse voltage drop in volts,  $I_f$  is the forward current in amps, and  $I_r$  is the reverse current, in amps.

$$R = |E_f| + \frac{|E_r|}{|I_f|} + |I_r| \quad (\text{Eq. 1})$$

### **Current Technology**

There are several commercially available tribometers on the market today. Only one commercially available option exists which satisfies our customer’s minimum requirements, but it has several unneeded functions which drive the cost for this product up. The most comparable tribometers which are commercially available today are manufactured by Nanovea, CSM Instruments and CETR.

Nanovea [5] has both pin-on-disk and linear reciprocating tribometers commercially available. Although both tribometers are arranged in the same test rig, only one type of test can be run at once. Therefore, user defined 2D path generation is not available. Figure 4 below shows both tribometers that Nanovea sells. The pin-on-disk tribometer meets our customer requirements for environmental control as it is able to control temperature and humidity to the ranges specified. The only other specifications Nanovea's pin-on-disk tribometer satisfies are requirements for speed, resistance detection, and testing within ASTM standards. Some unique concepts employed by their design include using several salt baths with a controlled circulating air module to control humidity levels, and a liquid heating module which heats up coils in the disk to control temperature.

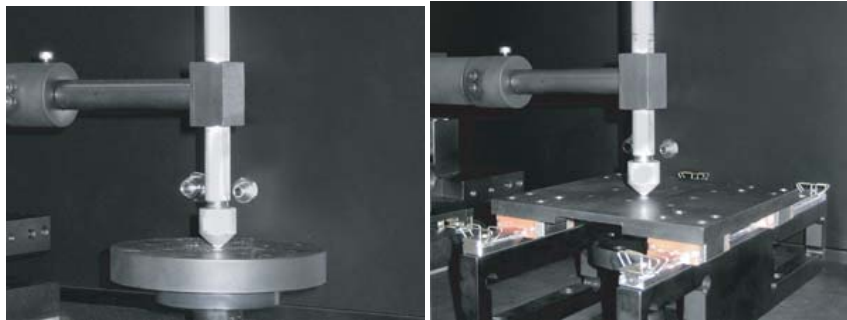


**Figure 4: Nanovea's Pin-on-Disk (Left) and Linear Reciprocating (Right) Tribometers [5]**

The Nanovea reciprocating tribometer also has acceptable environmental control, but fails to meet most of the other customer requirements. Both Nanovea tribometers come with a unique software data analysis program which provides the user with real-time displays of coefficient of friction, temperature, wear depth, and pin-substrate electrical contact information. It includes a set of features to setup the tribometer and 3D mechanical scanning software package to analyze surface roughness, critical dimensions, topography and a full pre/post test profile.

CSM Instruments [6] offers nano and micro tribometers for both linear reciprocating as well as pin-on-disk testing. Figure 5 below shows a CSM tribometer with environmental Plexiglas enclosure. Although one machine can do both linear and rotational tests, it cannot move in custom 2D paths. They offer ASTM compliant tribometers, but the test ranges for normal force and friction force are too low. Options include temperature control up to 1000 °C as well as humidity control. Testing with inert gasses is possible due to a Plexiglas enclosure. The tribometer has the ability to stop a test once a predefined coefficient of friction threshold has been reached. CSM Tribometers can be equipped with a depth measuring sensor for real-time display of wear properties.



**Figure 5: CSM Tribometer for linear and Rotational Testing with Environmental Enclosure [6]**

The most applicable tribometer on the market which most closely matches our customers' requirements is the Center for Tribology Research's Universal Micro-Tribometer (CETR-UMT) [7] shown in Figure 6 below. CETR-UMT currently has nano, micro, and macro testing capabilities. The micro tribometer setup can be seen in Figure 6 and is of the same measurement magnitudes that our sponsor has requested. The CETR-UMT device can conduct pin on disk, disk on disk, ball on disk, plate on plate, reciprocating and fretting, uni-directional and multi-directional wear tests. Among the unique functions of this machine is the ability to program any 2D path for wear analysis in any variety of path configurations. While this machine meets most of our customers' requirements, it has a base price around \$80,000. This doesn't include the modules necessary to run higher speed linear tests required by our customer. Even with these upgrades, speeds won't be sufficient for testing required by our customer.



**Figure 6: The most feasible currently available tribometer is the CETR-UMT tribometer capable of path generation in any 2D configuration [7]**

### **Proprietary Devices**

There are a variety of unique tribometers which have been designed and built by independent sources. We have made a visit to the Ford Research and Innovation Center in Dearborn, MI, where engineers conduct wear and friction tests for several automotive applications. They have developed their own tribometers to more accurately test different components unique to their studies. We have evaluated two of their linear

tribometers and two pin-on-disk tribometer and recognized several design characteristics which may be useful in our design of the customer's tribometer.

All four tribometers we saw were much smaller than that required by our customer. Linear/radial stroke length was limited to a few inches or less compared to the 10 inch stroke length required by our customer. Movement of the pin/ball on the linear tribometers was controlled by a rotating motor/cam system. This allowed the motor to run at a continuous speed without changing direction throughout the test. Motor speed was controlled by a closed loop feedback system with a sensor which measured flywheel speed. The normal force for one of the linear tribometers was applied via a closed loop spring/lever system. The others used a more traditional hanging weight approach. All four tribometers measured friction force by measuring deflection of the test rig. A noticeable feature of each test rig was a relatively weak base which allowed for larger deflections and more accurate friction force measurements. Strain gauges were hooked up to measure these deflections.

Three of the tribometers controlled temperature via a heated metal block element on which the specimen rests. Temperature is measured via a thermocouple immersed in the lubrication under test. Temperature could not be measured in a dry test. The other tribometer surrounded the sample with heat coils to heat the specimen by convective and radiative heat. Very coarse humidity control was used by boiling water in a closed environment.

*Note: The information included in "Proprietary Devices" is not to be shared with outside sources or duplicated for any reason without permission from Ford Motor Co.*

### Existing Patents

Existing design patents that correlate with the scope of this project were examined as well. Several patents of existing technology were found using [patentstorm.us](http://patentstorm.us) and are presented below. All contain aspects of design that may be valuable for the scope of this project.

Patent 1534014 [8], pictured below in Figure 7, describes a basic pin on disk wear device with a spring and mechanical measurement device used to measure the lateral frictional force. This is an old, simplistic design, but it provides a good starting point to the basic concepts and functions involved when developing a tribometer.

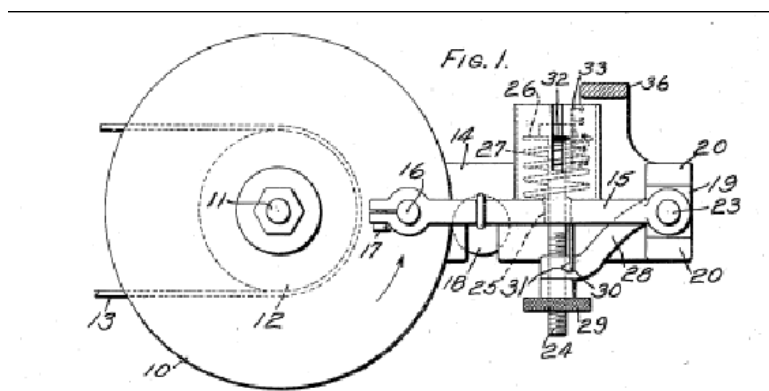


**Figure 7: Schematic for Patent 1534014 [8] – Basic pin on disk wear device**

Patent 4051713 [9] does not involve a pin apparatus, but instead measures the friction between two pads. It does, however, provide a way of specifying the normal force between the surfaces and provides good

motor control using an encoder device. While it is not exactly known what this project entails, it does contain components that may be transferrable and is shown below in Figure 8.

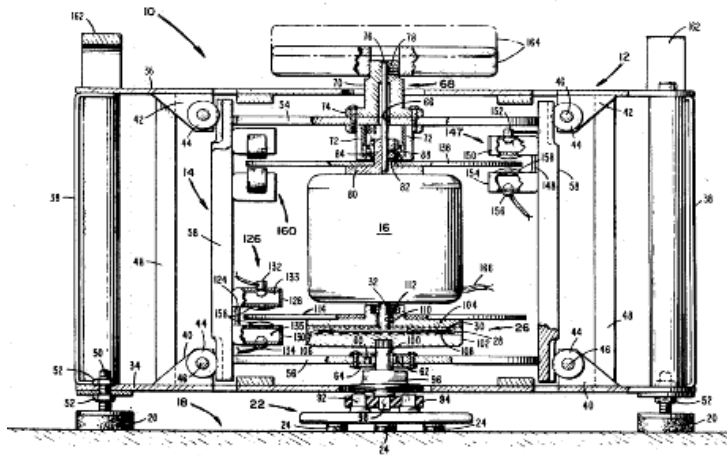


**Figure 8: Schematic for Patent 4051713 [9] – Wear device utilizing motor and force control**

Patent 6401058 [10] also does not use a pin device like this project requires but uses a rotating drum on a flat surface. The key features of this design are the data acquisition and control techniques as illustrated in Figure 9 below. This design also examines surface characteristics of the test sample which will be desirable for this project.

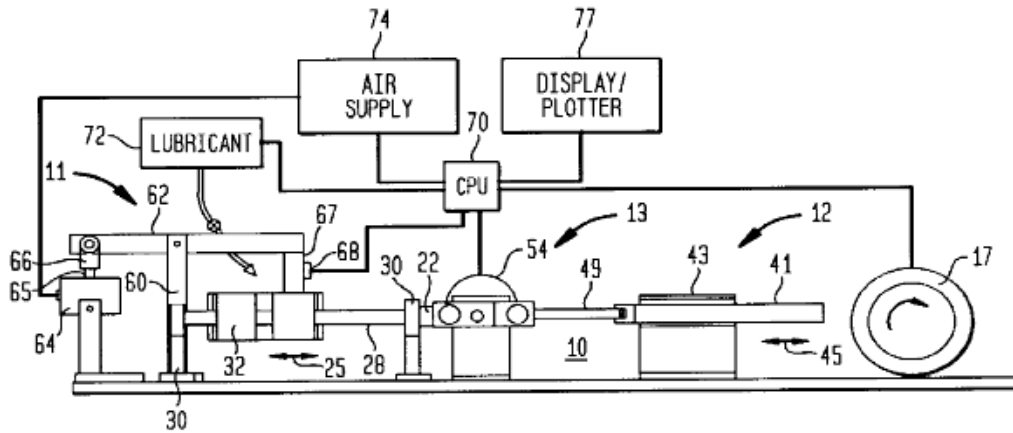


**Figure 9: Schematic for Patent 6401058 [10] – Wear device utilizing data acquisition, input control, and surface examination**

## DEVELOPMENT OF TARGET ENGINEERING SPECIFICATIONS

In order to set quantified targets for our project, we interviewed our sponsor, Prof. Krauss, and determined the functionality required of the device in order to meet his research needs. We researched wear testing, including a review of ASTM test standards and previous groups' work, conducted an interview with Dr. Arup Gangopadhyay of Ford Motor Company and toured his testing facility. We also benchmarked several commercially available tribometers to improve our understanding of the challenges of tribology. We then used this information to develop a list of customer requirements which we then reviewed with our sponsor to determine the relative importance of the requirements. Next we identified quantifiable engineering characteristics of the tribometer that could be used to meet these requirements.



We then organized this information in a Quality Function Deployment (QFD) chart which we used to correlate the customer requirements to the engineering characteristics that will be used to address them. We also used the QFD to identify engineering characteristics that might interact with each other leading to the need for tradeoffs or compromises in meeting different customer requirements. In order to develop target specification values for each of the characteristics, we tabulated values requested by the sponsor, those required by the ASTM standards, and specifications given for competitive products, which we evaluated against our customer requirements to help us identify which aspects of their designs were relevant to our efforts. This process is discussed in greater detail in the following sections and the resulting target specifications are tabulated in Table 3 on page 16. The QFD used in our analysis can be found in Appendix A.

### **Customer Requirements**

In order to meet the needs of Prof. Krauss' lab the tribometer must be capable of testing multiple wear path configurations under a wide range of environmental and loading conditions for a variety of specimen sizes. It must also be able to accurately and precisely control, measure and record the applied normal force, relative velocity of the samples, temperature, and humidity, as well as measure and record the lateral force generated, wear induced, and contact resistance across the samples and interface in real-time. The second column of Table 3 presents the minimum acceptable range for these test parameters as well as the required control tolerance, measurement precision, and sampling rate for data collection specified by the sponsor. Specifically, the tribometer must be able to conform to the ASTM G99 [1] and G133 [2] standards for linear reciprocating and pin-on disk tests, respectively, which are discussed above. It must be able to mount both pin and plate type samples of metals, ceramics, and polymers without damaging or altering their condition and must perform tests with or without the presence of lubricants or coatings. When testing custom 2-D wear paths, the leading point on the pin sample must be maintained in order to maintain a constant cross sectional wear profile. In addition to these testing capabilities, the tribometer must include features to safeguard the user from debris, moving parts, and high temperatures. It should also be designed to minimize maintenance and prevent the machinery from being damaged by moisture, temperature extremes, test fluids, material debris, and accidental misuse. The device must be sized to fit into the dedicated lab space provided and should allow viewing of the test in progress. Ideally it will also be automated to allow test samples to be loaded without the user being present so multiple tests may be run in succession without supervision. Finally, these things must be achieved for a significantly reduced cost relative to existing commercial products.

These priorities were quantified using a ranking system in which importance of each requirement relative to all others was assessed in pairs with a value of one given to the most important. The total score for each was tabulated and recorded in the QFD. This knowledge of the relative importance of the customer requirements to the customer will be important when two requirements are in conflict such as in the case of the requirement of shielding the user from debris and allowing the user to observe the test. Table 2 on page 15 summarizes our customer requirements in order of decreasing significance.

**Table 2: Customer Requirements ranked by relative importance**

Critical	Important	Useful
1. Meet ASTM standards	8. Test range of sample sizes	16. Tests wide range of environmental conditions
2. Safeguard user and device	9. Measure velocity in real time	17. Automated sample loading
3. Record forces in real time	10. Test custom 2D paths	
4. Test variety of materials	11. Measure temperature and humidity in real time	
5. Low Cost	12. Measure contact resistance in real time	
6. Low maintenance	13. Measure wear depth	
7. Fits in lab space	14. Constant pin orientation	
	15. Allows viewing of test	

### Engineering Characteristics

Most of the engineering characteristics we have identified arise from the need to closely control and measure the test parameters of normal force, velocity, temperature, and humidity. In order to do this we will need to use a feedback system with a sensor capable of detecting these parameters throughout the full range of values to which they may be set. The sensor will need to have a resolution that is sufficient to be able to detect physically significant variations so that the system can respond to maintain the desired setting. Similarly, the data acquisition system will need to be able to sample data at a rate that will allow the system to respond to variations before the parameters go out of tolerance. The tolerance itself will also have to be specified in order to optimize these resolutions and sampling rates. Similar sensor range, resolution, and sampling rate engineering characteristics arise relative to the need to measure the lateral force, contact resistance and wear depth outputs of the tests. These characteristics are also related to the requirement of meeting the ASTM standards which dictate the necessary tolerances for many of the test parameters.

Additional engineering specifications come from the physical requirements for the device and the tests it will perform. Overall device dimensions are required to ensure that it will fit in the lab space available. The capacity of the sample holders must be specified to ensure that the lab's specimens can be held securely by the tribometer. Similarly the maximum z-axis travel that the device can reach must be set to ensure that sufficient testing can be done and thick samples can be tested without damaging the device. We must also ensure that the tribometer has a sufficient lateral range of motion for the desired tests and that it can achieve the oscillation frequencies required to meet ASTM standards while still operating safely. In order to perform tests with custom 2-D wear paths and ensure that each pass overlaps and the pin is always oriented lead point first, we must specify the precision with which the device must position the specimen. Finally, the perpendicularity of the pin specimen to the plate specimen must be specified to conform to the ASTM guidelines.

The engineering characteristics discussed above and summarized in Table 3 on page 16 are by no means exhaustive. Additional engineering characteristics that will need to be developed as we continue our design efforts, but we believe that these will be the most important for use in evaluating potential working principles that we will consider for meeting the customer requirements. Most of them can be used to address multiple customer requirements to varying degrees. We have assessed these requirement-characteristic interactions and indicated their expected strength on the QFD chart using a rating system where 9 indicate strong, 3 modest, 1 weak, and no value a null interaction. Using these rankings and the weighted importance of the customer requirements, which we determined as discussed above, we were able to determine the relative degree of influence afforded by each parameter by summing the products of the requirement's weighted importance and the rating of the strength of the characteristic's influence on

the design's ability to meet the requirement. We found that the most important design specifications were the range of force, temperature, and linear and rotational speeds. This information will be useful in identifying which engineering characteristic it is most important to meet as well as what performance criteria will be affected if they are changed. Recognizing that many of the characteristics will depend upon or be affected by others, we have documented the interactions we expect to see for reference in the QFD. The interaction strengths are again ranked on a scale from 0-9. The most significant results from this exercise are that we expect to see temperature effects upon the sensor performances and also interactions between the control tolerance, sampling rate, and resolution of the measured parameters. The QFD can be seen in Appendix A.

### Specification Targets

For each of the engineering characteristics identified we have developed preliminary specification values to use as targets during the development of design concepts. To select these targets we considered the stated needs of our sponsor, the requirements set forth in the ASTM standards, and the specifications for aspects of the tribometers we benchmarked that met our customer requirements. The most rigorous requirements were selected to ensure that all customer requirements, as we understand them, would be met if these targets are achieved. These target specifications are presented in Table 3. In cases where it is desirable to maximize or minimize a specification, this is noted along with the minimum acceptable value. The target specification justification for specific characteristics is discussed in more detail in the following sections.

**Table 3:** Target Engineering Specifications and Sponsor Requests

Engineering Specification	Sponsor Request	Target Value	Control Tolerance
Normal Forces	≤ 200 N	≤ 200 N	1% (of nominal)
Linear Speed	0.01 – 1.0 m/s	0.01 – 1.0 m/s	1% (of nominal)
Oscillation Frequency	2-20 Hz	2-20 Hz	1% (of nominal)
Rotational Speed	1-600 rpm (maximize)	1-600 rpm (maximize)	1% (of nominal)
Temperature	0-150 C	0-150 C	2 C
Humidity	0-100 %	0-100 %	3 %
Contact Resistance	0-1000 ohm	0-1000 ohm (maximize)	
Measurement Resolution	1% (of nominal)	1% (of nominal)	
Data Sampling Rate	20 kHz	20 kHz	
Sample Dimensions: Pin	1.6 – 6.4 mm	1-8 mm	
Plate/Disk	25 – 254 mm	25 – 254 mm	
Specimen Perpendicularity		(90 ± 1)°	
Positioning Precision		± 0.025 mm	
Z-travel	15 mm	15 mm (maximize)	
Linear Travel	0 – 254 mm	0 – 254 mm	
Dimensions (l×w×h)	91x61x61 cm	91x61x61 cm	
Sample Visibility	100 %	100%	

**Control parameters:** The target ranges for the test conditions of applied normal force, linear and rotational speeds, linear oscillation frequency, temperature, and humidity were selected based upon those required for the lab's research. The allowable tolerance for the control of these parameters at constant nominal values were chosen based upon the ASTM standards, when specified, and upon the sponsor's experience of the tolerance needed to produce repeatable results.

**Data collection and contact resistance range:** The targets for the resolution and rate at which the normal and lateral forces, relative velocity, temperature, humidity, contact resistance, and wear depth were chosen based upon the sponsor's experience of what is required to produce meaningful results. A minimum resolution of 1% of the nominal value was proposed for all measurements. We also took into

consideration that the use of a feedback system will be required to achieve the stated control tolerances and the resolution of the sensors used must be at least as precise as the control tolerance. Additionally the sampling rate must be sufficient to allow the feedback system to respond before going out of tolerance. For the contact resistance range we have set the minimum capability based upon the performance of competitive products and the sponsor’s minimum requirement with the ultimate goal of maximizing the range.

**Sample holding and positioning:** The capacity of the sample mounts was determined from the stated needs of the sponsor’s lab and includes the sample sizes used in the ASTM standardized tests. The tolerance for the perpendicularity of the pin specimen to the plate specimen was taken from the ASTM G99 [1] standard. We have determined that the linear travel should allow the entire surface of the plate specimen to be tested and must therefore be equal to the length of the largest specimen to be tested. The oscillation frequency range was selected to allow testing at one half and two times the ASTM standard test rates. The z-axis travel was selected to accommodate the thickest samples the lab anticipates testing. The precision required for the displacement of the specimens in order to perform custom 2-D wear path tests was determined from the specifications for existing devices that meet our requirements.

**Physical constraints:** We have set limits for the overall dimensions of the tribometer based upon the lab space available for it. We have also determined that the design must enable the user to observe the test in progress and have set a target of 100% visibility.

## CONCEPT GENERATION

To begin the process of redesigning the tribometer, we broke the device into component subsystems and identified the required characteristics of each subsystem which will best meet the functionality demands for the overall device. We then further divided the subsystems as necessary and developed working principles for each major function. Using the relevant device specifications and additional subsystem specific criteria organized in Pugh charts, we identified the most suitable working principles for each subsystem and combined them to produce a number of potential concept designs. These designs were similarly evaluated and ranked and a preliminary selection was made and modified to include favorable aspects of other concepts. The following documents the working principles and concepts generated, as well as our selection process and a detailed description of the alpha design concept.

### Subsystems

We began the creative process by generating a function diagram to identify flow of information, material and energy through the tribometer and the individual functions performed. The resulting diagram can be seen on page 48 of Appendix A.2. The major subsystems identified are given in Table 5 below.

Table 5: Tribometer Subsystem Descriptions

Subsystem	Description
Motion Control	Produces smooth, controllable relative motion between samples at sufficient velocities and frequencies. Includes mechanisms for motion generation, transmission, and conversion between rotation and translation.
Force Application	Applies constant normal force in required range. Includes generation and transmission
Environmental Control	Contains and controls temperature and humidity of test environment. Includes heat and humidity generation and removal, containment, and delivery mechanisms.

Control System	Measures and records normal and lateral forces, relative velocity, temperature, humidity, wear depth, and contact resistance in real time. Adjusts signal to actuators to maintain test parameters. Includes sensors, controllers, and data storage devices. Includes a user interface to set test parameters and display results.
Sample Holding	Fixtures and interfaces for the securing of pin and plate type samples.

### Working Principles

For each of the subsystems identified we investigated methods for achieving part level functionality and used Pugh selection methods to narrow our focus to the most appropriate options for our application. The associated Pugh Charts may be found in Appendices A.3-A.15 on pages 49-62.

**Motion control system:** The motion control subsystem is further broken down into mechanisms to generate mechanical motion, transmit power, convert between rotational and translational motion, and to constrain and support those motions. Table on page 19 lists the working principles considered for each of these mechanisms. The motion control system must produce smooth motion in two dimensions at the specified speeds and frequency. This relative motion of the pin and plate samples can be achieved using a combination of translational and rotational motion or dual axis translation of one or both samples. The motion must be smooth in order to meet required speed control tolerance and must allow for precise positioning to enable 2D paths to be repeatably traced. The components must be able to withstand the lateral loads encountered, which are expected to be as much as 600 N, and must be suitable for the environment of the tests and require a minimum of maintenance. A detailed description of the most viable options identified is provided below.

Table 6: Motion Control Working Principles

Motion Generation	Transmission	Conversion	Constraint and Support
DC stepper motor	Belt or chain drive	Belt and linear stage	Bearings
DC servo motor	Gear train	Screw and nut	Bushings
AC servo motor	Shaft or screw	Rack and gear train	Rail guide or gantry
Linear servo motor	Piston	Cam and piston	Sliding Rods
Voice-coil actuator	Hydraulics or Pneumatics		
Gravity			

**Motion generation:** We have identified linear and traditional DC servo motors as the best option for handling the range of motion, speeds, loads, and control precision we require. Due to space restrictions we narrowed our attention to methods of generating motion using electric motors. We investigated both DC and AC options and determined that due to the need to vary test speeds and the high cost of AC controllers, the DC option best met our needs. Stepper motors would be able to provide us with high holding torques and precise positioning with the use of a micro-stepping controller and feedback system, but would not be able to provide the smooth motion required due to the discrete nature of its movements. A commutative, brushless DC motor, or voice-coil actuator, can provide the force, precision, and responsiveness we require, but is limited in stroke length. DC servo motors, both linear ServoTube and traditional rotational types, however can provide the smooth motion and rapid reversal of direction and include closed loop feedback control. They can also achieve the necessary speeds and frequencies in combination with appropriate transmission and friction reducing motion supports. These options are therefore the best for our application. Appendix A.3 on page 49 presents the relevant Pugh chart.

**Transmission and conversion:** We must be able to transmit and condition the output of the motors in order to drive the samples in either translation or rotation to achieve the required speeds, forces, and paths. We have eliminated hydraulic and pneumatic actuators as options for this application due to the

safety hazard associated with working with pressurized fluids and constraints on the size of the system. The following describes the options considered and justifies our selection. The relevant Pugh chart is in Appendix A.4 on page 60.

**Belt and chain drives:** These devices use a belt or chain to transmit rotation or convert it to translation by driving a stage on a linear guide. They are capable of high speed and high torques transmission which can be conditioned by altering the ratio of pulley diameters. However they often produce vibrations that would interfere with our sensors and introduce the potential for slipping, depending on the specific type chosen, which make them a poor choice for our high precision application. Slipping and vibration may be reduced by the use of a toothed timing belt and additional devices like belt tensioners, at the cost of increased complexity and maintenance needs. The timing belts also introduce backlash when reversing directions which will reduce positioning precision and make these drives a poor choice for our application

**Gear trains:** Gears can be used to transmit rotational motion from a driven pinion or worm to a second gear, or to convert to linear motion in the case of racks. They are capable of achieving the required speeds and torques and can be used to alter the axis of rotational motion as well. Backlash is an issue of concern in gear trains that will affect the responsiveness of the device to controller signals and the ability to control position and speed in tolerance. It can be minimized by using precisely manufactured herringbone and worm gears or preloaded shafts. Gears also present wear and maintenance problems as contaminants and operation at temperature extremes and in moist environments can cause deterioration and affect compliance. Gears are a viable option for rotation transmission if properly selected and isolated from the test environment.

**Screws and shafts:** Screws and shafts can be used to transmit rotational motion and screws can be used to convert to translation by driving a linear stage along the axis of rotation using a threaded nut. They are capable of handling the required speeds, loads, and range of motion and provide sufficient positioning precision and responsiveness with proper motor and controller pairing. Similar to gears they will require isolation from contaminants and will need to be carefully selected for the operating conditions in order to prevent wear and deterioration. Screws are the most favorable option for producing linear motion from a standard rotational motor.

**Pistons and cams:** Pistons can either transmit translational motion directly from a linear motor or voice-coil actuator, or produce translation when driven by a cam. The cam and piston system is not viable for our application due to the size of the cam that would be required for the stroke length desired as well as the inability to achieve various speed and position profiles with a single cam. Similarly, the voice coil driven piston is unable to achieve the stroke lengths required. The linear motor driven option is the simplest method to produce the required linear reciprocation and would eliminate the need for an intermediary conversion step. It is capable of achieving the speeds, loads, responsiveness and precise positioning required when paired with a suitable motor and does not present the wear and tooth shearing concerns associated with screws and gears. It is therefore the optimal method for linear actuation for design.

**Constraint and support:** It will be necessary to constrain the motion of the samples and minimize friction at moving interfaces in order to produce smooth motion within the required control tolerances and maximize the life of the device. The particular methods used to achieve this will be determined by the actuators chosen, but will include the options of bearings and bushings for friction reduction and sliding rods and rails for motion constraint. We will need bearings to support the rotating plate sample holder and any rotating or sliding shafts, as well as any translating parts in contact with other surface. We will make use of rolling friction as much as possible to improve device life and efficiency and reduce wear and vibrations that may interfere with data collection and device control.

**Best options:** We have determined that the ideal method for producing translational motion is the use of a linear ServoTube motor to directly drive the sample holder. This method can meet the load, speed, and positioning precision requirements and results in a simpler system. It eliminates the need to convert from rotational to translational motion and therefore eliminates loss of controllability due to inefficiencies and the complications introduced into the design to minimize such losses due to friction of part compliance. The next best option would be to use a DC servo motor driven ball or roller screw to drive the sample as these are the low friction and backlash devices. This option can also be optimized to meet the system requirements, but will introduce more rigorous assembly and manufacturing challenges than the prefabricated linear motor system. Depending on the DC servo motor selected it may also be necessary to have a separate control and feedback system if it is not included as it is in the ServoTube. Rotational motion will be driven by a DC servo motor and a gear train consisting of low backlash herringbone and worm gears.

**Force application system:** As one of the customer requirements, a normal force ranging from 0 – 200 N with a tolerance of  $\pm 1\%$  of the nominal value must be applied to the samples. This system will consist of force actuators and sensors to monitor their performance.

**Force actuators:** A normal force must be applied between the pin and plate samples during testing. The options considered for this application as well as the selection criteria used to determine the best options are presented below. The Pugh selection chart used to evaluate these designs is presented in Appendix A. 5 on page 51.

**Screw/Motor Application:** This concept, shown in Figure 10 below, would use a motor, with the potential use of a gear system, to spin a screw. The screw would move downward onto the pin applying a force between the samples. A spring would be added for elasticity to the system between the screw and the pin. The motor and gears would be rigidly attached to the linear reciprocating stage and the pin would be free to move vertically through a hole in the stage. This will allow the force to be transmitted to the pin sample. To measure the applied force a load cell could be used between the surface contact of the pin shaft and the spring or a potentiometer could be used to measure the displacement of the spring.

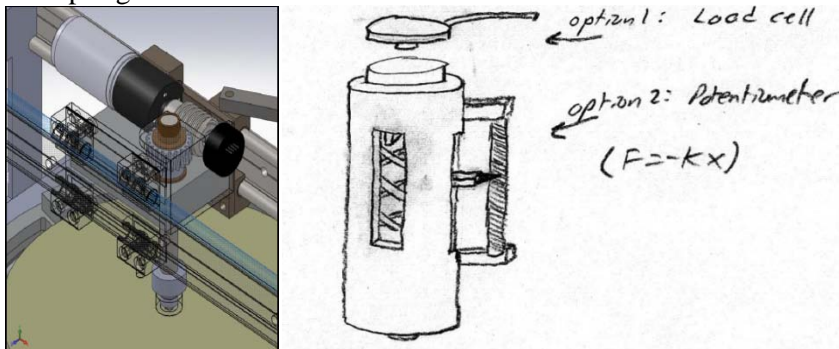
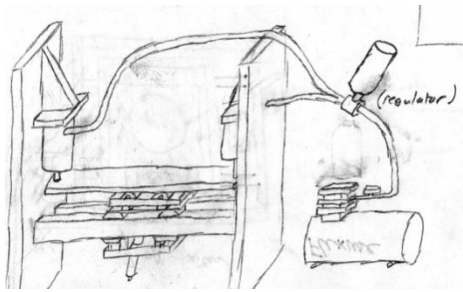


Figure 10: Screw actuated motor force application

**Spring/Lever System:** This concept would utilize spring force to apply the normal load to the pin. The lever system would allow this force to be transmitted from the spring to the pin. The idea for this concept was derived from the Ford tribology testing facility; however it is unlikely that this concept would be feasible in our design due to the size and complexity of the system

**Hydraulic/Pneumatic:** This concept, shown in Figure 11 below, would use a working fluid, either gas or liquid, to apply the force. The fluid would be regulated and pumped into a chamber to control the amount of force applied. The chamber would be secured at one end to the rigid stage with the other end free to move vertically, and thus apply a normal force.



**Figure 11: Hydraulic/pneumatic**

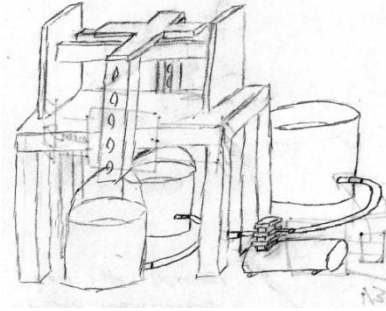


**Figure 12: Hanging weight force using water**

**Hanging Weights:** The most basic idea is to hang known weights from the device to achieve a constant normal force. The weights would hang to the side of the device, connect with a cross plate that would lower down onto the pin sample. Again this weight would be only transferred to the pin through the use of journal bearings feeding through the rigid stage. We proposed using water buckets for the weights so higher accuracy and continuous amounts of force could be achieved as shown in Figure 12 on page 21.

**Force Plate:** This concept, shown in Figure 13 below, would use contact force between a plate and the pin. The plate would be raised or lowered by a motor to control the normal force that is transmitted to the samples. The motor will be connected to two screws, one on either end of the device which will be spun at the same rate. Friction between the plate and the pin would be minimized by using a rolling contact at the contact point.

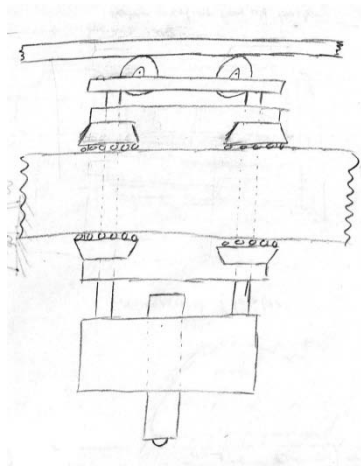


**Figure 13: Force plate**

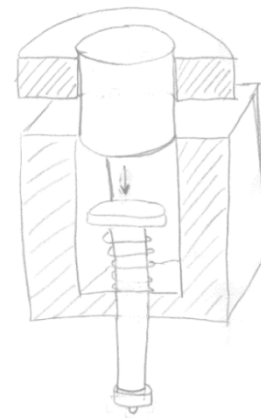


**Figure 14: Voice coil**

**Voice Coil:** This concept, shown in Figure 14 above, would use a voice coil, which is essentially a high force, low displacement linear motor. It uses magnetic forces to create a displacement which could be transferred to the pin shaft through a bearing, thus applying a normal force. The amount of force applied could potentially be measured by the amount of current supplied to the voice coil thus eliminating the need for a feedback control system. Also the voice coil itself could function as a spring eliminating another part and simplifying the design.

**Best options:** The best options to further consider are the spring application, the force plate, and the voice coil. The spring application would be more compact since one small screw and one small motor would be needed. Also, the previous team used this idea so it may be easier and more cost effective to implement since a motor is already available for use. There are several drawbacks, however. First, is that the motor will be held on the gantry so it will move with the pin. This adds weight to the gantry and the



motion may cause vibrations that affect the power transmission from the motor to the screw. Also, since the motor is on the gantry, the entire gantry will not be able to be inside the environmental chamber due to temperature affects on the motor.

The force plate idea is also a viable option. This may be more expensive since there will be more parts involved including a motor. This may also add more weight to the entire device. It may also be difficult to achieve the vertical motion with the machining tools available to us. Precision will be critical for this idea. This concept will, however, allow the controlling motor to be outside the working area and will allow the gantry to be enclosed in the environmental chamber if necessary.

The voice coil could be a suitable option as well. It eliminates the need for a spring and potentially a feedback system. It also would be more accurate than a rotational motor that is used for the other options. The voice coil does, however, weight a substantial amount which will again add weight to the system. Also, voice coils generate large amounts of heat, so for long testing periods a cooling device may be needed for it to function. This would counteract the benefits it would provide.

**Force measurement:** Lateral forces between the pin and the plate sample must be measured with high precision. To achieve this various ideas were generated and evaluated. The following section describes the working principles that could be used to measure the lateral force between the pin and the plate during testing. The Pugh selection chart for these principles can be found on page 53 of Appendix A. 6.

**Strain gauges:** This idea is the most basic and most cost effective. Strain gauges would be mounted on the pin shaft to measure the deflection of the pin which would correspond to a specific lateral force. The basic strain gauges would be purchased but will be mounted by the team. There is much uncertainty in the accuracy and reliability of such implementation and the previous team struggled with this concept. Also this idea relies on the deflection of the pin to measure the forces but since limiting the deflection to  $\pm 1^\circ$  is a critical engineering specification, the proper material would need to be utilized to ensure that we stay within this range.

**Professionally installed strain gauges:** The idea behind this is the same as the regular strain gauges but these will be able to measure the normal force as well. The professional installation, however, will add a sufficiently high degree of accuracy but also significant cost which must be evaluated by our sponsor. It may be necessary to achieve the engineering specifications, however.

**Load cells:** This concept, shown in Figure 15 below, will not rely on the displacement of the pin to measure the forces. The load cell would be mounted around the pin to measure all the lateral forces. Two one directional load cells could be used which would be mounted in box like device around the pin. The boxes would be restricted to translation in only one direction which is where the load cell would be located. This is also a costly principle that must be evaluated on performance.

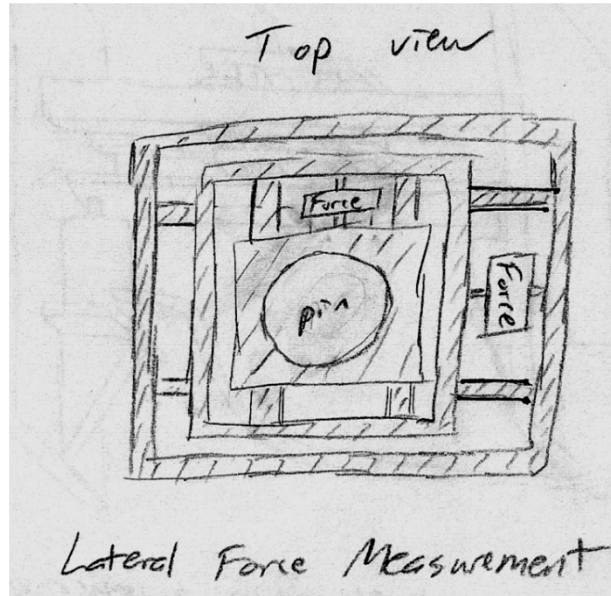


**Figure 15: Load cell configuration**

**Best option:** The options to further consider are professionally mounted strain gauges and load cells. They use different ideas to measure the forces which will be beneficial for our final concepts. The strain gauges use the pin deflection and the load cells measure the force directly. Since the amount of pin deflection is constrained to  $\pm 1^\circ$ , strain gauges may not be feasible, depending on the material properties used. They are much cheaper though than load cells.

**Environmental control system:** This system can be further broken down into the chamber that contains the test environment and the devices used to condition the temperature and humidity within the chamber. Table 7, below presents a list of the working principles investigated and Appendix A.10-13 on pages 57-61 present the Pugh selection chart used to evaluate them. A detailed description of the most promising principles follows.

**Table 7: Environmental Control Working Principles**

Heating	Cooling	Humidify	Dehumidify
Resistive Heating	Cold Plate	Air Misting	Salt Bath
Hot Plate	Evaporative Cooling	Heating Water Bath	Desiccant
Heat Pump	Refrigeration Cycle	Ultrasonic generation Water Wheel	Nitrogen gas

**Temperature control:** We have identified several methods for heating and cooling the test chamber as described below.

**Resistive heating:** Resistive heating works by passing a current through a resistive material and thus generates heat. The temperature of the heating element (usually a conductive wire coil) can be changed by controlling the amount of current passing through the coil. A household hairdryer makes use of this principle. Potential challenges to this method of heating involve risks involved with operating this type of device in a very moist environment.

**Hot Plate Heating:** Hot plates make use of resistive heating as well. They are commercially available and relatively cheap, but do not transfer heat as efficiently as a wound coil due to the limited surface area in contact with the surrounding air. Another option with a hot plate would be to heat the sample directly rather than heating the surrounding air.

**Evaporative Cooling:** Air is pushed through a saturated membrane, creating evaporation. Limitations to this design are the inability to function properly in humid conditions because less evaporation is possible in high relative humidity conditions. Because of this, evaporative cooling was dismissed as a viable option.

**Refrigeration Cycle:** By utilizing both heat transfer sections of the refrigeration cycle, we are able to generate both cold and hot chambers. We expect that we could reach temperatures at or below freezing, but temperatures much above ambient may not be possible. Although this principle may not be applicable for heating, we see it as the best option for cooling.

**Humidity control:** We have identified several methods for controlling humidity in the test chamber as described below.

**Air Misting:** Air misting makes use of the same principle that evaporative cooling employs. Water is sprayed on a membrane and air is passed through the membrane creating evaporation. Further control of evaporation rates can be controlled by setting the water temperature to be sprayed at a specific level. Because of the controllability and relative simplicity we see this as the most viable humidifying principle.

**Heating Water Bath:** Water is heated from a hot plate and air is forced over the surface of the water. By controlling both the air flow rate over the water as well as the water temperature itself, we can control evaporation rate.

**Ultrasonic Generation:** Ultrasonic waves are passed over a bath of water at a specific frequency. Water molecules begin to resonate, and vacuum pockets are generated. Vacuum pockets collide with one another and water molecules are displaced into the atmosphere. Due to the cost of this system and low moisture generation ability, we have dismissed this option.

**Salt Bath:** By controlling the concentration of moisture in a salt bath, various condensation rates have been observed. An option would be to place a salt bath with specific moisture content in the flow of our air recirculation system to decrease humidity.

**Nitrogen:** By injecting nitrogen gas into the chamber directly, we are able to displace moist air and fill the environmental chamber with mostly dry nitrogen gas. Either a constant supply of nitrogen and chamber equipped with a one-way valve would be needed, or a control system to regulate injection of nitrogen. This may be a viable option for very dry operating conditions.

**Desiccant:** A desiccant sucks moisture out of the air as do salt baths. The desiccant involved does eventually become saturated and recharging of the pellet is necessary by drying them out, which may delay test schedules. Also there is a limit to how much moisture these pellets are able to pull from moist air.

**Best options:** We have identified resistive heating in combination with a refrigeration cycle as the best methods for achieving the range of temperatures required. The best option for humidity control is the use of a misting system. These systems have the benefit of being relatively simple and readily available. They also make controlling humidity and temperature independently easier as they do not use water vapor to moderate temperature or heated water to control humidity.

**Data acquisition and control system:** One of the largest problems the last team faced while working on this project was in implementing a workable data acquisition and control system. The first problem they had was that the DAQ wasn't outputting a large enough voltage to be used by the motor controller. We should be able to solve this by implementing a voltage amplifier. The larger issue that we will have to design for is processing speed. The previous team claimed that the DAQ and PC-based LabVIEW program could not run at a high enough frequency. They believed the DAQ drivers were using software that took up too much computer bandwidth, that the software loop timing is insufficient for the needs of the motor controllers. With these problems in mind, we have investigated the following feedback control options.

**PC-based software processing:** One option would be to attempt to optimize the previous team's code to run faster. We could petition the help of someone with hardware programming experience to teach us how to implement hardware timing. Additionally, we could buy a faster DAQ and look into

using a PC with a faster processor. cursory discussions with some classmates in EECS majors indicates that running the controls and data acquisition system off of a standard desktop PC should be entirely feasible.

**FPGA processing:** If the previous team's assessment is correct a field programmable gate array (FPGA) processor could be used. An FPGA is essentially a user-programmable processor. The data acquisition and controller logic is written using a hardware programming code (traditionally Verilog), which is then compiled onto an FPGA chip. Because this chip exists externally from the PC, it can be custom built to work with our system hardware, and it will only be used to handle processes related to the tribometer. This custom programming will allow the individual data and control processes in our system can run in parallel. This will be faster than a PC-based processor system which executes tasks in series.

**Best option:** We believe, given the previous team's concerns, that an FPGA system is the best solution. FPGAs clearly offer a decisive advantage in processing speed and given that the functionality of this device is highly dependent on the ability to have a responsive feedback system we believe this option will best meet our needs.

**Sample holding:** In order to control the motion of the pin and plate samples it is first necessary to secure them to the testing platforms. We have investigated several methods for securing each of the samples as discussed below. The Pugh chart used to evaluate these methods can be found in Appendices A.8 and A.9 on pages 55-57.

**Pin sample holder:** There are two concepts for securing the pin sample free from rotation and translation. Both concepts use an applied normal force to clamp the pin into place.



**Figure 16: Threaded clamp**

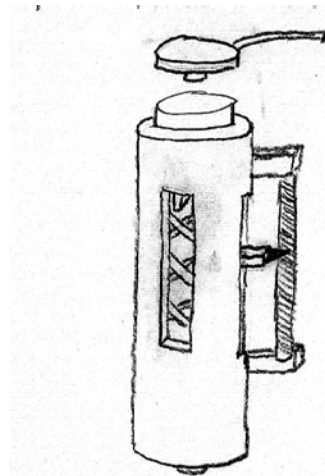


**Figure 17: Spring force clamp**

**Threaded clamp:** The threaded clamp concept, shown in Figure 16 above, places the ball sample into a fitted cap with a hole in the bottom to allow the surface of the ball to contact the plate sample without the pin holder interfering. The upper portion of the hole is threaded and fits on the main part of the pin holding device. By screwing the two pieces together, the ball sample is held in place securely.

**Spring force clamp:** The idea behind this concept, shown in Figure 17 above, is similar to the previous threaded clamp; however, the securing force is applied via a spring system instead of two threaded connectors. This concept may not secure the sample as well but will have the capability of measuring the applied normal force as a result of the displacement of the spring.

**Plate sample holder:** There are many more concepts for securing the plate samples.

**Modified radial clamp:** A variant of a radial clamp system can be seen in Figure 18 below. This system operates by forcing a metal strip closed around the disk sample with a series of set screws. This system differs from a regular radial clamp in that a regular radial clamp has a long band that is forced close by one bolt. The problems with a regular radial clamp are that the single closing bolt could cause a problematic asymmetrical moment of inertia when the system is at full speed, and there is no method for solidly fixing it to the base plate. This variant of the radial clamp attempts to solve both of those problems. First, by closing the clamp with a series of set screws, the device is more symmetrical, making it more stable at speed. Second, the fixed-size outer ring, through which the set screws operate, provides an area which can be solidly bolted to the base plate.

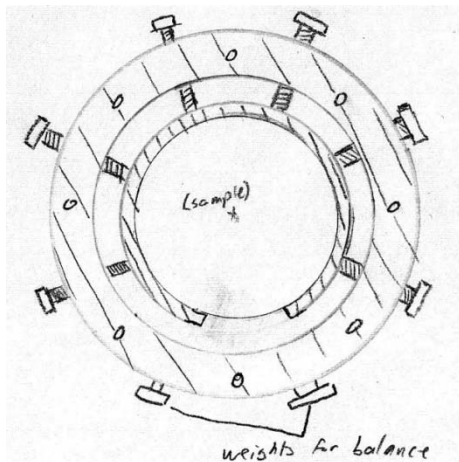


**Figure 18: Modified radial clamp**

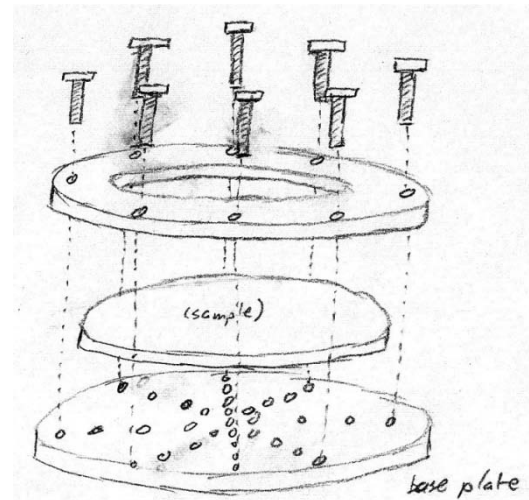


**Figure 19: Spring force clamp**

**Rigid ring clamp:** The vertical ring clamp, shown above in Figure 19 above, was designed to be a simpler alternative to the modified radial clamp presented above. This solution takes the outer ring from the radial clamp and decreases the inner diameter so that it overlaps the disk sample. This overlap between the ring plate and sample provides proper constraint on the sample when the ring plate is bolted to the base plate. Also, by using the ring plate, the stress concentrations seen in the previous team's solution (bolting the sample itself to the base plate) should be mostly dispersed.

**Chuck:** This concept will place grooves in the base plate that will allow L-shaped sliders to move back and forth to adjust for different sample sizes. Once the sliders are adjusted to the right size, they will be tightened down to the base plate.

**Large radial clamp with inserts:** This concept will use one large radial clamp placed on the outside of the base plate. A bolt will be used to tighten the radial clamp. To account for various sample sizes and dimensions, inserts of various sizes will be created to fill the space between the clamp and the sample and secure the sample into place.

**C-clamps:** This idea is to use a number of c-clamps around the outer edge of the base plate. These will apply concentrated forces between the sample and base plate.

**Individual bolted clamps:** This idea is similar to the rigid ring clamp, but a full ring will not be used. Instead, smaller individual clamps representing only a small section of the ring will be created. They will be bolted to the base plate, overlapping the sample to secure it. They will allow any size sample to be held with one set of clamps

**Magnetic:** This concept would involve magnets on the top of the sample and underneath the base plate. The magnetic forces would hold the sample in place.

**Adhesion:** For this concept, an adhesive would be applied between the sample and the base plate to secure it into place.

**Best options:** The best options to be further considered are individual bolted clamps, rigid ring clamps, and the chuck. The individual clamps would be a set of various sizes that could be mixed and matched depending on the sample size. Potential problems with this concept are that the overlap to secure the sample may interfere with the test path but it will be minimal. The other concern is that forces may become concentrated on the sample, which may affect the local properties in the sample and consequently the wear behavior.

The rigid ring clamps are similar to the individual clamps, but they more evenly distribute the securing load over the entire outer ring of the sample. They will not be a good option, however, if the samples are not circular and since they are of discrete sizes, many will have to be made which will add manufacturing time and material cost.

The chuck is another good option. Similarly to the individual clamps, it will be able to secure any size and shape sample. The chuck, however, will not interfere with any of the sample surface since the force is applied laterally, which is beneficial. The may be more difficult to manufacture with more small parts to adequately secure the samples.

## Concept Designs

We developed a number of preliminary concept designs by combining the optimal subsystem working principles identified above. Due to modular nature of the device it is convenient to design and optimize the tribometer and environmental chamber independently with consideration for the necessary interfaces. The concepts for each of these systems are described below and evaluated in the Pugh chart on page 62 of Appendix A.14.

**Tribometer concepts:** The tribometer is the portion of the overall system that generates force and relative motion of the samples. It comprises the main structural component and will include interfaces for mounting sample holders and an environmental chamber as well as sensors for data collection.

**Concept 1:** In this design, shown in Figure 20 on page 29, the lower plate type sample is held stationary while the pin sample is suspended from a gantry similar to that of a drill press. The pin sample holder is mounted to a ServoTube linear motor driven stage. The stage slides along a rail by way of roller bearings. The rail itself is mounted to a disk that is rotated by a gear train made up of a set of herringbone gears and a spur gear driven by a worm gear mounted to a DC servo motor as shown in the sketch above. By controlling translation and rotation independently 2D paths can be generated in a polar coordinate system. Normal force is applied by adjusting the height of the gantry using a ball screw driven by a stepper motor. The gantry system slides vertically within a supporting column. The stationary plate sample will be mounted to a table by bolting down the sample holder. A modular environmental chamber can be placed over the plate and secured by clamps (not shown). The interface between the pin sample and environmental chamber is discussed with environmental chamber designs.

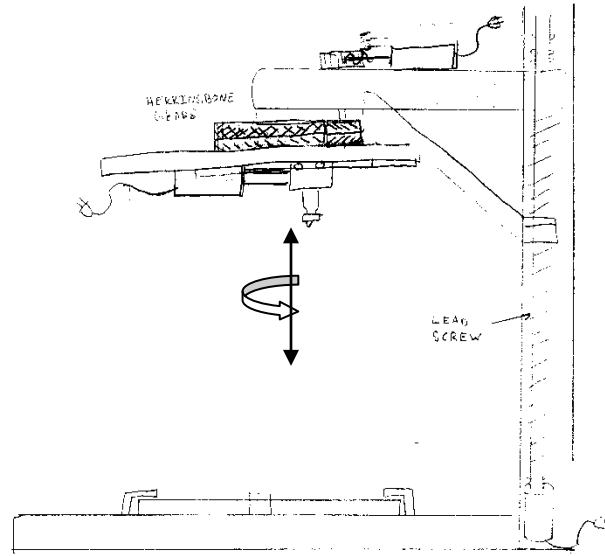


**Figure 20: Concept 1: Polar coordinate gantry**

The major benefit of this design is that the moving mechanical mechanisms can be completely isolated from the test environment which eliminates restrictions on material choice due to extreme temperatures, moisture and contaminants generated by the tests. It also reduces concerns raised by thermal expansion and its ramifications for compliance of parts. Controlling both rotation and translation within the gantry system introduces problems with balancing the system and preventing moments induced on the rails and shafts that might cause deflection, thus introducing friction and possibly affecting the ability to accurately position the pin. The linear ServoTube motor and DC servo will give us the ability to control the pin position to a high degree of accuracy and precision and the use of herringbone (aka double helix) and worm gears to transmit rotation will minimize backlash, further improving controllability. The stepper motor used to apply force and locate the gantry will provide a high holding torque which will be beneficial for maintaining constant pressure. However, micro-stepping and feedback controls will be required in order to meet the tolerances for force application.

**Concept 2:** In this design, shown in Figure 21 on page 30, the lower plate type sample is held stationary while the pin sample is suspended on a gantry. The gantry is designed to allow translation along two perpendicular axis thus allowing 2D paths to be produced in a Cartesian coordinate system. The pin sample holder is mounted to a ServoTube linear motor driven stage. The stage slides along the upper gantry rail which is in turn driven by a second ServoTube motor to slide along a set of parallel rails as shown. The entire gantry is held at a constant elevation. Force is applied using a voice coil actuator (not pictured) to drive the pin sample downward. The plate sample is secured by bolting its holding fixture, discussed later, to the table. The pin sample holder mounts into the linear stage and is secured by a shear pin passing through the both stage and pin.

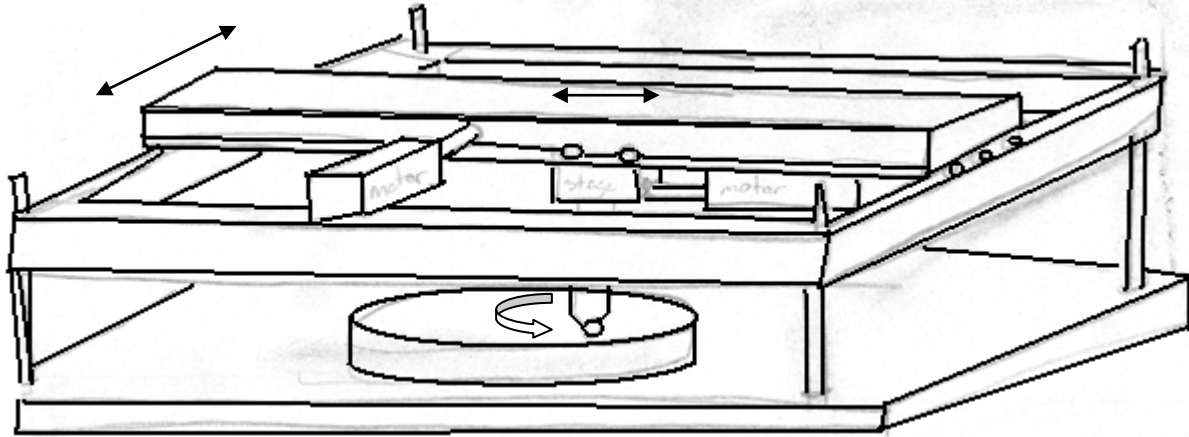
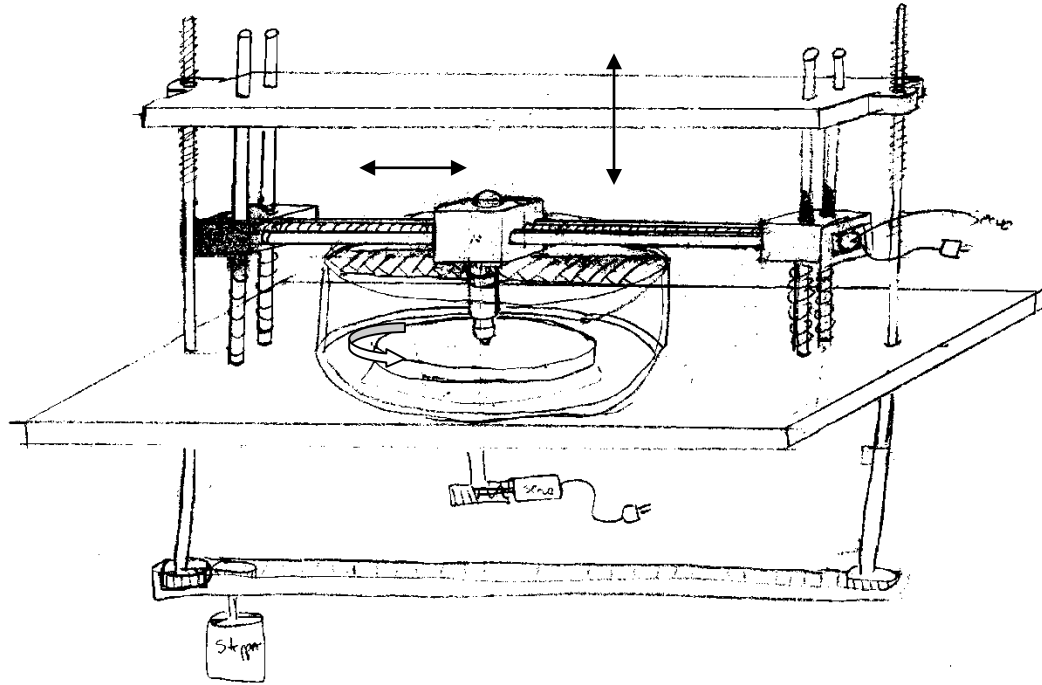


Figure 21: Concept 2: Dual translation gantry

Similar to Concept 1 the main benefit of this design is the isolation of the mechanical systems from the test environment. The elimination of rotation reduces concerns regarding balancing a spinning gantry and the resulting moments and varying inertia as the linear stage translates. The system is bulky, requiring multiple rail systems with high straightness tolerances. An foreseeable problem is that the pin sample would not maintain a single leading point unless an additional mechanism were implemented to rotate the pin as a function of its trajectory, which will significantly increase the difficulty of controls programming. The use of an extending pin is also a potential problem as a longer pin will deflect more under a given lateral load, which will complicate achieving tolerances on deflection over the full range of operation forces. The use of servo motors provides a high degree of positioning precision and controllability, but in order to take advantage of this it will be necessary to manufacture the gantry to high tolerances and use roller bearings to eliminate friction and sticking, thus increasing the complexity of the fabrication process.

**Concept 3:** In this design, shown in Figure 22 on page 31, the lower plate sample is rotated while the upper pin sample translates in a single direction. The linear motion is actuated by a DC servo motor driven ball screw and a sliding rod supported linear stage mounted to the nut. The rotating plate is driven by a second DC servo motor paired with a worm and spur gear. The plate is supported by a ring type ball bearing to prevent deflection. Normal force is applied by a screw actuated press that is lowered to come into contact with a roller mounted on top of the linear stage. The stage itself is suspended on a free-floating gantry supported by vertical sliding rods with springs to hold the pin sample off the plate when force is not applied. When force is applied the gantry is lowered until the pin mounted to the linear stage comes into contact with the plate sample and the desired normal force is achieved. The screws used to lower the plate are driven by a stepper motor and a belt drive in order to ensure both that both are lowered at the same rate.





**Figure 22: Concept 3: Screw actuated linear motion and force application**

This design's major strength is that the method of force application does not require the addition of a massive force actuator to the linear stage, which would increase the inertia of the system when reversing directions, thus increasing the requirements placed on the linear actuator. The stepper motor used to apply the force can provide a high holding torque to maintain constant force. However, the sliding rod suspension introduces the potential for sticking if the rods are not straight enough or a moment is induced on the gantry. Similar issues would be encountered with the lead screws controlling the press. Another strength of the design is that the pin sample is held off of the plate when force is not being applied. This will reduce the risk of user error when loading the pin holder as the pin cannot crash into and shatter brittle plate samples if dropped.

**Concept 4:** This design, shown in Figure 23 on page 32, is fundamentally unique from all other designs because linear motion is achieved by moving the base plate rather than moving the gantry and pin system from above. There are several advantages and disadvantages of using this type of approach. By achieving all motion (linear and rotational) in the base plate, we are able to hold the pin stationary. This reduces the total number of moving parts increasing overall reliability of the system. A nonmoving pin will not require a gantry and slide system. Since the pin will remain stationary throughout testing, it may be possible to increase accuracy of our lateral force measurements because we could. A moving pin introduces inertial forces due to acceleration and mass of the pin, adding error into lateral force measurements.

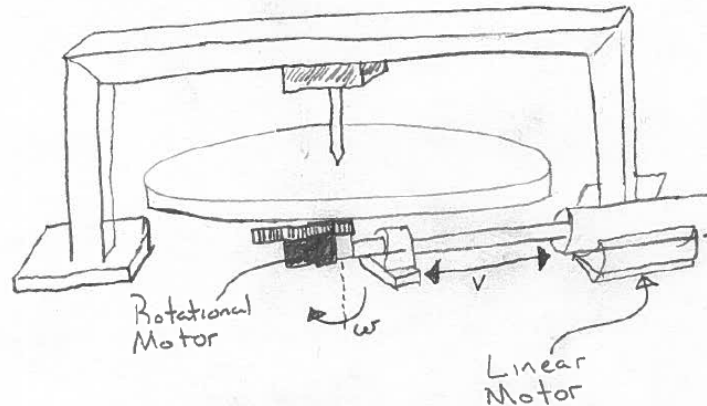


**Figure 23: Concept 4: Linear and rotational plate with fixed pin**

Although this approach reduces total number of moving parts and has potential to increase accuracy of lateral force measurement, our engineering team has decided a non-moving pin system is not the best approach for several reasons. If the base plate is capable of linear and rotational motion, the motor which drives rotation must be movable with the rotating plate. Also driving a rotating plate and motor system may be difficult due to its size and weight. It may be difficult to run tests which require high linear speeds due to the inertial forces required when accelerating the base plate. Because of this, either a very powerful linear motor will be required, or we will limit our high end velocity capability of the system. Although a moving pin system will also have inertial forces, we feel they will be negligible compared to lateral forces we expect to see don't foresee any issue by having a moving pin. Based on the above considerations, we have decided not to adopt this design concept.

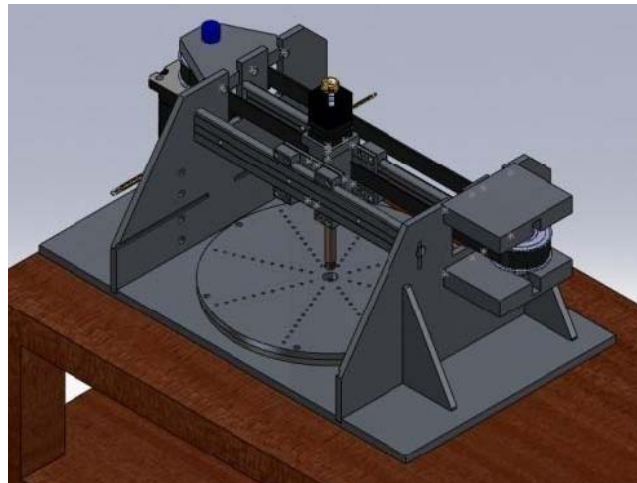


**Figure 24: Previous team's final design**

**Concept 5:** This design is based upon the previous team's prototype, shown above in Figure 24 above, which uses a spinning plate sample and translating pin sample. The disk is driven by a DC stepper motor and spur gears while the pin is translated on a linear stage and gantry rails using a stepper motor driven timing belt drive. Normal force is applied using a stepper motor controlled screw to press the pin holder downward into the plate. We would replace the ring bearing supporting the rotating disk as it is of poor quality and also replace the linear bushing on which the stage slides with roller bearings to reduce friction. A damper such as a spring or elastic material would be added to the force application system to provide a sort of suspension to reduce sensitivity of the applied force to variations in the sample surface. We would also have the strain gauges used to measure deflection of the pin sample and thus the lateral

force professionally mounted as the previous team was unable to obtain quality data with their gauges. Finally, in order to improve the smoothness of motion and positioning precision we will implement micro-stepping controllers with the stepper motors. The focus of this design is to use as much of the previous team's work as possible while making slight changes to improve its functionality. It cannot provide requested functionality as we believe can be achieved through a complete redesign, but has the benefit of being faster and less expensive to develop.

**Environmental control concepts:** Our sponsor has asked that our design have the ability to control temperature and humidity over a wide range. Temperatures ranging from 0 -  $150 \pm 2^\circ\text{C}$  and humidity levels ranging from 0-  $100 \pm 3\%$  relative humidity need to be achievable. To achieve this, we will need an environmental chamber which can be controlled by a temperature and humidity system. The following presents our concept designs for the chamber and temperature and humidity actuator.

**Environmental chamber:** The environmental chamber has several requirements. Its main function is to contain and isolate an environment. A secondary function will be to provide a safety mechanism to protect the user incase anything within the chamber becomes loose or breaks. To ensure isolation from the lab environment, the chamber must be airtight and well insulated. It must also have a window or way for the user to see the test being run to ensure everything is operating correctly. Since we have been asked to create environments which can potentially be corrosive to electronic and mechanical systems, we have restricted our focus chambers which will isolate the environment from the gantry system and house at most a rotating disk and sample. The gantry and most electronics will not be inside the chamber. To achieve this, some part of the chamber must have an interface which allows for the pin to slide linearly in the chamber. Several methods to do this are given below.

**Concept 1:** Figure 25 on page 34 shows a possible solution that makes use of an accordion type interface which is flexible enough to slide with the pin. This chamber includes ports to allow the flow of conditioned air through the system as well as inlets for the application of other gases and lubricants. The walls are constructed of two layers of transparent material with a layer of evacuated space in between to reduce heat transfer. The front panel is hinged for ease of sample loading.

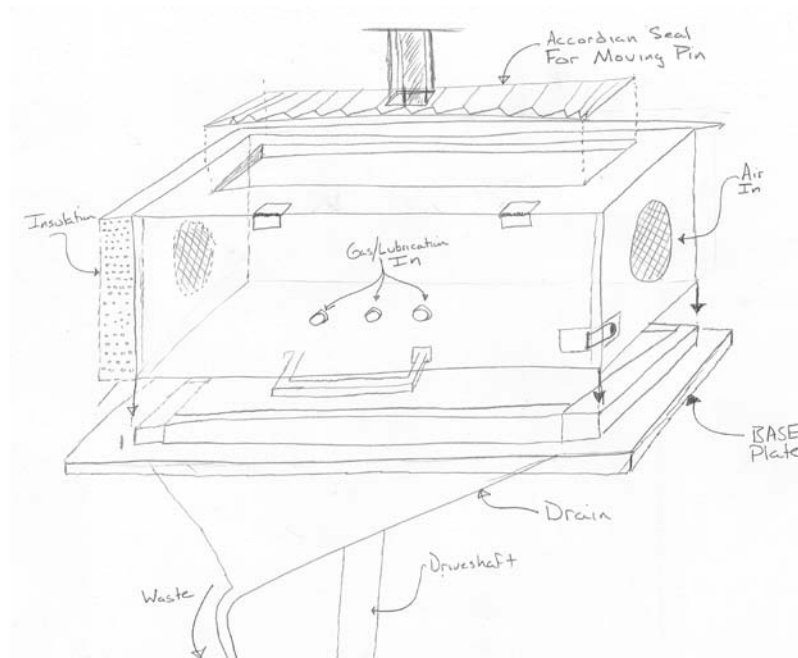


**Figure 25: Environmental Chamber with accordion seal**

**Concept 2:** Another method for achieving isolation of the mechanical system from the test environment uses a rubber barrier on the chamber along the length of the gantry rail, as can be seen in Figure 26 below. This rubber barrier would have a long slit in it which could flex around the pin as it traverses the disk. This design poses the problem of leaking from the chamber as well as the potential for friction as the pin slides through the seal.

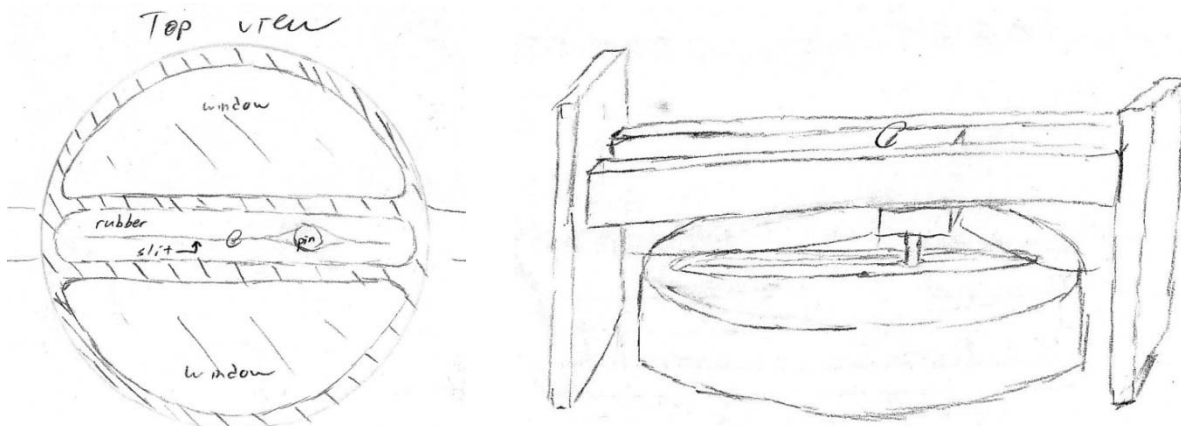


**Figure 26: Environmental chamber with rubber barrier**

**Temperature control:** After evaluating modes for heating and cooling, we have generated several concepts and selected a best option which is capable of generating temperatures in our required range of 0

– 150° C. This system would require divided forced air system to flow over either a set of cooling coils of a refrigeration system or resistive heating coils as seen in Figure 27 below. After heating or cooling the air, it would be fed into the environmental chamber. Air would be recirculated and controlled via a feedback system. The feedback system will gather temperature data from the chamber as well as temperatures from both the hot and cold divided air ducts using thermocouples. A baffle would be used to divide the airflow based on set temperature vs. actual condition, also seen in Figure 27 below.

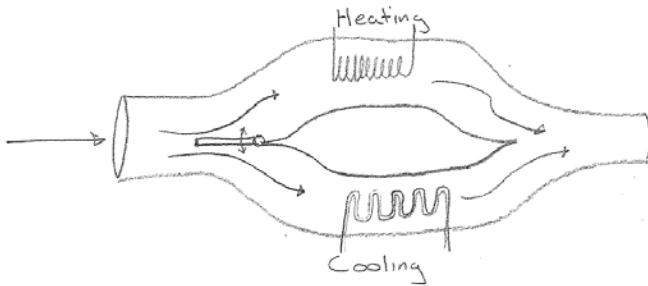


**Figure 27: Divided flow temperature control**

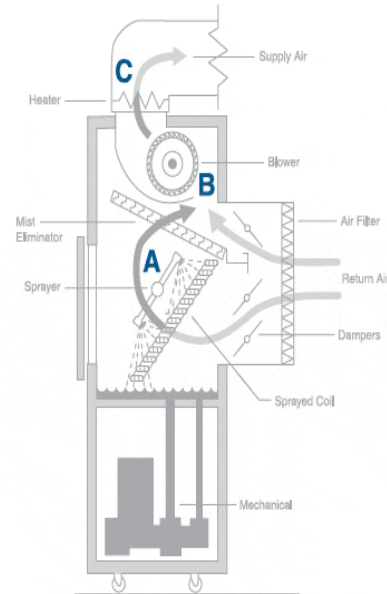


**Figure 28: Misting humidity control**

**Humidity Control Concept:** Several humidity control concepts were generated and a best option was chosen. Figure 28 above shows a humidity control system which uses a misting system to either increase or decrease the relative humidity of the test chamber. The water spray is adjusted to maintain the dew point temperature of the targeted condition. As the air passes through the water spray, it is cooled down to the temperature of the water and approaches saturation. The saturated air then flows over a heating coil to heat the air back up to the desired level. Commercially available systems which employ this technology are capable of reaching humidity levels of 22 – 83 ± .5% relative humidity. Temperature can be controlled to a range of 8 - 40 ± 0.1° C. One such commercially available system costs upward of \$35,000. A big part of the cost for these systems is the actual environmental chamber which holds the temperature/humidity specific gas. By designing our own chamber which can be catered to our specific needs, we hope to purchase systems which create the environment necessary, but don't have a chamber to house it. We will then interface it with our environmental chamber through the necessary number of insulated ducts.

**Evaluation:** After these concepts were developed, a mode of evaluation was needed to determine which design(s) would best fit the engineering specifications. First, a set of evaluation criteria was developed pertaining to the various engineering specifications determined previously. These criteria were listed in the left side of a table. Then, each of these criteria was given a weight as a percent (totaling 100%) to show the overall importance relative to other criteria. This information is placed in the column next to the criteria. From that, each design is given a rating between 1 and 5 (1 = worst, 5 = best) to evaluate how effectively each design meets the given criteria. These ratings are then multiplied by the importance percentage to obtain a weighted value for each criterion. These values are then added to determine the final score of each design, the higher the score the better the design. The Pugh chart used to evaluate the concept designs is shown on page 61 of Appendix A.10.

## ALPHA DESIGN

Using what we believe to be the best aspects of the previously described concepts designs, we have developed the proposed alpha design shown in Figure 29 below and described bellows.

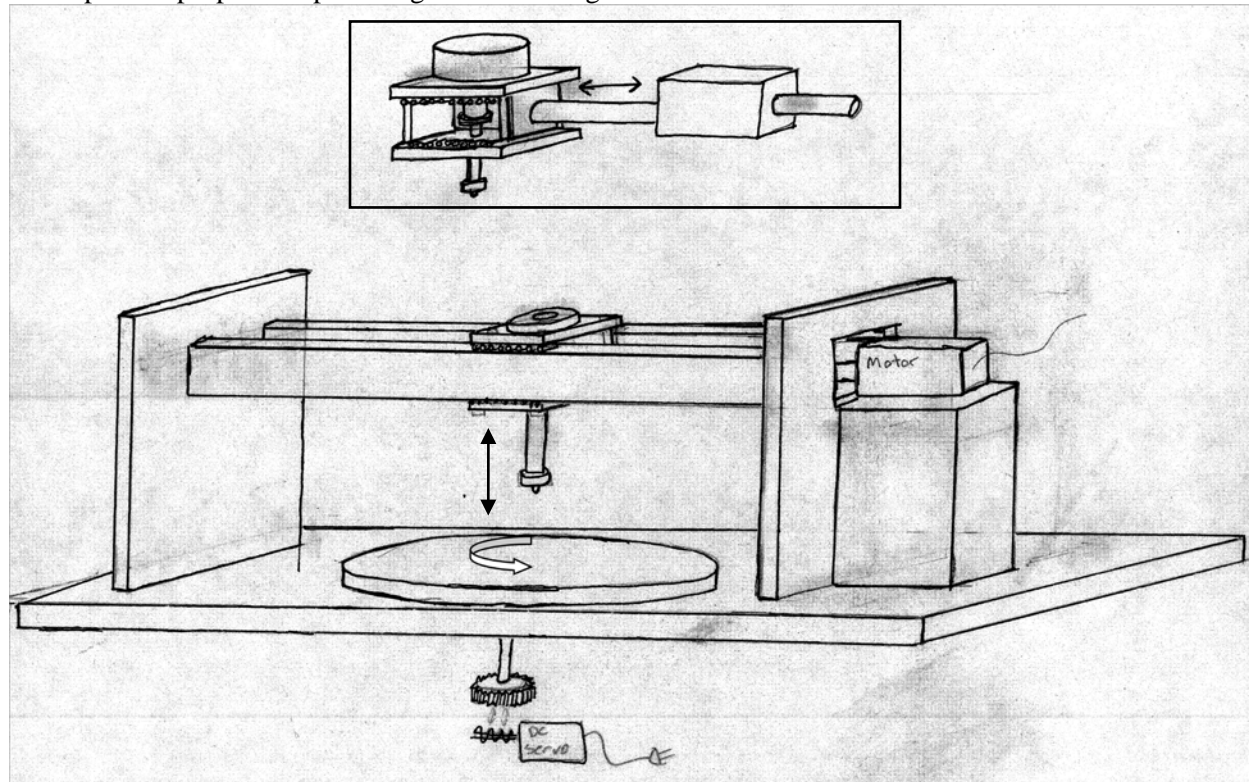


Figure 29: Alpha design

### Motion Actuation

In this design the lower plate sample is rotated while the upper pin system is translated. The plate is fixed to a rotating shaft driven by a herringbone gears and a DC servo motor. The plate is supported by a ring bearing mounted to the tribometer base to provide support and prevent bending moments on the shaft and displacement of the sample and plate. The pin sample will be mounted within a linear stage that slides along a rail gantry on roller bearing. The stage is driven directly by a linear ServoTube motor configured as shown in the inset of Figure 29 above.

### Force Application

In this design the normal force is applied using a voice coil actuator to drive the pin sample holder in the vertical direction. The voice coil actuator will be mounted on the linear stage as shown in the inset of Figure 29 and force applied will be controlled by the current through the voice coil, which determines the force exerted by the rod within the coil which is driven downward until it comes into contact with the head of the pin sample holder. A cross section view of this setup is shown in Figure 30 on page 37.

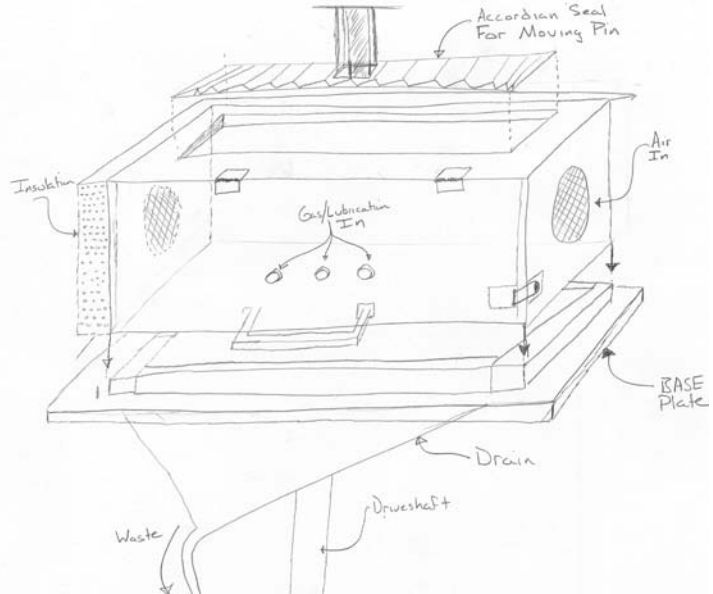
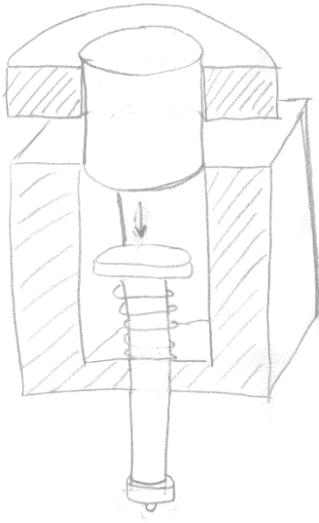


**Figure 30: Voice coil force application      Figure 31: Alpha design environmental chamber**

### **Environmental Chamber and Control**

The proposed design will implement a modular environmental chamber shown in Figure 31 above, which can be mounted to the tribometer base or removed as required. The pin sample interface will consist of a snap fitting ring that attaches to the sample holder. The ring will be located within a moving seal similar in appearance to an accordion diaphragm or pleated blinds. This seal will allow the pin to translate while still isolating the test environment. The chamber itself will be constructed of transparent material with double layer wall with an evacuated gap between them to minimize heat transfer. At the interface with the tribometer base a sealing strip similar to weather stripping will be used to minimize leaking. The front panel of the box will be hinged to allow sample loading and ports will be placed in the side walls to allow conditioned air or other gases to be circulated through the chamber. We recommend that the devices used to condition the temperature and humidity of the chamber be purchased and the interfaces of the chamber designed accordingly.

Controlling humidity to a close tolerance is extremely difficult because of its dependence upon temperature. For example, a 1°C increase in air temperature at 25°C and 55% relative humidity results in an 8% increase in relative humidity [11]. Because of this sensitive dependence of relative humidity on temperature, we expect that we will not be able to control relative humidity to our sponsor requirements of 0 – 100 ± 3% relative humidity. Currently available commercial systems such as Thunder Scientific’s 2500 model have the capability of thermal and humidity control to tolerances within our sponsor’s requirements, but not over the temperature or humidity range we have been asked to achieve. The base model from Thunder Scientific, the “Model 2500 Two Pressure Humidity Generator” costs \$35,000 [12]. The complexity needed to control both temperature and humidity over a range of 0 - 150°C and 0 – 100% humidity to within such precise tolerances is achieved only at such a great cost commercially that we don’t feel we will be able to achieve our sponsors requirements. We do believe that we can create some environmental control however, and have generated several working principles which either increase or decrease the humidity level.

## Control System

We plan to utilize LabVIEW for programming our control logic, sorting and storing measured data, and building a user interface. LabVIEW's graphic programming interface should ease the coding process. We plan to buy motors and actuators bundled with appropriate drivers and control units in order to avoid incompatibilities with the controllers and actuators. Procuring drivers and control units with the motors should alleviate the need for an FPGA system and allow us to run all of the control logic with a standard PC, but we may need to investigate intermediate solutions to the PC and LPGA, such as higher quality DAQ cards or a FPGA-based cRIO, if hardware timing becomes a problem.

## Feedback Sensors

We plan to utilize strain gauges to measure lateral. We will calculate the vertically applied force based on the value of the current applied to the voice coil actuator. Measurements of rotational motion of the disk should be provided for in the feedback system built into the servo motor we will buy. Likewise, feedback system in the linear ServoTube motor should return us information we can use to calculate the linear position of the gantry.

## Sample Holding

The proposed design will implement a pin sample holder similar to that used in the past semester's design shown in Figure 32 below. This holder uses a shaft with a threaded end and a threaded cap with a through hole smaller of a diameter slightly less than that of the pin sample. The pin is placed inside of the cap and screwed onto the shaft such that the ball is held stationary. A set of several plate or disk sample holders are being proposed due to the variety of sample geometries encountered. Figure 33 below shows the proposed ring clamps, one which applies force horizontally using set screws and a second that applies force vertically by clamping the sample between the rotating plate and a ring using bolts. Both of these holders mount to bolt holes in the rotating plate and distribute load on the samples to avoid stress concentrations. These holders will be made to accommodate the most common sample sizes tested and the interface on the tribometer's spinning plate will be designed for modularity to accommodate custom sample holders that may be required for odd sized samples.



Figure 32: Pin sample holder

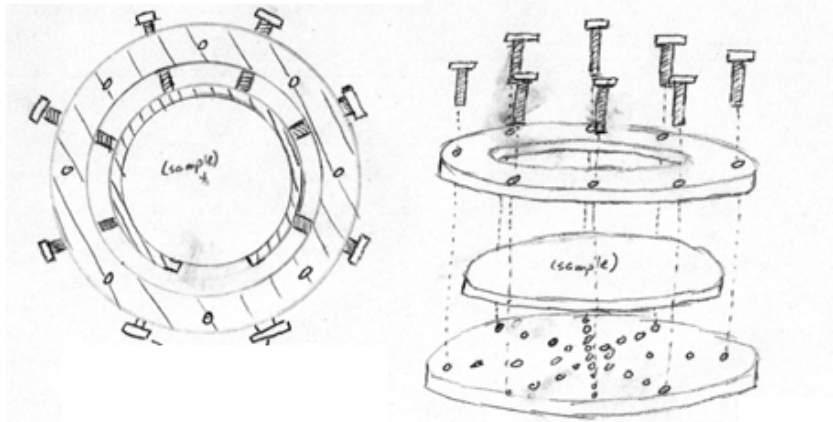


Figure 33: Plate sample holders



## **ENGINEERING ANALYSIS**

There will be many engineering fundamentals applied to analyze and optimize the parts of the proposed design in order to meet customer requirements and engineering specifications. Here we discuss the principles we expect to consider for each of our major applications.

### **Motion and Force Application**

Motion control and force application are combined because of the large similarities between the two systems. The first major engineering fundamental will be motor selection. For the two motion requirements the expected loads and maximum speeds set forth in the engineering requirements will need to be analyzed. From this the necessary torques needed to be transmitted to the rotating disk, and the forces seen by the linear motor can be evaluated. For the rotational disk, a gear train system can be used to transmit the motion from the actual motor and alter the torque as necessary. For the linear motor, no transmission device will be necessary but the forces needed to reciprocate the gantry will need to be analyzed to obtain a motor that can meet all of the engineering specifications. For the force application using a voice coil, which is essentially a smaller linear motor the same evaluation steps will need to be taken. The maximum normal forces needed, 200 N, plus some safety limit will need to be achieved by the voice coil over a long period of time.

Heating issues will need to be analyzed as well. The device is intended to run for long periods of time and motors running under these conditions will generate a large amount of heat. The amount of heat generated in each motor and the voice coil will need to be analyzed to determine if they can withstand the testing conditions. Heat sinks may need to be investigated as well to assist in cooling the devices.

### **Environmental Chamber Engineering Analysis**

Building and controlling an environmental chamber capable of controlling temperature and humidity to within 2% and 3% respectively requires thorough understanding of all engineering fundamentals at hand. This system will require very accurate modeling of the heat transfer and thermodynamic properties of the system. Because temperature will need to be controlled very accurately, we need to design a system which is very well insulated. A poorly insulated environmental chamber may limit our upper or lower end temperature ranges. Poor insulation may also result in a non-uniform temperature distribution within the test chamber due to large wall temperature differences compared to a target air temperature. Condensation may become an issue if wall temperatures are significantly lower than interior air temperatures at high humidity's. We plan to optimize our chamber by evaluating thermal properties of all materials which may be used to build the chamber and creating a chamber which resists heat flux as much as possible. By understanding the maximum heat transfer from the system in worst case scenarios (0°C and 150°C), we will be able to specify a heat pump or refrigeration system that has the power to keep our chamber at any temperature within this range.

Testing will be possible by introducing independent temperature and humidity sensors and placing them in the chamber to measure real-time environmental conditions. This will only be possible if our sponsor agrees to purchase additional temperature and humidity sensors. Data will be recorded in real time and will be monitored to see fluctuations in both temperature and humidity. If temperature and humidity remain within design specifications, we will know the chamber works correctly. Other test options include hiring a calibrations company which will test our equipment to ensure the systems accuracy. Due to humidity's sensitive dependence on temperature, we perceive that creating a well contained environmental chamber will be one of the key challenges in designing a chamber which meets our sponsor's requirements. Other important design drivers are the temperature and humidity actuators, which we plan to purchase due to the complexity a highly accurate system has.

### **Controller / Data Acquisition**

Signal communication and processing poses as major challenge to our project. In designing a control and data acquisition system, we are going to need to learn how to control how a multitude of varying

electronic devices sends and receives information. The main requirement we determined during the engineering specifications phase was that the data acquisition needs to occur at a rate of 20 kHz. This number by itself doesn't pose too great of a challenge, as the current DAQ card has the capability to collect data at this speed. Where the current system ran into problems was outputting signals back into the system. They could not output signals fast enough to control their stepper motors. Stepper motors are driven by a series of applied pulses. The previous team attempted to control the stepper motors by outputting an individual signal from LabVIEW for each pulse. The computer they were using couldn't run the control loop fast enough to output pulses at a high enough rate. Also, the output from the computer was at too low a voltage. So, we will need to find some sort of external pulse generator. In order to get the system to run fast enough, the computer should only be used to calculate the desired motor speed, which should then be sent to a driver whose sole job is to generate stepper motor pulses.

We will need to implement control schemes to determine what speed and force information needs to be sent to the motor and force actuators. To do this, we will write PID control loops in LabVIEW that will compare the user inputs to the actual system outputs. The PID will output gains that will adjust the actuators until the desired speeds and forces are achieved. This poses two additional challenges to the design. First, we will need to be able to model the dynamics of the physical system so that we can program a quality PID controller, and we will need to learn how to convert the resulting PID gains into appropriate signals that can be used by the actuator drivers.

As a matter of safety, the control system will need to have some sort of cutoff switch so that if the gantry traverses too far in one direction, the motors will be shutoff to avoid possible system damage or user injury.

### **Lateral Force Measurement**

We will need to determine appropriate sensors to measure the lateral forces generated between the samples. Our primary solution is to use strain gauges mounted to the pin. Thus, we will need to carefully select the material with which we manufacture the pin. It will need to be elastic enough that it provides a measurable deflection when testing lubricated samples under minimal load, but it will need to be inelastic enough to deflect less than 1° during an un-lubricated test at maximum load. We will also need to ensure that the strain gauges we select will have the range of deflection to measure the load at maximum load while retaining the precision to give usable measurements at minimal load.

### **Sample Holders**

Engineering fundamentals involved in the sample holding system include solid mechanics, material properties, and heat transfer. Since both the pin sample and the plate sample will be in the testing area inside the environmental chamber, material properties and heat transfer properties of the two will need to be heavily considered. Both the pin holder and the plate holder will need to withstand and be able to perform under the temperature conditions between 0 and 150 °C. It will be critical that the materials are not affected by this range. The opening of the pin holder must not open substantially such that the ball bearing falls through or begins to rotate, and it must not shrink such that the ball does not contact the plate sample. The bolts must not loosen at all, or tighten more than the sample can typically tolerate.

Solid mechanics will need to be evaluated as well. Since friction forces between the two samples may be quite large, in some foreseeable circumstances around 500 N, shear forces in both holders may become quite large as well, particularly in the bolts of the sample holder. Bending moments on the pin holder will be significant as well, especially where the pin connects to the linear reciprocating gantry. The structure of each holder must be evaluated to determine where maximum stress concentrations will be located and whether the holders, based on geometry and material properties, will be able to withstand such forces and moments to within some factor of safety.

## ENGINEERING DESIGN PARAMETER ANALYSIS

In this section we present the engineering analysis used to select components and design systems within the final prototype design. Each major subsystem is discussed and changes to the design specifications made by the sponsor are noted. The environmental chamber and universal sample holder subsystem requirements have been eliminated from this iteration of the design, however, sensors for humidity and temperature measurement and simple sample holders for proof of concept testing are included here.

### Force Application System

The final design of the force application system will utilize a worm gear and worm wheel system combined with the motor used by the previous team. This gear system will be used with a threaded bolt to apply a normal load to the pin. Gears have been selected and the system analysis is described below.

**Motor Selection and Gearing:** The motor from the previous design will be utilized for this design as well. This motor is a NEMA 17 stepper motor purchased from Keling with a holding torque of 62 oz-in, or 0.045 kg·m. The worm gear and worm wheel will be purchased from Quality Transmission Components with a gear ratio of 50:1. The worm gear will be mounted on the motor shaft using a set screw. To analyze the torque requirements the following equation 2 was used from [14]. In the equation,  $M$  is the torque on each gear,  $d$  is the pitch diameter of each gear,  $\alpha$  is the pressure angle,  $\mu$  is the coefficient of friction, and  $\gamma$  is the worm lead angle. The last term accounts for friction essentially and calculates to 4.31 when using the data provided from the gear manufacturer,  $\alpha = 20^\circ$ ,  $\mu = 0.1667$ , and  $\gamma = 3^\circ$

$$M_2 = M_1 \left( \frac{d_2}{d_1} \right) \left( \frac{\cos \alpha - \mu \tan \gamma}{\cos \alpha \tan \gamma + \mu} \right) \quad (\text{Eq. 2})$$

Using the gear pitch diameters of 40.06 mm and 14 mm for the worm wheel and worm gear, respectively, the output torque of the worm wheel is 0.557 kg·m. This torque is enough to apply the maximum 200 N load as specified in the engineering specifications. The maximum torque needed is determined using equation 3 below, where  $T$  is the torque,  $C$  is a thread coefficient of steel,  $D$  is the diameter of the bolt, and  $F$  is the maximum normal force.

$$T = CDF \quad (\text{Eq. 3})$$

The thread coefficient of steel is 0.2, and the worm wheel diameter again is 40.06 mm so the maximum torque needed is 0.160 kg·m. This gives a safety factor of 3.5 on the torque needed.

The system is also required to be able to control the amount of linear translation of the screw to 1 micron. A micron is equivalent to  $39.37 \times 10^{-6}$  inches. The bolt used has 18 threads per inch therefore for every rotation of the bolt, it will translate 0.055 inches. Since the gear ratio of the system is 50:1, one revolution of the motor will correspond to 1/50 revolution of the worm wheel and bolt. The stepper motor also operates with 200 steps per revolution. Combining these factors yields an output of  $5.5 \times 10^{-6}$  inches per step which is 7 times better than the required precision. This also means that motor would not need to be microstepped.

### Linear Reciprocating Motion System

This section discusses the design and selection of the power transmission mechanism, gantry, and motor used to drive the pin sample. In order to select these components we determined the expected loading during operation. Based upon the 200 N maximum normal load and a conservative estimated maximum

coefficient of friction of 1.5, based upon observed values for metal-on-metal contact, we have established a maximum expected loading of 300 N along the axis of translation. These requirements, in addition to the 254 mm stroke length and required maximum speed of 1 m/s can be met using a linear motor direct drive, a ball screw system. We also consider a belt drive with relaxed load and positioning precision requirements as a low cost option for proof-of-concept testing.

**Alpha design - Linear servomotor:** In accordance with our proposed alpha design, we investigated several linear motor options and found that while they provided precise positioning with a repeatability of 12 microns, the axial load for our application was at the upper limit of linear motor capability. Preliminary quotes from Nippon Pulse and Copley Controls indicated prices on the order of \$8,000 which made this option prohibitively expensive.

**Final design - Ball screw:** We have determined that a ball screw transmission can meet all engineering specifications at a significantly reduced cost from the linear servomotor system. It affords precise positioning with a repeatability of 25 microns and can achieve the required speeds and loads. We performed an analysis of the motor speed ( $\omega$ ) and torque ( $T$ ) required to meet our linear speed ( $v$ ) and axial load ( $F$ ) with different screw configurations using Equation 4, below. Using manufacturer’s data provided by Nook Industries provided in Appendix G.2, regarding the torque required to keep a 1 kN load in motion ( $T_{1000}$ ) for screws of varying geometry and material, we related driving motor torque in Nm to axial load in N,  $T_{1000}$  in kN, and the screw lead in mm and efficiency ( $e$ ) using Equation 5. We have established that a 25 mm lead precision alloy steel ball screw, which has  $T_{1000}$  of 2.235 kN,  $e$  of 0.9, and dynamic load rating of 10 kN, would provide the optimal performance by minimizing our motor torque and speed requirements. With this system we would require a driving torque of 2.96 Nm at a motor speed of 2400 rpm to achieve a speed of 1 m/s.

$$v = \omega l \quad \text{Eq. 4}$$

$$T = \frac{FlT_{1000}}{1000 * 2\pi e} \quad \text{Eq. 5}$$

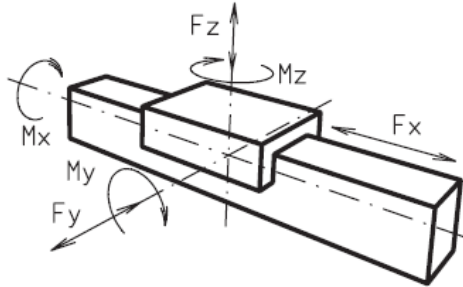
**In house construction:** We have investigated the option of manufacturing and assembling the ball screw drive, linear stage and gantry in house, as well as the option of purchasing a prefabricated ball screw driven linear actuator. The parts and estimated cost to fabricate the screw drive ourselves are listed in Table 8, below along with the estimated cost of the gantry and stage, the designs of which are addressed in a later section. For the loads and speeds required two singular radial bearing mounts will be required to support the screw ends. These are rated for a load of 1800 lbs (8 kN). A motor mount will also be needed to interface with the motor. The listed price is quoted by Nook Industries for a mount customized to any motor.

**Table 8:** Cost of in house ball screw actuator

<b>Part</b>	<b>Cost</b>
Ball screw: 25 mm lead x 25 mm diameter , steel	\$71
Ball nut: 25mm x 25 mm	\$384
End blocks: 25mm bore (x2)	\$1428
Gantry:	\$198
Linear stage:	\$50
Motor mount:	\$350
<b>Total</b>	<b>\$2481</b>

**Prefabricated actuator:** In order to select a prefabricated linear actuator capable of withstanding the expected loading, we calculated the expected bending moments that would be carried by the actuator guide rails and stage bearings in both the case of a linear reciprocating test and a rotational test. The

resulting maximum bending moments and forces are given in Figure 34 below and illustrated in the accompanying diagram. These were calculated assuming that the maximum 300 N lateral loading was applied to the tip of a 5 in. pin offset from the center of the linear stage by 2 in. Using coordinate system of Figure 34, the point of force application would be at coordinates (0, 5, 2), in inches, since the working orientation would be rotated 90 degrees about the x-axis from that shown. The maximum  $F_x$ ,  $M_y$ , and  $M_z$  will occur during the linear test and the maximum  $F_z$  and  $M_x$  during the rotational test. We have identified the Nook Industries ELK60 linear actuator with 25 mm lead screw option as a suitable system and secured a quote for the device of \$2,900.00 plus an additional \$350.00 for a custom motor mount.



<u>Maximum Loading</u>			
$F_x$	300 N	$M_x$	40 Nm
$F_y$	200 N	$M_y$	20 Nm
$F_z$	300 N	$M_z$	40 Nm

**Figure 34:** Linear actuator load diagram and maximum values

**Final design – DC servo motor:** We have determined that a DC servo motor will provide the best performance for the ball screw linear motion system. It provides superior speed control at a lower cost compared to AC motors and allows us to take full advantage of the positioning precision of the ball screw. We investigated the possibility of using the existing DC stepper motor with the standard 1.8 degree step size and found it was not able to meet our speed and torque requirements and would reduce the ball screw’s resolution since each step would translate to linear movement in increments of 125  $\mu\text{m}$ . Microstepping could improve this, but would reduce the maximum motor speed below that required. The stepper motor would also reduce the smoothness of motion at low velocities. Using the motor speed and torque requirements of 2400 rpm and 2.9 Nm (410 oz-in) determined previously, we have selected an Anaheim Automation BLZ482S-160V-3500 model dc servo motor with MDC15-120151 driver. The manufacturer’s torque-speed curve is shown below in Figure 35 and indicates that it meets the specifications for this system. The curve also shows that the maximum current required for our application is 10 A. The cost of the motor is \$550 and the driver \$296.

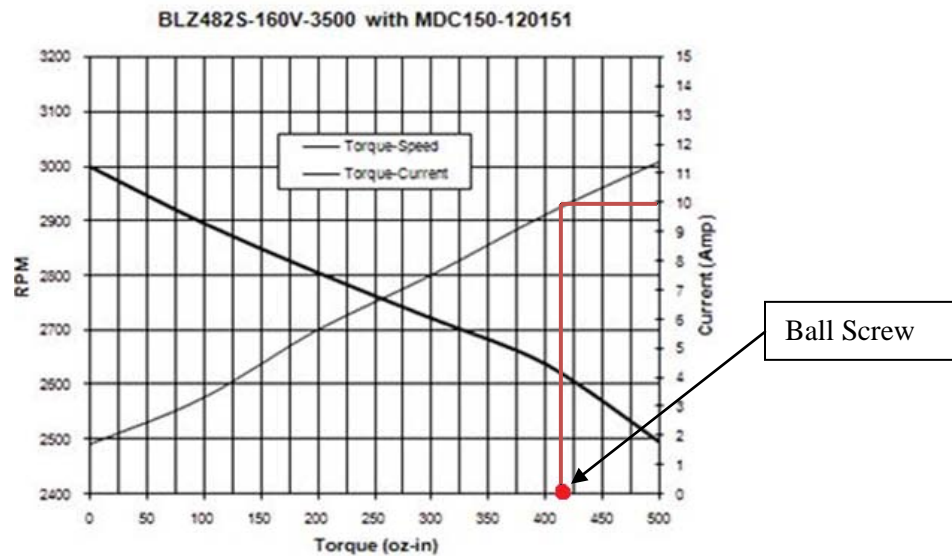


**Figure 35:** Linear motion DC servo motor torque-speed curve

**Prototype design - Belt drive:** Due to the expense of the final design's ball screw system and limited funding, our sponsor has requested that a proof-of-concept prototype be designed to modify the belt drive from the previous team's design and allow the device to be updated as funds become available. The existing design uses a Gates PowerGrip GT2 series timing belt with a pitch of 5 mm and a width of 25 mm and Gates GT2 5 mm pitch pulleys with a pitch diameter ( $d_p$ ) of 2.757". Using Equation 6, below, and the expected 300 N load (F) we have determined the belt's maximum torque load to be 10 Nm, which is within the capability quoted by the manufacturer of the existing belt system. The current belt drive is also rated for speeds of up to 8 m/s, which is sufficient for our design.

$$T_L = 0.5d_pP \quad (\text{Eq. 6})$$

$$\omega = 2/d_p \quad (\text{Eq. 7})$$

In order to keep the cost of upgrades minimal, the motor selected for the ball screw system will be used for the prototype as well. With this configuration, a motor speed of 735 rpm is required to achieve a 1 m/s test speed as calculated using Equation 7, above. At this speed the selected motor can provide 4.1 Nm of torque which is sufficient to carry a friction load of 125 N indicating that for materials with friction coefficients greater than 0.6, the full normal load range cannot be supported. Furthermore, the belt drive reduces the positioning precision of the tribometer to approximately 0.2 mm if the belt is properly tensioned. We have determined the optimal tension to be 58-64 lbs of tension using a program provided the manufacturer. This worksheet and results may be found in Appendix G1 and the tensioning system is described in the following section. This transmission option will be used in combination with a linear stage and gantry.

**Belt Tensioner:** The belt used to translate the linear stage must be tightened to a predetermined load. Because of this, we have designed a belt tensioning system which can be adjusted to preload the belt to a specific tension. Based on software from Gates, the belt manufacturer, we will require between 58 and 64 pounds to get the correct power transmission it was designed for. We have decided to use the same belt and pulley system previously implemented by last year's team to reduce cost as it fulfills the requirements for speed and power transmission we need. We will modify last year's team's design by adding bolts which allow for variable tension in the belt. The belt tension system we have designed can be seen in Figure 36 below.

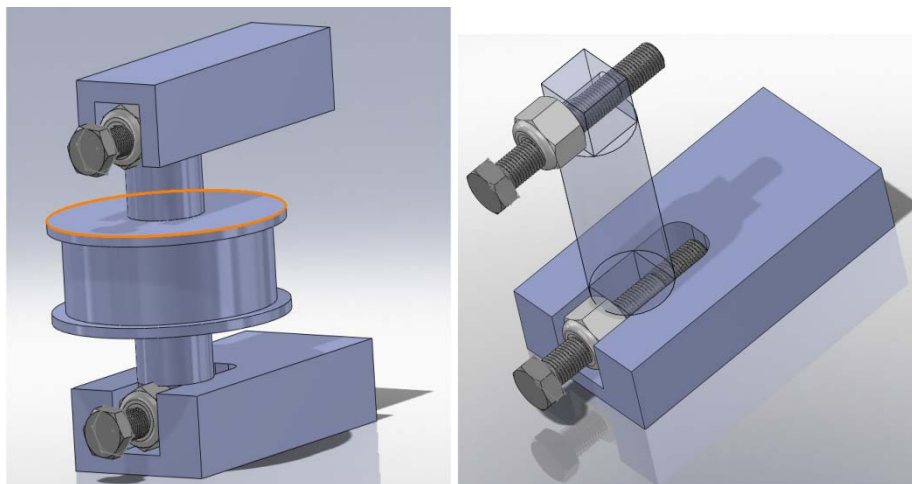


**Figure 36:** Belt Tensioning System with 2 Bolts for Applying Specific Tension to Belt

The tensioning system is implemented on the idler pulley of the linear system. Two screws, on either the top or bottom of the idler pulley, are screwed into the shaft which holds the pulley in place. As the bolts

are tightened, the pulley wheel is forced farther from the drive pulley, adding tension to the belt. A self-locking nut is placed on each bolt to prevent loosening of either bolt during testing.

To achieve a given tension in the belt, Equation 8 below can be used to determine the torque input required by the user. In Equation 8, *Torque* is the input torque required from the user,  $F_{belt}$  is the tension in the belt and  $D_{bolt}$  is the major diameter of the bolt shaft. This relationship is based on the assumption that regular series nuts and bolts with rolled threads are used, acting on surfaces without lubrication. To ensure the belt is tightened to a tension of 58 – 64 lbs, the user should apply a torque of 4.35 – 4.8 in-lbs to each bolt. This torque should be applied to each bolt by use of a torque wrench. Careful consideration should be employed when tightening each bolt; the user should alternate which bolt he/she is tightening every half-turn to avoid jamming the system.

$$Torque = .2F_{belt} D_{bolt} \qquad \text{Eq. 8}$$

**Linear Motor Drive Shaft:** One of the problems we identified in the previous team’s design was in the system that transmitted power to the linear stage belt from the motor. In their system, the drive pulley was mounted directly to the motor drive shaft (Fig. 37). This will cause off the forces in the belt drive to apply a moment to the drive shaft. This moment would have to be supported the internal bearing of the motor. This would drastically reduce the usable life of the motor, so we will have to redesign the system.

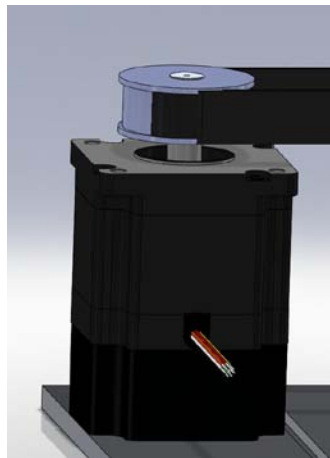


**Figure 37:** Previous team’s design for transferring motor power to the belt

**Prototype design: Linear gantry and stage:** We have designed a new gantry system for the prototype’s belt driven linear motion system that will constrain the pin sample motion. It consists of a solid aluminum carriage into which the previously discussed force application system is mounted. The timing belt clamps onto the side of the stage, and drives it along 5/8” diameter steel guide rails on a set of four linear bearings which are built into the stage body. These parts are summarized in Table 9 below

**Table 9:** Summary of guide rail and bearing selection

Component	Part Number	Inner Diameter	Outer Diameter	Price	Quantity
Linear Bearing	6489K51	0.625”	1.125”	\$24.78	4
Shaft	6253K57	-	0.625”	\$34.11	2

We analyzed this system to determine if it could handle the loads that will be seen during testing. To account for a wide range of materials a maximum friction force of 300N was assumed at the tip of the pin.

This produces bending moments on the guide rails and linear bearings that must be accounted for. The diagram that was used is pictured below in Figure 38. Based on our calculations, the maximum moment seen by the rails and bearings is 95 lbs if the bearings are perfectly aligned and the forces are assumed to be at the center. If the bearings are misaligned slightly however, the forces may be concentrated at the inner edge of the bearing which would cause the highest forces. This loading condition results in 189 lbs of force. Nonetheless, the linear bearings are rated for 620 lbs of dynamic load which gives a safety factor of at least 3.2.

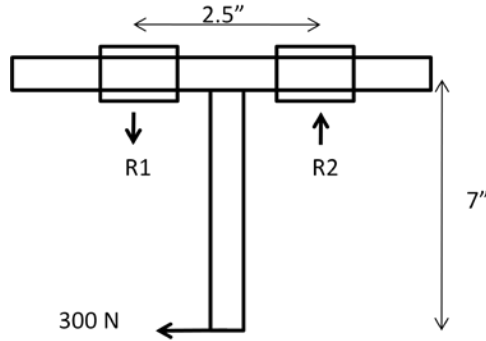


**Figure 38:** Moment diagram used for bearing loading calculations

The shafts will be mounted on the chassis and will run through the linear bearings – two bearings for each shaft. The bearings will be mounted in the stage which will linearly constrain the motion of the stage. This will ensure all motion provided by the motor and belt system will move the pin in a linear fashion. To attach the shafts to the chassis, they will be mounted in the chassis and secured using shaft collars on both ends. These collars will be secured using screws which will hold the shafts in place during testing.

### Rotational Motion System

The rotational motion system selected for our final design and prototype are the same. It makes use of the existing rotating plate driven by spur gears with modifications to the bearings and a more powerful motor. This section discusses the analysis performed to select the gears, support bearings, and motor required to meet the design specifications on load and speed while making use of the existing structural frame.

**Gear selection:** In order to confirm that the gears selected by the previous team can be successfully implemented in our redesign, we have performed an analysis of the gears' ability to withstand the expected loads and operating conditions. Given a maximum testing radius ( $r$ ) of 114 mm, or 4.5", a maximum force ( $F$ ) due to friction of 300 N and a maximum linear speed requirement ( $v$ ) of 1 m/s, the maximum torque and rotational speed on the follower gear ( $T_f, \omega_f$ ) and pinion ( $T_p, \omega_p$ ) were calculated using Equations 9-11 given below, where ( $k$ ) is the gear ratio of 3:1.

$$T_f = Fr \quad (\text{Eq. 9}) \quad \omega_f = 30v/\pi r \quad [\text{RPM}] \quad (\text{Eq. 10})$$

$$k = T_p/T_f = \omega_f/\omega_p \quad (\text{Eq. 11}) \quad \sigma = 6F_t L/bt^2 \quad (\text{Eq. 12})$$

$$F_t = \frac{44 T}{7\pi d_p} \quad [\text{lbf}] \quad (\text{Eq. 13})$$



Using the manufacturer’s specifications for the geometry and properties of the existing steel gears and Equation 12, above, we calculated the maximum bending moment induced in the gear teeth based upon the Lewis Equation [13]. The tangential force on the gear tooth ( $F_t$ ) is given by Equation 13 where  $T$  and  $d_p$  are in units of lb-in and in, respectively. The results of these analyses and the significant specifications used are listed below in Table 10 and indicate that the existing gears are sufficient for our design.

**Table 10:** Steel gear specifications, torque, speed and tooth stress at maximum load

		Gear ratio (k): 3:1		Follower		Pinion	
Gear Properties	Pressure angle	( $\phi$ )	20	deg.	20	deg.	
	Diametral pitch	(P)	16		16		
	Pitch circle diameter	( $d_p$ )	5"		1.5"		
	Tooth thickness	(b)	0.75"		0.75"		
	Tooth height	(L)	0.135"		0.135"		
	Tooth root width	(t)	0.135"		0.135"		
	Yield stress	(S)	50	ksi	50	ksi	
Results	Torque	(T)	34.3	Nm	11.4	Nm	
	Speed	( $\omega$ )	84	rpm	250	rpm	
	Tooth stress	( $\sigma$ )	8	ksi	9	ksi	

**Rotational motor selection:** In order to meet the speed and load specifications a motor capable of outputting 11.4 Nm torque at 250 rpm (1620 oz-in at 4.2 rps) is required. Evaluation of the existing motor’s torque speed curve shown in Appendix G.4, indicated that it was not suitable for our design. We have investigated DC servo and DC stepper type motors. Given the lower cost of stepper motors and the current plan to run the rotating plate in a single direction during testing such that sudden reversal of direction will does not pose the potential for step skipping in a stepper motor, we have selected a model 42Y112S-LW8 DC stepper motor manufactured by Anaheim Automation with MLA10641 driver, which is capable of meeting our torque-speed requirements as shown in Figure 39. This figure also indicates a maximum power requirement for the motor of 320 W. The cost of this system is \$252 for the motor and \$495 for the driver.

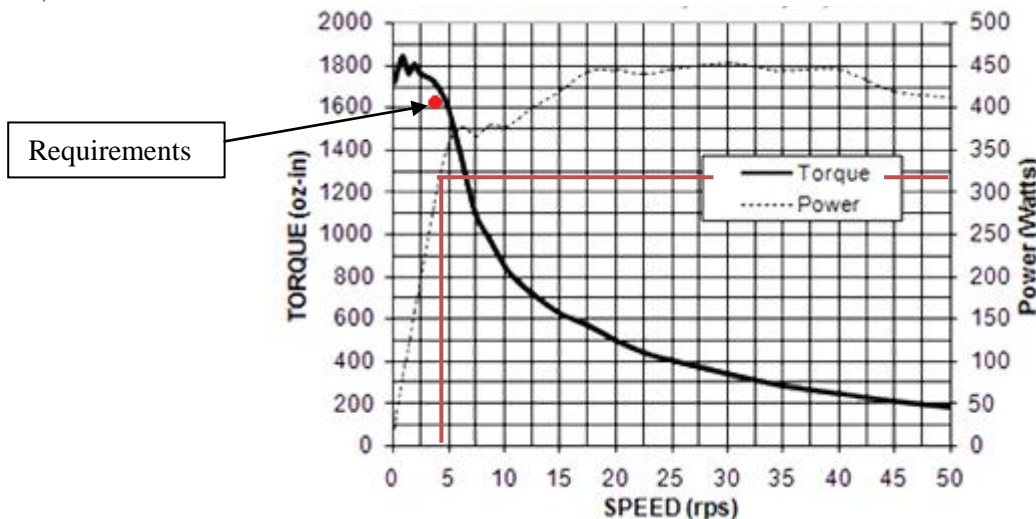


**Figure 39:** Rotational system DC stepper motor torque-speed curve

## Chassis

We plan to reuse some of last semester's chassis components. They chose aluminum 6061 for all chassis components. Aluminum 6061 was chosen for the entire chassis sub system for several reasons. Aluminum 6061 is relatively cheap, is readily available in a wide variety of shapes and sizes, is easily machineable and is strong and stiff enough for our applications. We agree with the previous team's reasoning and have agreed to make all new chassis components out of aluminum 6061 as well. The CES analysis used for this selection can be found in Appendix C along with the previous team's analysis. We do not expect this material selection to have a large environmental impact either due to the small production size of this product of about 100. A detailed environmental analysis is also in Appendix C.

## Pin Material Selection and Geometry Analysis

Before we could determine the specific parameters of the pin shaft, we had to first select what material it would be made out of. The material selection process was driven by the environmental conditions the shaft will be required to perform under as well as the specification that the pin cannot deflect more than  $1^\circ$  from vertical during any test. The deflection will be greatest when a test is performed with the highest normal force applied, 300N, and a coefficient of friction of 1.5. Due to the high temperatures seen by the shaft only metals were analyzed as possible options.

The engineering material selection program CES [27] was used to select various materials that could be used in our application. Steel was the first metal that was analyzed due to its high availability, high strength, and machinability. However, the shaft will be exposed to a relative humidity of up to 100% and steel is not corrosion resistant, so it was eliminated. Stainless steel was evaluated next because it is a corrosion resistant alloy of steel. Various alloys and grades of stainless steel were analyzed and Stainless Steel 303 was initially selected for the pin shaft. Upon further inspection, it was realized that only cold drawn 303 would be able to withstand the stresses seen at the highest loads. This variant was not readily available to purchase so additional alloys were identified as alternatives. However, the stainless steels that were available to purchase and strong enough to withstand the stresses in our application were either very difficult or impossible to machine. Threading, cutting, and drilling holes in the pin shaft would require special carbide bits and would be a highly tedious task. The difficulties of machining these stainless steels led us to search for other possibilities. Bronze was investigated, and eventually a high-strength bronze alloy that is corrosion resistant and easily machineable was selected. This alloy is known as Bronze 544. The material selection process for the shaft is described in detail in Appendix C. This material will also have minimum environmental impact due to the low number of products but it will have more of an impact than the Chassis due to the resources it uses and the fact that it will need to be replaced more often. A detailed environmental analysis is also in Appendix C

After we selected Bronze 544 we could determine the geometry of the pin shaft. The geometry was driven by the conditions that the shaft cannot deflect more than  $1^\circ$  from vertical and that the shaft should never yield due to stresses induced by the normal and frictional forces applied at the tip. A rod of circular cross-section was chosen over a rectangular or square cross-section to eliminate stress concentrations that would be present in the corners of the beam. A rod of circular cross-section will also be easier to thread at one end in order to attach the ball mount. Initial analysis of the shaft led us to change the design of the pin gantry system in DR2. Instead of having the spring at the bottom near the ball, we moved the spring to the top, closer to the motor. This eliminated the need of having a long hollow shaft to hold the spring and the threaded rod, which allows us to use a solid rod. The new design also greatly decreases the length of the threaded rod. We feel that this new design is much more robust because it involves fewer parts with more

simple geometries. These simpler geometries can be more accurately modeled using beam bending equations to predict what the resultant stresses and displacements of the shaft will be.

The deflection of the shaft was analyzed first. A safety factor of two was placed on the deflection because we cannot assume that the pin will be completely perpendicular to the disk to begin with. The shaft was then modeled as a cantilevered beam with a uniform diameter. To ensure the pin will never deflect more than 1° from normal, we modeled the worst case loading scenario ( $\mu=1.5$ ,  $F_B=300\text{N}$ ). The following equation was used to determine a minimum shaft diameter needed to ensure bending never exceeds 1° from perpendicularity. A safety factor of 2 was used in maximum allowable deflection (.5°). In eq. 14,  $F_B$  is the frictional force acting perpendicular to the pin shaft,  $L$  is the exposed length of the pin,  $E$  is the modulus of elasticity for Bronze 544 (15 MPsi) and  $r$  is the shaft radius.

$$\theta = \frac{2F_B L^2}{E(\pi r^4)} \quad (\text{Eq. 14})$$

Using the planned exposed length of pin of 3'' and maximum bending force of 300 N, we can determine that the minimum shaft radius necessary to prevent over-deflection (with a safety factor of 2) is .4. To ensure we could find a linear bearing capable of holding our pin secured, we decided to use a .5 inch diameter pin. When 0.25 in. is plugged into Equation 14 for  $r$ , and 3 in. is used for  $L$ , a deflection of .2° is observed. This results in a safety factor of 5 against deflecting more than 1° from vertical which will be sufficient to compensate for preliminary alignment errors. Because bronze becomes less stiff as temperature increases, we also analyzed the deflection at the maximum temperature of 150°C. At this temperature the Young's modulus for Bronze 544 is 14.4 MPsi, and the deflection increases slightly to .21°. Therefore, we are confident that the shaft will not deflect more than 1°, even at the most extreme temperature. Using these dimensions, the maximum stress from the normal force (Equation 15 where  $\sigma_N$  is the stress due to the normal force,  $F_N$ ) and the maximum bending stress (Equation 16 where  $\sigma_B$  is the bending stress due to the frictional force,  $F_B$  and  $r$  is the radius of the shaft) from the lateral friction force, can be determined. The maximum stress that will be seen by the pin is 15 Kpsi. This gives a safety factor of 3 versus the yield stress of bronze 544 (60 Kpsi).

$$\sigma_N = \frac{F_N}{\pi r^2} \quad (\text{Eq. 15})$$

$$\sigma_B = \frac{F_B L}{r} \quad (\text{Eq. 16})$$

The chassis that holds all of the Pin Gantry System parts and interfaces with the Linear Motion Control system will be made out of Aluminum 6061. Aluminum was selected because it is a strong, lightweight material that is easily machinable. Initial fabrication plans and methods for all machined parts are discussed in Appendix I1 and I2.

## Sensors and Feedback System

**Controls System:** To design a controls system, we first had to gain some experience in interfacing with motors and their associated drivers and power supplies. To do this, we obtained data sheets and wiring diagrams for the previous team's motors and drivers, and we enlisted the assistance of ME 450 Systems Engineer John Baker to teach us how to generate the signals needed for motor control. One of the first things we learned was that in order to run closed loop control logic and generate output signals fast enough to control motors, we need to control the system in "real time". He advised us that running the controller code on a computer's processor and then sending the output signals through a DAQ card (which was the previous team's solution) does not allow real time control. To achieve real time control, we need to compile our control code to an external processor.

**Data Acquisition:** The system must contain a way to interpret and store force data collected during experimentation. This requires that the system be able to convert the voltages received from the strain

gauges into units of strain, and then into units of force. This data needs to be stored in a format that can be exported to data analysis programs (MATLAB, for example), so our design must contain a system for storing the information on a PC. Additionally, vertical force measurement signals must be relayed to both the PC for storage and the controls processor for use in a closed loop feedback system.

## Sample Holding

Our system needs to be able to constrain the test samples. Machining the test samples themselves is not an option, so the samples must be constrained through a clamping mechanism. The parameters affecting our clamp design are:

- Must provide enough constraint to eliminate any slipping
- Must distribute constraint forces to avoid stress concentrations on the samples
- Must not interfere with the path of contact between the samples during the test
- Must be able to accommodate the sample sizes required by our sponsor
- Must be able to accommodate non standard or awkward sample shapes (disk sample)

## FINAL DESIGN DESCRIPTION

In this section we present a detailed description of the final recommended tribometer design, assembly details, and how the systems achieve the required performance. A full bill of materials with component names, vendors, part numbers, and quoted prices is provided in Appendix J along with additional dimensioned drawings of individual parts Appendix H.

### Normal Force Application System

The normal force application system will utilize a worm gear and worm wheel system (as engineered in the previous section) that will drive a threaded bolt down to apply the force to the pin. The current motor from the previous design will be used to drive the worm gear. As the motor rotates, the worm spins, mating with the worm wheel. The worm wheel is fixed from translating horizontally and vertically using a radial bearing and a thrust bearing. The inside of the worm wheel will be threaded and a bolt will thread through the gear. To prevent the bolt from rotating with the worm wheel, a hex socket will be secured on the bolt head. This will constrain the bolt to vertical motion only. On the tip of the bolt, a cap will be used to create a large flat surface to transmit the force. Beneath that, a rubber insert will be used to add elasticity to the system to account for small variations in alignment and surface roughness. This rubber insert will thread into the top of the pin. The pin will then pass through a linear bearing mounted to the linear stage. This will align the pin vertically, allow for smooth vertical translation, and absorb moments created by the frictional forces. A cross sectional view of the system is shown in Figure 40 and detailed descriptions and analyses of each component follow.

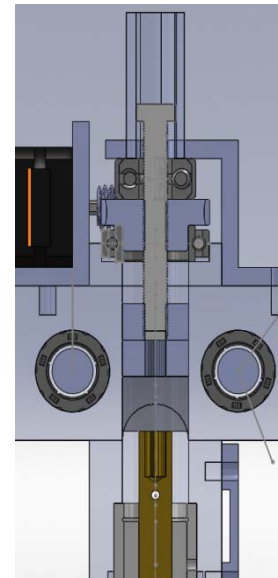


**Figure 40:** Cross sectional view of the normal force application system

### **Gear Constraint**

To keep the worm wheel from translating in the horizontal and vertical directions, a radial bearing and a thrust bearing will be used, respectively. For the radial bearing, the worm wheel will be press fit into the inner race of the bearing to ensure concentricity. The outer race of the bearing will be press fit into an aluminum casing in the linear stage. The thrust bearing will be placed on top of the worm wheel and will be secured using a Z-clamp that will be bolted to the linear stage. The bolt will go through the bore of the bearing, however the bore diameter is larger than the bolt diameter. This is to ensure free rotation of the bottom race with the worm wheel. To keep the upper race in place and to maintain concentricity, a cylindrical, hollow insert will be placed in the gap between the race and the bolt. The bearings will be ordered from McMaster-Carr and have part numbers 6455K88 (\$5.55) and 60715K11 (\$14.84).

### **Bolt Application**

A 3/8" diameter bolt with 18 threads per inch will be used to apply the normal force. It will be 3" long to ensure that there will always be room for the bolt to translate up or down as needed depending on load and sample height. The bolt will pass through the thrust bearing, thread through the worm wheel, and pass through the radial bearing. A cap will be secured to the tip of the bolt to create a larger surface area for the force application. To ensure that the bolt does not rotate with the worm wheel, a hex socket will be welded to the Z-clamp and fit over the head of the bolt. This component will be purchased to the size of the bolt head to minimize slop between the hex and the bolt. The socket will also hide the moving bolt from the users serving as a safety feature.

### **Elasticity**

To account for small changes in surface roughness on the samples and slight misalignment, we have decided to add rubber inserts between the pin and the normal force applicator. This will dampen the effects of any bumps on the sample surface and will reduce the stress on the system if only metal contacts were used. This will also absorb some of the additional forces produced which will make controlling the applicator motor much easier as well. The rubber stoppers will be purchased from Advanced Antivibration Components in New Hyde Park, New York. Since a wide range of normal forces must be applied, three different rubber inserts were selected that could handle the entire range. Before testing, the correct rubber insert must be selected for the best results. For selection of the three inserts, models were selected that would meet a portion of the force requirements while also considering the geometrical dimensions of the insert. It was important to select inserts that would be compatible with other parts of the system. Performance curves in the form of load vs. deflection were analyzed to ensure adequate performance under testing conditions. The three rubber inserts are summarized in the table below.

**Table 11:** Summary of rubber insert properties

Load	Part Number	OD (in.)	Height (in.)	Thread
0-10 N	V10Z 2-307A	0.750	0.375	1/4" - 20
10-90N	V10Z60MM3U2552	0.625	0.625	1/4" - 20
90-200N	V10Z 2-305B	1.000	0.53125	1/4" - 20



The strain in the rubber needed to be considered as well since it will be under compression during the entire test. The manufacturer accounts for this by indenting the side of the rubber face allowing for expansion during compression that does not extend past the outer diameter specification under the maximum loads. This will allow us to use the outer diameter specifications in our design of the rest of the normal force application and pin/gantry system. Strains under the compressive forces range from 0-12% of the nominal length for each rubber insert.

The selected rubber inserts have male threaded ends on each side of the rubber making attachment easy in this application. One end will be threaded directly into the pin while the other end will have a cap to increase surface area for the normal force application.

Spring systems were analyzed as well because they could have similar effects and would also allow for additional force measurement since the spring displacement and spring constant would be known. Springs, however would be less rigid than the rubber stoppers and the benefits can be achieved in other features of the design. Springs of different sizes and stiffness would complicate the design and would not allow for maximum performance for all testing loads. Securing the spring would be challenging as well. It would be difficult to hold the spring in place and constrain the loads to only in the axial direction to prevent buckling.

### **Pin Constraint**

The pin must be kept vertical and must be kept from rotating during testing. To keep the pin from rotating during testing shoulder bolts will be used. There are slots machined into the linear stage for these shoulder bolts and holes are tapped into the pin for connection. This system was used by the previous team so the pin holes are already machined. To keep the pin vertical, a linear bearing will be used that will be mounted to the underside of the linear stage and housed inside the linear stage. Moment calculations were done on the linear bearing to determine if the pin would be able to slide through the bearing. The maximum concentrated forces seen on the bearing assuming a maximum friction force of 300N is 202 lbs. This is well within the rated load of 1950 lbs.

### **Wear Depth Measurement**

To measure the wear of the ball and disk, the number of motor steps will be recorded and will keep track of how far the motor has rotated. As the ball wears, the normal force between the pin and disk will decrease. In order to maintain the force, the motor will turn the screw to keep the damper compressed a fixed amount. By measuring how much the motor rotates, we can find the vertical distance the screw has travelled which will equal the amount of wear that has occurred.

## **Linear Motion System**

Linear reciprocating motion of the pin sample relative to the plate sample will be achieved using prefabricated ball screw driven linear actuator consisting of a linear stage on guide rails and a 25 mm lead steel ball screw and nut assembly. This gantry system will be purchased prefabricated from Nook Industries. The optimal model for this application is the Nook ELK 60 with 25 mm lead screw shown in Figure 41, below. The manufacturer's specifications for this model can be found in Appendix G3. A custom built motor mount will also be required to interface with the Anaheim Automation BLZ482S-160V-3500 model DC servo motor selected to drive the screw. This mount will be manufactured by Nook Industries upon submission of motor CAD diagrams. The quoted price for the transmission system is \$2900 for the actuator and \$350 for the motor mount. The servo motor will cost \$550 plus \$296 for the accompanying MDC15-120151 driver for a total system cost of \$4096.

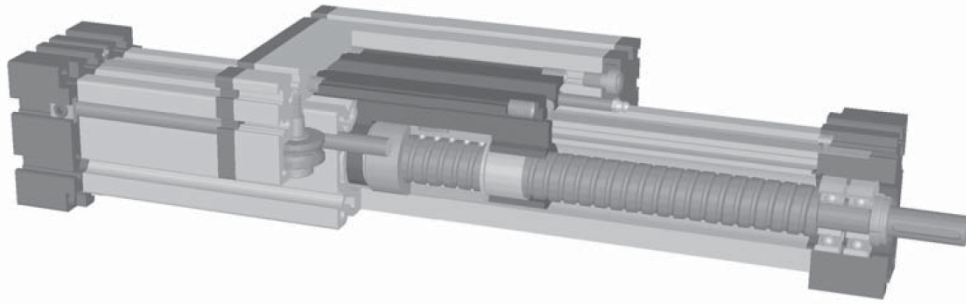


**Figure 41:** Nook Industries NLK60 ball screw driven linear actuator – cross section view

The actuator will be mounted into the aluminum sidewalls of the tribometer chassis and oriented on its side, rotated 90 degrees about the axis of translation. The end mounts will be secured to the sidewalls using t-bolts matched to the prefabricated mounting T-slots and bolt holes on the actuator. The previously described force application system will then be mounted to face of the linear stage using T-bolts. Finally the DC servo motor will be coupled to the ball screw using the motor mount and secured to the tribometer chassis's base plate using bolts.

This linear motion system will provide sufficient torque to perform ASTM standard linear reciprocating tests as well as 2D path tests with normal loads of up to 200 N on materials with kinematic coefficients of friction as large as 1.5 and can withstand the moments induced on the actuator for all test configurations under these loading conditions. Due to the low friction in the ball screw assembly and the use of a dc servo motor, smooth translation will be possible throughout the target speed range of 1 cm/s to 1 m/s. Positioning precision of 25  $\mu\text{m}$  will be attainable with proper motor control, as discussed in the following Controls and Feedback section. This means that for a 300 mm stroke length, after a full cycle, the pin can be returned to the same position within 25  $\mu\text{m}$ , which will allow for 2D paths to be reliably retraced.

We have recommended the prefabricated option be taken over in house fabrication, which would provide savings of \$770, due to the need for precise positioning, which we feel we would be unable to guarantee with our limited machining experience. Furthermore, the transition from prototype to final design would be significantly easier for a third party to implement in the case that a single module needs to be traded, as opposed to requiring the design and fabrication with an internal ball screw nut. Such design would require that the stage be either a multiple piece part, which has the potential to reduce performance due to loosening of fasteners or misalignment and mismatch, or it would need made from a polymer m, molded around the nut, which would be far more expensive than the prefabricated part due to tooling expenses.

### **Rotational Motion System**

Rotational motion of the plate sample relative to the pin sample will be achieved using a rotating disk. The disk itself will be reused from the previous design iteration and is constructed of 6061-T4 aluminum which provides sufficient stiffness at a minimal weight and cost for this application. Motion of the disk relative to the base plate of the tribometer chassis will be facilitated by a set of three miniature ball transfer units mounted to the base plate at 120 degree intervals and a radius of 5.27" from the center of the disk as shown in Figure 42, below and the dimensioned drawings in Appendix H. These units will support the disk in the vertical direction and prevent precession of the disk during tests due to moments caused by loading in the normal direction, which will be necessary in order to maintain constant normal loading and repeatable test results. The disk will be constrained from lateral motion by two deep-groove ball

bearings spaced on a shaft which is press fit into the follower gear mounted to the rotating plate as shown in Figure 42. These bearings will prevent the frictional load on the plate from inducing bending or translation. This bearing configuration was chosen to replace the previous team’s turntable bearing as that bearing was not rated for the loads and speeds encountered during testing. Slew and large diameter ring bearings were also considered but proved excessively expensive; \$600 compared to the \$142 for this system.

The follower gear mounted to the underside of the aluminum plate will be driven by a pinion gear mounted to the shaft of the Anaheim Automation 42Y112S-LW8 model stepper motor using a key shaft. This system provides a 3:1 gear ratio in order to reduce the driving torque required to a level achievable with a stepper motor. With the \$252 the motor, the total cost of the rotational system is \$404.

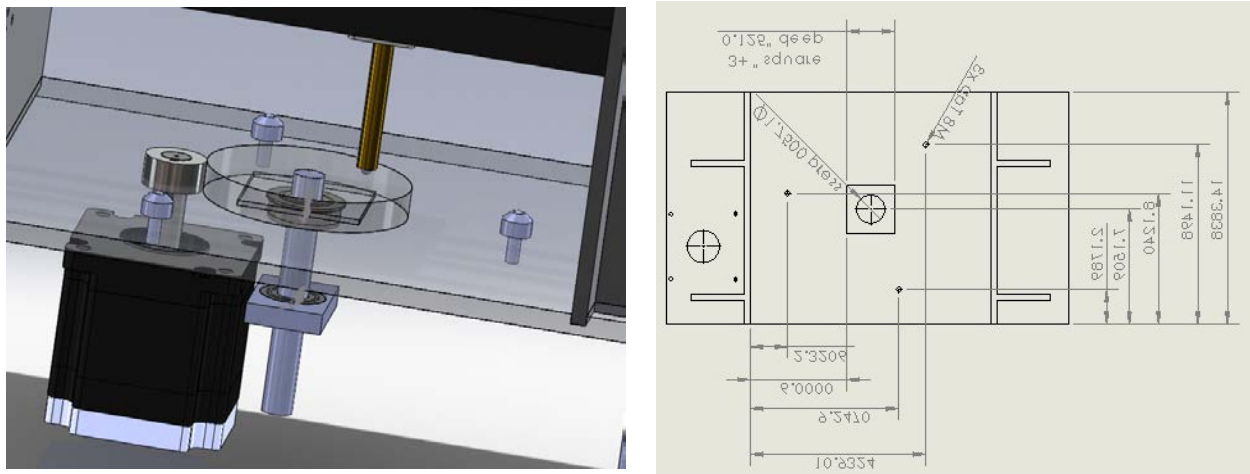


**Figure 42:** Motor, gears, and bearings for rotational motion system and dimensioned sketch

The rotational system will be assembled as follows. The ball transfer unit will be screwed into M8 threaded holes in the base plate and the flanged upper ball bearing will be press fit into the base plate. The second ball bearing will be press fit into an aluminum block which will then be attached to the base plate by bolts running through the base plate, test stand, and aluminum bearing block. The follower gear will be bolted to the aluminum disk and a steel drive shaft will press fit into it. The shaft will then be inserted through the two ball bearings and the assembly lowered onto the ball transfer units taking care to properly mesh the follower gear with the pinion which protrudes through the base plate from the motor shaft. The motor itself will be mounted to the underside of the base plate using bolts.

This rotational system allows ASTM standard pin-on-disk tests at a maximum radius of 4.5” as well as 2D path tests with normal loads of up to 200 N on materials with kinematic coefficients of friction as large as 1.5. It has been designed to achieve speeds of 1 m/s under these loading conditions while withstanding the applied load without bending or rotation out of plane. At low speeds there may be some roughness due to the discrete steps of the stepper motor and additional micro stepping will be employed if necessary as determined by testing once fabrication is completed.

## Chassis Design



The chassis assembly will consist of a wood base table from IKEA for stability, an aluminum base plate mounted to the table, four triangular brackets for stability and alignment, and two side walls that will hold the guide rails and linear stage. A CAD model of this setup is shown below in Figure 43. The aluminum base plate will be secured to the top of the wood table using 3 bolts. Rubber spacers will be used between the two surfaces to maintain a level surface and to allow room for bolt heads on the underside of the base plate. The four triangular brackets will be pressed into their corresponding slots and bolted to the base plate. It is critical that these brackets be perpendicular to the base plate before continuing with the assembly of the side walls. The first side wall will then slide into the slot in the base plate, while also sliding along the face of the triangular brackets. Once in place the side wall will be bolted to the brackets. This will constrain all motion of the side wall except for in the vertical direction. The other side wall will be mounted similarly, however the slots and bolt holes in the side wall will be slightly larger to allow for alignment. The linear stage and guide rails will first be secured into the first mounted side wall. The second side wall will then be slid into place. The guide rails will then be inserted through the corresponding holes in the second side wall. With the additional space machined out in the slots, the second wall will be slid perpendicular to the rails and triangular brackets while a team member simultaneously slides the gantry back and forth. Adjustments will be made until there is smooth motion of the gantry with no little friction. The second side wall will then be secured in place with bolts to the triangular bracket.



**Figure 43:** Tribometer chassis and stand

This design and alignment strategy will allow us to achieve smooth, precise linear motion that our requirements specify. It will also ensure that the guide rails and rotating disk are a constant distance from each other within the tolerances of the purchased and pre-manufactured components. The triangular brackets will also add stability to the design to maintain this alignment during testing under high speeds and high forces. The wood table will stabilize the entire device to minimize vibration of the system during testing which would affect the results during a test.

### **Force Measurement**

The purpose of this section is to outline in detail how normal and lateral forces exerted on the pin shaft will be measured. Strain will be measured at 4 locations around the pin perimeter using a total of 8 strain

gauges. Strain gages measure strain through changes in resistance of a metal wire attached to the surface of a specimen. As the specimen is extended or compressed, the metal wire either stretches or compresses. This increase/ decrease in wire length increases/ decreases the wires resistance. By knowing the location of the strain gages and the material and geometrical properties of the shaft itself, the loads applied to the shaft can be determined by measuring these changes in resistance.

**Strain Gage Pin Orientation:** To measure the normal force and the frictional force, 8 strain gauges will be placed on the shaft. These strain gauges will be placed in pairs in a “T” configuration at four locations on the outside of the shaft as seen in figure 44 below. Each strain gauge set will be  $90^\circ$  apart from each other and as far up the shaft as possible (approximately .5- 1 inch from the linear bearing support depending on sample size). This will allow the gauges to see the maximum possible strain experienced in the pin increasing the precision of our measurements. The 8 strain gauges will be arranged according to figure 43. Each pad contains two gauges set perpendicular to each other.

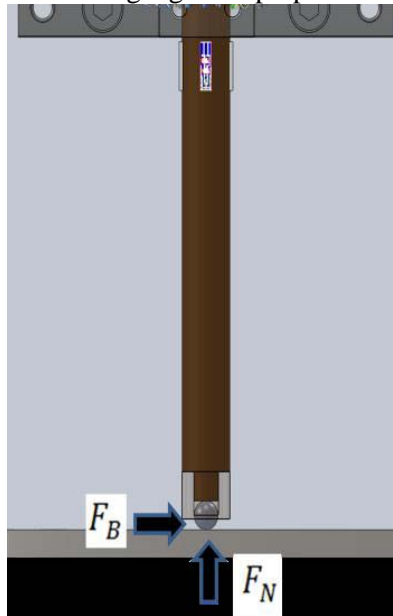
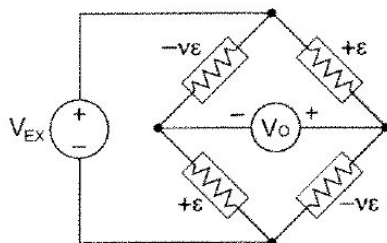


**Figure 44:** Strain gauge location on pin will measure normal and lateral forces

4 of the strain gauges will be arranged in a full Wheatstone bridge and the 2 gauge sets will be arranged on the pin  $180^\circ$  from each other. The remaining 2 sets will be arranged in 2 separate half Wheatstone bridges, also  $180^\circ$  from each other. The combination of all four sets allows for equally accurate measurement of forces in all directions. The full Wheatstone and half Wheatstone bridges can be seen in figure 45 below. For a full bridge configuration, all four resistors in the Wheatstone bridge are active strain gauges and are arranged in pairs. For each pair, one gauge measures strain in the axial direction, while the other measures poisson's strain ( $-\nu\epsilon$ ). The half Wheatstone strain gages that are  $180^\circ$  from each other will be used to measure both the normal force and the component of the frictional force along the axis of which these gauges are aligned (see eq. 17 – 22). The remaining full Wheatstone strain gages will be used to measure the remaining component of the frictional force. By configuring the remaining 2 sets in a full Wheatstone bridge, the sensitivity of the output voltage is doubled, increasing our measurement precision and accuracy.



58

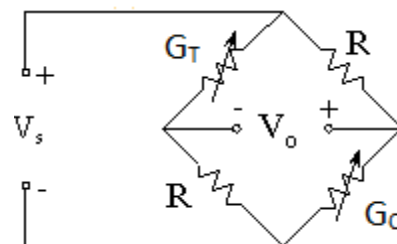


**Figure 45:** Full- Bridge (left) and Half- Bridge (right) strain gauge configurations

Each strain gage pair in the half bridge will be in a tee rosette configuration in which strain gages are placed perpendicular to one another so that one is strained axially and the other is strained in the opposite sign in the Poisson direction.

Equations 17 - 22 show how the strain readings of the two half bridges that are 180° from each other can be used to determine the normal force and lateral force exerted on the shaft. The forces and strain gages referred to in these equations are depicted in Figure 45. Equations 17 and 18 show that the strain measured is the sum of the strain from the normal force compression and the bending strain from the lateral force. The strain from the normal force is equal on all strain gages in both sign and magnitude. The strain from the lateral force, however, is equal in magnitude and opposite in sign because this force will put one side of the shaft into tension and the other into compression. Because of this, equations 21 and 22 below can be used to determine the normal force and frictional force.

$$\varepsilon_1 = \varepsilon_N + \varepsilon_B \quad \text{Eq. 17}$$

$$\varepsilon_2 = \varepsilon_N - \varepsilon_B \quad \text{Eq. 18}$$

Using equations 19 and 20 below, the strains measured above can be used to calculate the overall axial and bending strains.

$$\frac{\varepsilon_1 + \varepsilon_2}{2} = \varepsilon_N \quad \text{Eq. 19}$$

$$\frac{\varepsilon_1 - \varepsilon_2}{2} = \varepsilon_B \quad \text{Eq. 20}$$

These strains can then be used to determine the normal force (Equation 21) and the lateral force along the line of the two strain gages being read (Equation 22).

$$F_N = \frac{E \varepsilon_N \pi D^2}{4} \quad \text{Eq. 21}$$

$$F_B = \frac{E \varepsilon_B \pi R^3}{4L} \quad \text{Eq. 22}$$

Because forces may act on the pin from any direction in a complex 2D path test, two more sets of gauges are required to detect strains acting off axis from the two half bridge gauges previously mentioned. The remaining two gauges will be mounted 90° from either of the half bridge gauges, and will be wired in a full bridge to increase measurement resolution. We will be able to use the strain measurement from these gauges to determine lateral forces in this direction by subtracting the strain from axial loads found in eq. 21 above. Once the lateral forces along two axes are determined, the magnitude of the lateral force can be determined using Equation 23 below.

$$|F_F| = \sqrt{F_{B_x}^2 + F_{B_y}^2} \quad \text{Eq. 23}$$

Using the equations above, and plugging in the largest and smallest forces that will be seen according to the specifications, the minimum ( $1.49 \times 10^{-6}$ ) and maximum ( $8.96 \times 10^{-4}$ ) strain expected to be seen can

be determined. Based on these strain ranges, and our required force measurement accuracy, we have chosen a suitable strain gauge which meets our sponsors requirements.

**Strain Gage Selection:** Typical strain gages are only accurate to 1 micro-strain. This strain resolution will not meet our customer’s specifications. Micron Instruments makes semi-conductor strain gages that can, “Perform like a foil gage except that the resistive change is 30 to 55 times greater.” When this was discussed with their application engineer, he stated that their backed semiconductor strain gage half-bridge can easily read  $1/10 \mu\text{strain}$ , and with accurate calibration it is possible to read  $.004 \mu\text{strain}$ . This gage, shown in Figure 46, is already configured in a half-bridge. The two gauges are placed perpendicular to each other such that one gauge reads axial strain and the other reads strain induced from the Poisson effect. Figure 46 also shows a silicone covering over the strain gages in green. This covering will help to eliminate damage from contact to the strain gages. It will also stop condensation and oils due to handling from changing the resistance of the strain gages. This gage will be used to measure the strain on the four locations mentioned previously on the pin.

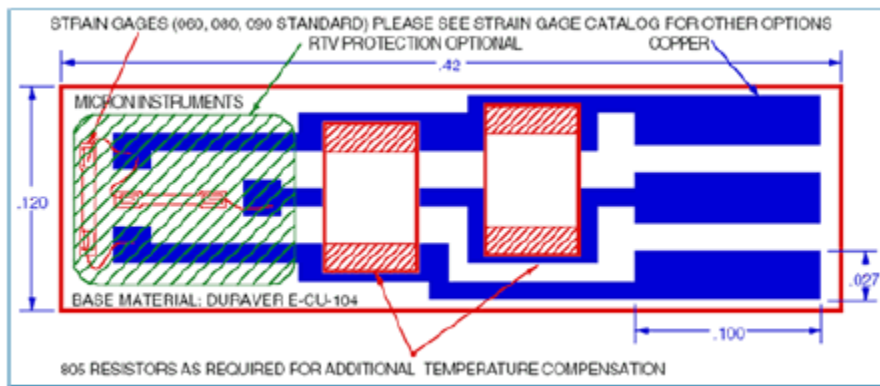


**Figure 46:** Micron Instrument SSGH Half-Bridge Gage [19]

If these gages only read  $1/10$  micro-strain accurately, we expect to be able to read up to  $.08 \text{ N}$  of lateral force accurately. If the gages read  $.004 \mu\text{strain}$  accurately, they will read up to  $.003 \text{ N}$  of lateral force accurately. This would meet the specified low range measurement of  $.01 \text{ N}$  of lateral force. In the conversation with their application engineer he also said that the calibration needed to read  $1/100$  micro-strain accurately is difficult and reading such a small strain may be impossible because at that level the wind from the shaft moving may cause the gauges to show strain.

He also stated that these gauges are not recommended for long term readings as they will see creep over time. To alleviate this issue, Micron Instruments has the capability to professionally mount strain gauges which do not have creep tendencies. We have looked into this option, but because the lead time required to get our pin professionally mounted is too long, we will use the backed strain gauges as a much cheaper proof of concept. If we can validate that these strain gauges do indeed work as they say, we will recommend that our sponsor send our pin to Micron Instruments to get the gauges professionally mounted by their staff. Herb Chelner, Micron’s President, has provided us a quote for this service and details regarding the mounting can be found in Appendix F. To professionally mount one pin with 4 gauges, our sponsor can expect to pay approximately \$650.

**Analog to Digital Conversion:** The next step in this process is to insure that the output voltage measurement can be read and stored by our data collection hardware. This will require that the device can correctly convert the analog voltage signal to a digital signal. The range of the voltage signals expected from the half bridge and full bridge configurations can be determined using Equations 24 and 25, respectively. In this equation the gage factor ( $GF$ , the change of a gage’s resistance per unit strain) is

determined by equation 26. This equation compensates for the fact that the gage in the Poisson direction will only see part of the strain that the gage in the axial direction will see.

$$V_{0 \text{ half bridge}} = \frac{V_s GF \epsilon}{2} \quad \text{Eq. 24}$$

$$V_{0 \text{ full bridge}} = -GF \epsilon V_s \quad \text{Eq. 25}$$

$$GF = \frac{GF_0(1+\nu)}{2} \quad \text{Eq. 26}$$

From the specifications given by Micron Instruments for the strain gage, the gage factor was determined to be 97.5. If we use the recommend excitation voltage of 5V and a minimum and maximum strain of 1.5  $\mu$ strain and 1.22 X 10<sup>-3</sup> respectively, we can determine that the range of the output voltage will be 3.65 X 10<sup>-4</sup> to .608 V. This low range voltage is well below the A/D converters lower converting range of 37.5 mV. For this reason, we will need to incorporate an inverting amplifier with a constant gain to amplify the signal so that the low end voltage will be high enough that it will be read by the A/D converter. The schematic of this circuit is shown in Figure 47 below. The voltage that will be read after gain can be calculated using Equation 27 below.

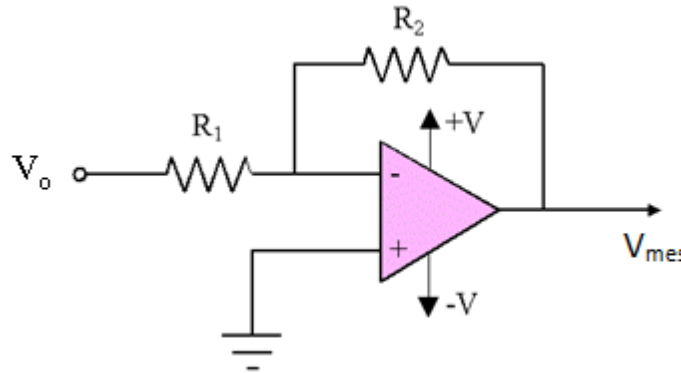


**Figure 47:** Strain Gauge Output ( $V_0$ ) Amplification Circuit with Fixed Gain.

$$V_{mes} = \frac{-R_2}{R_1} V_0 \quad \text{Eq. 27}$$

It is important to note that the A/D converter we plan to use will only read up to 20V. Because of this restriction, the team will also have to create a way to change the gain of the amplifier. To create a low cost system, the supply voltage will be 5V, the same as the excitation voltage for the gages. By changing out the resistors, different gains can be achieved. By having many different resistors whose gain is well understood, the voltage measured can always be near 5 volts. By always getting close to this voltage, the measurement will be converted from analog to digital more accurately.

**Pin manufacturing:** Because we will be using a previously designed pin with incorrectly mounted strain gauges, we must first carefully remove the damaged strain gauges and clean the epoxy off of our pin. Once this is done, the strain gauges will be bonded onto the shaft using a high temperature bond that will ensure that the strain gauges will work over the specified temperature range. The procedure that will be used is outlined by documents provided by Vishay Micro-Measurements and will be done under the supervision of Todd Webber, who has experience mounting strain gauges. The procedure that will be used can be found in Appendix F. Because last year's team had difficulty mounting these gauges, we plan to discuss in detail with Todd Webber the mounting procedure, and will be present during this operation to

minimize mistakes. The operational amplifier needed to boost the output signal from the strain gauges was previously made and we plan to use this amplifier. Last year's team also made use of a 15 pin VGA connector to easily disconnect the pin from the tribometer system. We also will use their VGA connector so that the pin is easily removable from the tribometer system.

The wires that will be attached to the strain gages will be soldered using solder that will not melt at the 150°C that the shaft may experience in operation. These wires will also be stressed relieved with tie wraps that will not melt at this temperature.

Both of the processes required for completing this system involve the risk of burning skin. This could be done with a solder iron needed to apply the solder to complete circuits or on the shaft when the bond is cured in an oven. During both of these activities special care will be taken to insure that injury is avoided. When soldering, we will be sure to always be aware of the solder iron.

**Cost Analysis:** A breakdown of the cost for the entire force measurement subsystem can be found in Table 12 below. By using several previously purchased components from last year's team, we plan to spend ~\$100 for the cost of two additional Micron Instruments strain gauges. We will be able to reuse last year's team's assembled operational amplifier, 15 pin VGA D-Sub connectors (male and female) and DC adapter. The power supply to the operational amplifier and strain gauges (5 V) will be supplied from previously purchased power supplies used in our control board.

**Table 12: Cost Breakdown of Force Measurement System**

Part	Supplier	Part #	Quantity	Cost/ Part	Total
Backed Half Bridge Strain Gauge	Micron Instrument	SS-080-050-1000PB-SSGH	2	46.49	92.98
				<b>Total</b>	92.98

**Data Acquisition and Control System**

The controller that we have selected for use in our project is the Arduino Mega (Figure 48). The other option real time control option is an FPGA as described in the Concept Generation section of this report. Most FPGA's are expensive (between \$1700 and \$3000), and require knowledge of Verilog to implement, which made them a very undesirable option. An Arduino board is more desirable in the scope of this system. Like an FPGA, it has its own processor, which can operate independently of a PC, allowing real time control. The computing power of this processor is significantly less than an FPGA, which provides a significant price saving (an Arduino Mega costs \$64).



**Figure 48:** Arduino Mega control processor

The main drawback to the Arduino board in comparison to an FPGA is that the Arduino board does not have the ability to communicate signals to a PC for storage. We will need to use a separate DAQ card to collect experimental data and sort it for storage on a PC. The DAQ that we have chosen is a National Instruments USB 6009 (Figure 49). The USB 6009 is a simple, low cost device (\$280), and at a sampling rate of 48 kHz, it exceeds the sponsor's requirements. The data will be collected and stored via a LabVIEW program running on a common PC.



**Figure 49:** NI USB 6009 data acquisition PC card

## Sample Holding

We have developed fixtures for securing both ball and plate/disk type samples for testing of a range of sizes and shapes.

**Ball sample:** To constrain the ball sample in the pin, we plan to reuse the previous team's solution, which is to create a cup with interior threads which can be screwed on to the end of the pin (Fig. 50).

After examining the existing system, we found that this method works well, and it is same method we found on most of the commercial pin-on-disk tribometers. Three of these threaded cups will be needed to accommodate the various sample sizes specified by our sponsor.

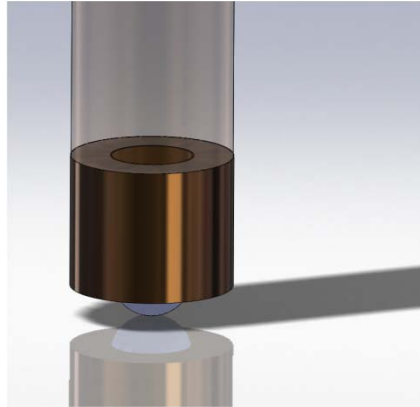


**Figure 50:** Design for ball sample holder

**Plate sample:** We designed two clamping systems to constrain the plate/disk sample, both of which can be used on the plate manufactured by the previous team. The first is a set of two crescent-shaped clamps (Fig. 51). These are designed to accommodate large circular samples. The crescents span a large arc length with the purpose of distributing the constraining force over a large area. A crescent shape was chosen to avoid interference with the pin during rotational tests. Two rows of holes are to be drilled into clamps to allow them to be mounted at different locations on the disk corresponding to disk samples of different diameters.

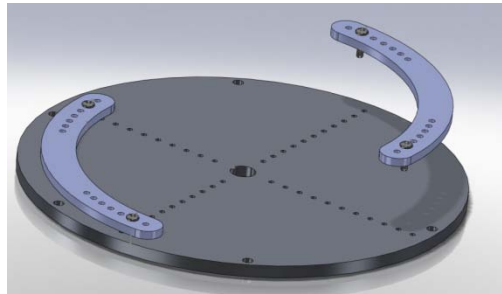


**Figure 51:** Disk constraining system based on crescent-shaped clamps

However, there are two drawbacks to the crescent clamps. First, they cannot accommodate small samples. At a small enough radius, the crescent clamps will interfere with each other. Second, they may not be effective at constraining certain awkwardly shaped samples, as they were designed specifically to constrain large circular samples. Because of these drawbacks, we designed a second clamping system specifically to constrain small and/or awkwardly shaped samples. This system is a set of four fork-shaped clamps (Fig. 52). By using a system of four small clamps instead of two big ones, the clamps can be placed closer together, which allows the system to accommodate smaller sample sizes. Each clamp bolts to only one row on the plate, as opposed to the crescent solution, which bolted across two rows. This allows for greater flexibility in clamp placement, which in turn allows for greater flexibility in sample shapes that can be accommodated.



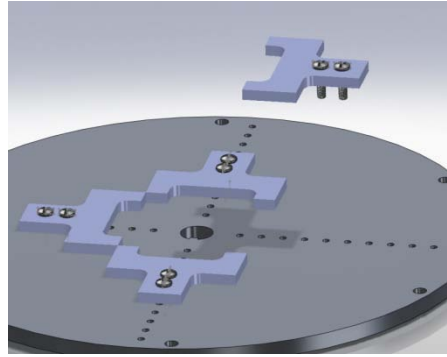


**Figure 52:** Disk constraining system based on fork-shaped clamps

## Environmental Control

Based on the scope of our project and strict time requirements, we have agreed with our sponsor that a full environmental system is beyond the abilities of our group for this semester. Although we will not be creating an environmental system, our final design has the ability to incorporate an environmental system in the future. We have designed components which would be exposed to harsh temperature and humidity conditions such that they will function correctly in any expected environment.



**Figure 53** Temperature and Humidity Sensor (Omega RH-USB)

Although we do not plan to design/ manufacture a full environmental system, our design will have the capability to measure both temperature and humidity. We plan to implement a humidity/ temperature probe which will mount to one of our side walls, and will plug directly into the lab computer via a USB interface. The sensor (Omega RH-USB) will be capable of measuring temperature in the range of  $-40$  to  $49 \pm 1^\circ\text{C}$  and humidity in the range of  $2 - 98 \pm 3\%$ . Initially our sponsor requested that temperature and humidity be measured from  $0-150 \pm .5^\circ\text{C}$  and  $0 - 100 \pm 1\%$  respectively, however because sensors which meet these specifications cost upwards of \$1,600 and we will only be measuring atmospheric conditions, we have decided to use the Omega RH-USB as a temporary solution. The cost of the Omega RH-USB is \$145 and can be seen in Figure 53 above.

## PROTOTYPE DESIGN EXPLANATION

Due to restricted funding it has been requested that our team produce a one-off version of the proposed tribometer design for proof-of-concept testing. It incorporates a less expensive linear motion system

which reuses the previous design's timing belt and can be easily updated to the ball screw system due to the modular nature of the design. We have added of a belt tensioning system and flexible motor coupling to improve performance as well. Additionally, due to time constraints and budget, we have opted to mount the strain gauges in house for the prototype and recommend having this done professionally for the final product to achieve the necessary force resolution. All other systems will be identical to those of the final design as detailed in the previous Final Design Description section. Additional dimensioned drawings and CAD renderings of the prototype can be found in Appendix H.

## Linear Motion System

The prototype linear motion system will consist of the previous design's Gates PowerGrip GT2 series timing belt with a pitch of 5 mm and a width of 25 mm and Gates GT2 5 mm pitch pulleys with pitch diameters of 2.757". The drive pulley is driven by the same Anaheim Automation BLZ482S-160V-3500 model DC servo motor with MDC15-120151 driver as selected for the final design. The drive pulley is mounted on a separate shaft that is coupled to the motor shaft through a flexible connector that prevents the bending moment induced on the pulley shaft due to tension in the belt from being transmitted to the motor, which could severely reduce motor life. We have also designed a system for applying tension to the timing belt by adjusting the position of the idler pulley shaft using threaded bolts.

This prototype linear motion system will be capable of operating at the full range of test velocities from 1 cm/s to 1 m/s so long as proper tension is maintained on the belt. It cannot, however, achieve the specified positioning precision or operate under the full range of normal loads. The precision is limited to 0.2 mm and for a kinetic coefficient of friction of 1.5 only 120 N of normal force can be applied at full speed. This should be sufficient, however to show that this tribometer design implementing a translating gantry with a rotating plate is capable of performing the ASTM standard tests and able to repeatably produce closed 2D paths.

**Flexible motor coupling:** As described in the parameter analysis, we needed to redesign the system through which motion is transferred to the belt from the motor. In order to eliminate large moments from being applied to the internal bearings of the motor, we separated the drive pulley shaft from the motor shaft with a flexible coupling (Fig. 53). The flexible coupling consists of two independent hubs. One hub is to be rigidly fixed to each of the two sides of the separated shafts. In between the two hubs is a rubber spider gear. The torque from the motor is transmitted to the drive shaft through this spider gear. There is no rigid connection between either of the hubs or the spider gear, which means that the flexible coupling cannot support bending moments, and the internal bearing of the motor will be protected desired. Also, because the spider gear is made of a flexible rubber, it allows for a small amount of misalignment between the two shafts, which will aid in manufacturing.

By using a flexible coupling, we eliminated the need for the motor to support bending moments. However, in doing so we also removed the support for the drive pulley. To support the pulley, we designed a simple system that uses radial bearing above and below the drive pulley to secure it to the chassis (Fig. 54). The bearing provides a fixed axis about which the drive shaft can spin, and they support the horizontal loads imposed on the pulley by the drive belt.

The shaft we chose to use for the drive pulley is a 3/4" outer diameter steel shaft with a keyway. We chose these dimensions because they will allow us to reuse the previous team's drive pulley. We are able to do this even though the new motor will have a different shaft diameter because we can choose flexible coupling hubs to have different inner diameters. In this way, we can step down the shaft diameter without any complicated machining.

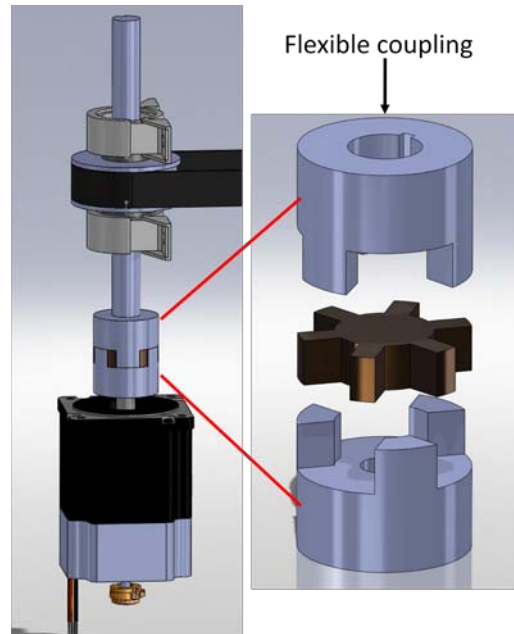


**Figure 54:** Redesign of linear stage drive shaft with flexible coupling

**Belt tensioner:** The drive pulley of the belt drive will be mounted on a drive shaft that passes through pillow block ball bearing mounted to the outer sidewall of the chassis directly above and below the pulley. The lower end of the shaft will secure into the upper end of the flexible motor coupling, while the motor shaft is secured to the opposite end of the coupling. The motor itself will be mounted to the base plate of the chassis using bolts. The idler pulley is mounted on the stationary shaft of the belt tensioner, which is in turn bolted to the outside wall of the chassis wall opposite the drive pulley. Once the belt is mounted on the pulleys, tension is applied by rotating the bolts of the tensioner to draw the idler shaft away from the drive shaft until the desired 58-64 lbs is reached. This device is shown in Figure 55 below.

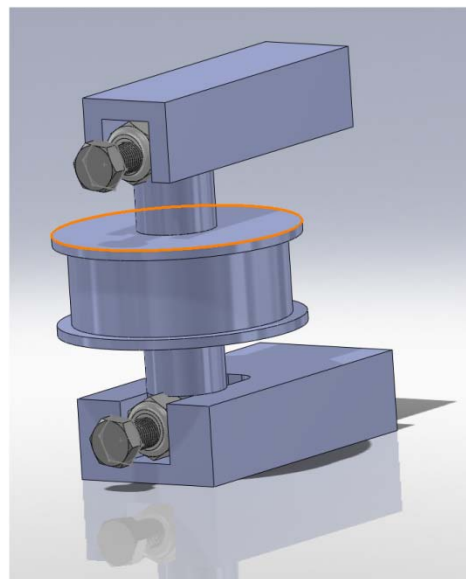


**Figure 55:** Belt tensioning device

## **INITIAL FABRICATION PLAN**

Production of the prototype will involve the manufacturing of a number of aluminum pieces, including the linear stage, chassis sidewalls, motor mounts, shaft mounts and various spacers. Alterations will also be made to the chassis base to employ the updated rotational motion bearing system. These pieces will be fabricated using CNC milling in the case of the base plate and linear stage due to the complexity of the shapes required and the need to produce high tolerance holes for press fitting of bearings, which cannot be achieved by drilling and reaming due to the size of the hole diameters exceeding that of the available tooling. End milling on a manual mill will be employed for the motor and shaft mounts as well as the rectangular spacers. Holes will be drilled on the mill and reamed to tolerance where necessary. Milling has been selected for these processes due to its economy for low production runs. Several circular aluminum spacers and a steel drive shaft will be drilled and cut to length using a manual lathe and a steel drive shaft will be cut to length using a band saw. Water-jet cutting will also be employed to fabricate the plate sample holders due to their thin, re-entrant geometries and curved features, which would be difficult to achieve using a mill. All parts will be subsequently deburred and sharp edges removed and a number of holes will be threaded using a hand tap. Detailed manufacturing plans indicating the step-by-step process, machines and tools used, and relevant speeds and feed rates can be found in Appendix I1.

Assembly will occur as parts become available due to varying lead times on purchased parts. The chassis walls and base will be manufactured first in order to allow for the motion systems to be mounted and motors secured. The force application system will be assembled separately and mounted on the gantry rails once complete. Special consideration will be given to the alignment of the chassis walls in order to attain parallel orientation of the gantry rails features have been included in the base plate and walls to a proper placement relative one another and the base plate to ensure that the axis of translation runs through the center of the rotating disk. Once one wall is in place, the gantry rails secured, and the linear stage mounted on the rails, the second wall will be put in place and its position adjusted, while sliding the stage along the rails, until the position that minimizes resistance to the motion, indicating optimal alignment, is found. A similar process will be followed for the alignment of bearings along the pulley drive shaft and rotational disk shaft. For the pulley shaft the lower bearing block will be mounted to the chassis wall and the shaft inserted. The upper bearing block will then be adjusted and secured once such that the shaft spins freely. The same procedure will be followed for the rotating disk shaft with the lower bearing being adjusted. The final assembly steps will be to attach and tension the timing belt, mount gauges and sensors, and wire the circuitry for the DAQ and motor controls. Detailed step-by-step assembly plans can be found in Appendix I2 along with a full bill of materials in Appendix J and dimensioned drawings of individual parts to be manufactured in house in Appendix H.

## **VALIDATION TESTS AND RESULTS**

Due to limitations in time and difficulties encountered with the processing unit of our prototype we were unable to perform full validation testing. In this section we provide the results of the tests that were completed as well as descriptions of the planned tests, which we recommend be carried out once the processor issues are resolved.

### **Force Measurement Validation and Verification**

Force measurement was validated to ensure the designed system met our sponsor's requirements. The normal and frictional force measurement system is comprised of 8 strain gauges mounted on the bronze pin sample in varying arrangements. Four gauges were mounted 90° from each other around the pin and

wired in two half bridge configurations to measure bending in any direction. From measured bending strains, friction force and ultimately a coefficient of friction can be determined. The remaining four gauges were mounted in one full bridge configuration to measure axial strain and ultimately normal force applied to the test sample. This force is required for the closed loop normal force application system as well as for test purposes.

Two types of tests were run to validate our measurement system. First, bending was measured by applying a known load to the tip of the pin via hanging milk jugs. Known masses of water were added to the jugs and then they were hung from the pin tip and strains were measured. From equations derived in the Force Measurement section of Parameter Analysis, we were able to determine a measured force and compare this force to the actual known load. Figure 56 below shows the results from bending tests.

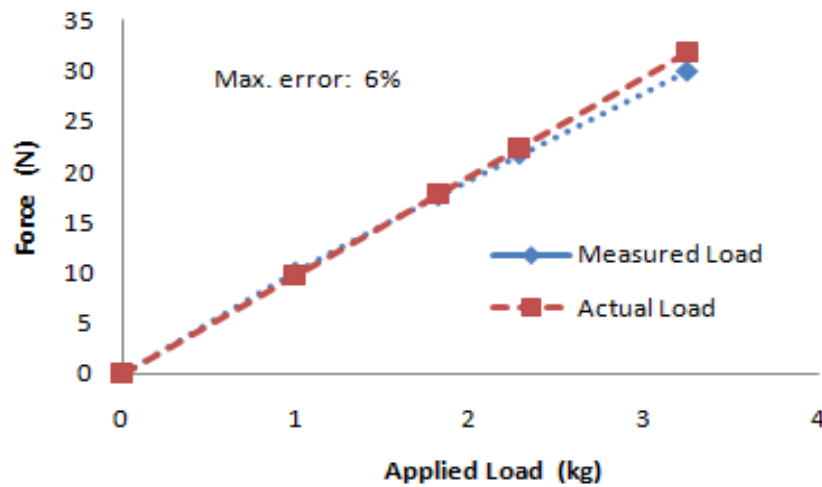


**Figure 56:** Measured load from bending test is accurate to within 6% of actual applied load

Varying loads were applied and data was taken for 5 seconds at 500 samples per second. Voltages were averaged and a corresponding load was calculated. Each test load was removed from the pin and reapplied twice to mitigate any initial force application differences. To account for creep seen in the strain gauges, initial offset voltage for the unstrained pin was recorded to increase measurement accuracy. Because the pin will experience friction forces in all directions, the pin was rotated in 20° increments and tested again to ensure accuracy in all directions. From these tests, a calibration curve was generated to directly convert a measured strained voltage to a friction force. The calibration curves for bending strains are shown in Figure 57 below. The forces determined from these curves are for on axis bending only. Equation 23 from the Parameter Analysis section must be used to calculate off axis bending.

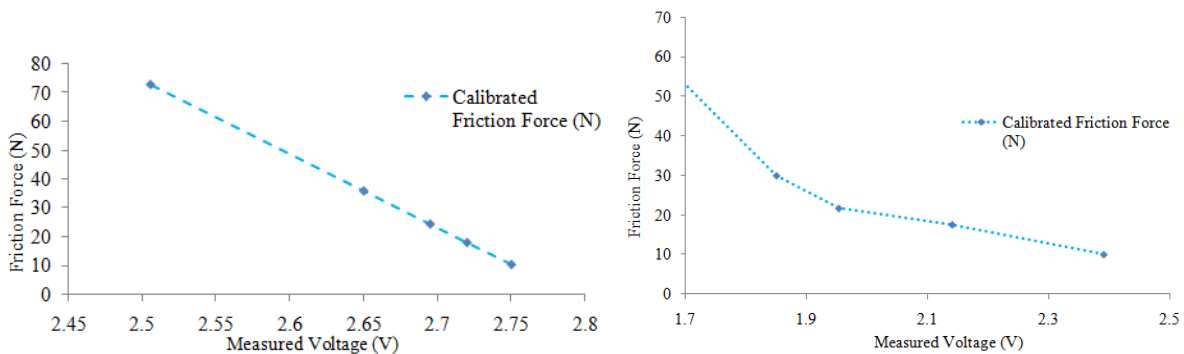


**Figure 57:** Principle axis bending calibration curves for black (left) and green (right) frictional force measurement

To validate the normal force measurement, a similar technique was used. The pin was oriented vertically to allow for axial compression when the same masses of water were hung. For this test, the masses were attached to a metal bar and balanced from the top of the pin to compress the pin. Varying loads were applied and data was taken for 5 seconds at 500 samples per second. Voltages were averaged and a corresponding load was calculated. Each test load was removed from the pin and reapplied twice to mitigate any initial force application differences. To account for creep seen in the strain gauges, initial offset voltage for the unstrained pin was recorded to increase measurement accuracy. From equations derived in section Parameter Analysis, we were able to determine a measured force and compare this force to the actual known load. Figures 58 and 59 below show the results from axial tests as well as a calibration curve for axial force measurement.

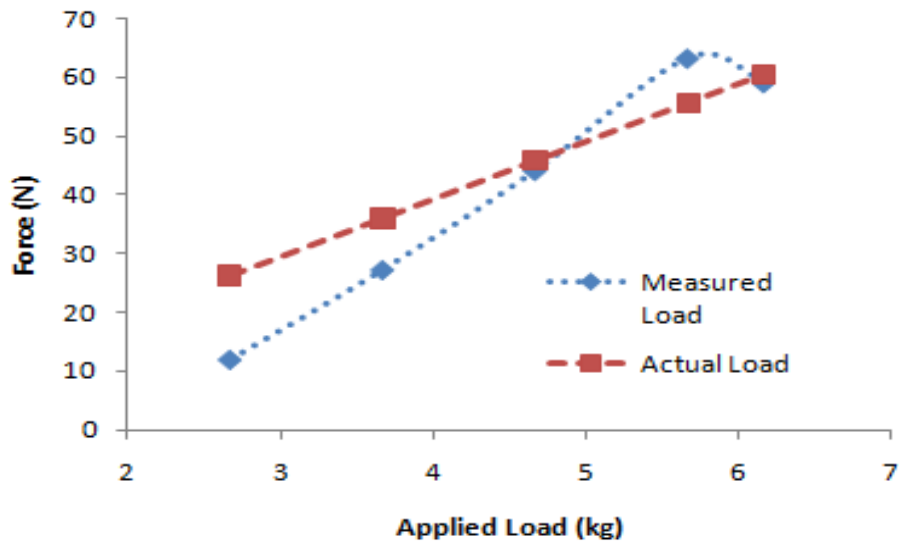


**Figure 58:** Axial Force test measured load compared to actual applied load.

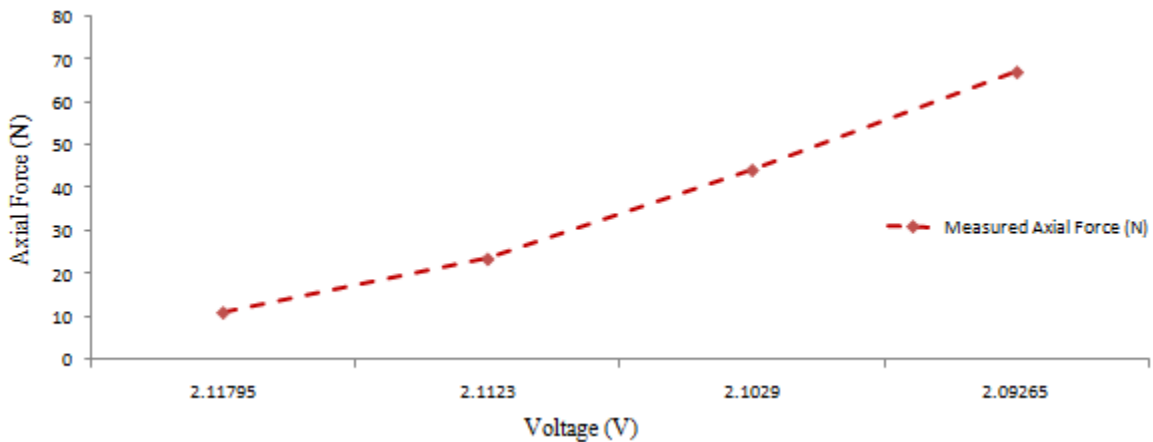


**Figure 59:** Axial force calibration curve for applied axial loads up to 65 N

From Figure 58, it can be seen that initially the measured load underestimates the applied load, but as time goes on and more tests are run, the measured load begins to overestimate the applied load. We were warned by the strain gauge manufacturer that creep will be an issue in the type of strain gauge used when applying gauges ourselves, but not when Micron Instruments applies gauges directly. Because of this, we were forced to determine the creep rate of the gauges under a given load to ensure accurate

measurements. To determine the creep rate, 65N of water was hung from the top of the pin and allowed to sit for one hour. Voltage measurements were measured at 500 samples per second, and the results plotted to determine a creep rate. Figure 60 below shows the results from this test. From this figure, the creep of the gauges was seen to be linear with a correlation coefficient of .9. With this linear approximation for creep rate, a time-varying offset voltage can be determined. Under a 65 N load, creep was determined to occur at a rate of approximately 1.2 N per minute.

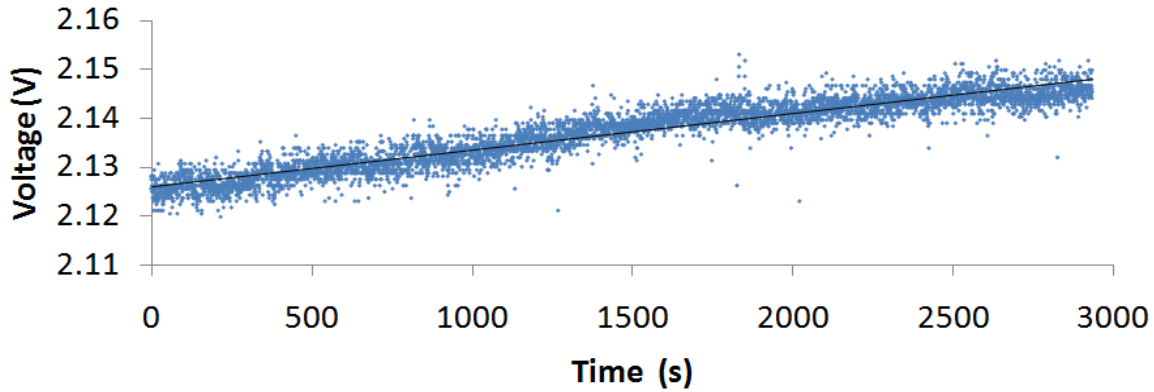


**Figure 60:** Normal Force gauges experience creep under applied axial loads in a linear fashion

Further testing is required to fully determine creep rates for all test loads since creep may change depending on applied load. Creep tests must also be completed for the gauges which measure bending strain. We did not need to determine creep for these tests since we re-measured offset voltage before each test. Since we expect frictional forces up to 300N and axial forces up to 200N, further testing must also be completed to calibrate the full test envelope of expected forces.

### Vertical Force Application

Our system has been designed to measure applied vertical force using the strain gauges on the pin. Once the strain gauges have been calibrated, they can be used to validate the accuracy of our force application system. However, to ensure that there is no error in the strain gauge calibration or in the feedback system controlling force application, the applied force should be tested independently of the system. To do this, we plan to use a load cell. The load cell will be placed between the ball sample and the disk sample, and the force application system will be run with the motion generation systems disabled (Fig 61). The readings from the load cell will be compared with the readings from the strain gauges and with the desired vertical load to validate the system.

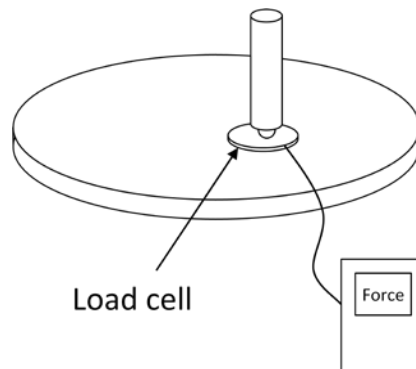


**Figure 61:** Diagram of vertical force validation

## Friction Force Measurement

Our system is designed to measure lateral friction forces between the two samples using strain gauges mounted on the pin. Proper calibration of the strain gauges will ensure that the lateral friction force measurements are accurate. To validate the calibration of the strain gauges, we will apply known lateral forces to the pin using a tension gauge (Fig. 62) and compare those known forces to the force calculated from the readings from the strain gauges.

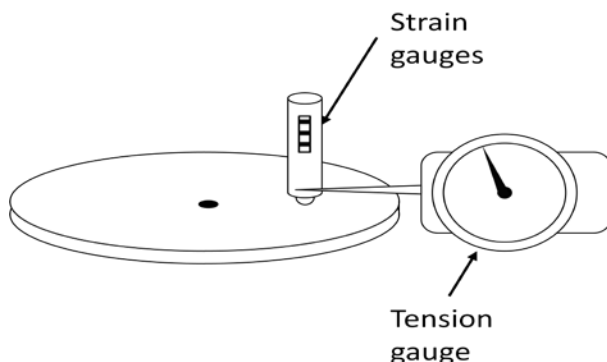


**Figure 62:** Diagram of friction force measurement validation

## Velocity of Linear Stage

Validation of the velocity of the linear stage will not require any special tests. During operation, our system will be constantly performing linear velocity validation. This is part of our design because the DC servo motor driving the linear stage must be controlled with a closed loop feedback. To achieve this feedback, the drive shaft will be fitted with an optical encoder to constantly monitor the velocity output by the motor.

## Rotational Velocity of Disk Sample

Validation of the rotational velocity of the disk sample should not require any special tests. This is because the motion is generated using a stepper motor. Every time a stepper motor is given a signal, it advances one step of known angular displacement. However, we will have to validate that the motor is not skipping steps. To do this, we plan to use a stroboscope or similar tachometer to independently validate that the rotational velocity profile of the disk sample matches the velocity profile that was input to the controller (Fig. 58).

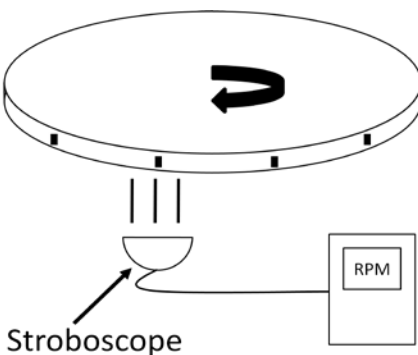


**Figure 63:** Diagram of rotational velocity validation



## Position Accuracy Validation

In order to produce useful and measureable wear paths, our system must be able to move the pin sample across the disk sample in the exact same path throughout an entire test. To validate that our system is achieves the precision necessary to accomplish this, we will carry out several wear tests. Lack of positioning precision will be indicated by drifting wear paths, as illustrated in Figure 64.

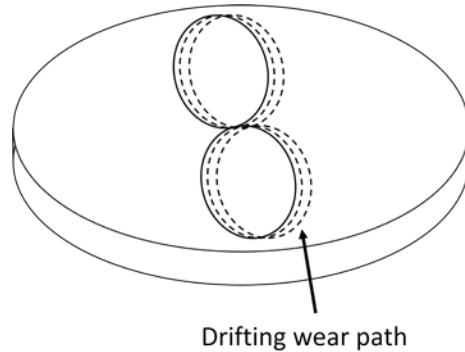


**Figure 64:** Diagram of drifting wear paths that would result from poor positioning precision

## DISCUSSION

Overall we believe that our final design is of good quality and will be able to meet the sponsor's requirements. The one-off prototype developed is mechanically sound and demonstrates the feasibility of the proposed final design with the exception of the ball screw actuator, which we are confident will perform well based upon the success of our prototype gantry system which operate under similar principles and the calculations done to confirm the suitability of the selected Nook Industries NLK-60 ball screw actuator. The current force application system is capable of achieving the required range of loads and the rotational motion system has been demonstrated to work as intended, though due to time constraints, additional testing is still needed to establish whether the intended maximum speed can be safely reached. Furthermore, the pin sample holder design is capable of holding the full requested range of sample sizes and to provide the proper range of deflection under the conditions encountered during testing to obtain usable strain gage data while remaining within the 1 degree maximum deflection limit. The plate/disk sample holders have also been successfully demonstrated and the mounting plate design provides the option of easily creating compatible custom clamps for non-standard samples.

The main shortcomings of the current recommended final design as demonstrated by our prototype lie in the area of controls and electronics. We found during our testing that an Arduino board may not have enough processing power to run 2D wear path tests. Running all three motors at once with two feedback loops takes too much time, and the Arduino board cannot repeat the function loops fast enough to control the system. We believe that a large part of the problem may lie in the force feedback loop. This loop gets analog feedback data from a strain gauge signal amplifier. This process of reading an analog signal takes 100 microseconds, which is a large amount of processor time in the scope of our controller. The force feedback loop must also perform several math functions before the data can be compared with the desired force to determine the system response. This feedback loop will undoubtedly interfere with motion controlling loops unless the Arduino board can be coded to run in true parallel processing. If that is not possible or sufficient, then the use of an FPGA processor will need to be investigated. An additional complication was that the strain gage measurements used in the force feedback system were observed to contain a problematic amount of noise induced by the power supply as well as drift over long testing

periods. The drift is highly predictable and could be accounted for in the controller programming, however a filter will be needed to reduce noise in the strain measurements to reach the precision and accuracy required for the device. This should also be improved in the final design by the use of professionally mounted high resolution gages, but a filter would still be recommended.

Mechanically several issues arose during testing that should be addressed in future design iterations. We found that during testing the large DC stepper and DC servo motors became extremely hot during operation. In order to ensure that no damage is caused to the motor and that the tests are not affected by the increased temperature, we recommend that a heat sink and fan cooling system be considered. We also encountered the issue that the rotational system is loud when running at high speeds due to vibrations at the steel ball transfer-aluminum plate interface. Application of a masking tape to the bottom of the plate reduced this slightly. A more robust solution may be desirable if a wear resistant linear bearing material can be found. This may also be of benefit in reducing noise in the strain measurements. Finally, the current prototype has expose moving parts which we had intended to build housings for, but were unable to due to time constraints. We recommend that this be done as part of any further work.

## **RECOMMENDATIONS**

Based upon the issues identified in the Discussion section above, we have compiled the following list of recommendations for future work. We emphasize the fact that the current mechanical systems are mechanically sound and not in need of redesign. Future work would do well to focus on improvement of the control, processing, and electronic systems, addition of an environmental chamber and safety features, and implementation of a cooling system for the motors.

### **Controls Recommendations**

The main issue currently facing our controls system is processing speed. The Arduino board cannot run all of the control code and feedback loops fast enough to drive the motors with the necessary speed or precision. There are three things we recommend doing to resolve this issue.

First, we recommend investigating the possibility of coding the Arduino to run processes in parallel. The success of this method will depend a lot on whether or not the board is physically capable of running true parallel processing. Our current code already uses a series of interrupts for the optical encoder so that position feedback is performed in pseudo-parallel with the main motor driver loops. Similar code optimization techniques, when coupled with parallel processing, will decrease the processing time.

If it is not possible to code the Arduino board to run in parallel, then we recommend looking into physically setting up a parallel processing system. This could be accomplished by using a separate Arduino board to run each motor. By delegating the motor running tasks, to other boards, the main control board would not need to run with such low processing speeds. The main speed issue currently is that the stepper motors require pulse changes every 200 microseconds. By delegating the pulse train generation to a separate board, the main control board could send a simple speed command to the sub-controller at much larger intervals, which would free up a lot of processing power.

In the event that multiple Arduino boards cannot be tied together to form a parallel processing system, then an FPGA will need to be employed. An FPGA can be written so that physical portions of its processor are partitioned off to run specific tasks, so it is capable of running a true parallel system. An FPGA will definitely be able to run the system, but it is the least desirable option, as it is by far the most expensive, and coding is traditionally done in Verilog, which is not something a mechanical engineering undergrad can be expected to learn in one semester.

## Strain Gauge Recommendations

Force measurement was completed using 8 strain gauges purchased from Micron Instruments. Although it was recommended to us to have the gauges professionally mounted to achieve the accuracy in force measurement we needed, we decided to purchase the gauges and have them shipped to us here in Ann Arbor, where we would mount them ourselves. The gauges would be used as a “proof-of-concept” and if they could demonstrate the accuracy of a backed semiconductor gauge specified on the company’s website, we would recommend that the bronze pin be sent to micron instruments where the same gauge configuration could be mounted by a trained professional.

Because we have been limited by both our data acquisition hardware and Arduino board, we were unable to accurately determine the accuracy of the gauges. We feel that the limitation at this point does not come from the accuracy or resolution of our strain gauges, but rather in the resolution of our DAQ. We feel this way because the best accuracy we were able to achieve was at the same level as our DAQ. We recommend purchasing a better DAQ unit as well as a higher bit arduino board and then re-testing according to our testing procedure documented in our validation section.

We also recommend using the same method of strain gauge application. We used 3 circuits to measure bending and axial forces independently. Two of the three circuits involved 2 backed semiconductor strain gauges (P/N SS-080-050-1000PB-S2) mounted in series on opposite sides of the pin, to complete half of a Wheatstone bridge circuit as seen in Figure X below. The other half of these bridges is completed with inactive resistors ( $R_1$  and  $R_2$  in Figure X), and by wiring them this way, we were able to measure bending of the pin in any direction independently of applied axial forces on the pin. The mounting and circuit diagram for these half-bridge gauges is shown below in Figure 65.

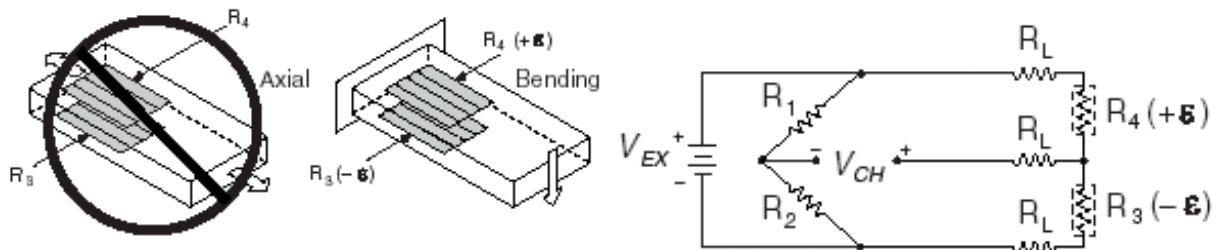


**Figure 65:** Recommended mounting (left) and wiring (right) diagrams for half bridge strain gauges measuring bending strains only

The Third circuit we implemented is a full-bridge measuring axial strain but not any bending strains. This gave us readings for axial forces regardless of any bending moment on the pin. The gauges we used, and recommend any future team use, is two backed half bridge strain gauges (P/N SS-080-050-1000PB-SSGH) wired together to make a full bridge according to Figure 67 below.

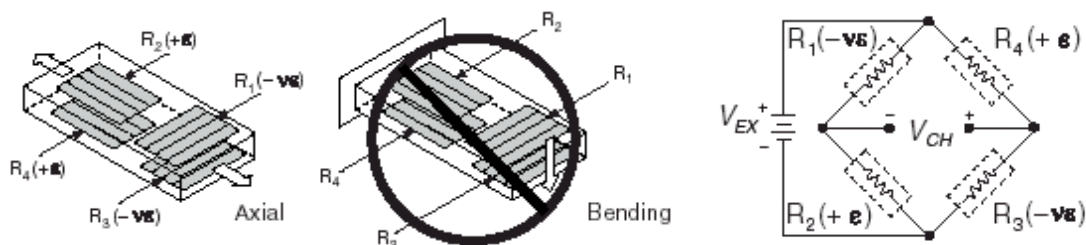


**Figure 67:** Recommended mounting (left) and wiring (right) diagrams for full bridge system measuring axial pin force only

These diagrams were retrieved from the National Instruments website. We have found this website to be extremely useful in strain gauge applications, and recommend any future team to first check this website to resolve any issues encountered with strain gauges.

### Strain Gauge Signal Conditioning Recommendations

In order to accurately measure friction forces on the order of several Newtons, we must amplify the signal coming from the strain gauges. To do this, we used a non-inverting amplifier to amplify each half bridge by a known amount. Figure 68 below shows the non-inverting amplifier circuit we used in our design.

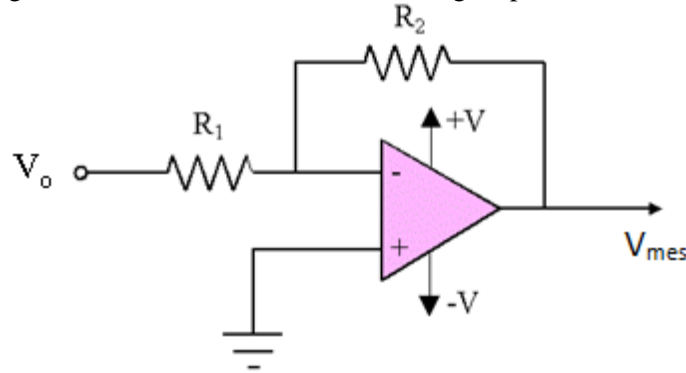


**Figure 68:** Non-inverting operational amplifier used to boost strain gauge signals

One issue which arose with amplification was that we were amplifying noise present in the signal, as well as the offset voltage present in the gauges. The offset voltage was a result of the strain gauges not being exactly equal in initial resistance, creating a difference in voltage drop over the two gauges. Once amplified, this offset was also amplified, and drove the signal to be clipped if amplification was too large. To alleviate this issue, we recommend adding a voltage divider (a simple potentiometer in parallel with the signal prior to the amplifier would work) to tune the offset voltage to be as close to the neutral reading of 2.5 V as possible. This would allow for larger amplification without clipping of the signal. To reduce noise in the system incurred from fluctuations in the voltage source (wall outlet), we recommend adding a low pass filter to the signal before the signal is amplified. We did not do this because the magnitude of the noise seen in the signal was smaller than the resolution of the DAQ, and therefore was not an issue when paired with our DAQ. Once a better DAQ and FPGA are implemented into the system, it will be advantageous to add a filter to reduce signal noise as well as add a potentiometer voltage divider to reduce initial offset voltage readings from the gauges.

### Environmental Chamber Recommendations

Because an environmental chamber is needed eventually, we recommend incorporating this chamber into the safety design to minimize design complexity and overall cost. We recommend isolating the environmental chamber so that controlled temperature and humidity air is only exposed to the sample, and not motors or many moving parts due to the potential hazards and detrimental effects high/low temperature and humidity settings may have on motors or moving parts. That being said, we have designed the strain gauge/ pin system to be able to withstand temperatures from 0 - 150°C and humidities from 0 – 100%. The gauges on the pin are temperature compensated so changes in temperature do not change readings. No other subsystems have been designed with temperature or humidity changes in mind, and we do not recommend exposing the entire system to an environmental chamber.

## **Safety Recommendations**

There are many moving parts in our tribometer system. Three motor shafts actively spin, and a bulky carriage assembly moves at speeds up to 1 m/s. Because of this, we recommend future teams to either add a housing for each individual moving piece, or one larger housing encompassing the entire tribometer. The housing should be rigid enough to withstand the forces expected if the system or sample were to break.

## **Motor Overheating Recommendations**

As we began running our system, we noticed that both the linear motor and rotational motors became very hot during just a few minutes of continuous operation. Since our system is required to run tests for several hours (up to a full day), we recommend designing/ implementing a cooling system to ensure that overheating of the motors is not a problem. A simple fan system may suffice, as heat sink fans are already installed on each motor.

## **Rotational Bearing System Recommendations**

The current rotational bearings are insufficient for the accuracy and speeds required of our system. They are loud and do not maintain accurate enough position of the aluminum disk. We chose to go with these bearings as a temporary cost savings, as the thrust bearing we recommended cost upwards of \$500 and did not fit our budget for the semester. We recommend future teams change the rotational bearing and upgrade to a sturdier but more expensive model.

## **CONCLUSION**

Our team was asked to design and fabricate a tribometer, or wear testing device, which had the capability to perform not only ASTM standard linear reciprocating and in-on disk wear test, but also two-dimensional wear path tests for the purpose of approximating actual operational conditions and determining the path dependence of wear and friction phenomena. A comprehensive list of customer requirements and corresponding engineering specifications may be found in Tables 2 and 3 on pages 17 and 18 of this report, respectively. The most significant of these are that the device must be able to operate at speeds of 0.01 to 1 m/s and apply a normal load of 1 to 200 N while collecting speed, force, temperature, humidity, and wear depth data in real time (~20 kHz sampling rate). Furthermore, in order to repeatably trace complex wear paths, a positioning precision of 25 micrometers is required. The device is intended for use within the EAST laboratory of the University of Michigan mechanical Engineering Department and must provide a significant savings over those available commercially.

The final design proposal that we have developed to fully meet the sponsor's requirements is documented in detail in the Final Design section of the previous report beginning on page 51. It achieves motion of a pin-type sample relative to a flat plate or disk type sample by one of several methods. For all tests the pin sample, consisting of a spherical sample, often a ball bearing, is mounted at the end of a vertical rod which is attached to the stage of a linear, sliding rod gantry and the flat sample is clamped to a flat disk mounting plate. Normal force is applied using a screw actuator driven by a DC stepper motor and worm and spur gear train as described on page 51. In the linear reciprocating test configuration, the plate sample is held stationary and the pin sample is driven back and forth on the gantry using a DC servo motor using a 25 mm lead ball screw. This system was selected due to its ability to precisely and repeatably position the samples and achieve the speeds required and is described on page 53. For the pin-on-disk test configuration, the pin sample is held stationary at a specific radius relative to the center of the lower mounting plate. The plate is then rotated at a constant velocity using a DC stepper motor with a spur gear

train with 3:1 gear ratio to step down the torque requirement of the motor. The disk is supported in the horizontal direction by radial bearings and in the vertical direction by a series of ball transfer units. Additional details are given on page 54. To achieve two dimensional wear path configurations, the two previously discussed configurations are run in parallel. Normal and friction force measurements are taken by measuring the strain induced in the bronze pin sample holder using professionally mounted strain gages. Temperature and humidity data monitored using an Omega RH-USB relative humidity sensor. Data acquisition is enabled by an NI USB 6009 DAQ system and control and feedback processing is done using an Arduino board, though this recommendation is subject to change pending validation of the ability of the board to be retrofit to handle multiple processes at once, which is necessary to run the large DC stepper motor controlling the rotating plate with any of the other systems. The body of the device and the linear stage itself are constructed of 6061 aluminum to reduce weight and provide stiffness and support to the mechanical systems.

At the request of our sponsor and due to budgetary limitation, we have fabricated a one-off prototype based upon the proposed final design with several major modifications. This prototype implements a timing belt-drive with tensioning system and flexible motor coupling, in place of the ball screw actuator, to drive the linear stage. Additionally, the professionally mounted strain gages have been replaced with foil gages mounted by our team. All other aspects of the device are as described for the final design. The total cost of the prototype is \$2910. The cost to upgrade the linear actuator and strain gages from the current prototype is \$3150.

Our team was able to conduct limited validation testing due to limitations of the current Arduino processor which prevented us from being able to run the rotational DC stepper motor with any additional motors due to the demands placed on the processor to send high frequency pulses to control it. We have completed calibration of the strain gages and provided the calibration curves in figures 58 and 59 on page 69. We expect improvement in the resolution of these gages once a suitable filter has been applied to the system to reduce noise caused by the power supply. We have also confirmed that the full range of normal forces requested can be met by the device. Testing of the full range of linear and rotational speeds was not completed due to time constraints and validation of the ability of the prototype to repeatably trace a 2D path was not possible due to the aforementioned processing limitations. However, the system has been demonstrated to be mechanically sound and we are confident that once the controller and processor aspects of the design can be improved, the device will operate as intended based upon the design analyses performed.

We have provided a full critique of the final design based upon complications encountered in the prototype and made recommendations for changes and additions in future design iterations. We recommend that the bulk of the mechanical design be left unchanged. The majority of work will involve the controls and processing of signals and data. To resolve the processing power limitations we have recommended that methods for improving the Arduino function or implementation of an FPGA processor be considered in future iterations. Other major areas for future work will be the implementation of a modular environmental chamber and implementation of additional safety features such as housings for moving parts. Details may be found in the Recommendations section of this report on page 73.

## **ACKNOWLEDGEMENTS**

This project would not have been completed without the assistance of numerous other individuals. Our team would first like to thank our sponsor Gordon Krauss, section instructor Shorya Awtar, and systems and design engineer John Baker for their assistance with the design and operation of the project. We would also like to thank GSI Phil Bonkoski for his assistance as well. Bob Coury and Marv Cressey provided insight and assistance with all of the machining processes and we would like to thank them for

that as well. Thanks also to Todd Wilber for his assistance in strain gage mounting. We would also like to thank Dr. Gangopadhay of the Ford Motor Company for allowing us to tour his lab providing insight on tribology. Lastly we would like to thank Amanda Gaytan, Tracie Straub, and the rest of the ME administrative team for their assistance with purchasing materials.

## REFERENCES

- [1] American Society for Testing Materials Standard G99, 2005, “Standard Test Method for Wear Testing with a Pin-on-Disk Apparatus”, ASTM International, West Conshohocken, PA.
- [2] American Society for Testing Materials Standard G133, 2005, “Standard Test Method for Linearly Reciprocating Ball-on-Flat Sliding Wear”, ASTM International, West Conshohocken, PA.
- [3] American Society for Testing Materials Standard G115, 2004, “Standard Guide for Measuring And Reporting Friction Coefficients”, ASTM International, West Conshohocken, PA.
- [4] American Society for Testing Materials Standard B539, 2008, “Standard Test Methods for Measuring Resistance of Electrical Connections (Static Contacts)”, ASTM International, West Conshohocken, PA.
- [5] Nanovea. (n.d.). *www.nanovea.com*. Retrieved January 14, 2010, from [www.nanovea.com](http://www.nanovea.com)
- [6] CSM Instruments. (n.d.). *CSM Instruments*. Retrieved Jan 14, 2010, from <http://www.csm-instruments.com>: <http://www.csm-instruments.com>
- [7] Center for Tribology Research. (n.d.). Retrieved January 14, 2010, from CETR: <http://www.cetr.com/eng/products/umt-2.html>
- [8] Gilett, C.E., US Patent 1534014, April 14, 1925, “Grading Machine,” Norton Company, Worcester, MA. Obtained from <http://uspto.gov>
- [9] Bao, Frank W., Hummeldorf, James L., Parker, Stephen D., US Patent 4051713, October 4, 1977, “Friction Measuring and Testing Method and Apparatus,” Actus, Inc, Florence, KY. Obtained from <http://www.patentstorm.us>
- [10] Akalin, Ozgen, Newaz, Golam M., US Patent 6401058, June 4, 2002, “Reciprocating System for Simulating Friction and Wear,” Wayne State University, Detroit, MI. Obtained from <http://www.patentstorm.us>
- [11] Relative Humidity. (n.d.). Retrieved from Hyperphysics.com: <http://hyperphysics.phy-astr.gsu.edu/HBASE/Kinetic/relhum.html>
- [12] Scientific, T. (n.d.). Model 2500 Benchtop/Mobile Two Pressure Humidity Generator. Retrieved from Thunder Scientific Corporation: [http://thunderscientific.com/humidity\\_equipment/model\\_2500.html](http://thunderscientific.com/humidity_equipment/model_2500.html)
- [13] Deutschman, Aaron D., Walter J. Michels, and Charles E. Wilson. *Machine Design: Theory and Practice*. New York: Macmillan, Inc., 1975
- [14] Worm Gears. Retrieved March 12, 2010 [http://www.roytech.co.uk/Useful\\_Tables/Drive/Worm\\_Gears.html](http://www.roytech.co.uk/Useful_Tables/Drive/Worm_Gears.html)
- [15] McMaster Carr. “McMaster Carr – Bronze.” Web. <http://www.mcmaster.com/#bronze/=4x6hw2>
- [16] CES EduPack. Software. Granta Design Limited, 2009.



## TEAM MEMBER BIOS



### Bob Chlum

I grew up in Lockport, Illinois, a suburban town south of Chicago. Throughout my childhood and adolescence, I was always fooling about with technical sorts of things, starting with Lincoln Logs, Legos, and Erector Sets, and eventually worked my way up through bicycles, lawn mowers, and computers. It was in high school where my enjoyment of math and physics led me to decide that my future was in engineering.

Within a year of starting my studies at Michigan I declared into the mechanical engineering program, after briefly considering aerospace and computer science. In between classes and studying, I play the trumpet in the marching band.

Between semesters I did odd jobs for a construction company back in Chicago. After graduation I plan to gain some engineering industry experience before pursuing a master's degree.



### Kelsey Hanson

I am a senior undergraduate/1<sup>st</sup> term SGUS student in Mechanical Engineering. I don't really have a home town since I haven't lived in the same place for more than a few years since I was little. I have lived in Michigan most of my life, barring a few years of high school in Golden, Colorado. I grew up in a family dedicated to doing-it-yourself and doing it well. Much of my childhood and adolescence were spent helping with home improvement projects, repairing appliances, and figuring out how things worked.

I have always enjoyed doing hands on work and building things and I decided to pursue a career in engineering to put those skills to use. In addition to my course work at U of M I have had the opportunity

to work for the U.S. Navy characterizing explosives. My greatest interest however is in the fields of design and manufacturing. One of the most unique experiences I have had was as a guest student at CalTech where I worked with a team of students in Guatemala to develop equipment to support the growing honey business in the impoverished rural communities.

When I am not studying I am most likely participating in some sort of sport or photography. I spend as much time as possible rock climbing, surfing, snowboarding and playing sports. I am eternally grateful that I have an aptitude for math and science since I would probably end up spending my life as a surf bum otherwise. It is my ultimate goal to combine my engineering background with my love of sports to pursue a career in sports equipment design. Someday I hope to build my own company to produce snowboards and surfboards that are completely designed and manufactured in the U.S.



### **Stephen Lindsay**

I grew up in a small town on the west side of the state called Ludington. I always liked building things and getting my hands dirty so it seemed interesting to me that I could make it my profession by becoming a mechanical engineer. My parents run a furniture store in Ludington, and seeing the stresses they have gone through by owning a small business has helped lead me away from following in their footsteps and into something completely different and new.

I have worked for about 1.5 years in the “real world” working for Toyota as a design engineering intern in their Instrument Panel group as well as a Powertrain Controls intern this past semester. I spent the past summer working for the Air Force at Edwards Air Force Base in their Electronic Warfare Group as a test engineering intern. I have a big interest in aircraft (especially military aircraft) and I found this internship to be a great experience and will probably go back this summer to intern again.



When not in school or working, I spend my time playing sports and hanging out with friends. I play indoor and intramural soccer, but I think my favorite sport is football.

I also enjoy traveling and try to spend as much time outdoors as possible. As much as I LOVE school, I am looking forward to graduating in December and (hopefully) entering the real world with a job I enjoy.

### **Ben Pascoe**

I'm a senior from Saline, MI, which is located just a stone's throw away from Ann Arbor. Growing up so close to Ann Arbor, I always knew I would come to the University of Michigan. My interest in mechanical engineering began in high school as I always gravitated toward math and science and wanted to know how things worked. My dad, uncle, and grandpa are all engineers as well so being around them definitely contributed to my interest too.



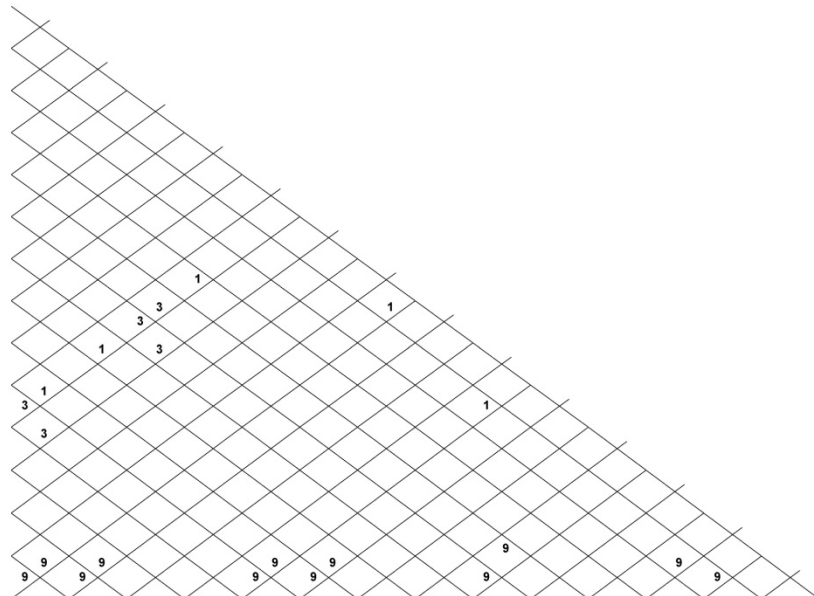
After undergrad, I plan on getting my Master's degree in Mechanical Engineering and graduating next year. I'm still keeping my options open for future jobs but I'm interested in design, sustainability, and making things more efficient. My only requirement is that the job's located in a warm climate.

Outside of schoolwork and engineering, I enjoy playing and watching sports, especially football and basketball. On the weekends you can find me at the gym or in front of the television watching the Detroit Lions lose yet another game. I also like to travel and I spent 2 months studying abroad in Shanghai, China during the summer after my 2<sup>nd</sup> year here.

# APPENDIX A: DESIGN TOOLS

## A.1: QFD

Customer Attribute	Importance (%)	Engineering Characteristics					Linear Speed				Rotational Speed				Temperature				
		Dimensions (height, width, length)	Specimen Perpendicularity	Linear Travel / Stroke	Oscillation Frequency	Positioning Precision	Range	Resolution	Control Tolerance	Sampling Rate	Range	Resolution	Control Tolerance	Sampling Rate	Range	Resolution	Control Tolerance	Sampling Rate	
		min	max	max	max	max	max	max	max	max	max	max	max	max	max	max	max	max	max
Meet ASTM standard test requirements	12%	1	9	3	3	1	3		9	3	3		9	3	3		9	3	3
Safeguards user and equipment	11%	1		1	9		9		1		9				9				3
Measure and record lateral and normal forces in real time	10%		3	3	3		3			3				1					1
Test variety of materials	10%	1		1			3			3				3					3
Low cost	9%	9	3	9	3	9	9	9	9	9	9	9	9	9	9	9	9	9	9
Low maintenance	8%	1	3	3	3	1	1		3		1		3		9		3		9
Fits in dedicated lab space	8%	9		9	1	1	1							3			3		3
Measure and record relative velocity in real time	7%			3	1	3	9	9		9	9	9		9	1				
Secure std. and custom sample sizes (pin, plate)	6%	9		3															
Perform custom tests (2d paths)	6%	9		3		9	9	3	9		9	3	9						
Measure and record temperature and humidity in real time	5%													3	9			9	3
Measure and record contact resistance of sample in real time	4%				3		1			1				1					
Maintains constant leading point on pin sample	3%		3	1	1	9	9	3	9	9	9	3	9	9					
Measure and record wear volume	3%			1		1	3		1		3		1		1				
Allows viewing of test	2%	1		1			1												
Test under wide range of environmental conditions	1%	1												9			9		9
Automated sample loading	1%		9			9													
<b>Direction of Improvement</b>		min	max	max	max	max	max	max	max	max	max	max	max	max	max	max	max	max	max
<b>Units</b>		cm	degree	mm	Hz	mm	m/s	% of nominal	% of nominal	kHz	rpm	% of nominal	% of nominal	kHz	C	C	C	kHz	%
<b>Current Device (F09 prototype)</b>		61.61.91	±1	0-254		1	0.01-1	1		20	2.9-600	1		20	0-150	5 C		20	0-100
<b>CSM Nano Tribometer</b>				30µm-10	0.1-10		<0.01				1-100								
<b>CSM Microtribometer</b>				60	1.6-10		<0.1				0.3-1500			25-150					
<b>IIT Cryogenic Tribometer</b>				15			0.6-45				850-36k								
<b>Nanovea</b>				50	120	0.0025	0.1				0.1-6000			1000 max					0-100
<b>CETR Nano/Micro Tribometer UMT-2</b>														1200					
<b>ASTM Std</b>			±1	10	5-10		0.1-0.2	1		60-600	1	1				2			
<b>Sponsor Request</b>		61.61.91		0-254	2-20		0.0001	1	20	1->600		1	1	20	0-150	1		20	0-100
<b>Target (Plan)</b>		61.61.91	±1	0-254	maximize	0.0025	0.01-1	0.0001	1	20	maximize	1	1	20	0-150	1	2	20	0-100
<b>Total</b>		42	30	41	27	43	61	24	41	30	59	24	40	30	52	18	33	21	43
<b>weight absolute</b>		3.02797	2.07692	3.29371	2.51049	2.21678	4.54545	1.72028	3.0979	2.11888	4.44755	1.72028	2.98601	2.11888	3.97902	1.25874	2.4965	1.61538	3.16783
<b>weight percent</b>		4%	3%	4%	3%	3%	6%	2%	4%	3%	5%	2%	4%	3%	5%	2%	3%	2%	4%



**Engineering Characteristics**

**Customer Attribute**

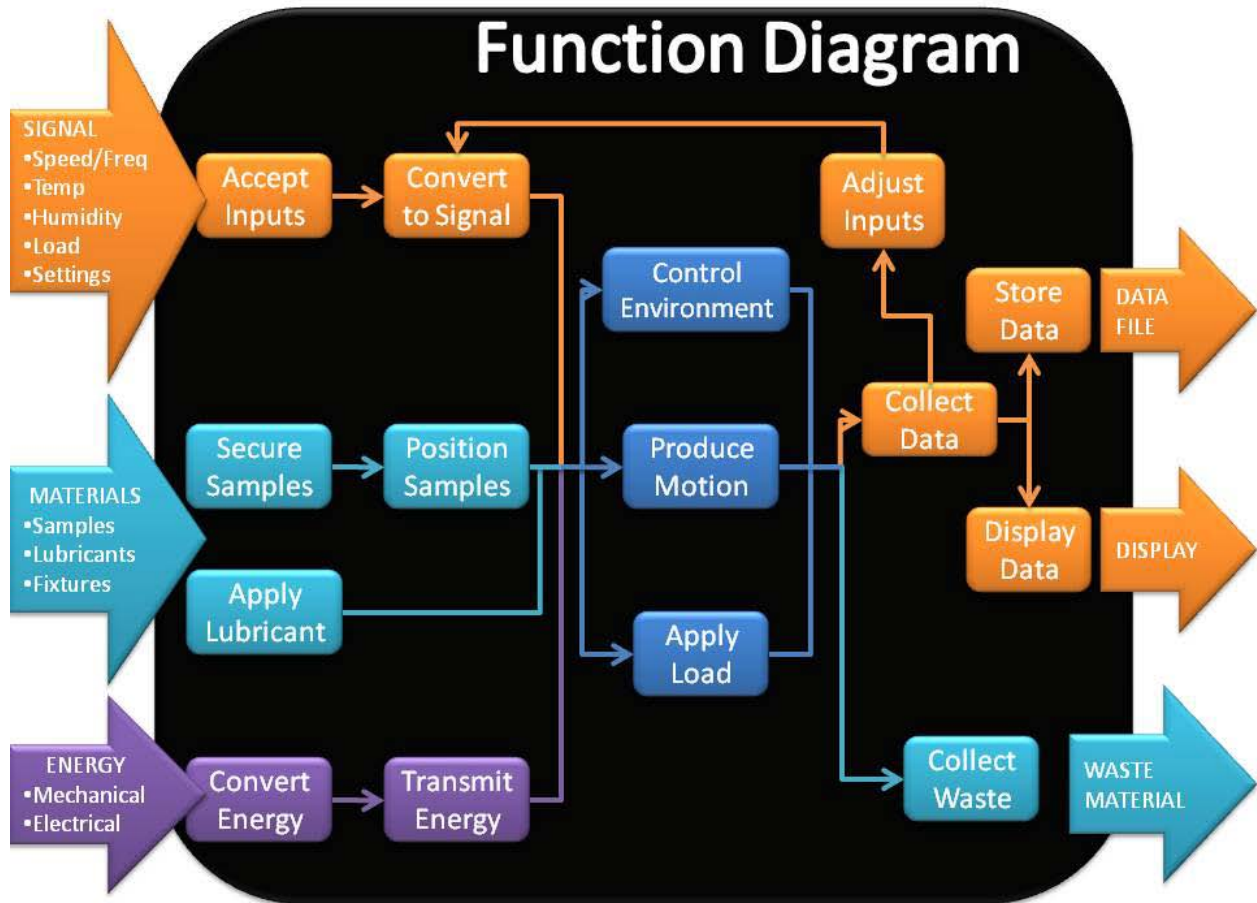
Customer Attribute	Importance (%)
Meet ASTM standard test requirements	12%
Safeguards user and equipment	11%
Measure and record lateral and normal forces in real time	10%
Test variety of materials	10%
Low cost	9%
Low maintenance	8%
Fits in dedicated lab space	8%
Measure and record relative velocity in real time	7%
Secure std. and custom sample sizes (pin, plate)	6%
Perform custom tests (2d paths)	6%
Measure and record temperature and humidity in real time	5%
Measure and record contact resistance of sample in real time	4%
Maintains constant leading point on pin sample	3%
Measure and record wear volume	3%
Allows viewing of test	2%
Test under wide range of environmental conditions	1%
Automated sample loading	1%

Engineering Characteristics	Humidity			Normal and Lateral Forces			Contact Resistance			Pin Sample Size Range	Disk Sample Size Range	Vertical Travel	Visibility of specimen during tests
	Resolution	Control Tolerance	Sampling Rate	Range (Normal)	Resolution	Control Tolerance	Sampling Rate	Range	Resolution				
Meet ASTM standard test requirements		9	3	9	9	9	9			9	3	3	
Safeguards user and equipment				9				3				3	3
Measure and record lateral and normal forces in real time				9	9		9						
Test variety of materials				9		3				9	9	9	
Low cost	9	9	9	9	9	9	9	9	9	1	3	1	1
Low maintenance		3		9		3		1					3
Fits in dedicated lab space		3		3		1				1	9	1	
Measure and record relative velocity in real time													
Secure std. and custom sample sizes (pin, plate)										9	9	3	
Perform custom tests (2d paths)				3						1	1	1	
Measure and record temperature and humidity in real time	9		9										
Measure and record contact resistance of sample in real time								9	9	9	1	1	1
Maintains constant leading point on pin sample				1		3					1		
Measure and record wear volume				1						1	3	9	
Allows viewing of test										1	1		9
Test under wide range of environmental conditions	9												
Automated sample loading										9	9	9	

Direction of Improvement	max	max	max	max	max	max	max	max	max	max	max	max	max	
Units	%	%	kHz	N	N	% of nominal	kHz	ohm	%	kHz	mm (diam)	mm (diam)	mm (depth)	% visible
Current Device (F09 prototype)	3		20	0.1-200	0.001		20	0-1000	1 ohm	20	1.6-6.4	25.4-254	0-3.18	
CSM Nano Tribometer				50 µN - 1	1 µN			0-1000						100
CSM Microtribometer				0-60	30 mN									100
IIT Cryogenic Tribometer				0-50										100
Nanovea				0-60	30 mN									100
CETR Nano/Micro Tribometer UMT-2				0-200										100
ASTM Std		3		25-200		2					2-10	.3-1.0		
Sponsor Request			20	≤200	1	1	20	0-1000		20	1.6-6.4	25-254	15	100
Target (Plan)	1	1	20	≤200	0.001	1	20	maximize	1	20	1-8	25-254	maximize	100
Total weight absolute	18	33	21	62	27	28	27	22	18	18	43	48	40	16
weight percent	1.25874	2.4965	1.61538	5.93706	2.83217	2.61538	2.83217	1.61538	1.1958	1.1958	2.93007	3.03497	2.34266	0.86713
	2%	3%	2%	7%	3%	3%	3%	2%	1%	1%	4%	4%	3%	1%

	F09 prototype	CSM Nano Tribometer	CSM Microtribometer	IIT Cryogenic Tribometer	Nanovea	CETR Nano/Micro Tribometer UMT-2
	1	5	5	1	5	5
	1	5	5	5	5	5
	1	5	5	5	5	5
	1	5	5	3	5	5
	5	-	-	1	-	1
	1	4	4	3	4	3
	1	5	5	5	3	3
	1	5	5	5	5	5
	1	5	5	2	5	5
	1	1	1	1	1	5
	1	5	5	1	5	5
	1	1	5	1	5	5
	1	3	3	5	3	3
	1	3	3	5	5	5
	5	5	5	1	5	5
	1	5	5	2	5	5
	1	5	5	5	5	5

## A.2: Function Diagram



A.3: Motion Generation Pugh Chart

Selection Criteria	Weight [%]	DC Step		DC Servo		AC Servo		Linear Motor		Voice Coil Actuator	
		Grade	Score	Grade	Score	Grade	Score	Grade	Score	Grade	Score
Speed range	14	1	0.14	5	0.7	1	0.14	5	0.7	5	0.7
Torque/Force	19	4	0.76	4	0.76	4	0.76	4	0.76	5	0.95
Positioning precision	24	4	0.96	4	0.96	4	0.96	5	1.2	5	1.2
Responsiveness	14	3	0.42	5	0.7	4	0.56	5	0.7	4	0.56
Motion Range	10	5	0.5	5	0.5	5	0.5	5	0.5	1	0.1
Smoothness	19	1	0.19	5	0.95	4	0.76	5	0.95	4	0.76
<b>Total Score</b>			2.97		4.57		3.68		4.81		4.27

A.4: Motion Transmission Pugh Chart

Selection Criteria	Weight [%]	Belt Drive		Screw		Gear Train		Cam		Linear Motor	
		Grade	Score	Grade	Score	Grade	Score	Grade	Score	Grade	Score
Smooth motion	25	1	0.25	5	1.25	4	1	4	1	5	1.25
Precise positioning/ responsiveness	15	1	0.15	4	0.6	3	0.45	3	0.45	5	0.75
Sufficient speed	15	5	0.75	4	0.6	4	0.6	4	0.6	5	0.75
Range of Motion	20	5	0.75	5	0.75	3	0.45	1	0.15	4	0.6
Load Capacity	15	3	0.45	5	0.75	5	0.75	5	0.75	4	0.6
Low Maintenance	10	3	0.3	3	0.3	3	0.3	4	0.4	5	0.5
<b>Total Score</b>			2.65		4.25		3.55		3.35		4.45



A.5: Force Application Pugh Chart

Selection Criteria	Weight [%]	Voice Coil		Screw Application		Plate Clamp	
		Grade	Score	Grade	Score	Grade	Score
Accuracy	15	5	0.75	4	0.6	3	0.45
Reliability	18	4	0.72	3	0.54	3	0.54
Long Lifetime	5	3	0.15	4	0.2	5	0.25
Low Cost	15	1	0.15	3	0.45	4	0.6
Size	10	3	0.3	4	0.4	2	0.2
Safety	10	4	0.4	3	0.3	3	0.3
Setup time	2	4	0.08	4	0.08	3	0.06
Manufactuability	10	4	0.4	5	0.5	4	0.4
Applies adequate range	15	5	0.75	4	0.6	5	0.75
<b>Total Score</b>			<b>3.85</b>		<b>3.87</b>		<b>3.75</b>

A.5: Force Application Pugh Chart (Continued)

Selection Criteria	Weight [%]	Hanging Weight		Spring/Lever Arm		Hydraulic/Pneumatic	
		Grade	Score	Grade	Score	Grade	Score
Accuracy	15	2	0.3	3	0.45	3	0.45
Reliability	18	1	0.18	4	0.72	3	0.54
Long Lifetime	5	5	0.25	4	0.2	4	0.2
Low Cost	15	5	0.75	4	0.6	3	0.45
Size	10	2	0.2	4	0.4	2	0.2
Safety	10	2	0.2	3	0.3	2	0.2
Setup time	2	4	0.08	2	0.04	2	0.04
Manufacturability	10	4	0.4	3	0.3	3	0.3
Applies adequate range	15	4	0.6	3	0.45	5	0.75
<b>Total Score</b>			<b>3.16</b>		<b>3.66</b>		<b>3.18</b>

A.6: Force Measurement Pugh

Selection Criteria	Weight [%]	Micron Instruments Gauged Pin		Glued on strain gauge rosette		Load Cells	
		Grade	Score	Grade	Score	Grade	Score
Accuracy	20	5	1	3	0.6	5	1
Reliability	18	5	0.9	3	0.54	5	0.9
Long Lifetime	5	4	0.2	4	0.2	4	0.2
Low Cost	15	1	0.15	5	0.75	1	0.15
Size	10	4	0.4	4	0.4	2	0.2
Setup time	2	3	0.06	4	0.08	2	0.04
Manufacturability	15	4	0.6	5	0.75	3	0.45
Measures adequate range	15	5	0.75	4	0.6	5	0.75
Low Maintenance	5	3	0.15	4	0.2	3	0.15
<b>Total Score</b>			4.21		4.12		3.84

A.7: Data/Control Pugh Chart

Selection Criteria	Weight [%]	DAQ/PC		FPGA	
		Grade	Score	Grade	Score
High Cycle Speed	0.5	1	0.5	5	2.5
Low Cost	0.3	5	1.5	1	0.3
Ease of programming	0.2	2	0.4	1	0.2
<b>Total Score</b>			<b>2.4</b>		<b>3</b>

A.8: Plate Sample Holding Pugh Chart

Selection Criteria	Weight [%]	Individual Clamp		Ring Clamp		Chuck		Adhesion	
		Grade	Score	Grade	Score	Grade	Score	Grade	Score
Reliability	20	4	0.8	4	0.8	5	1	2	0.4
Low Cost	10	5	0.5	4	0.4	3	0.3	4	0.4
No interference	15	4	0.6	3	0.45	5	0.75	5	0.75
Safety	10	4	0.4	5	0.5	3	0.3	3	0.3
Setup time	10	4	0.4	4	0.4	3	0.3	2	0.2
Manufacturability	15	4	0.6	4	0.6	3	0.45	4	0.6
Accommodates all sample sizes	20	5	1	2	0.4	5	1	5	1
Low Maintenance	5	4	0.2	4	0.2	4	0.2	1	0.05
<b>Total Score</b>		4.5		3.75		4.3		3.7	

A.8: Plate Sample Holding Pugh Chart (Continued)

Selection Criteria	Weight [%]	Perpendicular Bolts		Radial Clamp w/inserts		C-Clamps		Magnetic	
		Grade	Score	Grade	Score	Grade	Score	Grade	Score
Reliability	20	4	0.8	3	0.6	3	0.6	2	0.4
Low Cost	10	2	0.2	4	0.4	5	0.5	3	0.3
No interference	15	5	0.75	5	0.75	3	0.45	3	0.45
Safety	10	3	0.3	3	0.3	3	0.3	3	0.3
Setup time	10	3	0.3	2	0.2	4	0.4	4	0.4
Manufacturability	15	2	0.3	3	0.45	4	0.6	5	0.75
Accommodates all sample sizes	20	3	0.6	4	0.8	2	0.4	4	0.8
Low Maintenance	5	3	0.15	4	0.2	5	0.25	3	0.15
<b>Total Score</b>		3.4		3.7		3.5		3.55	

A.9 Pin Sample Holding Pugh Chart

Selection Criteria	Weight [%]	Spring Force		Threaded Clamp	
		Grade	Score	Grade	Score
Reliability	20	3	0.6	4	0.8
Low Cost	10	3	0.3	3	0.3
No interference	15	4	0.6	4	0.6
Safety	10	4	0.4	4	0.4
Setup time	10	3	0.3	5	0.5
Manufacturability	15	4	0.6	4	0.6
Accommodates all sample sizes	20	5	1	5	1
Low Maintenance	5	4	0.2	4	0.2
<b>Total Score</b>			<b>4.0</b>		<b>4.4</b>

A.10: Humidification Pugh Chart

Selection Criteria	Weight [%]	Divided Air Mist		Hot Plate and Water		Ultrasonic Generation		Water Wheel	
		Grade	Score	Grade	Score	Grade	Score	Grade	Score
Controllable	30	5	1.5	4	1.2	4	1.2	4	1.2
Able to Achieve Temperature and Humidity Range	35	4	1.4	4	1.4	3	1.05	3	1.05
Accurate to within required test tolerances	20	3	0.6	3	0.6	3	0.6	3	0.6
Minimize Parts	5	2	0.1	3	0.15	2	0.1	4	0.2
Low Maintenance	10	3	0.3	4	0.4	4	0.4	4	0.4
<b>Total Score</b>		3.9		3.75		3.35		3.45	



A.11: Dehumidification Pugh Chart

Selection Criteria	Weight [%]	Divided Air Mist		Salt Bath		Condensation Plate		Desiccant		Nitrogen	
		Grade	Score	Grade	Score	Grade	Score	Grade	Score	Grade	Score
Controllable	30	5	1.5	1	0.3	5	1.5	3	0.9	3	0.9
Able to Achieve Temperature and Humidity Range	35	4	1.4	2	0.7	4	1.4	3	1.05	5	1.75
Accurate to within required test tolerances	20	3	0.6	2	0.4	3	0.6	3	0.6	4	0.8
Minimize Parts	5	2	0.1	5	0.25	5	0.25	5	0.25	3	0.15
Low Maintenance	10	3	0.3	5	0.5	4	0.4	4	0.4	3	0.3
<b>Total Score</b>		3.9		2.15		4.15		3.2		3.9	

A.12: Heating Pugh Chart

Selection Criteria	Weight [%]	Resistive Heating		Hot Plate	
		Grade	Score	Grade	Score
Controllable	30	5	1.5	5	1.5
Able to Achieve Heating Temp	35	5	1.75	4	1.4
Accurate to within required test tolerances	20	5	1	4	0.8
Minimize Parts	5	4	0.2	3	0.15
Low Maintenance	10	4	0.4	4	0.4
<b>Total Score</b>					
			4.85	4.25	

A.13 Cooling Pugh Chart

Selection Criteria	Weight [%]	Refrigeration Cycle		Compressed air expansion		Ice Block		Evaporative Cooling	
		Grade	Score	Grade	Score	Grade	Score	Grade	Score
<b>Controllable</b>	30	5	1.5	3	0.9	3	0.9	4	1.2
<b>Able to Cool to Desired Temp</b>	35	5	1.75	4	1.4	3	1.05	3	1.05
<b>Accurate to within required test tolerances</b>	20	5	1	3	0.6	3	0.6	3	0.6
<b>Minimize Parts</b>	5	3	0.15	3	0.15	5	0.25	4	0.2
<b>Low Maintenance</b>	10	4	0.4	3	0.3	4	0.4	4	0.4
<b>Total Score</b>		4.8		3.35		3.2		3.45	

**A.14: Full Tribometer Concept Pugh Chart**

	<b>Low Cost</b>				<b>Screw</b>						
	<b>Retro Fit</b>		<b>Polar Pin</b>		<b>Alpha Design</b>		<b>X-Y Axes</b>		<b>Application</b>		
<b>Selection Criteria</b>	<b>Weight [%]</b>	<b>Grade</b>	<b>Score</b>	<b>Grade</b>	<b>Score</b>	<b>Grade</b>	<b>Score</b>	<b>Grade</b>	<b>Score</b>	<b>Grade</b>	<b>Score</b>
<b>Motion:</b>											
Smooth motion	9	1	0.09	3	0.27	5	0.45	5	0.45	4	0.36
Precise positioning	10	1	0.1	3	0.3	5	0.5	5	0.5	4	0.4
Sufficient speed	8	4	0.32	2	0.16	5	0.4	4	0.32	4	0.32
Load capacity	7	3	0.21	3	0.21	5	0.35	3	0.21	5	0.35
<b>Force</b>											
Accuracy of measurement	10	2	0.2	3	0.3	5	0.5	5	0.5	5	0.5
Accuracy of application	5	2	0.1	4	0.2	5	0.25	5	0.25	2	0.1
Range of force	9	3	0.27	5	0.45	3	0.27	2	0.18	5	0.45
<b>Overall:</b>											
Low maintenance	5	5	0.25	3	0.15	4	0.2	3	0.15	2	0.1
Low cost	4	5	0.2	1	0.04	1	0.04	1	0.04	3	0.12
Reliability	6	2	0.12	2	0.12	4	0.24	4	0.24	2	0.12
Longevity	5	2	0.1	2	0.1	4	0.2	3	0.15	3	0.15
Manufacturability	8	5	0.4	1	0.08	5	0.4	2	0.16	1	0.08
Set-up time	2	5	0.1	4	0.08	2	0.04	2	0.04	3	0.06
Safety	9	3	0.27	2	0.18	3	0.27	2	0.18	2	0.18
Size	3	5	0.15	3	0.09	2	0.06	1	0.03	1	0.03
<b>Total Score</b>			<b>2.88</b>		<b>2.73</b>		<b>4.17</b>		<b>3.4</b>		<b>3.32</b>

## APPENDIX B: DESCRIPTION OF ENGINEERING CHANGES

1. **What has changed?** Instead of using the purchased linear bearing for the pin to travel through we will now be manufacturing our own sleeve bearing to serve the same function. There was too much play in the purchased bearing that allowed the pin to deviate more than  $1^\circ$  from vertical. The new design keeps the pin alignment within the engineering specifications.

**What is impacted?** The normal force application system will be improved and the lateral force measuring will be improved as well since there is more rigidity in the system now. The pin will still be able to translate vertically but there will be more friction than using the purchased bearing. This will not significantly affect the system, however.

**Who made the change?** Steve Lindsay

**Who authorized the change?** Gordon Krauss

2. **What has changed?** Limit switches will be added to the linear motion system. They will be mounted on the chassis side wall and will cut power from to the motor when tripped to stop the system if there is any malfunction in the programming or operation of the DC servo motor. Bumps will be added onto the belt to trip the switch at a specific location.

**What is impacted?** The linear system will be safer with the limit switches. They will also prevent damage to the chassis if there are any malfunctions.

**Who made the change?** Bob Chlum

**Who authorized the change?** Gordon Krauss

3. **What has changed?** A bearing has been placed on the belt tensioner to constrain the vertical motion of the pulley. This will keep the belt system aligned and will allow for smooth motion of the idler pulley.

**What is impacted?** The linear system will be improved again and the belt will be constrained to one operating location which is desired.

**Who made the change?** Ben Pascoe

**Who authorized the change?** Gordon Krauss

4. **What has changed?** We will now be using 6 ball transfer units instead of the 3 that were initially in the design. The reason for the change was that the manufacturer shipped more than were ordered.

**What is impacted?** The rotational motion system will be more stable with 6 units instead of 3. This will also expand the maximum radius that the force can be applied at which benefits the entire system

**Who made the change?** Kelsey Hanson

**Who authorized the change?** Gordon Krauss

- 5. What has changed?** We will be adding a motor mounting block to the rotational system. The block will be mounted under the base plate and secured to the top of the motor. This block will keep the motor more stable and ensure that the shaft is perpendicular to the base plate.

**What is impacted?** The rotational motion system will be improved because the motor will be more stable. There will be less chance of failure of the system and more consistency in the motion.

**Who made the change?** Ben Pascoe

**Who authorized the change?** Gordon Krauss

- 6. What has changed?** We will be water jet cutting a hex socket instead of using the purchased hex socket from the design. The purchased hex socket did not allow for the travel distance we thought it would need. Also there was more play in the socket than was expected. The water jet hex socket gives us adequate travel distance and more constraint on the bolt.

**What is impacted?** The normal force application system is improved with this piece. The bolt will be constrained from rotating and will be able to travel the necessary distance.

**Who made the change?** Steve Lindsay

**Who authorized the change?** Gordon Krauss

## APPENDIX C: DESIGN ANALYSIS ASSIGNMENT

### Chassis Material Selection

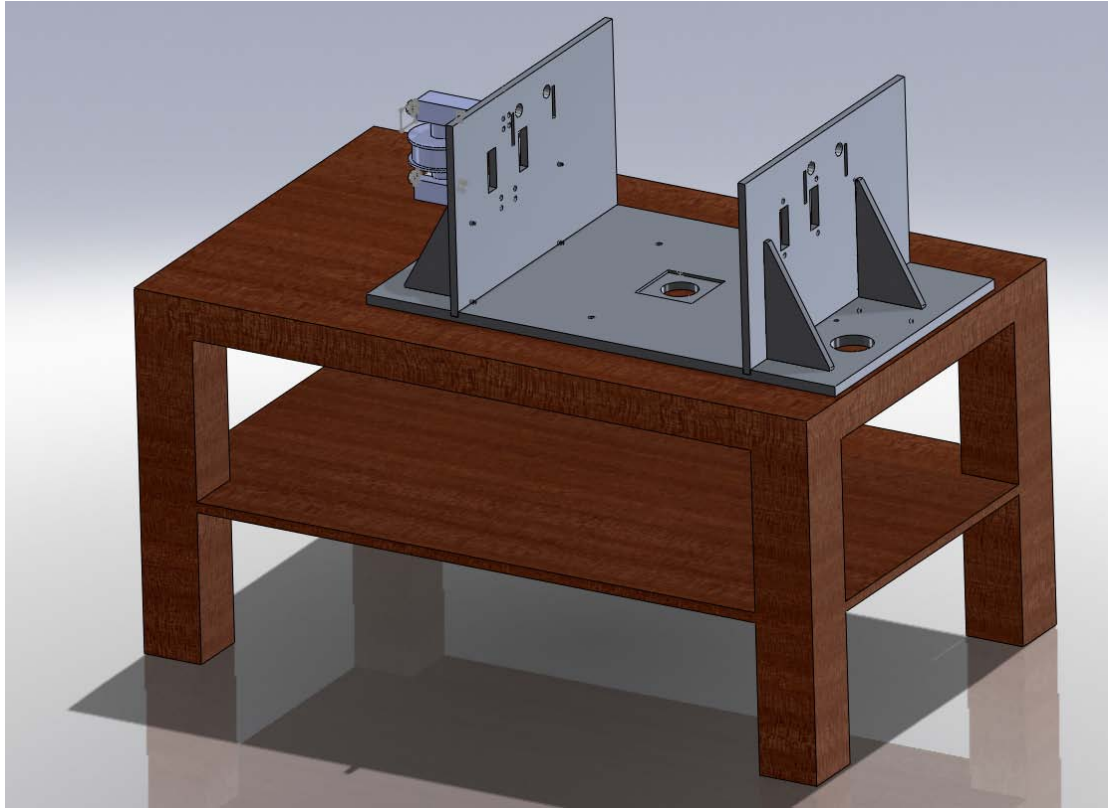


**Figure C1:** Full Chassis with aluminum side walls and rib supports

These sides are used to support the linear rails that the pin-gantry system is mounted to. These sides also support the motor, belt drive, and idler that are used to create the required linear motion. The sides must be able to withstand the cyclic forces that will be applied because of the force application performed by the pin-gantry system and the reciprocating motion. The sides must also be as light weight as possible so that the device is portable. These pieces also have many holes and slots that require the selected material to be machinable to high tolerances. These parts must also have a high stiffness and low cost. Finally, the sides must be able to withstand temperatures up to 150°C and high humidity. The first step that was taken to find the optimal material was to create a material indice. This is a process by which we create a parameter that consists of material properties that we want to maximize. In this case, we can start by using a parameter that is used to find the ratio of stiffness of a material to the density and cost of a material. The indice used is shown in the equation below where  $E$  is the Young's modulus,  $C_m$  is the cost of the material, and  $\rho$  is the density of the material.

$$M = \frac{E^5}{C_m \rho} \quad \text{Eq. C1}$$

By plotting this indice's denominator versus its numerator for several materials, we can determine how different materials compare to each other based on this parameter. The following figure shows a logarithmic graph of wide range of materials plotted against each other. The materials in the upper left corner of the graph are rated the highest on this parameter, while the materials in the lower right corner are the materials that rate the lowest.

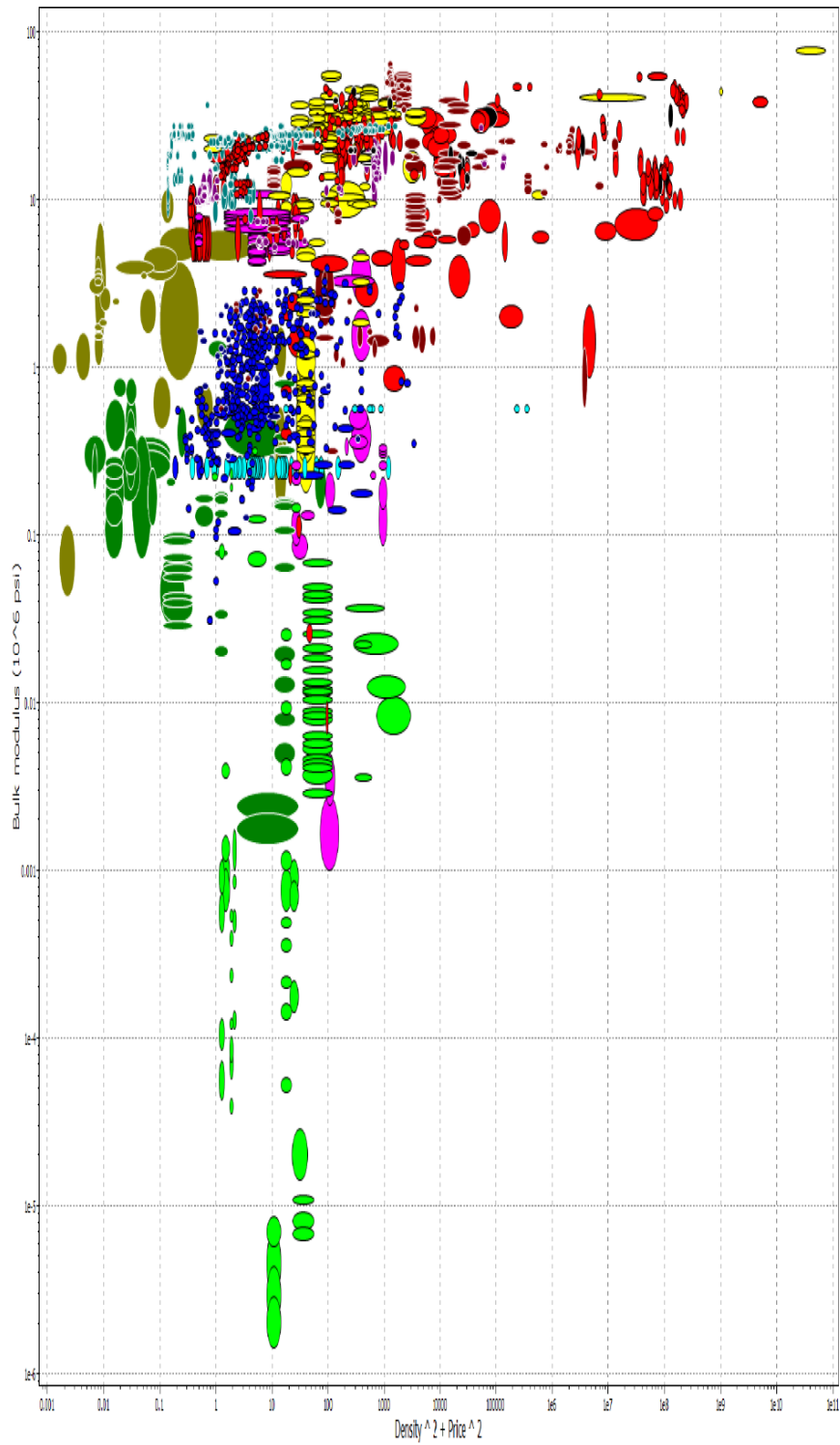


**Figure C2:** Comparison of Various Materials based on Material Index



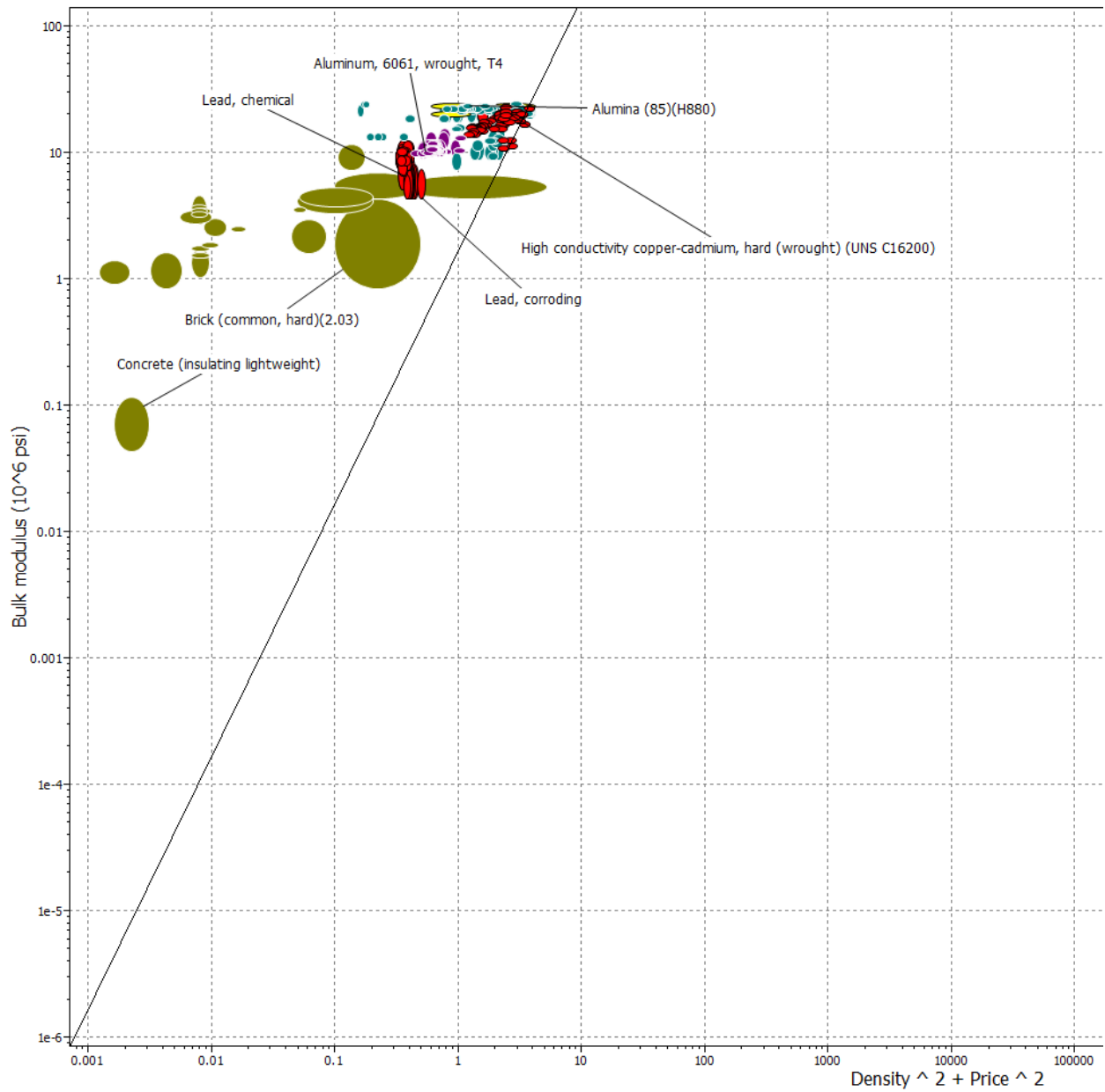


**Figure C3:** Comparison of Materials that can withstand the Expected Conditions Based on Material Index

From this process we can select five materials that have met the requirements that we have specified so far. These materials are Aluminum 6061, Copper-Cadmium, Alumina 85, Lead, and Concrete. We can then further analyze these materials based on some of the material properties already discussed as well as others. Significant properties are listed for these materials in Table C1.

**Table C1:** Comparison of Selected Materials

<b>Properties</b>	<b>Concrete</b>	<b>Cu-Cd</b>	<b>Alum 6061</b>	<b>Lead</b>	<b>Alumina 85</b>
<b>Yield Strength (KSI)</b>	.0145	49.3	28	.87	24.8
<b>Young's Modulus (MPSI)</b>	.087	48.3	9.86	1.89	35.4
<b>Fatigue Strength at 10<sup>7</sup> Cycles (KSI in<sub>1/2</sub>)</b>	.0218	32.6	30	.725	21.1
<b>Price (\$/lb)</b>	.0188	1.45	.713	.438	.752
<b>Density (lb/in<sup>3</sup>)</b>	.0325	.323	.0965	.409	.125
<b>Notes</b>	Low Wear Resistance	Not resistant to Acids	Used for Heavy Duty Structures	Poisonous	Only Machined by Water Jets

Using the information in Table C1, we decided that aluminum 6061-T4 is the best material to make the sides out of. This material maximizes stiffness to cost and density. It also has high fatigue strength and Young's modulus, while being able to withstand the expected conditions. Concrete was eliminated because of its low fatigue strength and its susceptibility to wear. Copper-cadmium was eliminated due to its not being able to withstand acids which may be used as lubricants and its high price. Lead was eliminated because it is poisonous to humans. Alumina was eliminated because it cannot be machined with mills as would be required for us to machine.

### **Chassis Sides Mass Production**

Due to the small demand for tribometers, we expect that only 100 of these devices would be sold if the device was made commercially available. This means that only 200 sides would be made in mass production. Due to a low amount of parts being made and the requirement for high tolerances, mass production of the sides would most likely be done on a CNC Mill. According to CES[16], aluminum 6061 can be easily machined on a mill. The process by which this would be done can be found in Appendix I. All required machining could be performed on this CNC Mill and would only require that the part be mounted in the mill twice. Once a program is written to do the machining, this part will require limited attention by an employee. For this reason, and the fact that most companies already own a CNC Mill, we believe this is the best option for mass producing this part.

## Pin Shaft Material Selection

This section will discuss, in detail, how the material was selected for the pin shaft of the pin gantry system. The shaft is pictured in the figure below.



**Figure C4: Pin Shaft**

The pin shaft of the tribometer performs multiple functions and is one of the most important parts of the design. The primary purpose of the shaft is to transmit a constant normal force between the ball at the tip of the shaft and the disk. It must also withstand the forces seen due to friction without deflecting more than  $1^\circ$  from vertical. The highest normal load that the shaft must be able to achieve is 200N, and the highest coefficient of friction applied is specified to be 1.5. Therefore, the shaft must be sufficiently strong to withstand these maximum specified loads. However, the pin shaft is also used to measure the forces by using strain gauges attached directly to the surface. Because strain gauges measure the forces by displacements on the surface, the shaft must be flexible enough to allow the measurement of very low normal and frictional loads. The tip of the shaft will also be exposed to the extreme environmental conditions of the environmental control box, so it must also be able to withstand temperatures from  $0^\circ$  -  $150^\circ$  C and 100% RH.

Appropriate material indices were derived by first determining which objectives and constraints were driving the design of the pin shaft. The shaft is subjected to both compressive and bending forces, however, the stresses due to bending are much greater than those seen from compression, so the pin was assumed to function as a beam. It was also assumed to have a circular cross-section because circular shafts can be evaluated quite easily and are commonly manufactured and sold in nearly all materials.

The objective was to minimize the weight of the beam because a light-weight pin gantry system will be less difficult to move in a linear reciprocating test. Two constraints were looked at – strength prescribed and stiffness prescribed. The pin beam must never plastically deform as this would ruin the alignment, force application, and force measurement aspects of the design. Therefore, a material index for a beam with minimum weight and strength prescribed, as given in Ashby's Materials Basics is:

$$M = \frac{\sigma_y^2}{\rho} \quad \text{Eq. C2}$$

Where  $\sigma_y$  is the yield stress and  $\rho$  is the material density. This index should be maximized to give the strongest, lightest beam possible. By plotting the numerator vs the denominator with CES, we are able to observe how different materials compare to each other with respect to strength and density. A plot of the graph is shown below.

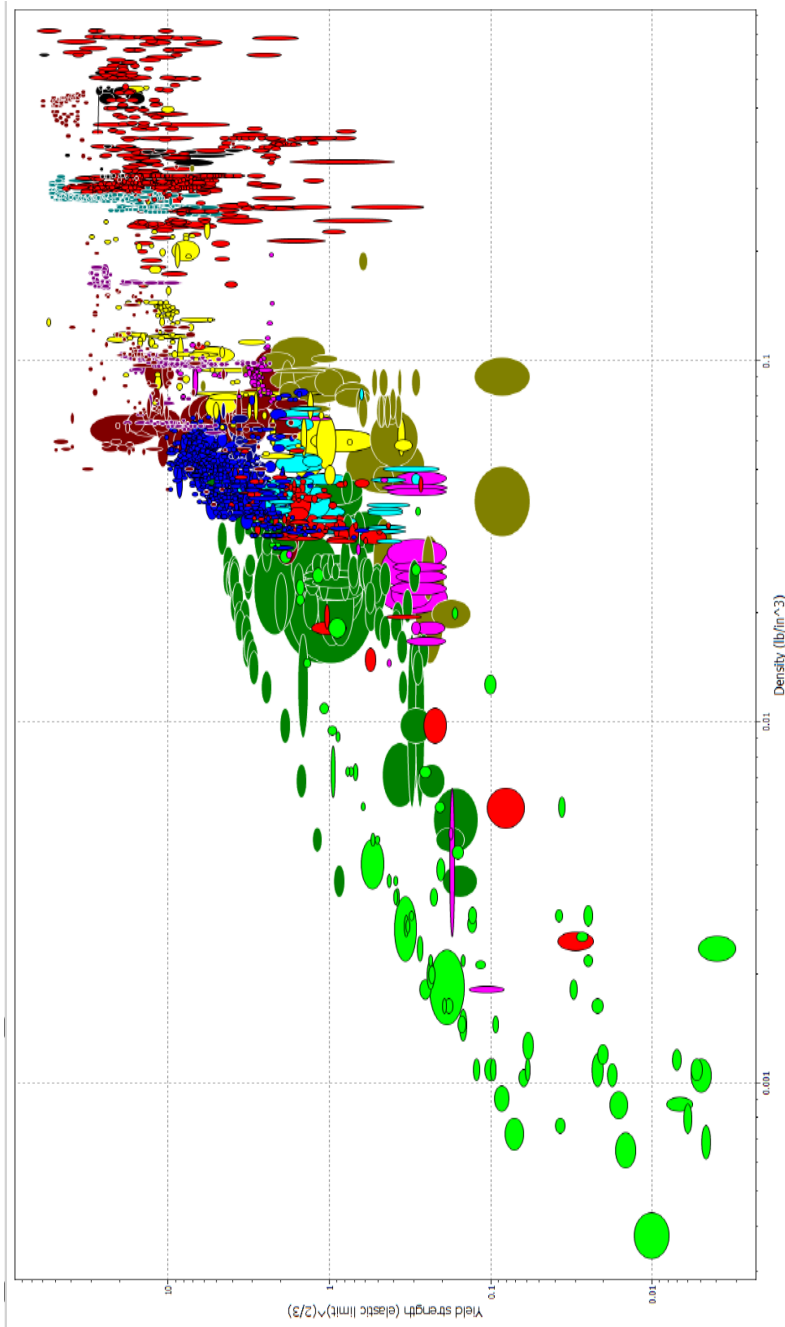


**FIGURE C5: GRAPH COMPARING MATERIAL INDEX**

corrosion resistance, and stiffness. A graph showing a reduced sample of suitable materials is shown below.

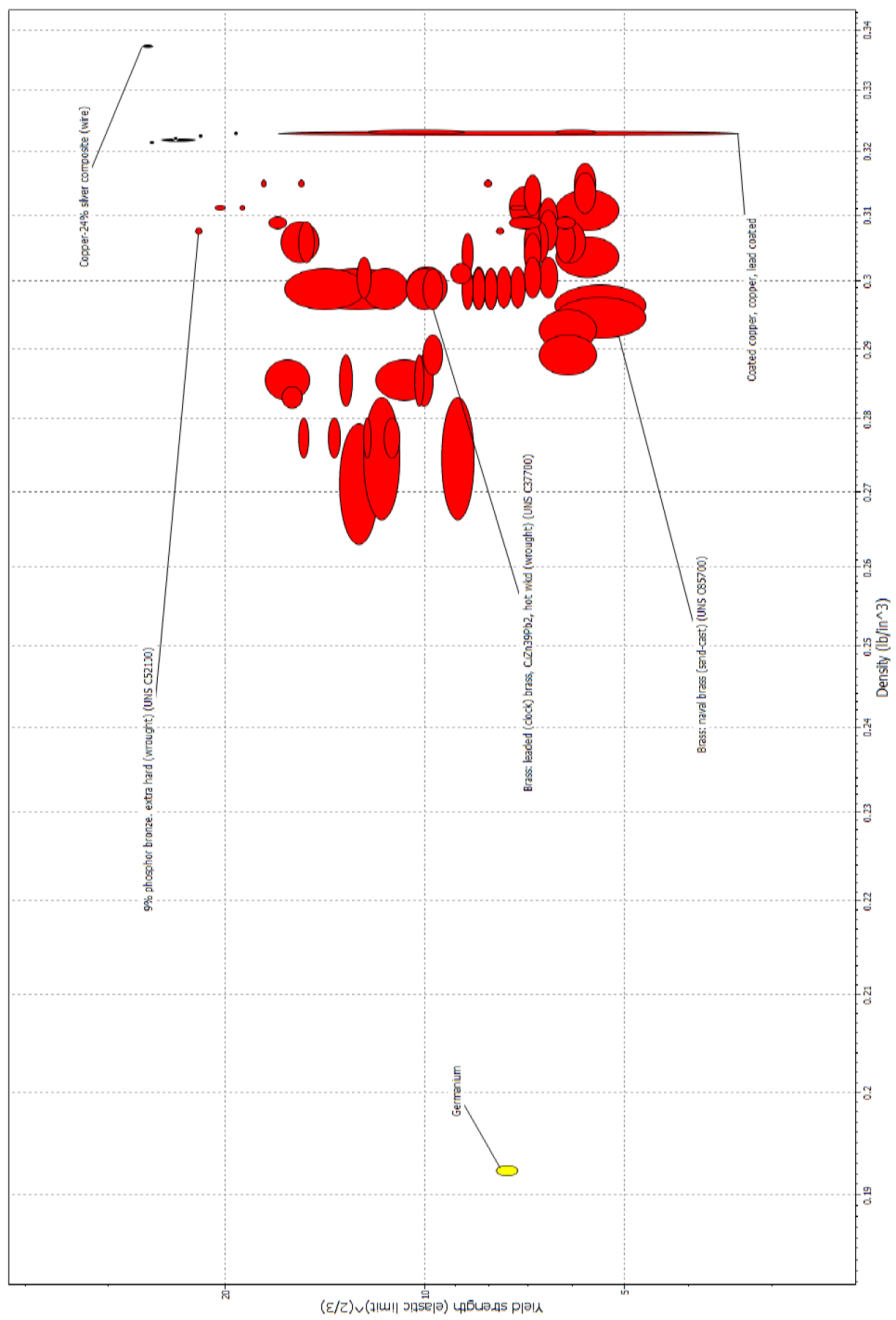


**Figure C6:** Comparison of suitable materials

After identifying which materials would be strong enough for the pin shaft, we then looked at the stiffness requirement. We did not want a beam that was too stiff and would not deflect enough, but it had to be stiff enough to achieve the specification of not deflecting more than 1° from vertical. By taking a safety factor

of 2 into account, we determined the minimum value of Young’s Modulus,  $E$ , that would allow the pin to deflect no more than  $0.5^\circ$  from vertical at the highest normal and frictional loads. The materials that had been previously identified for their high strength to weight ratios were then examined for their stiffness properties. A strong material with a Young’s Modulus that was as low as possible without deflecting too much was desired. The top five materials identified using the CES software are displayed below.

**Table C2: Comparison of top 5 materials for pin**

<b>Properties</b>	<b>Bronze Alloy 544</b>	<b>Manganese Bronze, C86500</b>	<b>Aluminum Bronze E, forged</b>	<b>Naval Brass</b>	<b>Silicon Bronze CuSi3Mn1</b>
<b>Yield Strength (KSI)</b>	60	24.9	36.3	10.2	65.3
<b>Young’s Modulus (MPSI)</b>	15	14.9	16.7	13.8	14.8
<b>Fatigue Strength at <math>10^7</math> Cycles (KSI in<math>_{1/2}</math>)</b>	34.5	21.8	35.1	18.9	33.4
<b>Price (\$/lb)</b>	1.62	1.04	1.57	1.15	1.43
<b>Density (lb/in<math>^3</math>)</b>	.321	.299	.275	.292	.308
<b>Notes</b>	Easily machinable.	Parts in contact w/ salt and fresh water	Used in marine shafts	Sand cast	Hard (wrought)

The final choice for the pin shaft was Bronze Alloy 544. It was chosen because it was strong enough to withstand the highest loads seen in our application, while also deflecting enough to allow the measurement of very low loads. It is also corrosion resistant and able to function in the temperature ranges that it will be exposed to in our device. What sets it apart from the other materials in the table is that it is readily available, and highly machinable. It is a little more expensive than the other materials, but less than 0.5 lbs of the material is required for the shaft in our design.

**Pin Shaft Mass Production**

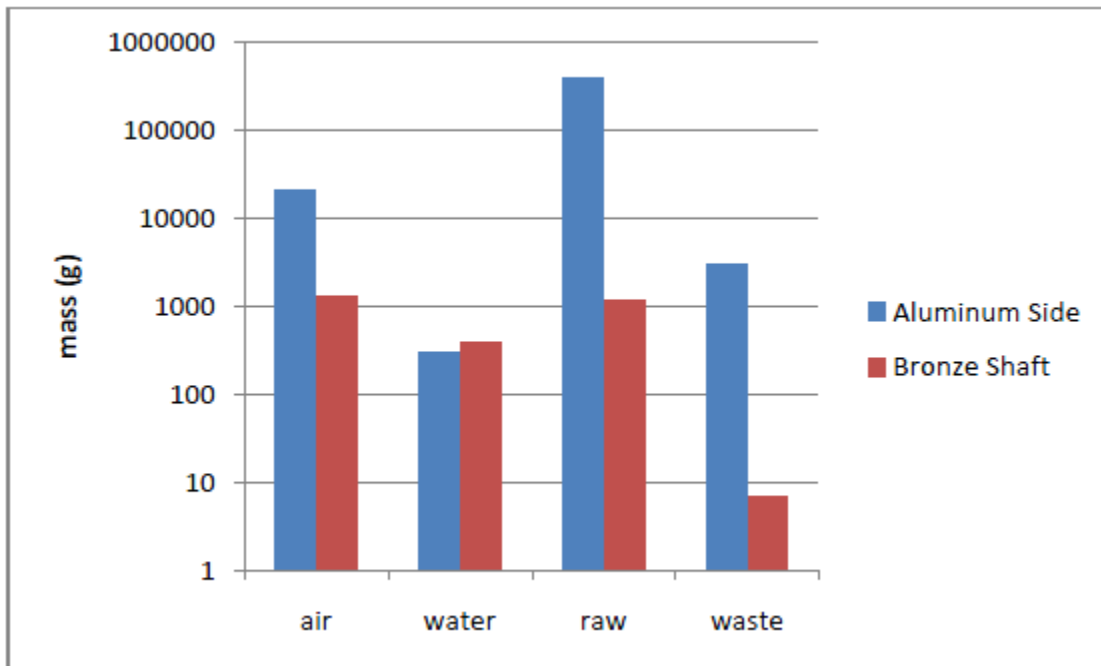
Due to the small demand for tribometers, we expect that only 100 of these devices would be sold if the device was made commercially available. This means that only 100 pin shafts would be made in mass production. Due to the low amount of parts being made and the requirement for high tolerances, mass production of the shafts would most likely be done on a lathe and CNC Mill.

According to both the CES[16] software and the supplier’s website [15], bronze 544 can be easily machined. The process by which this would be done can be found in Appendix I. The machining to be performed on the lathe would be performed first, and then the part would be finished on a CNC Mill, in a rotational chuck. Once a program is written to do the machining, this part will require limited attention by an employee. For this reason, and the fact that most companies already own lathes and CNC Mills, we believe this is the best option for mass producing this part.

## Environmental Performance

To analyze the environmental impact of the selected materials we used a program called SimaPro. This program allows you to select materials, put in the weight of those materials, and it gives you the ways that those materials impact the environment and how much of an impact they have.

The first thing we did was to see how much air emissions, water emissions, raw materials, and solid waste would be created by each part. A graph logarithmic graph showing this can be found below. This graph indicates that the aluminum sides create a lot of damage to the environment, most significantly in raw materials. Most of the mass in the raw materials section is the water that is used in making the materials.



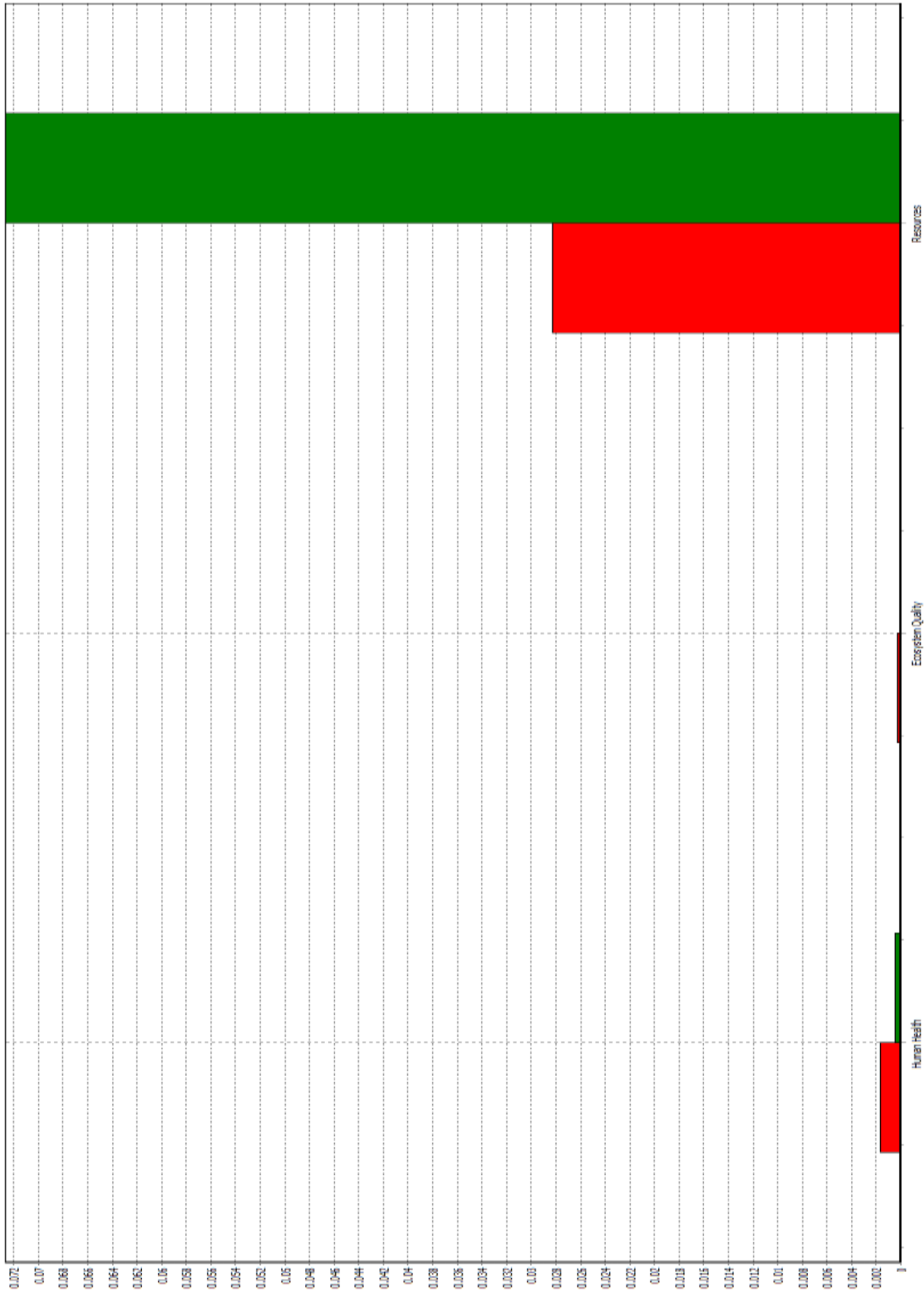
We then graphed E199 impact categories. This graph shows how the two materials compare in these categories. The material with the most impact is shown as 100% and the other material is shown in percentage of the one with the most impact. This graph shows that again the aluminum sides will make more of an environmental impact than the bronze shaft. This is true in every category except for minerals. This graph is shown on the next page.

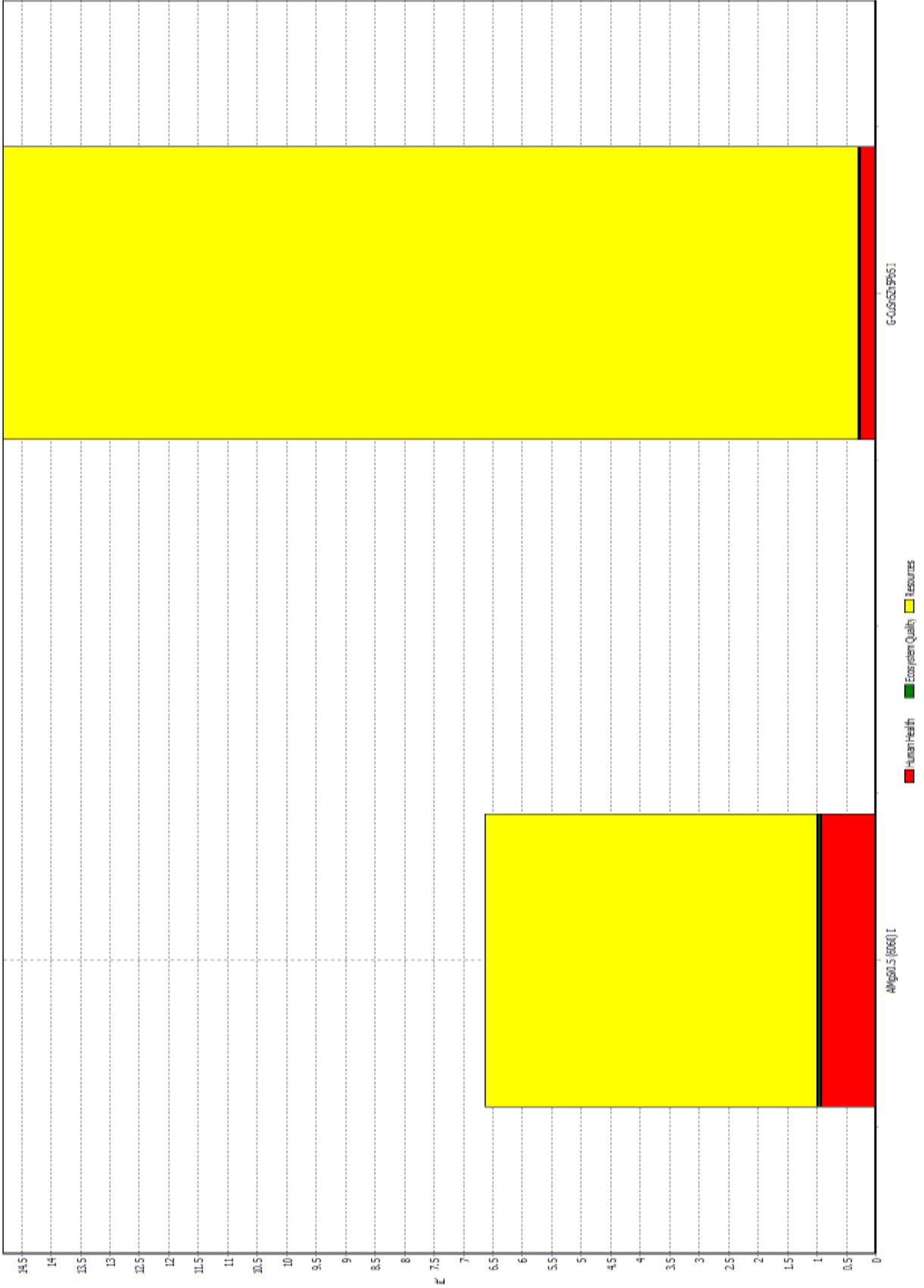
We also create a graph that shows the normalized “meta-categories.” These categories include the impact on human health, the ecosystem, and resources. The categories are plotted versus the percentage of damaged caused by an average European in one year. This graph, on Pg. 103 shows that the resources used to make both parts are more significant than the damage caused to human health or ecosystem quality and even this impact is significantly less than 1%.

Lastly, we made a chart showing how each material scores in total E199 points. This chart is shown on Page 104 and indicates that the bronze shaft has more of an environmental impact due to its use of resources.









After considering all the things, we can still consider what will happen to the device over its life cycle. For both of these products, a long life time is expected, with the shaft having a lesser life time. This is because it will see large cyclic loading and eventually break. When this happens, the shaft will need to be replaced, but the old shaft can be melted down and recycled. The same can be done with the aluminum sides when the tribometer will no longer be used. Because the shaft will most likely need to be replaced several times over the lifetime of a tribometer, we have determined it will have more of an environmental impact; however, overall, neither material will make a significant impact to the environment because very few tribometers are expected to be built.

## APPENDIX D: MOTOR CONTROL CODE

### CONTROLLER LOGIC

This section will explain the mechanisms and logic used to control the motion and force generation of our tribometer.

#### **Running the Stepper Motors**

A stepper motor is driven by rapidly changing the polarity of the steps within the motor. Both of the stepper motors we used were supplied with drivers that expect digital pulse input to dictate the rate of step polarity change. That means that in order to make the motor advance one step, the pulse input on the driver must receive one rising edge (0 to 5 V change) followed by one falling edge (5 V to 0 change). The speed of the motor is determined by rapidly this digital input changes.

In addition to pulse commands, the stepper motor drivers expect two other digital control inputs: direction and enable. “Direction” simply controls which way the motor rotates. A digital “HIGH” value will cause rotation in one direction while a digital “LOW” value will cause rotation in the other direction. “Enable” controls whether or not the motor will accept inputs. If the motor is not given an “Enable” command, it should not spin. It should be noted, however, that the proper “Enable” command is not always the digital “HIGH” state. It will depend on whether or not the input signals are set up to source current or to sink current. The wiring diagrams supplied with each driver will specify how to set up both sinking and sourcing configurations. Caution should be exercised if the motor is wired such that it is enabled with a digital “LOW” input.

A simple code to drive one of our stepper motors with an Arduino board is shown in Figure D1. This code also contains logic to reverse the direction of motion after 800 steps. This corresponds to two revolutions, as we had our 200 steps/rev motors driven by ½ step microstepping.

```

/*
Stepper motor tester
Bob Chlum
March 2010
Runs the motor forward one revolution, reverse one revolution, repeats
*/

// Digital I/O Pins

int Pul = 31;    // position increment/decrement line
int Dir = 33;    // direction line
int Enable = 35; // arms motor

// State Variables

int dirVec = 0; // direction of rotation
int count = 0; // step count (indicates position)

void setup() {
  // initialize output pins
  pinMode(Pul, OUTPUT);
  pinMode(Dir, OUTPUT);
  pinMode(Enable, OUTPUT);
  // set output defaults
  digitalWrite(Pul, HIGH); // no pulse signal
  digitalWrite(Dir, dirVec); // default direc. set to val. given in var. def.
  digitalWrite(Enable, LOW); // Motor defaults to "on"
}

void loop() {
  // run motor:
  digitalWrite(Pul, LOW); // rising edge
  delayMicroseconds(600); // .6 ms
  digitalWrite(Pul, HIGH); // falling edge
  delayMicroseconds(600); // .6 ms
  count++; // Advance step counter
  // After one revolution (if 10000 steps = 1 rev), reverse direction
  if(800 <= count) {
    count = 0; // reset counter
    dirVec = dirVec ^ 1; // Flip direction variable
    digitalWrite(Dir, dirVec); // Output new direction
  }
}

```

**Figure D1:** Basic stepper motor control code

The main problem with the code in Figure D1 above is that it uses “delay” commands. These become very problematic in larger programs, as delays cause the processor to do nothing during the specified time of the delay. In order to execute code that can do more than drive one open-loop stepper motor, the processor will need to be able to execute other operations during the pause between pulse changes. The code in Figure D2 below drives a stepper motor with exactly the same motion as Figure X above, but without use of any “delay” commands.

```

/*
Stepper motor tester without delay() commands
Bob Chlum
March 2010
Runs forward 2 revs, then reverses
*/

// Define I/O pins
int Pul = 37;          // Pulse generator (LOW = step high)
int DirSTEP = 39;     // direction line (LOW = ?CW)
int EnableSTEP = 41; // run-stop line (LOW = ENABLE)

// State variables
int direcstep = 0;    // rotation direction (0 = pin down)
int Step = 0;         // Pulse state
int count = 0;        // Step counter
unsigned long StepTime = 0; // time since last step
unsigned long StepLast = 0; // time of last step

void setup() {
  // initialize output pins
  pinMode(Pul, OUTPUT);
  pinMode(DirSTEP, OUTPUT);
  pinMode(EnableSTEP, OUTPUT);
  // set output defaults
  digitalWrite(Pul, Step);          // step high
  digitalWrite(DirSTEP, direcstep); // direction
  digitalWrite(EnableSTEP, HIGH);   // motor enabled
}

void loop() {
  // run stepper at 1 RPM (200 step/rev)
  StepTime = micros() - StepLast; // Calculate time since last half-step
  if(200 <= StepTime) {           // Check if its time to advance
    digitalWrite(Pul, Step);      // Send motor new signal
    StepLast = micros();          // Reset time of last half-step
    if(0 == Step) {               // Check for full step
      count ++;                   // Update step counter
    }
    Step = Step ^ 1;              // Flip step state
  }
  if(800 <= count) {              // Check if 2 revs have finished
    direcstep = direcstep ^ 1;    // Flip direction var
    digitalWrite(DirSTEP, direcstep); // Flip direction
    count = 0;                    // Reset counter
  }
}

```

**Figure D2:** Stepper control without delay commands

Another challenge in controlling stepper motors is that they cannot snap to desired speeds. The motor needs to be able to physically advance to the desired step before the next pulse change occurs, otherwise the motor may stall. If a motor is connected to a system with too much friction or inertia, the time it takes to accelerate will be slower, and so the motor will need to be “ramped up” to the desired speed so that pulse changes do not out-accelerate the motor rotor. Figure D3 below provides coding which gradually ramps of the speed of a stepper motor. This code was successfully implements on our disk-sample-driving motor while it was attached to its gear train and the disk.

```

/*
Stepper ramp program
Bob Chlum
April 2010
Starts the motor slowly and then increases speed.
*/

// Define I/O pins
int PulB = 31;      // Pulse generator
int DirB = 33;      // Direction line
int EnableB = 35;   // run-stop line

// State variables
unsigned int wait = 2400; // Initial pulse delay [us]
unsigned int countB = 0;  // step counter
unsigned long STB = 0;    // time since last step
unsigned long SLB = 0;    // time of last step
int Step = 0;            // Step state

void setup() {
  // Initialize I/O pins
  pinMode(PulB, OUTPUT);
  pinMode(DirB, OUTPUT);
  pinMode(EnableB, OUTPUT);
  // Set output defaults
  digitalWrite(PulB, HIGH); // No pulse signal
  digitalWrite(DirB, HIGH);
  digitalWrite(EnableB, LOW); // Motor defaults to 'on'
}

void loop() {
  STB = micros() - SLB; // Calculate time since last step
  if(wait <= STB) {     // Check if its time to advance
    digitalWrite(PulB, Step); // Advance a step
    SLB = micros();        // Reset time of last step
    Step = Step ^ 1;       // Flip step state
    countB ++;            // Advance step counter
  }
  if(601 <= wait) {
    if(4 <= countB) {
      wait = wait - 4; // Decrease pulse delay
      countB = 0;      // Reset step counter
    }
  } else if(401 <= wait) {
    if(8 <= countB) {
      wait--; // Decrease pulse delay (less aggressive)
      countB = 0;
    }
  }
}
}

```

**Figure D3:** Stepper motor ramp program

A disadvantage of all of the code that has been presented thus far is that it executes as soon as it is finished compiling on the Arduino board. Figure D4 below shows a way to run the ramp program from Figure D3 above only when a specific command is entered into a connected laptop.

```

/*
Stepper ramp program
Bob Chlum
April 2010
Starts the motor slowly and then increases speed
w/ serial interface
*/

// Define I/O pins
int PulB = 31;      // Pulse generator
int DirB = 33;      // Direction line
int EnableB = 35;   // run-stop line

// State variables
unsigned int wait = 2400; // Initial pulse delay [us]
unsigned int countB = 0; // step counter
unsigned long STB = 0;    // time since last step
unsigned long SLB = 0;    // time of last step
int Step = 0;            // Step state
unsigned int cmdKey = 0;  // User input variable
unsigned int terma = 0;   // Termination variable (from user)
unsigned int term = 0;    // Termination flag

void setup() {
  // Initialize I/O pins
  pinMode(PulB, OUTPUT);
  pinMode(DirB, OUTPUT);
  pinMode(EnableB, OUTPUT);
  // Set output defaults
  digitalWrite(PulB, HIGH);
  digitalWrite(DirB, HIGH);
  digitalWrite(EnableB, LOW);
  Serial.begin(9600); // Begin serial comm. with computer
}

void loop() {
  if(Serial.available() > 0) { // Check if the user has send a command
    cmdKey = Serial.read();    // Store user command in cmdKey
  } else {
    cmdKey = 0;                // If no user input, set 0
  }

  switch(cmdKey) { // User command option switch
    case 'b':
      while(term != 1) {
        STB = micros() - SLB; // Calculate time since last step
        if(wait <= STB) { // Check if its time to advance
          digitalWrite(PulB, Step); // Advance a step
          SLB = micros(); // Reset time of last step
          Step = Step ^ 1; // Flip step state
          countB++; // Advance step counter
        }
        if(601 <= wait) {
          if(4 <= countB) {
            wait = wait - 4; // Decrease pulse delay
            countB = 0; // Reset step counter
          }
        } else if(401 <= wait) {
          if(8 <= countB) {
            wait--;
            countB = 0;
          }
        }
        terma = Serial.read();
        if('s' == terma) { // Check for termination cmd. from user
          term = 1; // Set term flag
        } else {
        }
      }
      break;
    default: // If no user input, do nothing
      break;
  }
}

```

**Figure D4:** Stepper ramp program with serial user input

### **Normal Force Motor with Feedback**

The code shown in Figure D5 below is the logic developed to provide feedback control for the normal force applied to the pin. This code is quite crude due to the high levels of noise we were getting from the strain gauges. Before this code can be tuned, the strain gauges measuring the pin compression (or, more accurately, the Op Amps processing the signal from said strain gauges) must be fine tuned to produce steady and readable outputs. Additionally, there should to be a way to average the inputs from the strain gauges to condition out noise, where this code only takes random samples at 100 millisecond intervals. However, this code does work, if roughly.

It should be noted that the normal force calculation and feedback logic can severely hinder the performance of the Arduino board.. The “analogRead()” command takes about 100 microseconds to execute, which is a huge amount of time in the scope stepper motor control. This doesn’t cause a huge problem in the code in Figure D5, but when the Arduino needs to control multiple motors, this time loss will cause large problems.



```

/*
Feedback control for normal force application
Bob Chlum
April 2010
WARNING: Do not use run this program for long periods of time
until you have validated the strain gauge outputs and the force
calculations in this code.
WARNING: Check that the right direction vars are used
*/

#include <math.h> // Math library

// Define I/O pins
int Pul = 37; // Pulse generator (LOW = step high)
int Dir = 39; // Direction line
int Enable = 41; // run-stop line (LOW = high)
int Gauge = 15; // Strain gauge line

// State variables

double SVolt = 0; // Gauge reading
double F = 0; // Applied normal force (measured)
double Fwant = 40; // Desired normal force
double Fhigh = Fwant+8; // Acceptable force upper bound
double Flow = Fwant-8; // Acceptable force lower bound
double Gain = 200; // OpAmp gain
double GF = 9; // Gauge factor
double Vr = 0;
double Strain = 0; // Strain
double creep = 0; // creep rate
double Voff = 0; // Total voltage offset
long E = 103000; // Young's modulus [MPa]
double R = 6.41; // pin radius [mm]
double v = 0.34; // pin Poisson's ratio
double Vunstr = 2.32; // Unstrained SVolt reading
int Vex = 5; // Gauge supply voltage
double D = 2*R; // pin diameter
unsigned long STF = 0; // time since last force motor step
unsigned long SLF = 0; // time of last force motor step
int StepF = 0; // Pulse state
unsigned long Ctime = 0; // time since last force calc
unsigned long Clast = 0; // time since of last force calc

void setup() {
// initialize output pins
pinMode(Pul, OUTPUT);
pinMode(Dir, OUTPUT);
pinMode(Enable, OUTPUT);
pinMode(Gauge, INPUT);
// set output defaults
digitalWrite(Pul, HIGH); // no pulse signal
digitalWrite(Dir, LOW);
digitalWrite(Enable, HIGH); // Motor defaults to 'on'
}

Serial.begin(9600); // serial comm with computer

}

void loop() {
// Determine currently applied normal force
Ctime = millis()-Clast;
if(100 <= Ctime) {
Clast = millis();
SVolt = analogRead(Gauge)/204.6; // Read strain gauge
Voff = Vunstr+creep*millis()/1000;
Vr = (SVolt-Voff)/Vex;
Strain = ((-2*Vr)/(GF*((1+v)-Vr*(v-1))))/Gain;
F = (Strain*3.14159*D*D*E)/8-24;
Serial.print(F, DEC); // Display force reading
Serial.print("\t");
}

if(Flow >= F) { // Determine if applied force is too low
STF = micros() - SLF; // Calculate time since last 1/2 step
digitalWrite(Dir, HIGH); // Set direction [CHECK THIS!]
if(200 <= STF) {
digitalWrite(Pul, StepF); // Advance force motor 1/2 step
SLF = micros(); // Reset time of last 1/2 step
StepF = StepF ^ 1; // Flip step state
}
} else if(Fhigh <= F) { // Determine if applied force is too high
STF = micros() - SLF; // Calculate time since last 1/2 step
digitalWrite(Dir, LOW); // Set direction [CHECK THIS!]
if(200 <= STF) {
digitalWrite(Pul, StepF); // Advance force motor 1/2 step
SLF = micros(); // Reset time off last 1/2 step
StepF = StepF ^ 1; // Flip step state
}
} else {
}
}
}

```

**Figure D5:** Normal force motor feedback control

## Running the DC Motor

Similar to the stepper motors, the DC motor was supplied with a driver that powers the motor based on simplified inputs. There are four main inputs to be concerned with for control programming: speed, direction, freewheel, and enable (marked “run-stop” on the driver).

The driver expects the speed input to come in the form of a 10 kilo-Ohm potentiometer connected to three “Pot” pins. We planned send speed inputs to the driver using a pulse-width modulated (PWM) output pin on the Arduino board, along with an optical isolator and a low-pass filter, as shown in the schematic in Figure D6. However, we had trouble getting the isolator to work properly, so we conducted the bulk of our testing by plugging a physical 10K potentiometer into the driver “Pot” pins.

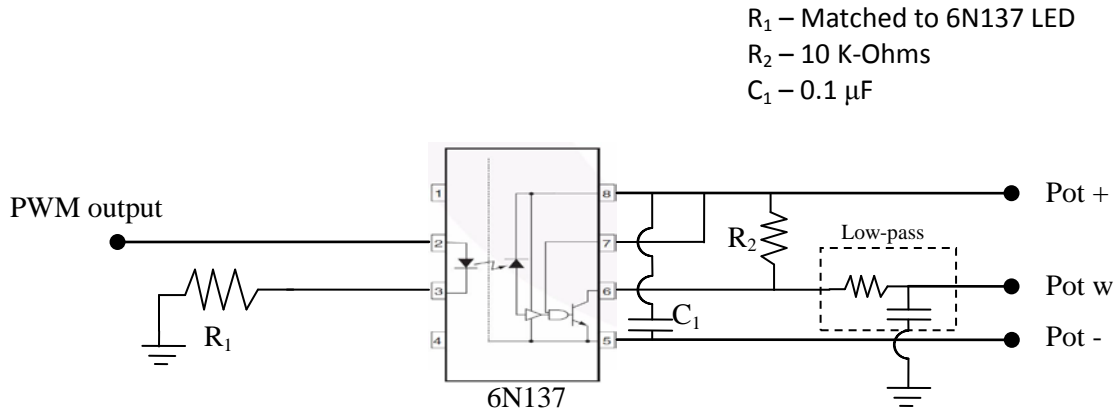


**Figure D6:** Schematic diagram of opto-isolator circuit to join controller PWM to driver “Pot”

The direction input works the same as it did on the stepper motor driver. A digital “HIGH” value causes the motor to rotate counter-clockwise and a digital “LOW” value causes the motor to rotate clockwise.

The freewheel input provides for the ability for the motor to coast. When a digital “HIGH” value is passed to this input, the motor will no longer accept speed input and will coast. The driver documentation warns that it is bad to change the direction variable during motor operation. This is because at high speeds, the inertia of the motor is large enough that the resulting back-EMF sudden direction changes could damage the circuitry of the driver. To account for this issue, we used the freewheel option extensively to bring the motor to a low speed before switching the direction.

The enable (run-stop) input works the same as it did on the stepper motor drivers. The driver will run the motor when passed a digital “HIGH” value, and it will stop the motor when passed a digital “LOW” value. It should be noted that changing the enable state to “LOW” during operation does not produce the same result as using the freewheel function. Changing the enable state to low will cause the motor to stop very rapidly. When operating at high speeds, the freewheel function should be used to bleed off speed before the enable state is changed to “LOW”.

Figure D7 below shows the code we used to verify the functionality of the DC motor and driver. It contains a serial switch case which allows the user to specify several different options. The user can choose to run the motor at constant speed, coast and then stop the motor, and change the direction of rotation of the motor.

```

/*
DC motor tester
Bob Chlum
March 2010
Runs the motor forward, then backwards, repeats
Speed is controlled with an external 10K potentiometer
*/

// Define I/O pins
int Dir = 23; // Direction line (HIGH = CCW)
int Frwhl = 25; // Run-stop line (HIGH = ENABLE)
int Enable = 27; // Freewheel line (HIGH = COAST)

// Define variables
int direc = 0; // direction, defaults to CW
unsigned long Time = 0; // Time operation has been running
volatile unsigned int cmdKey = 0; // User input variable

void setup() {
  // initialize output pins
  pinMode(Dir, OUTPUT);
  pinMode(Enable, OUTPUT);
  pinMode(Frwhl, OUTPUT);
  // set output defaults
  digitalWrite(Dir, direc); // Sets initial rotation direction
  digitalWrite(Enable, LOW); // Motor initially disabled
  digitalWrite(Frwhl, LOW); // Driver initially accepts speed inputs
  Serial.begin(9600); // Begin serial comm. with computer
}

void loop() {
  if (Serial.available() > 0) { // Check if user has sent a command
    cmdKey = Serial.read(); // Store user command
  } else {
    cmdKey = 0; // If no user input, store 0
  }

  switch(cmdKey) { // User command switch
    // Run motor
    case 'g':
      digitalWrite(Frwhl, LOW); // For input g, set motor to run
      digitalWrite(Enable, HIGH);
      break;
    // Coast, then stop motor
    case 'f':
      digitalWrite(Frwhl, HIGH); // For input f, coast motor
      delay(1000);
      digitalWrite(Enable, LOW); // ...then stop motor.
      break;
    // Run motor for 5 seconds
    case 't':
      digitalWrite(Frwhl, LOW); // For input t, run for 5 seconds
      digitalWrite(Enable, HIGH);
      delay(5000);
      digitalWrite(Frwhl, HIGH); // ... then coast for 5 seconds
      delay(5000);
      digitalWrite(Enable, LOW); // ... then stop.
      break;
    // Change direction (motor must then be restarted)
    case 'd':
      digitalWrite(Frwhl, HIGH); // For input d, coast for 3 seconds
      delay(3000);
      digitalWrite(Enable, LOW); // ... then stop.
      direc = direc ^ 1; // Flip the direction variable
      digitalWrite(Dir, direc); // Output the new direction
      break;
    // Quick change direction (no coast stage)
    // This case should only be run after stopping the motor
    case 'dq':
      direc = direc ^ 1; // Flip the direction variable
      digitalWrite(Dir, direc); // Output the new direction
      break;
    // Motor reset (toggles enable state)
    case 'reset':
      digitalWrite(Enable, LOW); // Toggle enable state
      delay(50); // Allow time for driver to toggle
      break;
    // Default case
    default:
      break; // No input => do nothing
  }
}

```

**Figure D7:** Code for testing the DC motor (without speed control)

## **Reading the Optical Encoder**

In order to have position control over a DC motor, we need to have a position feedback mechanism. We implemented a 1000 ppr (pulses per revolution) two channel optical encoder to provide this feedback. The code we used to read the encoder can be seen in Figure D8 below. The code is based on interrupts. By using interrupts, the code to calculate and update position only runs when the input from one of the encoder changes. This increases the processing efficiency of the board, because the encoder functions stay hidden except for when the encoder signals actually change. The code in Figure D8 was provided for us by Professor Brent Gillespie. We tested this code by running the DC motor for a specific number of revolutions and then calling for the encoder position through the serial monitor. This test produced no discernable errors in the encoder measurement.

```

/*
Optical encoder reader using interrupts
Provided by Professor Brent Gillespie
Edited by Bob Chlum
April 2010
*/

// ISR pins on Arduino Mega
#define ENCPINA 21 // Encoder Channel A
#define ENCPINB 20 // Encoder Channel B
// Define variables
volatile unsigned int cmdKey=0; // For serial input
volatile int encPos=0; // Encoder position

void setup() {
  pinMode(ENCPINA, INPUT);
  pinMode(ENCPINB, INPUT);
  digitalWrite(ENCPINA, HIGH);
  digitalWrite(ENCPINB, HIGH);
  // Attach interrupts - readsEncoder interrupts 'loop' when encoder input changes
  attachInterrupt(2, readEncoderA, CHANGE);
  attachInterrupt(3, readEncoderB, CHANGE);
  Serial.begin(9600);
}

void loop(){

  if (Serial.available() > 0) // Checks for user input
    cmdKey = Serial.read();
  else
    cmdKey = 0;

  switch(cmdKey){
    // User input 'a' returns the current encoder position to the serial monitor
    case 'a':
      Serial.print(encPos,DEC);
      Serial.print("\n");
      break;
    // User input ' ' zeroes encoder position
    case ' ':
      encPos=0;
      break;
    default:
      break;
  }
}

// Updates the measured position whenever encoder signal A changes
void readEncoderA(){
  if(digitalRead(ENCPINA) ^ digitalRead(ENCPINB))
    encPos--;
  else
    encPos++;
}

// Updates the measured position whenever encoder signal B changes
void readEncoderB(){
  if(digitalRead(ENCPINA) ^ digitalRead(ENCPINB))
    encPos++;
  else
    encPos--;
}

```

**Figure D8:** Code to read the optical encoder

### **Running a Linear-Reciprocating Pattern with the DC Motor**

After successfully implementing code to run the DC motor and to read the optical encoder, we then combined the two to create a code that could run a repeating pattern upon to form the basis of a linear reciprocating test. This code can be seen in Figures X and X below.



```

break;
// Case r runs the motor at constant speed
case 'r':
digitalWrite(Dir, direc);
digitalWrite(Frwhl, LOW);
digitalWrite(Enable, HIGH);
break;
// Case a returns the measured encoder position
case 'a':
Serial.print(encPos,DEC);
Serial.print("\t");
break;
// Case f coasts then stops the motor
case 'f':
digitalWrite(Frwhl, HIGH);
delay(1000);
digitalWrite(Enable, LOW);
break;
// Case d stops the motor and flips the direc. command
case 'd':
digitalWrite(Frwhl, HIGH);
delay(3000);
digitalWrite(Enable, LOW);
direc = direc ^ 1;
digitalWrite(Dir, direc);
break;
// Encoder interrupt for channel A
void readEncoderA() {
  if(digitalRead(ENCPINA) ^ digitalRead(ENCPINB)) {
    encPos--;
  } else {
    encPos++;
  }
}
// Case dq flips the direction command
case 'dq':
direc = direc ^ 1;
digitalWrite(Dir, direc);
break;
// Resets the program
case 'reset':
digitalWrite(Enable, LOW);
encPos = 0;
break;
// No case -- do nothing
default:
break;
}
}
}
// Encoder interrupt for channel B
void readEncoderB() {
  if(digitalRead(ENCPINA) ^ digitalRead(ENCPINB)) {
    encPos++;
  } else {
    encPos--;
  }
}
}
}

```

**Figure D10:** Linear reciprocating motion code, Part 2 of 2

### **Generating 2D Paths**

We attempted to combine the control coding for all three motors to try to generate two-dimensional wear paths, but the Arduino board could not execute the code fast enough. The time required for all of the individual tasks was greater than the time delay between pulse changes for the stepper motors, and as a result the stepper motors could not spin at the desired speeds. During our test, the disk sample motor stalled completely, as the timing problems severely threw off the ramp program. As a reference, the combined code that we attempted to execute is included here as Figure X.

```

/*
2D wear path test code
Bob Chlum
April 2010
Attempts to run all three motors (w/ force & position feedback)
Note: This code is for achival purposes only -
THIS DOES NOT WORK!
*/

// Define I/O pins
#define ENCPINA 21
#define ENCPINB 20
int Dir = 23; // Direction line (LOW = CCW) Digital output
int Frwhl = 25; // Run-stop line (LOW = ENABLE) Digital output
int Enable = 27; // Freewheel line (LOW = COAST) Digital output

// Define variables
int direc = 1;
volatile unsigned int cmdKey = 0;
volatile long encPos = 0;
volatile int count = 0;
int wait = 50;
volatile unsigned int encVar = 0;
volatile unsigned int turnVar = 0;
volatile unsigned long time = 0;

// Define I/O pins
int Pul = 37; // Pulse generator (LOW = step high)
int DirF = 39; // Direction line
int EnableF = 41; // run-stop line (LOW = high)
int Gauge = 15; // Strain gauge line

// State variables (force feedback)
double SVolt = 0; // Gauge reading
double F = 0; // Applied normal force (measured)
double Fwant = 5.667*9.81; // Desired normal force
double Fhigh = Fwant+8; // Acceptable force upper bound
double Flow = Fwant-8; // Acceptable force lower bound
double Gain = 200; // OpAmp gain
double GF = 9; // Gauge factor
double Vr = 0;
double Strain = 0; // Strain
double creep = 0; // creep rate
double Voff = 0; // Total voltage offset
long E = 103000; // Young's modulus [MPa]
double R = 6.41; // pin radius [mm]
double v = 0.34; // pin Poisson's ratio
double Vunstr = 2.32; // Unstrained SVolt reading
int Vex = 5; // Gauge supply voltage
double D = 2*R; // pin diameter
unsigned long STF = 0; // time since last force motor step
unsigned long SLF = 0; // time of last force motor step
int StepF = 0; // Pulse state

unsigned long Ctime = 0;
unsigned long Clast = 0;

// Define I/O pins
int PulB = 31; // Pulse generator
int DirB = 33; // Direction line
int EnableB = 35; // run-stop line

// State variables
unsigned int waitB = 2400; // Initial pulse delay [us]
unsigned int countB = 0; // step counter
unsigned long STB = 0; // time since last step
unsigned long SLB = 0; // time of last step
int Step = 0; // Step state

void setup() {
// DC Motor I/O
pinMode(ENCPINA, INPUT);
pinMode(ENCPINB, INPUT);
pinMode(Dir, OUTPUT);
pinMode(Enable, OUTPUT);
pinMode(Frwhl, OUTPUT);
// set output defaults
digitalWrite(ENCPINA, HIGH);
digitalWrite(ENCPINB, HIGH);
digitalWrite(Dir, direc); // Sets initial rotation direction
digitalWrite(Enable, LOW); // motor initially disabled
digitalWrite(Frwhl, LOW); // Driver initially accepts speed input
attachInterrupt(2, readEncoderA, CHANGE);
attachInterrupt(3, readEncoderB, CHANGE);
Serial.begin(9600);
// Force motor I/O
pinMode(Pul, OUTPUT);
pinMode(DirF, OUTPUT);
pinMode(EnableF, OUTPUT);
pinMode(Gauge, INPUT);
// set output defaults
digitalWrite(Pul, HIGH); // no pulse signal
digitalWrite(DirF, LOW);
digitalWrite(EnableF, HIGH); // Motor defaults to 'on'
// Disk Motor I/O
pinMode(PulB, OUTPUT);
pinMode(DirB, OUTPUT);
pinMode(EnableB, OUTPUT);
// Set output defaults
digitalWrite(PulB, HIGH);
digitalWrite(DirB, HIGH);
digitalWrite(EnableB, LOW);
}

void loop() {

```

**Figure D11:** Code attempting to generate 2D paths, Part 1 of 3 (cont'd →)

```

if (Serial.available() > 0) {
  cmdKey = Serial.read();
} else {
  cmdKey = 0;
}

switch(cmdKey) {
  case 'g':
    while(100 >= count) {
      if(400 <= encPos) {
        if(1 != turnVar) {
          encVar = 2;
        } else {
          encVar = 1;
        }
      } else if(-400 >= encPos) {
        if(1 != turnVar) {
          encVar = 3;
        } else {
          encVar = 1;
        }
      } else {
        encVar = 1;
        turnVar = 0;
      }
      switch(encVar) {
        case 1:
          digitalWrite(Frwhl, LOW);
          digitalWrite(Enable, HIGH);
          break;
        case 2:
          time = millis();
          while(wait >= millis()-time) {
            digitalWrite(Frwhl, HIGH);
          }
          direc = 1;
          digitalWrite(Enable, LOW);
          digitalWrite(Dir, direc);
          turnVar = 1;
          break;
        case 3:
          time = millis();
          while(wait >= millis()-time) {
            digitalWrite(Frwhl, HIGH);
          }
          direc = 0;
          digitalWrite(Enable, LOW);
          digitalWrite(Dir, direc);
          turnVar = 1;
          break;
      }
    }

    Ctime = millis()-Clast;
    if(100 <= Ctime) {
      Clast = millis();
      SVolt = analogRead(Gauge)/204.6; // Read strain gauge
      Voff = Vunstr+creep*milis()/1000;
      Vr = (SVolt-Voff)/Vex;
      Strain = ((-2*Vr)/(GF*((1+v)-Vr*(v-1)))/Gain;
      F = (Strain*3.14159*D*D*E)/8-24;
    }

    if(Flow >= F) { // Determine if applied force is too low
      STF = micros() - SLF; // Calculate time since last 1/2 step
      digitalWrite(DirF, HIGH); // Set direction [CHECK THIS!]
      if(200 <= STF) {
        digitalWrite(Pul, StepF); // Advance force motor 1/2 step
        SLF = micros(); // Reset time of last 1/2 step
        StepF = StepF ^ 1; // Flip step state
      }
    } else if(Fhigh <= F) { // Determine if applied force is too high
      STF = micros() - SLF; // Calculate time since last 1/2 step
      digitalWrite(DirF, LOW); // Set direction [CHECK THIS!]
      if(200 <= STF) {
        digitalWrite(Pul, StepF); // Advance force motor 1/2 step
        SLF = micros(); // Reset time of last 1/2 step
        StepF = StepF ^ 1; // Flip step state
      }
    } else {
      STB = micros() - SLB; // Calculate time since last step
      if(waitB <= STB) { // Check if its time to advance
        digitalWrite(PulB, Step); // Advance a step
        SLB = micros(); // Reset time of last step
        Step = Step ^ 1; // Flip step state
        countB ++; // Advance step counter
      }
      if(601 <= waitB) {
        if(4 <= countB) {
          waitB = waitB - 4; // Decrease pulse delay
          countB = 0; // Reset step counter
        }
      }
      if(100 <= count) {
        digitalWrite(Enable, LOW);
      }
    }
    break;
  case 'r':
    digitalWrite(Dir, direc);
    digitalWrite(Frwhl, LOW);

```

**Figure D12:** Code attempting to generate 2D paths, Part 2 of 3 (cont'd →)



```

digitalWrite(Enable, HIGH);
break;
case 'a':
    Serial.print(encPos,DEC);
    Serial.print("\t");
break;
case 'f':
digitalWrite(Frwhl, HIGH);
delay(1000);
digitalWrite(Enable, LOW);
break;
case 'd':
digitalWrite(Frwhl, HIGH);
delay(3000);
digitalWrite(Enable, LOW);
direc = direc ^ 1;
digitalWrite(Dir, direc);
break;
case 'dq':
direc = direc ^ 1;
digitalWrite(Dir, direc);
break;
case 'reset':
digitalWrite(Enable, LOW);
encPos = 0;
break;
default:
break;
}
}

void readEncoderA() {
    if(digitalRead(ENCPINA) ^ digitalRead(ENCPINB)) {
        encPos--;
    } else {
        encPos++;
    }
}

void readEncoderE() {
    if(digitalRead(ENCPINA) ^ digitalRead(ENCPINB)) {
        encPos++;
    } else {
        encPos--;
    }
}
}

```

**Figure D13:** Code attempting to generate 2D paths, Part 3 of 3

## APPENDIX E: MICRON INSTRUMENTS DESIGN FOR FORCE MEASUREMENT

This appendix describes the force measurement system that could be built by Micron Instruments to improve the accuracy of the tribometer.

This system will use semi conductor bar gages and will be arranged similarly to the system described in the report. These strain gages would be arranged in a tee rosette and wired in both a half bridge and full bridge to amplify the signal and to compensate for temperature. We have selected a bar gage unit (part# SS-060-033-1000P) which will meet the requirements. This unit is pictured in Figure E.1, below. For the unit selected the dimension for X is .06", for Y is .033", and for Z is .008".

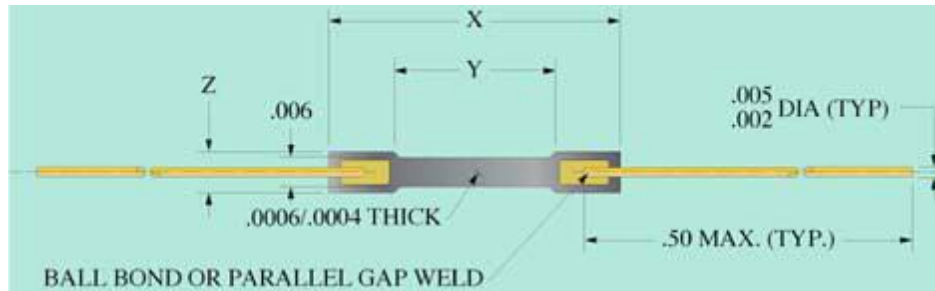


**Figure E1: Micron Instruments Bar Gauge**

The strain gages will need to be placed and bonded to the outside of the shaft and wired in the correct bridges by Micron Instruments. This should be done by Micron Instruments because of the accuracy required and the size of the gages that we have selected. It has been advised that the gages be bonded on , placed in the Wheatstone bridges and balanced by someone with experience, to achieve the accuracy required. It has been determined that the money needed to have Micron Instruments perform these tasks is well worth the price. A cost break down given to us by Micron can be found in on the next page.

This price also shows a silicone covering for the strain gages. This covering will help to eliminate damage from contact to the strain gages. It will also stop condensation and oils from handing from changing the resistance of the strain gages. Lastly, this covering will help to keep thermal gradients from changing the resistance of the strain gages from the lights. (Herb Chelner) This price also includes putting the wires on that we will use to read the output from the bridges and apply the excitation voltage.

If this strain gage system is used in an ensuing project, Herb Chelner at Micron Instruments should be contacted. He is the President at Micron Instruments and has been very helpful in suggesting this design. He is also the one who created the quote listed. His contact information is as follows: phone: 805-522-1468 email: hchelner@microninstruments.com. It should be noted that this process would require a detail drawing be made of the system and that when the shaft is delivered to Micron Instruments it will take an estimated three weeks for them to return a finished product.

	COSTS				
<b>Materials</b>					
<b>Gages per rod</b>		<b>rods</b>	<b>1</b>	<b>2</b>	<b>3</b>
<b>SS-060-033-1000P</b>		S2	2	4	6
		S4	1	2	3
gage cost per rod		40.14	80.28	160.56	192.84
		81.43	81.43	162.86	244.29
		32.14			
Gaging	126.2		126.2		
	50		100		
	92.87			185.74	
	45			180	
	75.01				225.03
	40				240
Bal. TC	11.91	3	35.73		
	6.75	6		40.5	
	5.75	9			51.75
Bridge Completion on rods					
	35.36	3	106.08		
	26.19	6		157.14	
	19.64	9			176.76
Silicone			30	45	55
Exit wires plus strap		8	24	40	48
Final balance output mv/temp					
	31	3	93		
	20	6		120	
	15	9			135
<b>tot</b>			<b>676.72</b>	<b>1091.8</b>	<b>1368.67</b>
<b>Unit cost</b>			<b>676.72</b>	<b>545.9</b>	<b>456.2233</b>

**Figure E2:** Cost Quote from Micron Instruments

## APPENDIX F: STRAIN GAUGE BONDING PROCEDURE

The following procedure for mounting strain gauges will be used to mount any strain gauge used in our design:



VISHAY MICRO-MEASUREMENTS

Application Note B-129-8

### Surface Preparation for Strain Gage Bonding

#### 1.0 Introduction

Strain gages can be satisfactorily bonded to almost any solid material if the material surface is *properly* prepared. While a properly prepared surface can be achieved in more than one way, the specific procedures and techniques described here offer a number of advantages. To begin with, they constitute a carefully developed and thoroughly proven system; and, when the instructions are followed precisely (along with those for gage and adhesive handling), the consistent result will be strong stable bonds. The procedures are simple to learn, easy to perform, and readily reproducible.

Furthermore, the surface preparation materials used in these procedures are, unless otherwise noted, generally low in toxicity, and do not require special ventilation systems or other stringent safety measures. Of course, as with any materials containing solvents or producing vapors, adequate ventilation is necessary.

The importance of attention to detail, and precise adherence to instructions, cannot be overstressed in surface preparation for strain gage bonding. Less thorough, or even casual, approaches to surface preparation may sometimes yield satisfactory gage installations; but for *consistent* success in achieving high-quality bonds, the methods given here can be recommended without qualification. Fundamental to the Vishay Micro-Measurements system of surface preparation is an understanding of *cleanliness* and *contamination*. All open surfaces not thoroughly and freshly cleaned must be considered contaminated, and require cleaning immediately prior to gage bonding. Similarly, it is imperative that the materials used in the surface preparation be fresh, clean, and uncontaminated. It is worth noting that strain gages as received from Vishay Micro-Measurements are chemically clean, and specially treated on the underside to promote adhesion. Simply touching the gages with the fingers (which are always contaminated) can be detrimental to bond quality.

The Vishay Micro-Measurements system of surface preparation includes five basic operations. These are, in the usual order of execution:

1. Solvent degreasing
2. Abrading (*dry and wet*)
3. Application of gage layout lines
4. Conditioning
5. Neutralizing

These five operations are varied and modified for compati-

bility with different test material properties, and exceptions are introduced as appropriate for certain special materials and situations.

The surface preparation operations are described individually in *Section 2.0*, following a summary of the general principles applicable to the entire process. *Section 3.0* discusses special precautions and considerations which should be borne in mind when working with unusual materials and/or surface conditions.

The various surface preparation and installation accessories referred to throughout this Application Note are Vishay Micro-Measurements Accessories, listed in Strain Gage Accessories Data Book and available directly from Vishay Micro-Measurements.

As a convenience to the gage installer in quickly determining the specific surface preparation steps applicable to any particular test material, *Section 4.0* includes a chart listing approximately 75 common (and uncommon) materials and the corresponding surface preparation treatments.

#### 2.0 Basic Surface Preparation Operations and Techniques

##### 2.1 General Principles of Surface Preparation for Strain Gage Bonding

The purpose of surface preparation is to develop a chemically clean surface having a roughness appropriate to the gage installation requirements, a surface alkalinity corresponding to a pH of 7 or so, and visible gage layout lines for locating and orienting the strain gage. It is toward this purpose that the operations described here are directed.

As noted earlier, cleanliness is vital throughout the surface preparation process. It is also important to guard against recontamination of a once-cleaned surface. Following are several examples of surface recontamination to be avoided:

- a. Touching the cleaned surface with the fingers.
- b. Wiping back and forth with a gauze sponge, or reusing a once-used surface of the sponge (or of a cotton swab).
- c. Dragging contaminants into the cleaned area from the uncleaned boundary of that area.
- d. Allowing a cleaning solution to evaporate on the surface.
- e. Allowing a cleaned surface to sit for more than a few minutes before gage installation, or allowing a partially prepared surface to sit between steps in the cleaning procedure.

APPLICATION NOTE



## Surface Preparation for Strain Gage Bonding

Beyond the above, it is good practice to approach the surface preparation task with freshly washed hands, and to wash hands as needed during the procedure.

### 2.2 Solvent Degreasing

Degreasing is performed to remove oils, greases, organic contaminants, and soluble chemical residues. Degreasing should always be the first operation. This is to avoid having subsequent abrading operations drive surface contaminants into the surface material. Porous materials such as titanium, cast iron, and cast aluminum may require heating to drive off absorbed hydrocarbons or other liquids.

Degreasing can be accomplished using a hot vapor degreaser, an ultrasonically agitated liquid bath, aerosol type spray cans of CSM-2 Degreaser, or wiping with GC-6 Isopropyl Alcohol. One-way applicators, such as the aerosol type, of cleaning solvents are always preferable because dissolved contaminants cannot be carried back into the parent solvent. Whenever possible, the entire test piece should be degreased. In the case of large bulky objects which cannot be completely degreased, an area covering 4 to 6 in [100 to 150mm] on all sides of the gage area should be cleaned. This will minimize the chance of recontamination in subsequent operations, and will provide an area adequately large for applying protective coatings in the final stage of gage installation.

### 2.3 Surface Abrading

**General** — In preparation for gage installation, the surface is abraded to remove any loosely bonded adherents (scale, rust, paint, galvanized coatings, oxides, etc.), and to develop a surface texture suitable for bonding. The abrading operation can be performed in a variety of ways, depending upon the initial condition of the surface and the desired finish for gage installation. For rough or coarse surfaces, it may be necessary to start with a grinder, disc sander, or file. (*Note: Before performing any abrading operations, see Section 3.1 for safety precautions.*) Finish abrading is done with silicon-carbide paper of the appropriate grit, and recommended grit sizes for specific materials are given in Section 4.0.

If grit blasting is used instead of abrading, either clean alumina or silica (100 to 400 grit) is satisfactory. In any case, the air supply should be well filtered to remove oil and other contaminant vapors coming from the air compressor. The grit used in blasting should not be recycled or used again in surface preparation for bonding strain gages.

The optimum surface finish for gage bonding depends somewhat upon the nature and purpose of the installation. For general stress analysis applications, a relatively smooth surface (in the order of 100µin [2.5µm] rms) is suitable, and has the advantage over rougher surfaces that it can be cleaned more easily and thoroughly. Smoother surfaces, compatible with the thin "gluelines" required for minimum creep, are used for transducer installations. In contrast,

when very high elongations must be measured, a rougher (and preferably cross-hatched) surface should be prepared. The recommended surface finishes for several classes of gage installations are summarized in Table I, below.

TABLE I

CLASS OF INSTALLATION	SURFACE FINISH, rms	
	µin	µm
General stress analysis	63 - 125	1.6 - 3.2
High elongation	>250	>6.4
	cross-hatched	
Transducers	16 - 63	0.4 - 1.6

**Wet Abrading** — Whenever *M-Prep* Conditioner A is compatible with the test material (see Section 4.0), the abrading should be done while keeping the surface wet with this solution, if physically practicable. Conditioner A is a mildly acidic solution which generally accelerates the cleaning process and, on some materials, acts as a gentle etchant. It is not recommended for use on magnesium, synthetic rubber, or wood.

### 2.4 Gage-Location Layout Lines

The normal method of accurately locating and orienting a strain gage on the test surface is to first mark the surface with a pair of crossed reference lines at the point where the strain measurement is to be made. The lines are made perpendicular to one another, with one line oriented in the direction of strain measurement. The gage is then installed so that the triangular index marks defining the longitudinal and transverse axes of the grid are aligned with the reference lines on the test surface.

The reference, or layout, lines should be made with a tool that *burnishes*, rather than scores or scribes, the surface. A scribed line may raise a burr or create a stress concentration. In either case, such a line can be detrimental to strain gage performance and to the fatigue life of the test part. On aluminum and most other nonferrous alloys, a 4H drafting pencil is a satisfactory and convenient burnishing tool. However, graphite pencils should never be used on high-temperature alloys, where the operating temperature might cause a carbon embrittlement problem. On these and other hard alloys, burnished alignment marks can be made with a ballpoint pen or a round-pointed brass rod. Layout lines are ordinarily applied following the abrading operation and before final cleaning. All residue from the burnishing operation should be removed by scrubbing with Conditioner A as described in the following section.

### 2.5 Surface Conditioning

After the layout lines are marked, Conditioner A should be applied repeatedly, and the surface scrubbed with cotton tipped applicators until a clean tip is no longer discolored by the scrubbing. During this process the surface should be kept constantly wet with Conditioner A until the cleaning is completed. *Cleaning solutions should never be allowed to*



## Surface Preparation for Strain Gage Bonding

*dry on the surface.* When clean, the surface should be dried by wiping through the cleaned area with a single slow stroke of a gauze sponge. The stroke should begin inside the cleaned area to avoid dragging contaminants in from the boundary of the area. Then, with a fresh sponge, a single slow stroke is made in the opposite direction. The sponge should never be wiped back and forth, since this may re-deposit the contaminants on the cleaned surface.

### 2.6 Neutralizing

The final step in surface preparation is to bring the surface condition back to an optimum alkalinity of 7.0 to 7.5pH, which is suitable for all Vishay Micro-Measurements strain gage adhesive systems. This should be done by liberally applying *M-Prep* Neutralizer 5A to the cleaned surface, and scrubbing the surface with a clean cotton-tipped applicator. The cleaned surface should be kept completely wet with Neutralizer 5A throughout this operation. When neutralized, the surface should be dried by wiping through the cleaned area with a *single* slow stroke of a clean gauze sponge. With a fresh sponge, a *single* stroke should then be made in the opposite direction, beginning with the cleaned area to avoid recontamination from the uncleaned boundary.

If the foregoing instructions are followed precisely, the surface is now properly prepared for gage bonding, and the gage or gages should be installed as soon as possible.

### 3.0 Special Precautions and Considerations

#### 3.1 Safety Precautions

As in any technical activity, safety should always be a prime consideration in surface preparation for strain gage bonding. For example, when grinding, disc sanding, or filing, the operator should wear safety glasses and take such other safety precautions as specified by his organization or by the Occupational Safety and Health Administration (OSHA).

*When dealing with toxic materials such as beryllium, lead, uranium, plutonium, etc., all procedures and safety measures should be approved by the safety officer of the establishment before commencing surface preparation.*

#### 3.2 Surfaces Requiring Special Treatment

**Concrete** — Concrete surfaces are usually uneven, rough, and porous. In order to develop a proper substrate for gage bonding, it is necessary to apply a leveling and sealing precoat of epoxy adhesive to the concrete. Before applying the precoat, the concrete surface must be prepared by a procedure which accounts for the porosity of this material.

Contamination from oils, greases, plant growth, and other soils should be removed by vigorous scrubbing with a stiff-bristled brush and a mild detergent solution. The surface is then rinsed with clean water. Surface irregularities can be removed by wire brushing, disc sanding, or grit blasting, after which all loose dust should be blown or brushed

from the surface.

The next step is to apply Conditioner A generously to the surface in and around the gaging area, and scrub the area with a stiff-bristled brush. Contaminated Conditioner A should be blotted with gauze sponges, and then the surface should be rinsed thoroughly with clean water. Following the water rinse, the surface acidity must be reduced by scrubbing with Neutralizer 5A, blotting with gauze sponges, and rinsing with water. A final thorough rinse with distilled water is useful to remove the residual traces of water-soluble cleaning solutions. Before precoating, the cleaned surface must be thoroughly dried. Warming the surface gently with a propane torch or electric heat gun will hasten evaporation.

Vishay Micro-Measurements M-Bond AE-10 room-temperature-curing epoxy adhesive is an ideal material for pre-coating the concrete. For those cases in which the test temperature may exceed the specified maximum operating temperature of AE-10 (+200°F [+95°C]), it will be necessary to fill the surface with a higher temperature resin system such as M-Bond GA-61.

In applying the coating to the porous material, the adhesive should be worked into any voids, and leveled to form a smooth surface. When the adhesive is completely cured, it should be abraded until the base material begins to be exposed again. Following this, the epoxy surface is cleaned and prepared conventionally, according to the procedure specified in *Section 4.0* for bonding gages to epoxies.

**Plated Surfaces** — In general, plated surfaces are detrimental to strain gage stability, and it is preferable to remove the plating at the gage location, if this is permissible. Cadmium and nickel plating are particularly subject to creep, and even harder platings may creep because of the imperfect bond between the plating and the base metal. When it is not permissible to remove the plating, the surface should be prepared according to the procedure given in *Section 4.0* for the specific plating involved. Note that it may be necessary to adjust testing procedures to minimize the effects of creep.

**Use of Solvents on Plastics** — Plastics vary widely in their reactivity to solvents such as those employed in the surface preparation procedures described here. Before applying a solvent to any plastic, *Section 4.0*, which includes most common plastics, should be referred to for the recommended compatible solvent. For plastics not listed in *Section 4.0*, the manufacturer of the material should be consulted, or tests should be performed to verify nonreactivity between the solvent and the plastic.

**Dimensional or Mechanical Changes Due to Surface Preparation** — For most materials, strain measurement results are usually not significantly changed by the surface preparation procedures described in this Application Note. Even with appreciable material removal, effects on the static mechanical properties of the test part are generally negli-



## Surface Preparation for Strain Gage Bonding

ble compared to other error sources in the experiment. It should be understood, however, that removal of a plated or hardened surface layer, or of a surface layer with significant residual stresses, may noticeably affect the fatigue life or the wear characteristics of the part when operated under dynamic service conditions.

**Silicone Contamination** —The properties of silicones which make them excellent lubricants and mold-release agents also make them the enemies of adhesion, and therefore potentially the most serious of contaminants to be encountered in the practice of bonding strain gages. The problem is compounded by the high natural affinity of the silicones for most materials, and by their tendency to migrate. Furthermore, since silicones are relatively inert chemically, and unaffected by most solvents, they are among the most difficult surface contaminants to remove.

The best practice is to keep the gage-bonding area free of silicones. This may not be as easy as it sounds, since the widely used silicones can be introduced from a variety of sources. For instance, many hand creams and cosmetics contain silicones, and these should not be used by persons involved in gage installation. Some of the machining lubricants also contain silicones, and such lubricants should be avoided when machining parts that are to have strain gages installed. Similarly, silicone-saturated cleaning tissues for eyeglasses should not be used in the gage-bonding area or by gage-installation personnel.

Regardless of efforts to avoid silicones, contamination may still occur. Light contamination can sometimes be removed by cleaning with Conditioner A, preferably heated to +200°F [+95°C]. More severe cases may require special cleaning solutions and procedures, recommendations for which should be obtained from the manufacturer of the silicone compound involved in the contamination.

### 4.0 Index of Test Materials and Surface Preparation Procedures

In this section, the specific step-by-step surface preparation procedures are given for approximately 75 different materials. For compactness, and convenient, quick access to the procedure for any particular material, the information is presented in chart form in Table II. The test materials are listed alphabetically, from ABS Plastics to Zirconium; and the complete procedure for each material is defined by one or more digits in each of the applicable operations columns of the table. Each digit identifies the required operation and specifies the step number for that operation in the complete procedure.

For example, assume that the necessity arises for bonding one or more strain gages to a brass test specimen. Reading down the *Specimen Material* column of Table II to Brass, and following that row across the table to the right, the first step in surface preparation consists of degreasing the specimen with CSM-2 Degreaser. The symbol (1) in the *Isopro-*

*pyl Alcohol* column indicates that this is a suitable substitute degreasing operation. Continuing across the row, the second operation calls for abrading the specimen surface with 320-grit silicon-carbide paper. In the third operation the specimen is reabraded with 400-grit silicon-carbide paper, wet lapping with Conditioner A if feasible. The fourth and fifth operations consist of applying layout lines for locating the gages, and scrubbing the surface clean with Conditioner A. Cleaning with isopropyl alcohol is the final operation in the procedure.

In the *Remarks* column, it is recommended that the gages be installed within 20 minutes after completing the surface preparation, because the freshly bared brass surface tends to oxidize rapidly. In addition, in the *Grit Blast* column, the gage installer is specifically advised not to substitute grit blasting for other surface abrading methods, in order to avoid significantly altering the surface condition of this relatively soft material. Surface preparation procedures for other materials are defined similarly in the table, and, in many cases, accompanied by special warnings or recommendations in the *Remarks* column. When an operation not included in the first ten column headings is required, it is indexed in the *Other* column, with an arrow pointing to the *Remarks* column where the operation is specified.

### Additional References

For additional information, refer to Instruction Bulletins listed below:

B-127, "Strain Gage Installations with M-Bond 200 Adhesive".

B-130, "Strain Gage Installations with M-Bond 43-B, 600, and 610 Adhesives".

B-137, "Strain Gage Applications with M-Bond AE-10, AE-15, and GA-2 Adhesive Systems".

### Important Notice

The procedures, operations, and chemical agents recommended in this Application Note are, to the best knowledge of Vishay Micro-Measurements, reliable and fit for the purposes for which recommended. This information on surface preparation for strain gage bonding is presented in good faith as an aid to the strain gage installer; but no warranty, expressed or implied, is given, nor shall Vishay Micro-Measurements be liable for any injury, loss, or damage, direct or consequential, connected with the use of the information. Before applying the procedures to any material, the user is urged to carefully review the application with respect to human health and safety, and to environmental quality.



## Surface Preparation for Strain Gage Bonding

**TABLE II**  
Index of Test Materials and Surface Preparation Procedures (Sheet 1 of 3)

See Section:	2.2		2.3			2.4	2.5	2.6	REMARKS		
	CSM-2 DEGREASER	GC-6 ISOPROPYL ALCOHOL	GRIT-BLAST	220-GRIT ABRASIVE PAPER	320-GRIT ABRASIVE PAPER	400-GRIT ABRASIVE PAPER†	GAGE LOCATION LAYOUT	CONDITIONER A (SCRUB)		NEUTRALIZER 5A	OTHER
ABS PLASTICS		1	No			2	3	4	5		ABS plastics may be affected by ketones, esters, aromatics, and chlorinated hydrocarbons.
ACRYLICS		1				2	3	4	5		Acrylics may be affected by ketones, esters, aromatics, and chlorinated hydrocarbons.
ALUMINUM, ALCLAD	1					2	3	4	5		Alclad coating must be removed prior to gage installation by abrading with 180-grit or 220-grit silicon-carbide paper. Test for completeness of Alclad removal: (a) swab area with 10% sodium hydroxide solution - area will darken within 60 sec if cladding is completely removed; (b) neutralize surface with Conditioner A; (c) flush area with distilled water. Proceed with surface preparation as specified at left.
ALUMINUM, ANODIZED	1					2	3	4	5		Black or colored anodizing must be removed prior to gage installation. Use nonchlorinated household cleaner to strip sealer. Clear anodized surface acceptable for elastic strain level only.
ALUMINUM, CASTINGS	1		(2)	(2)	2	3	4	5	6		Gages should be bonded within 30 min after final surface preparation.
ALUMINUM, WROUGHT	1		(2)		2	3	4	5	6		Gages should be bonded within 30 min after final surface preparation.
ANTIMONY		1	No			2	3	4	5		
ASPHALT		1	No				3		4	2	Often necessary to grind, disc sand, or file surface.
BERYLLIUM	1		No				3	4	5	2	Obtain safety department approval for surface removal. Abraded particles must be kept wet to prevent becoming airborne, and must be properly disposed of. Some individuals may develop allergic reaction. Gloves should be worn.
BERYLLIUM COPPER	1*	(1)*				3	4	5	6	2	Obtain safety department approval for surface removal. Abraded particles must be kept wet to prevent becoming airborne, and must be properly disposed of. Some individuals may develop allergic reaction.
BISMUTH		1	No			2	3	4	5		
BONE		(3)								1,2,3	Clean with ether under proper ventilation, then scrape surface, and redry with ether.
BORON-EPOXY COMPOSITES		1,5*	No			2	3	4	(5*)	(2)	Scrub with a slurry of pumice powder and Conditioner A.
BRASS	1	(1)	No		2	3	4	5**			Install gages within 20 min of final surface preparation.
BRICK		1,3*							4*	2	Wire-brush or disc-sand, and remove dust with dry paint brush. Fill and seal surface with epoxy adhesive, such as Micro-Measurements AE-10, and sand smooth after adhesive is cured.
BRONZE	1	(1)			2	3	4	5**			Install gages within 20 min of final surface preparation.
CADMIUM PLATE	1	(1)	No		2	3	4	5	6		Cadmium plating has a tendency to creep, and the plating should be removed if permissible.
CARBON (see GRAPHITE)											
CERAMICS		1*			2		3	4	5*		
CHROMIUM PLATE	1	(1)			2		3	4	5		Chromium plating should be removed at gage installation site if permissible.
CONCRETE										1	See Concrete Section 3.2 in text.
COPPER AND COPPER-BASED ALLOYS	1	(1)	No		2	3	4	5**	No		Install gages within 20 min after final surface preparation.

**SPECIAL NOTES**  
 \* Heating specimen will help drive out oils, moisture, and solvent.  
 \*\* Rinse with distilled water, and wipe dry.  
 † Use clean (filtered), dry air. Do not recycle alumina or silica grits.  
 †† Wet lap with Conditioner A when compatibility is indicated by "Conditioner A (Scrub)" column.  
 ( ) Parentheses indicate alternate step(s).

APPLICATION NOTE





## Strain Gage Installations with M-Bond 43-B, 600, and 610 Adhesive Systems

### INTRODUCTION

Vishay Micro-Measurements M-Bond 43-B, 600, and 610 adhesives are high-performance epoxy resins, formulated specifically for bonding strain gages and special-purpose sensors. When properly cured, these adhesives are useful for temperatures ranging from -452° to +350°F [-269° to +175°C] with M-Bond 43-B, and to +700°F [+370°C] for short periods with M-Bond 600 and 610. In common with other organic materials, life is limited by oxidation and sublimation effects at elevated temperatures. M-Bond 43-B is particularly recommended for transducer applications up to +250°F [+120°C], and M-Bond 610 for transducers up to +450°F [+230°C].

For proper results, the procedures and techniques presented in this bulletin should be used with qualified Vishay Micro-Measurements installation accessory products (refer to Vishay Micro-Measurements Strain Gage Accessories Databook). Accessories used in this procedure are:

- |   |                                       |
|---|---------------------------------------|
| CSP-1 Cotton Applicators                | CSP-1 Cotton Applicators              |
| MJG-2 Mylar® Tape                       | MJG-2 Mylar® Tape                     |
| TFE-1 Teflon® Film                      | TFE-1 Teflon® Film                    |
| HSC-X Spring Clamp                      | HSC-X Spring Clamp                    |
| GT-14 Pressure Pads and Backup Plates   | GT-14 Pressure Pads and Backup Plates |
| CSM Degreaser or GC-6 Isopropyl Alcohol |                                       |
| Silicon-Carbide Paper                   |                                       |
| M-Prep Conditioner A                    |                                       |
| M-Prep Neutralizer 5A                   |                                       |
| GSP-1 Gauze Sponges                     |                                       |

### MIXING INSTRUCTIONS

Since M-Bond 43-B is a solvent-thinned, pre-catalyzed epoxy mixture, it is applied at room temperature directly as received. The M-Bond 600 and 610, on the other hand, are two-component systems. These must be mixed as follows:

1. Resin and curing agent bottles must be at room temperature before opening.
2. Using the disposable plastic funnel, empty contents of bottle labeled "Curing Agent" into bottle of resin labeled "Adhesive". Discard funnel.
3. After tightening the brush cap (included separately), thoroughly mix contents of this "Adhesive" bottle by vigorously shaking it for 10 seconds.
4. Mark bottle with date mixed in space provided on the label.

Allow this freshly mixed adhesive to stand for at least one hour before using.

### SURFACE PREPARATION

The extensive subject of surface preparation techniques is covered in Application Note B-129. Metal surface cleaning procedures usually involve solvent degreasing with either CSM Degreaser or GC-6 Isopropyl Alcohol, abrading, and cleaning with M-Prep Conditioner A, followed by application of M-Prep Neutralizer 5A. When practical, these preparation procedures should be applied to an area significantly larger than that occupied by the gage. Surfaces should be free from pits and irregularities. Porous surfaces may be pre-coated with a filled epoxy, such as M-Bond GA-61, which is then cured and abraded.

### SHELF LIFE AND POT LIFE

At room temperature, M-Bond 600 has a useful storage life of approximately three months, while M-Bond 43-B and M-Bond 610 will last about nine months.

Once opened and mixed, M-Bond 600 and 610 have room-temperature pot lives of two weeks and six weeks, respectively. Since M-Bond 43-B is supplied already mixed, its pot life is about the same as its shelf life when kept in a tightly closed container.

These periods of adhesive usefulness can be increased by refrigeration at +30° to +40°F [0° to +5°C]. Check individual adhesive kit labels for details. Never open a refrigerated bottle until it has reached room temperature.

### GAGE INSTALLATION

The basic steps for bonding gages using M-Bond 43-B, 600, and 610 adhesives are given on the following pages.

HANDLING PRECAUTIONS
Epoxy resins and hardeners may cause dermatitis or other allergic reactions, particularly in sensitive persons. The user is cautioned to: (1) avoid contact with either the resin or hardener; (2) avoid prolonged or repeated breathing of the vapors; and (3) use these materials only in well-ventilated areas. If skin contact occurs, thoroughly wash the contaminated area with soap and water immediately. In case of eye contact, flush immediately and secure medical attention. Rubber gloves and aprons are recommended, and care should be taken not to contaminate working surfaces, tools, container handles, etc. Spills should be cleaned up immediately. For additional health and safety information, consult the Material Safety Data Sheet, which is available upon request.

### Strain Gage Installations with M-Bond 43-B, 600, and 610 Adhesive Systems



## Instruction Bulletin B-130

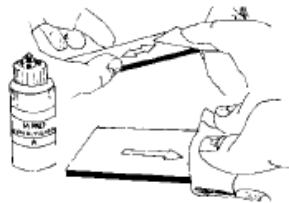
### Vishay Micro-Measurements

#### Step 1



Thoroughly degrease the gaging area with solvent, such as CSM Degreaser or GC-6 Isopropyl Alcohol. The former is preferred, but there are some materials (e.g., titanium and many plastics) that react with CSM. In these cases, GC-6 Isopropyl Alcohol should be considered. All degreasing should be done with uncontaminated solvents—thus the use of “one-way” containers, such as aerosol cans, is highly advisable.

#### Step 2



Preliminary dry abrading with 220- or 320-grit silicon-carbide paper is generally required if there is any surface scale or oxide. Final abrading is done by using 320- or 400-grit silicon-carbide paper on surfaces thoroughly wetted with M-Prep Conditioner A; this is followed by wiping dry with a gauze sponge.

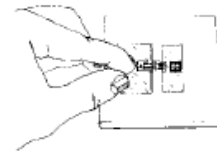
With a 4H pencil (on aluminum) or a ballpoint pen (on steel), burnish (do not scribe) whatever alignment marks are needed on the specimen. Repeatedly apply Conditioner A and scrub with cotton-tipped applicators until a clean tip is no longer discolored. Remove all residue and Conditioner by again slowly wiping through with a gauze sponge. Never allow any solution to dry on this surface because this invariably leaves a contaminating film and reduces chances of a good bond.

#### Step 3



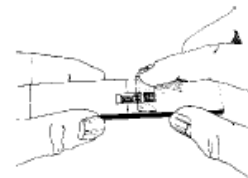
Now apply a liberal amount of M-Prep Neutralizer 5A and scrub with a cotton-tipped applicator. With a single, slow wiping motion of a gauze sponge, carefully dry this surface. Do not wipe back and forth because this may allow contaminants to be redeposited on the cleaned surface.

#### Step 4



Remove a gage from its mylar envelope with tweezers, making certain not to touch any exposed foil. Place the gage, bonding side down, onto a chemically clean glass plate or empty gage box. If a solder terminal is to be incorporated, position it next to the gage. While holding the gage in position with a mylar envelope, place a short length of MJG-2 mylar tape down over about half of the gage tabs and the entire terminals.

#### Step 5



Remove the gage/tape/terminal assembly by peeling tape at a shallow angle (about 30°) and transferring it onto the specimen. Make sure gage alignment marks coincide with specimen layout lines. If misalignment does occur, lift the end of the tape at a shallow angle until assembly is free. Realign and replace. Use of a pair of tweezers often facilitates this handling.

### Strain Gage Installations with M-Bond 43-B, 600, and 610 Adhesive Systems

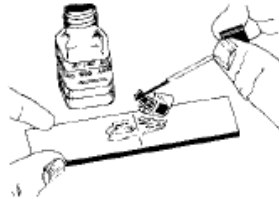


## Instruction Bulletin B-130

### Vishay Micro-Measurements

**Note:** A "hot-tack" method of positioning can be used, which eliminates need for taping. This method is explained after Step 9.

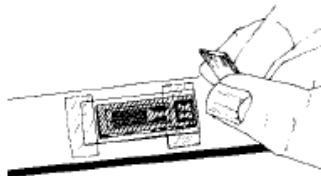
#### Step 6



Now, by lifting at a shallow angle, peel back one end of the taped assembly so as to raise both gage and terminal. By curling this mylar tape back upon itself, it will remain in position, ready to be accurately repositioned after application of adhesive.

Coat the gage backing, terminal, and specimen surface with a thin layer of adhesive. Also coat the foil side of open-faced gages. Do not allow the adhesive applicator to touch the tape mastic. Permit adhesive to air-dry, by solvent evaporation, for 5 to 30 minutes at +75°F [+24°C] and 50% relative humidity. Longer air-drying times are required at lower temperatures and/or higher humidities. **Note:** An additional drying step with 43-B is beneficial for large gages. Place the unclamped installation in an oven for 30 minutes at +175°F [+85°C] following the air-dry step above.

#### Step 7

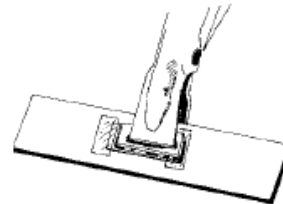


Return the gage/terminal assembly to its original position over the layout marks. Use only enough pressure to allow the assembly to be tacked down. Overlay the gage/terminal area with a piece of thin Teflon sheet (TFE-1). If necessary, anchor the Teflon in position across one end with a piece of mylar tape.

Cut a 3/32-in [2.5-mm] thick silicone gum pad and a metal backup plate (GT-14) to a size slightly larger than the gage/terminal areas, and carefully center these. Larger pads may restrict proper spreading of adhesive, and entrap residual solvents during cure process.

**Note:** Steps 6, 7, and 8 must be completed within 30 minutes with M-Bond 600, 4 hours with M-Bond 610, and 24 hours with M-Bond 43-B.

#### Step 8



Either spring clamps or deadweight can be used to apply pressure during the curing cycle. For transducers, 40 to 50 psi [275 to 350 kN/m<sup>2</sup>] is recommended and 10 to 70 psi [70 to 480 kN/m<sup>2</sup>] for general work. Place the clamped gage/specimen into a cool oven and raise temperature to the desired curing level at a rate of 5° to 20°F [3° to 11°C] per minute. Air bubbles trapped in the adhesive, uneven gluelines, and high adhesive film stresses often result from starting with a hot oven. Time-versus-temperature recommendations for curing each adhesive are given on the next page.

#### Step 9

Upon completion of the curing cycle, allow oven temperature to drop to at least 100°F [55°C] before removing the specimen. Remove clamping pieces and mylar tape. It is advisable to wash off the entire gage area with either RSK Rosin Solvent or toluene. This should remove all residual mastic and other contamination. Blot dry with a gauze sponge.

#### "Hot-Tack" Method of Gage Installation

This procedure eliminates all need for taping to prevent movement of the gage during mounting, and is especially suited to M-Bond 43-B and M-Bond 600.

1. After completing the preceding Steps 1, 2, and 3, remove a gage from its mylar envelope using clean tweezers.
2. Coat the bonding side of gage and gaging area of the specimen with adhesive, and set each aside to air-dry for at least 15 minutes. M-Bond 43-B may dry for up to 24 hours.

### Strain Gage Installations with M-Bond 43-B, 600, and 610 Adhesive Systems



# Instruction Bulletin B-130

## Vishay Micro-Measurements

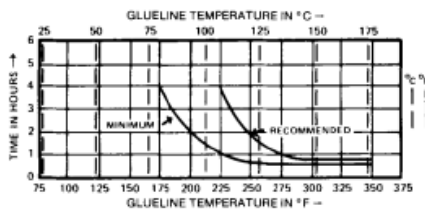
- Using tweezers, position gage onto the specimen. A properly cleaned dental probe may help.
- To anchor the gage, use a 15- to 25-watt soldering iron with a new conical tip. This is usually done by hot-tack-setting the adhesive at two spots (such as opposite gage-alignment marks) while temporarily holding the gage down with a mylar envelope. A little experimentation may be required to learn the correct iron temperature and hot tip contact time. These depend upon type of adhesive used and thermal conductivity of the base material.
- If the gage is open-faced, apply a thin coating of adhesive to its face and allow to dry for at least five minutes before overlaying with a Teflon sheet (as described in Step 7). Proceed with Steps 8 and 9.

### RECOMMENDED CURE SCHEDULE

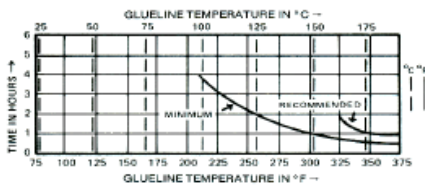
It should be noted that the following curves represent a range of time-versus-temperature; however, the upper limits of both time and temperature should be employed whenever possible, while keeping in mind the possible effect on the heat treat condition of the substrate material.

**M-Bond 43-B:** 2 hours at +375°F [+190°C].

**M-Bond 600:** Cure at temperature for time period specified by graph below.



**M-Bond 610:** Cure at temperature for time period specified by graph below.



### POSTCURING

Postcures with the clamping fixture removed are usually required for stable transducer applications. Postcuring can be done following Step 9 above, or after wiring the transducer (subject to temperature limits of solder and wire insulation).

**M-Bond 43-B:** 2 hours at +400°F [+205°C].

**M-Bond 600:** 1 to 2 hours at 50°F [30°C] above maximum operating or curing temperature, whichever is greater.

**M-Bond 610:** 2 hours at 50° to 75°F [30° to 40°C] above maximum operating or curing temperature, whichever is greater.

### FINAL INSTALLATION PROCEDURES

1. Refer to Strain Gage Accessories Databook to select an appropriate solder, and attach leadwires. Be sure to remove solder flux with Rosin Solvent. Gage tabs and terminals can be cleaned prior to soldering by light abrading with pumice to remove the adhesive film. This pumicing is not required with gages having integral leads (Options L and LE) or pre-attached solder dots. See Application Note TT-606, "Soldering Techniques for Lead Attachment to Strain Gages with Solder Dots." General soldering instructions are discussed in Application Note TT-609, "Strain Gage Soldering Techniques."

2. Select and apply protective coatings according to recommendations given in Strain Gage Accessories Databook.

### ELONGATION CAPABILITIES

**M-Bond 43-B:**

1% at -452°F [-269°C]; 4% at +75°F [+24°C]; 2% at +300°F [+150°C].

**M-Bond 600 & 610:**

1% at -452°F [-269°C]; 3% from room temperature to 500°F [+260°C].

Mylar and Teflon are Registered Trademarks of DuPont.

### Strain Gage Installations with M-Bond 43-B, 600, and 610 Adhesive Systems

# APPENDIX G: PARAMETER VALIDATION SUPPLEMENTARY INFORMATION

Figure G.1: Gates Design Pro Flex belt selection criteria and results

The screenshot displays the Gates Design Pro Flex software interface. The top navigation bar includes 'File', 'Drive Options', 'Tools', and 'Help'. The main window is titled '450 Team 21 Linear Belt Drive'.

**Desired Belt Line:** A tree view on the left shows selected options: Synchronous, Poly Chain Carbon, PowerGrip GT2, TruMotion, PowerGrip Timing, Poly Chain GT2, PowerGrip HTD, and PowerGrip GT. Below this are dropdowns for Length and Width.

**Motor:** Electric Motor is selected. Power is 15 N-m, RPM is 375, and Motor Eff. is 88%. Motor Frame is Unspecified. Gearbox Speed Ratio is 1, Output RPM is 375. Drive Service Factor is Synchronous at 1.6.

**Application Title:** 450 Team 21 Linear Belt Drive

**DriveN Pulley Speed:** Min. RPM 360 (-4%), Nominal RPM 375 (+/-4%), Max. RPM 390 (+4%). Speed Ratio is 1. Speed Up is unchecked.

**Center Distance Between Shafts:** Min. CD 18 (-10%), Nominal CD 20 (+/-10%), Max. CD 22 (+10%). Unit is in.

**Bushings to Consider:** QD, Taper-Lock, Minimum Plain Bore, and ACHE Sprockets are checked.

**Material:** Standard Materials is checked. Stainless Steel and Nickel Plated are unchecked.

**DriveR Pulley:** Shaft Dia., Shaft Len., Max. O.D., and Max. Width are Unspecified. Known DriveR Size is 44 Teeth.

**DriveN Pulley:** Shaft Dia., Shaft Len., Max. O.D., and Max. Width are Unspecified. Known DriveN Size is 44 Teeth.

Buttons for 'Design', 'Set Savings Numbers', and 'Clear' are visible in the top right.



Figure G.3: Nook Industries ELK 60 Linear Actuator

1

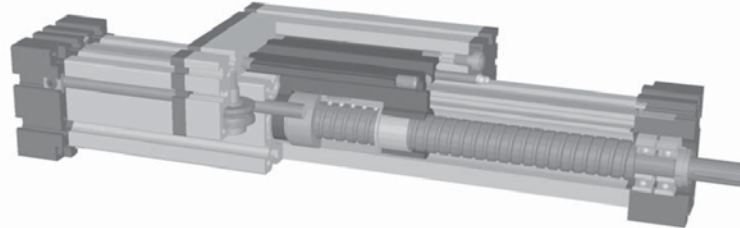
## Modular Linear Actuator

### ELT, ELK 30, 40, 60, 80, 80S, 100, 125

Acme or Ball Screw Driven, Right and Left-handed Thread or Divided Screws



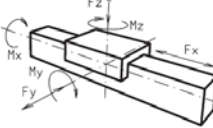
**NOOK**  
INDUSTRIES  
...THE LINEAR MOTION PEOPLE



**Function:**

This unit consists of an aluminium extrusion body with integral, parallel ground and hardened steel guide rods. The carriage has play-adjustable ball-bearing rollers which ride on the guide rods. The rotating screw causes linear motion of the nut, which is connected to the carriage. The slot in the profile is covered by a stainless steel strip, making the unit dust and splash-proof. Lateral alignment adjustment for parallel units, or when two carriages are mounted on one unit, is provided for the carriages in the nut mounting.

- Fitting length:** As required, Max. length 3,000 mm  
**Carriage mounting:** T-slots and tapped holes  
**Unit mounting:** T-slots

Forces and torques	Size	EL 30		EL 40		EL 60		EL 80		EL 80S		EL 100		EL 125			
	Forces/Torques	static	dyna.	static	dyna.	static	dyna.	static	dyna.	static	dyna.	static	dyna.	static	dyna.		
	F <sub>x</sub> [N]	750	600	1500	1200	2500	2000	5000	4000	5000	4000	10000	8000	15000	12000		
	F <sub>y</sub> [N]	90	60	1200	700	3000	2000	3000	2000	4600	3600	8000	6500	12000	9000		
	F <sub>z</sub> [N]	90	60	900	650	1700	1100	1700	1100	3000	1800	3600	2200	6000	4500		
	M <sub>x</sub> [Nm]	12	10	25	20	67	43	90	55	170	140	300	230	600	450		
	M <sub>y</sub> [Nm]	12	10	32	18	90	70	110	80	270	230	400	270	750	600		
	M <sub>z</sub> [Nm]	15	12	35	25	120	100	150	120	300	220	750	500	1350	1150		
<b>No-load torque</b>																	
Acme Screw		10x3		18x4/18x8		24x5/24x10		28x5/28x10		28x5/28x10		32x6/32x12		40x7/40x14			
		[Nm]		0,3		0,4/0,5		0,6/0,8		0,8/1,0		0,8/1,0		0,9/1,1		1,2/1,4	
Ball Screw		8x2,5		16x5/16x10		25x5/25x10		32x5/32x10		32x5/32x10		32x5/32x10		40x10/40x20			
		[Nm]		0,15		0,2/0,4		0,4/0,6		0,6/0,8		0,6/0,8		0,7/0,9		1,0/1,2	
<b>Geometrical moments of inertia of aluminium profile</b>																	
I <sub>x</sub> mm <sup>4</sup>		4,09x10 <sup>4</sup>		1,32x10 <sup>5</sup>		6,79x10 <sup>5</sup>		18,99x10 <sup>5</sup>		18,99x10 <sup>5</sup>		44,4x10 <sup>5</sup>		101,5x10 <sup>5</sup>			
I <sub>y</sub> mm <sup>4</sup>		4,00x10 <sup>4</sup>		1,34x10 <sup>5</sup>		6,97x10 <sup>5</sup>		18,97x10 <sup>5</sup>		18,97x10 <sup>5</sup>		44,8x10 <sup>5</sup>		101,5x10 <sup>5</sup>			
E-Modulus N/mm <sup>2</sup>		70000		70000		70000		70000		70000		70000		70000			

**Formula: EGTH**

Driving torque:

$$M_b = \frac{F \cdot P \cdot S}{2000 \cdot \pi \cdot \mu} + M_{\text{ver}}$$

$$P_o = \frac{M_b \cdot n}{9550}$$

- F = force [N]
- P = thread pitch [mm]
- S<sub>1</sub> = safety factor 1,2 ... 2
- M<sub>ver</sub> = no-load torque [Nm]
- n = rpm of screw [min<sup>-1</sup>]
- M<sub>b</sub> = driving torque [Nm]
- μ = screw efficiency ~ 1,22
- w = friction coefficient
- P<sub>o</sub> = motor power [KW]

Efficiency (η)

Ball Screws = 0.900

Acme Screws

- Tr 18x4 = 0.399      Tr 18x8 = 0.565
- Tr 24x5 = 0.384      Tr 24x10 = 0.550
- Tr 28x5 = 0.349      Tr 28x10 = 0.513

$$f = \frac{F \cdot l^3}{E \cdot I \cdot 192}$$



- f = deflection [mm]
- F = load [N]
- l = free length [mm]
- E = elastic modulus 70000 [N/mm<sup>2</sup>]
- I = second moment of area [mm<sup>4</sup>]

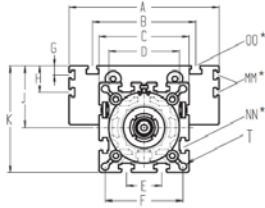
Figure G.3: Nook Industries ELK 60 Linear Actuator (Cont.)



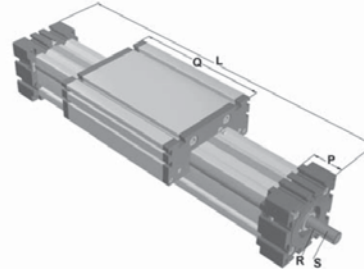
**Modular Linear Actuator ELT/ELK 30, 40, 60, 80, 80S, 100, 125**

Dimensions (mm)

1



Increasing the carriage length will increase the basic length by the same amount.



\* For Trnuts refer to the accessory section

Size	Basic length L	A	B	C	D	E	F	G	H	J	K	MM	NN	OO	P	Q	R	S Ø x length	T Ø	Basic weight	Additional Weight per 100 mm
EL 30	120	70	56	42	40x1	13	35	-	-	26	47	-	M6	M6	18	82	-	5x16	4,2	0,7 kg	0,16 kg
EL 40	125	100	66	58	48x1	18	47	-	-	35	64	-	M6	M6	25	122	3x3x25	10x27	6,5	1,7 kg	0,32 kg
EL 60	245	144	96	82	62x1	30	69	-	-	49	90	-	M8	M8	35	168	5x5x28	14x35	8,5	5,1 kg	0,89 kg
EL 80	285	170	117	102	80x1	40	88	10	30	70	121	M6	M10	M10	45	194	6x6x40	18x45	8,5	10,0 kg	1,48 kg
EL 80S	305	190	126	102	80x1	40	88	12,5	30	71	122	M6	M10	M8	45	214	6x6x40	18x45	8,5	11,0 kg	1,48 kg
EL 100	410	230	155	130	110x1	50	112	-	30	90	155	M10	M10	M10	55	300	6x6x40	22x45	10,5	19,0 kg	2,00 kg
EL 125	510	295	200	165	130x1	60	142	-	30	107,5	190	M10	M12	M12	65	365	8x7x50	25x55	13,0	33,0 kg	2,89 kg

**Screw Type:**  
**(T)** Acme Screw      **(K)** Ball Screw

**Selection of screw hand:**  
**(1)** right-hand   **(2)** left-hand (ball screw by inquiry)

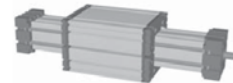
**Choice of guide body profile:**  
**(0)** standard   **(1)** stainless guide rod   **(2)** stainless guide rods and screws   **(3)** stainless guide rods, rollers and screws

**Choice of carriages:**

**(0)**



**(1)**



For standard carriage length see 'Q' in table. The carriages can be provided in any non-standard length on request; the longer the carriage, the greater the load capacity.

Top and bottom carriages are rigidly joined, enabling higher loads to be applied. This increases the basic length by 12-24 mm. For thickness of jointing plate refer to the accessory section.

**Choice of journal:**  
**(0)** one shaft (standard)   **(2)** shaft on both sides

**Selection of screw:**

Size	acme screw (trapezoidal)		ball screw	
	Standard	Multistart-screw	Standard	Multistart-screw
30	<b>(0)</b> Tr 10x3		<b>(0)</b> kg 8x2,5	
40	<b>(0)</b> Tr 18x4	<b>(1)</b> Tr 18x8	<b>(0)</b> kg 16x5	<b>(1)</b> kg 16x10
60	<b>(0)</b> Tr 24x5	<b>(1)</b> Tr 24x10	<b>(0)</b> kg 25x5	<b>(1)</b> kg 20x20 <b>(2)</b> kg 25x10 <b>(3)</b> kg 20x50
80	<b>(0)</b> Tr 28x5	<b>(1)</b> Tr 28x10	<b>(0)</b> kg 32x5	<b>(1)</b> kg 25x25 <b>(2)</b> kg 32x10
100	<b>(0)</b> Tr 32x6	<b>(1)</b> Tr 32x12	<b>(0)</b> kg 32x5	<b>(1)</b> kg 32x10 <b>(2)</b> kg 32x20 <b>(3)</b> kg 32x32
125	<b>(0)</b> Tr 40x7	<b>(1)</b> Tr 40x14	<b>(0)</b> kg 40x10	<b>(1)</b> kg 40x20

**Ball Screw pitch accuracy:**  
**(0)** 0,1 mm / 300 mm (Standard)   **(1)** 0,05 mm / 300 mm   **(2)** 0,025 mm / 300 mm

**End play of ball nut:**  
**(0)** 0,04 mm (Standard),   **(1)** < 0,02 mm,   **(2)** 2% apply preload

**Repeatability:**  
 ± 0,2 mm Acme Screw  
 ± 0,025 mm Ball Screw

**1500** basic length + stroke = total length

EL T 40 1 0 0 0 0 0 0 0 1500  
 Pos. 1 2 3 4 5 6 7

Sample ordering code:  
 ELT40 with acme right-hand screw, standard body profile, top carriage, one shaft, 18x4 screw, 1325 mm stroke

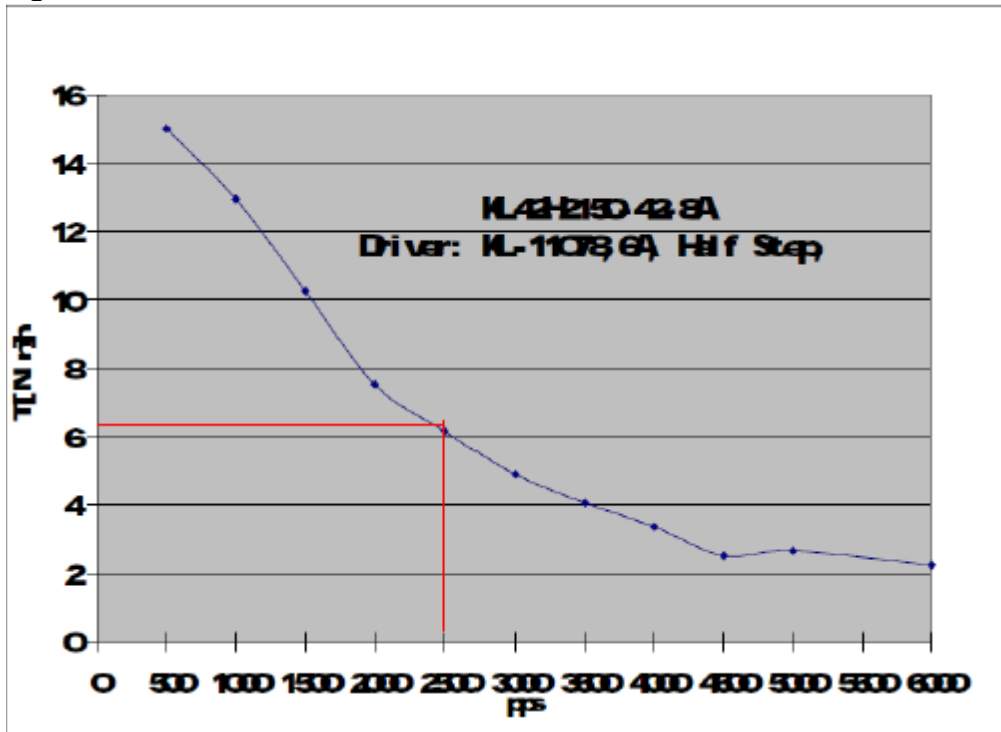
toll-free (877) 915-7100

www.precisionactuator.com

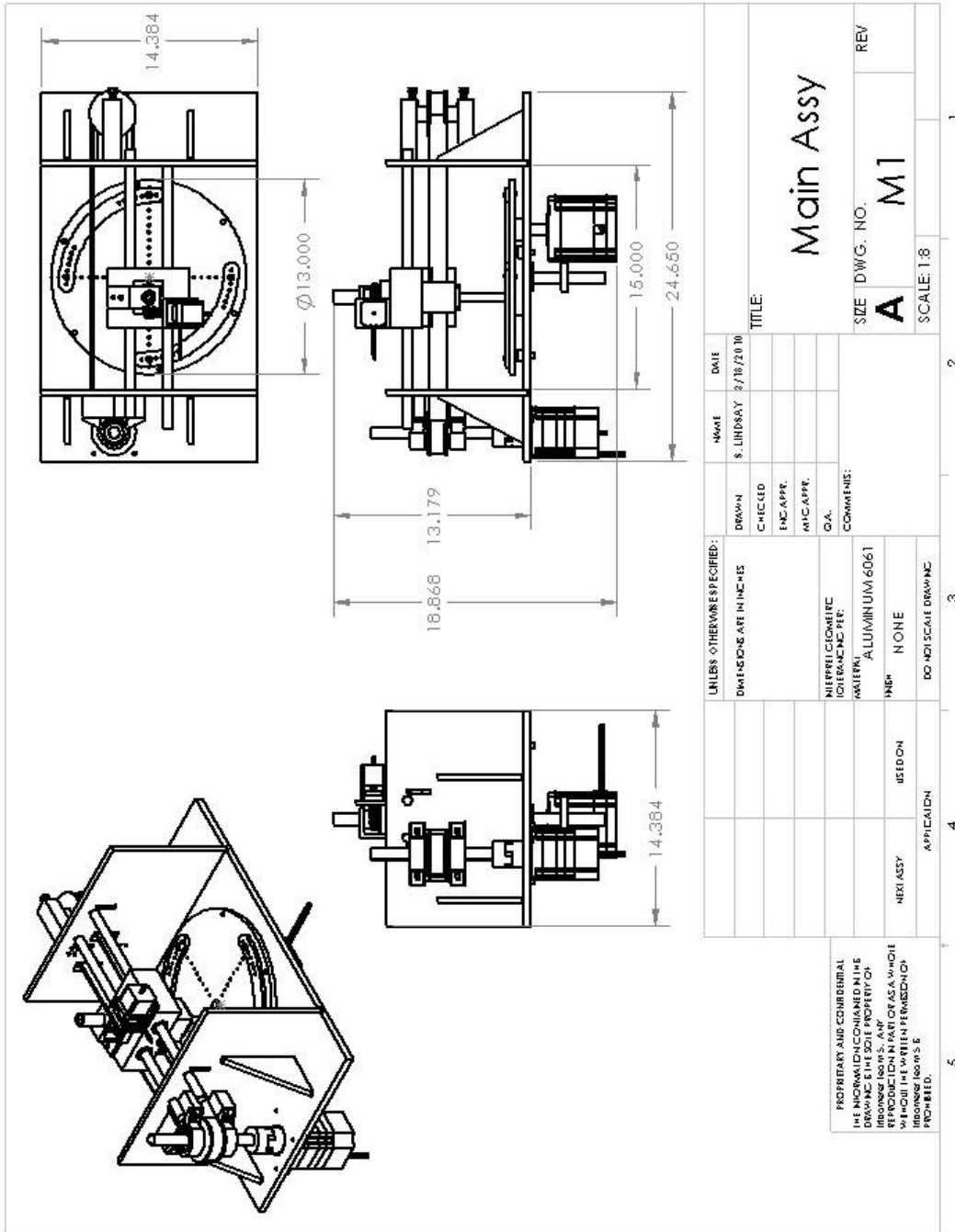
11



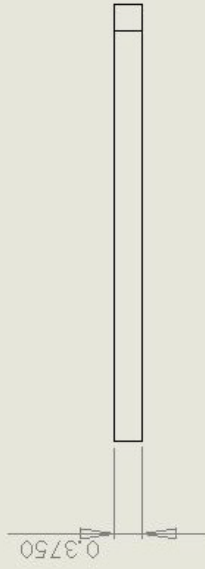
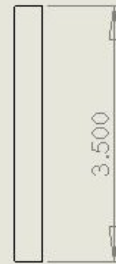
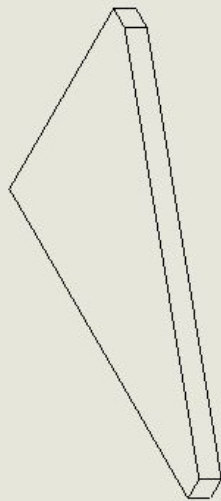
Figure G.4: Previous Year's Motor Curves



APPENDIX H: MANUFACTURING DRAWINGS AND PROCEDURE





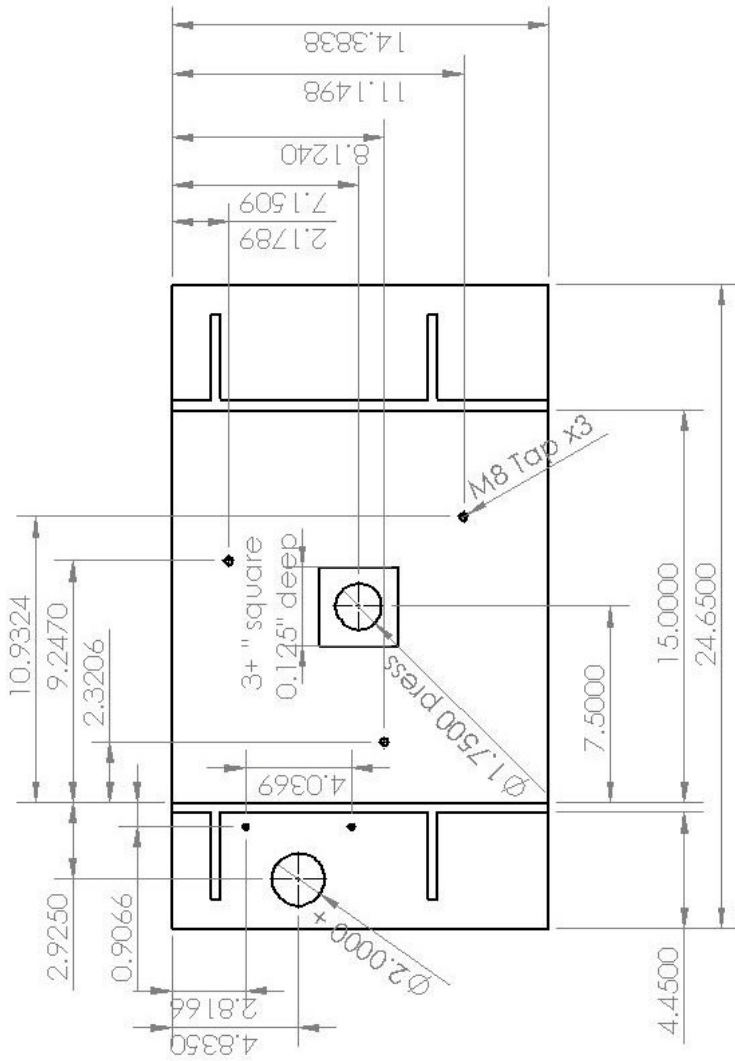


PROPRIETARY AND CONFIDENTIAL  
 THE INFORMATION CONTAINED IN THIS  
 DRAWING IS THE SOLE PROPERTY OF  
 INTERTECHNICAL SYSTEMS, INC. ANY  
 REPRODUCTION OR TRANSMISSION OF  
 THIS INFORMATION IN ANY FORM OR BY  
 ANY MEANS WITHOUT THE WRITTEN PERMISSION  
 OF INTERTECHNICAL SYSTEMS, INC. IS  
 PROHIBITED.

UNLESS OTHERWISE SPECIFIED:		NAME	DATE
DRAWN	S. LINDSAY		9/18/2010
CHECKED			
ENG APPR.			
MFG APPR.			
Q.A.			
COMMENTS:			
TOLERANCING PER:			
MATERIAL: ALUMINUM 6061			
FINISH: NONE			
NEXT ASSY	USED ON	SCALE: 1:2	
APPLICATION		SIZE	DWG. NO.
4		A	C_2
5		REV	
3		1	
2		1	
1		1	

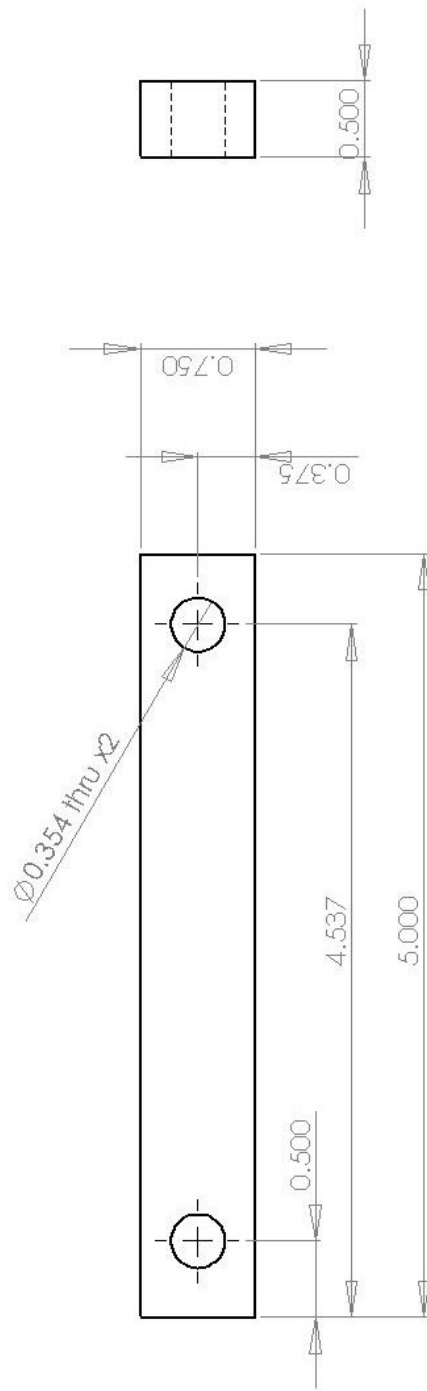
# Wall Rib

TITLE:



PROPRIETARY AND CONFIDENTIAL  
 THE INFORMATION CONTAINED IN THIS  
 DRAWING IS THE SOLE PROPERTY OF  
 TRICOORDER, INC. ANY REPRODUCTION  
 OR TRANSMISSION IN ANY FORM OR BY  
 ANY MEANS WITHOUT THE WRITTEN PERMISSION OF  
 TRICOORDER, INC. IS PROHIBITED.  
 Tricoorder Team 5-B

UNLESS OTHERWISE SPECIFIED:		NAME	DATE
DRAWN	IN INCHES	S. LINDSAY	3/18/2010
CHECKED			
ENG APPR.			
MFG APPR.			
G.A.			
COMMENTS:			
INTERPRET GEOMETRIC TOLERANCING PER:			
MATERIAL	ALUMINUM 6061		
FINISH	NONE		
USED ON			
APPLICATION			
NEXT ASSY			
TITLE:		SCALE: 1:10	
BASE PLATE		SIZE DWG. NO.	REV
		A C3	



UNLESS OTHERWISE SPECIFIED:		NAME	DATE
DIMENSIONS ARE IN INCHES		S. LINDSAY	3/18/2010
INTERPRET GEOMETRIC TO LEADING PER:		DRAWN	
MATERIAL		CHECKED	
FINISH		ENG. APPR.	
NEXT ASSY		MFG APPR.	
USED ON		Q.A.	
APPLICATION		COMMENTS:	
DO NOT SCALE DRAWING			

TITLE:

# Motor Connector

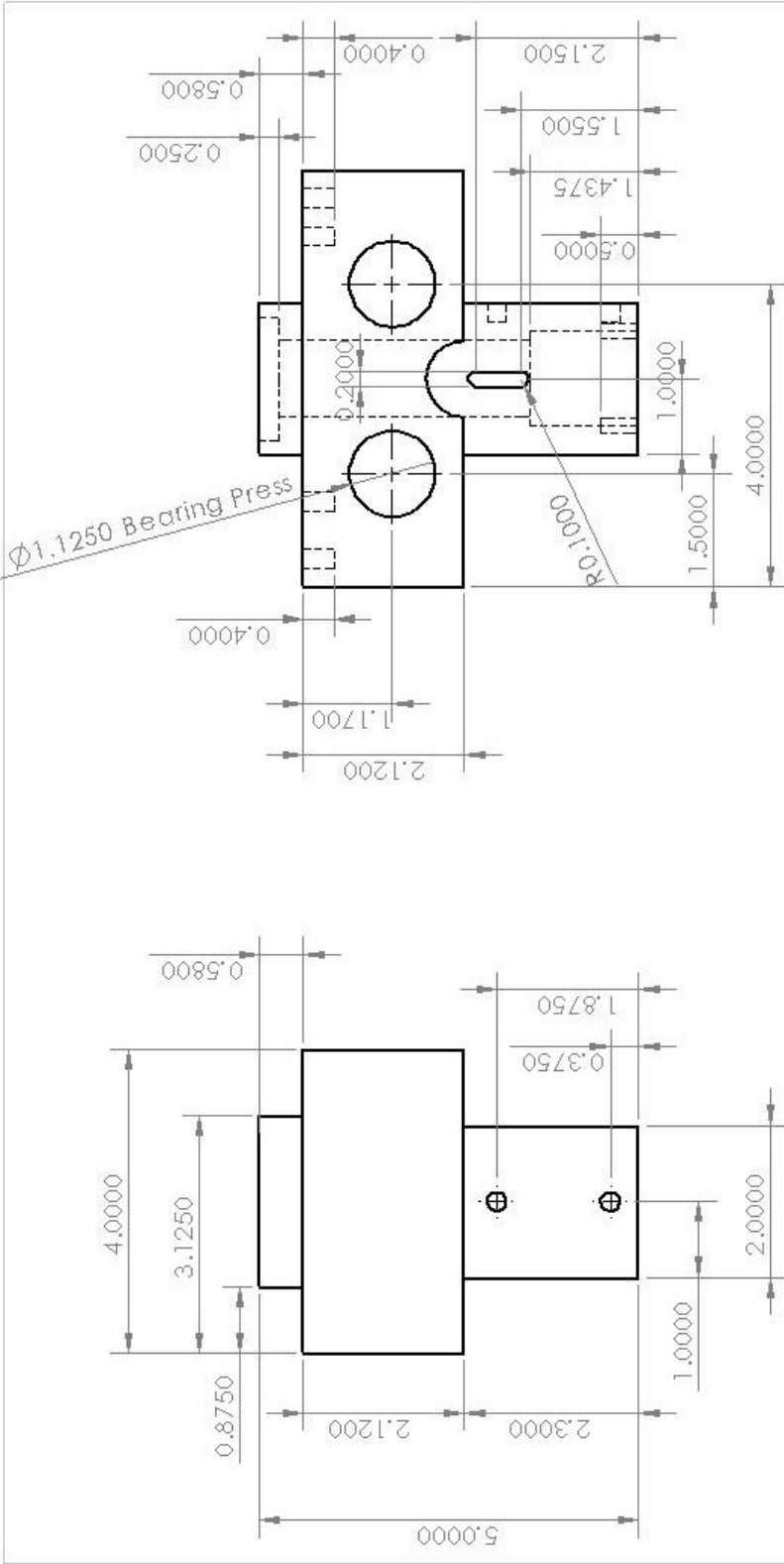
SIZE DWG. NO. REV

**A** **C4**

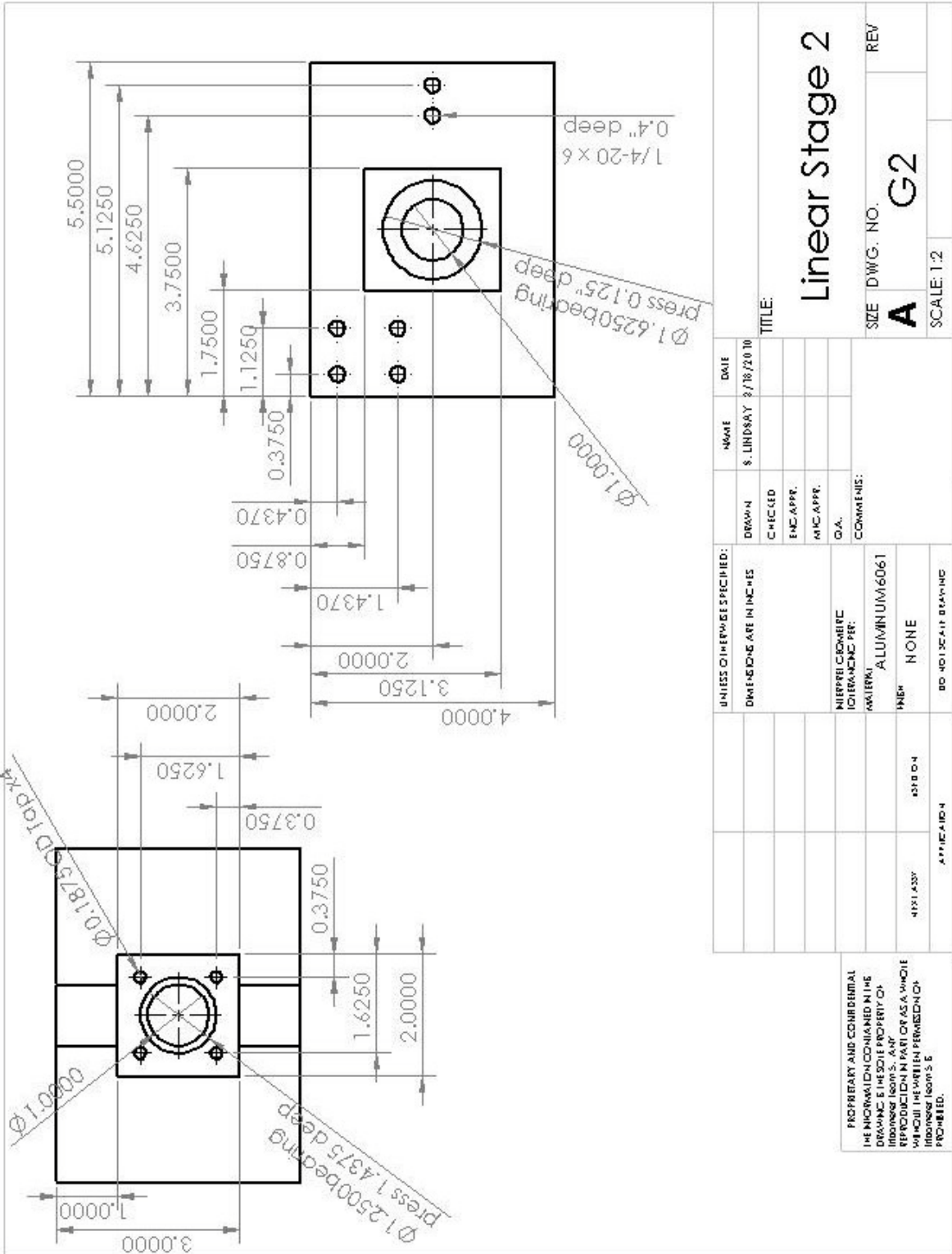
SCALE: 1:1

PROPRIETARY AND CONFIDENTIAL  
 THE INFORMATION CONTAINED IN THIS DRAWING IS THE SOLE PROPERTY OF  
 Tribometer Team S. NY  
 REPRODUCTION IN PART OR AS A WHOLE  
 WITHOUT THE WRITTEN PERMISSION OF  
 Tribometer Team S. NY  
 IS PROHIBITED.

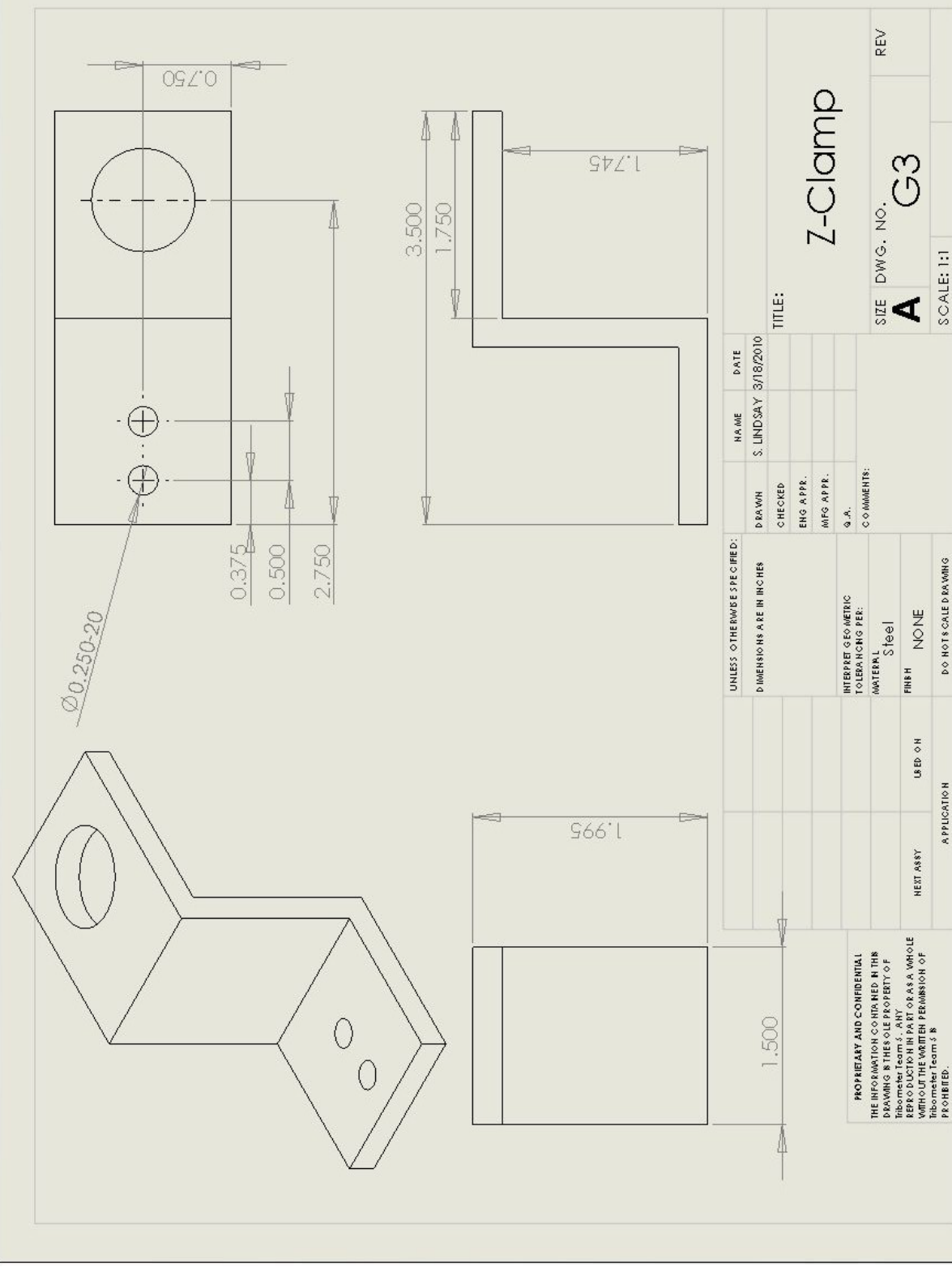
5 4 3 2 1

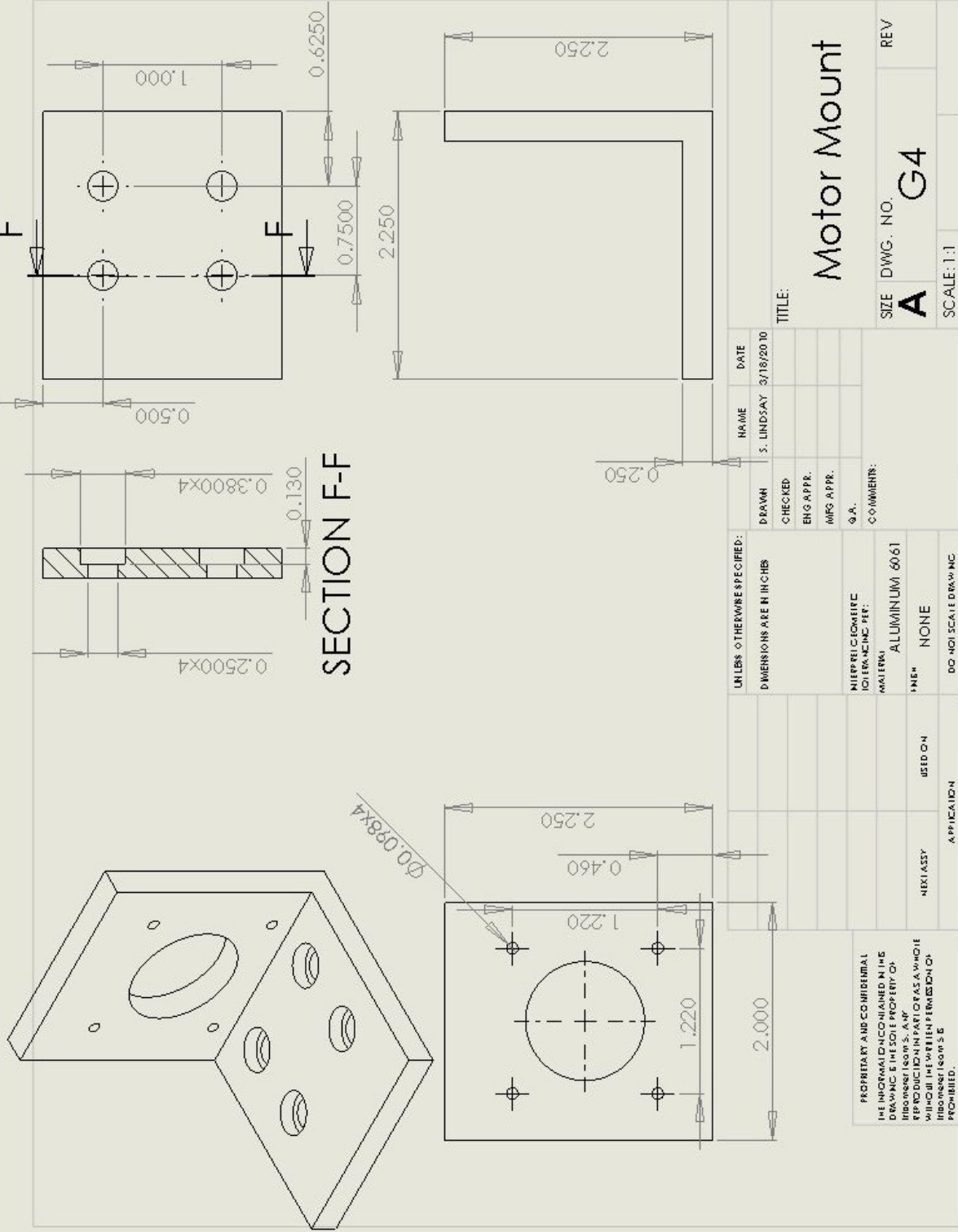


UNLESS OTHERWISE SPECIFIED: DIMENSIONS ARE IN INCHES		NAME S. LINDSAY	DATE 3/18/2010
DRAWN		CHECKED	TITLE: <b>Linear Stage</b>
ENG APPR.		ENG APPR.	SIZE DWG. NO. <b>A G1</b>
MFG APPR.		MFG APPR.	REV
Q.A.		Q.A.	SCALE: 1:2
COMMENTS:		1	
INTERPRET GEOMETRIC TO LEADING PER:		2	
MATERIAL ALUMINUM 6061		3	
FINISH NONE		4	
DOWNSCALE DRAWING		5	
NEXT ASSY		APPLICATION	
USED ON			
<p>PROPRIETARY AND CONFIDENTIAL THE INFORMATION CONTAINED IN THIS DRAWING IS THE SOLE PROPERTY OF THE COMPANY. ANY REPRODUCTION IN PART OR AS A WHOLE WITHOUT THE WRITTEN PERMISSION OF THE COMPANY IS PROHIBITED.</p>			



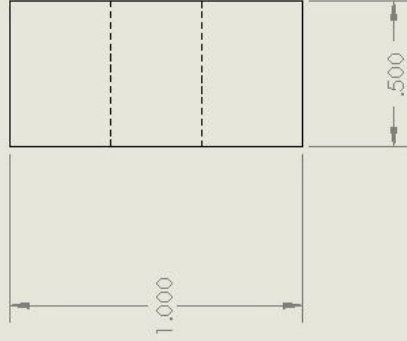
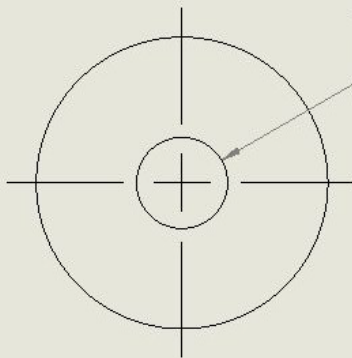
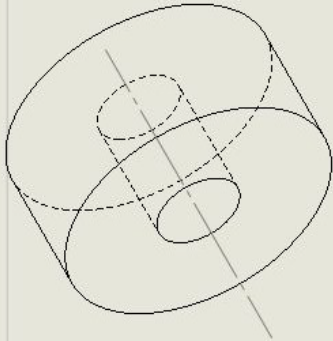






UNLESS OTHERWISE SPECIFIED: DIMENSIONS ARE IN INCHES		NAME	DATE
DRAWN	CHECKED	S. LINDSAY	3/18/2010
ENG APPR.	ENG APPR.		
MFG APPR.	MFG APPR.		
Q.A.	Q.A.		
TOLERANCES UNLESS SPECIFIED:		TITLE: Motor Mount	
FRACTIONAL	DECIMAL	SIZE	DWG. NO.
		A	G4
MATERIAL: ALUMINUM 6061		REV	
FINISH: NONE		SCALE: 1:1	
DO NOT SCALE DRAWING			
NECESSARY	USED ON		
APPLICATION			

PROPRIETARY AND CONFIDENTIAL  
 THE INFORMATION CONTAINED IN THIS  
 DRAWING IS THE SOLE PROPERTY OF  
 IRIDIUM TECHNOLOGIES, AND IS TO BE  
 USED FOR THE INTENDED APPLICATION  
 ONLY. REPRODUCTION OR TRANSMISSION  
 IN ANY FORM OR BY ANY MEANS IS  
 PROHIBITED.



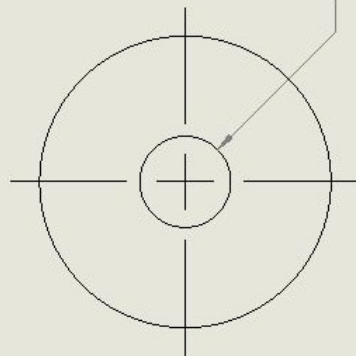
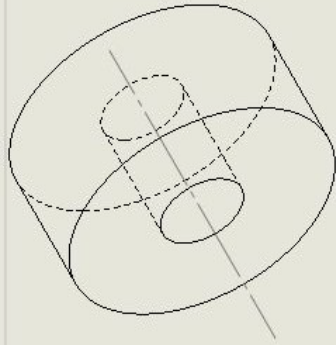
PROPRIETARY AND CONFIDENTIAL  
 THE INFORMATION CONTAINED IN THIS  
 DRAWING IS THE SOLE PROPERTY OF  
 GEORGE A. HANCOCK COMPANY. ANY  
 REPRODUCTION IN PART OR AS A WHOLE  
 WITHOUT THE WRITTEN PERMISSION OF  
 GEORGE A. HANCOCK COMPANY IS  
 PROHIBITED.

UNLESS OTHERWISE SPECIFIED:		NAME	DATE
DIMENSIONS ARE IN CHES	DRAWN	S. LINDSAY	
TOLERANCING PER:	CHECKED		
INTERPRET GEOMETRIC	ENG APPR.		
TOLERANCING PER:	MFG APPR.		
MATERIAL	Q. A.		
FINISH	COMMENTS:		
NEXT ASSY	USED ON		
APPLICATION	DO NOT SCALE DRAWING		

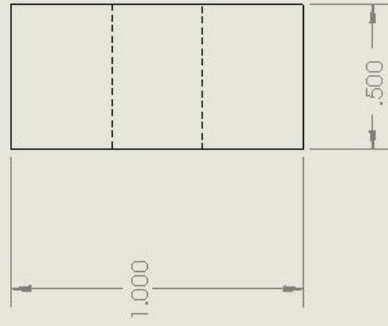
TITLE:  
**Screw End Cap**

SIZE DWG. NO. REV  
**A G5**

SCALE: 2:1 WEIGHT: SHEET 1 OF 1



$\phi$ .250-20 Through Tapped

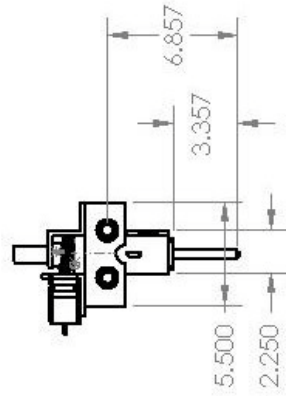
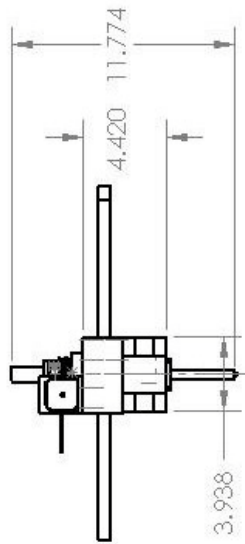
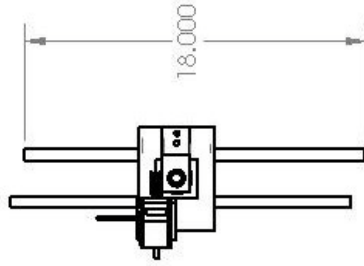
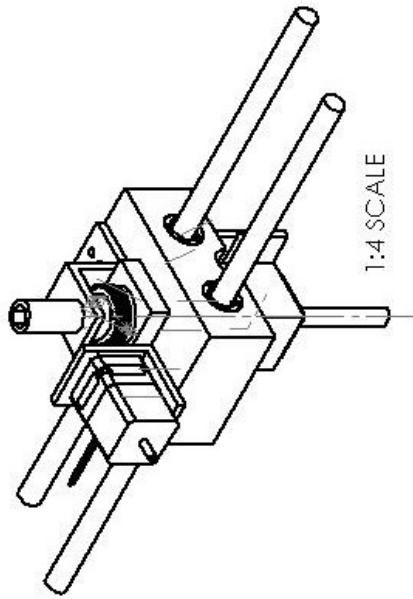


PROPRIETARY AND CONFIDENTIAL  
 THE INFORMATION CONTAINED IN THIS  
 DRAWING IS THE SOLE PROPERTY OF  
 WESTERN AIRCRAFT MANUFACTURING  
 SERVICE COMPANY. IT IS TO BE KEPT  
 SECRET IN ALL PARTS OF THE WORLD  
 WITHOUT THE WRITTEN PERMISSION OF  
 WESTERN AIRCRAFT MANUFACTURING  
 SERVICE COMPANY. NAME HEREIN IS  
 PROHIBITED.

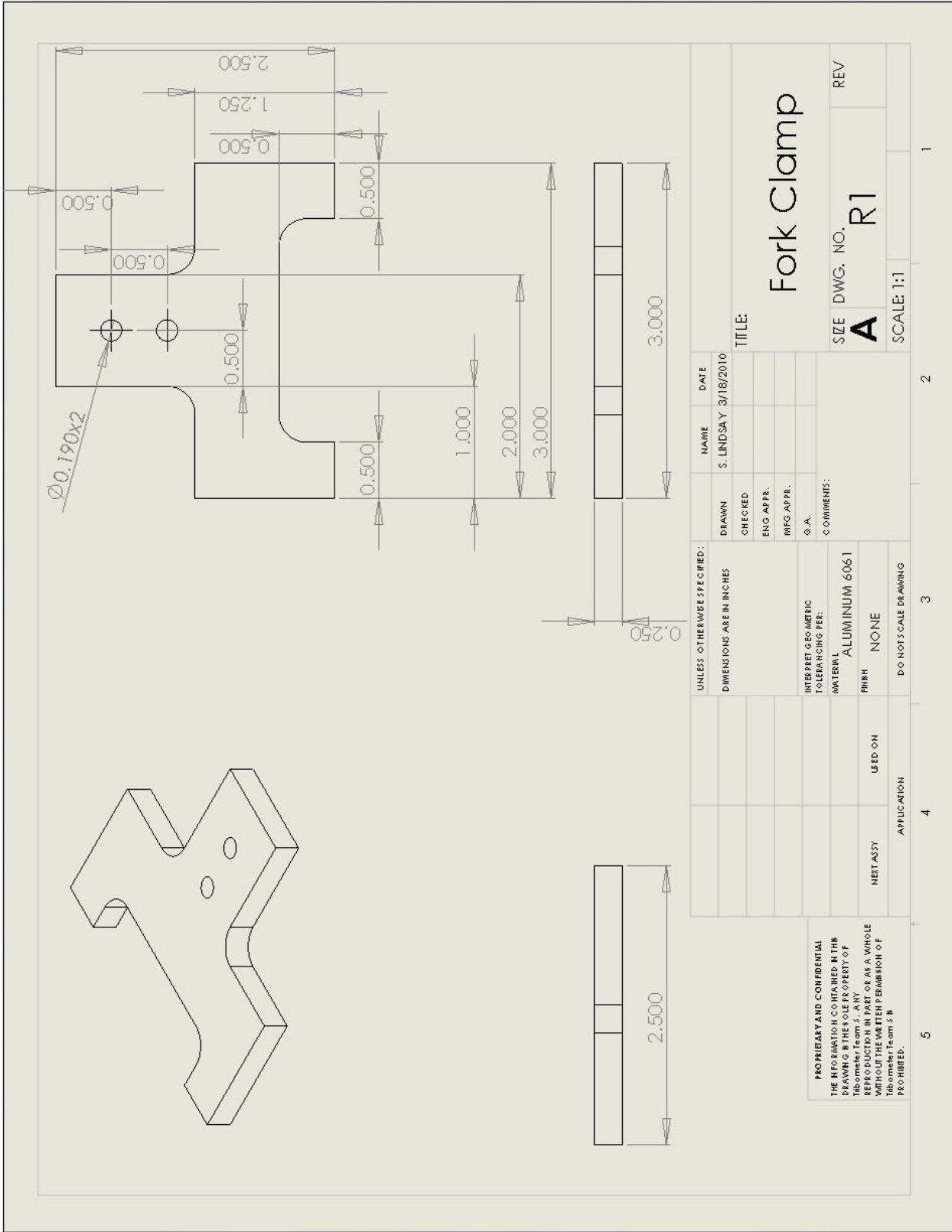
UNLESS OTHERWISE SPECIFIED:		NAME	DATE
DIMENSIONS ARE IN INCHES	DRAWN	S. LINDSAY	
TOLERANCES:	CHECKED		
FRACTIONAL: ±	ENG APP R.		
DECIMAL: ±	MFG APP R.		
ANGLE: MACH: ±	Q. A.		
TWO PLACE DECIMAL: ±	COMMENTS:		
THREE PLACE DECIMAL: ±			
INTERPRET GEOMETRIC TOLERANCING PER:			
MATERIAL:			
FINISH:			
HEAT ASSY:	USED ON:		
APPLICATION:			

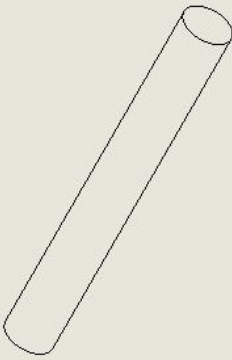
### Damper End Cap

SIZE DWG. NO. **A G6** REV  
 SCALE: 2:1 WEIGHT: SHEET 1 OF 1



UNLESS OTHERWISE SPECIFIED: DIMENSIONS ARE IN INCHES		NAME S. LINDSAY	DATE 3/18/2010
INTERPRETING/REWORKING REF:		DRAWN CHECKED	TITLE: <b>Carriage Assy</b>
MATERIAL: ALUMINUM 6061		ENG APPR.	SIZE DWG. NO. REV <b>A G7</b>
FINISH: NONE		MFG APPR.	SCALE: 1:8
DO NOT SCALE DRAWING		COMMENTS:	
PROPERTY AND CONFIDENTIAL THE INFORMATION CONTAINED IN THIS DRAWING IS THE SOLE PROPERTY OF HOMERSON S. A. ANY REPRODUCTION IN PART OR AS A WHOLE WITHOUT THE WRITTEN PERMISSION OF HOMERSON S. A. IS PROHIBITED.	HEAT TREAT	APPLICATION	
1	2	3	4
5	6	7	8





PROPRIETARY AND CONFIDENTIAL  
 THE INFORMATION CONTAINED IN THIS  
 DRAWING IS THE SOLE PROPERTY OF  
 TRICOMER TEAM S. A. ANY  
 REPRODUCTION OR TRANSMISSION  
 OF THIS DRAWING OR ANY PART  
 THEREOF WITHOUT THE WRITTEN PERMISSION OF  
 TRICOMER TEAM S. A.  
 PROHIBITED.

UNLESS OTHERWISE SPECIFIED:		NAME	DATE
DIMENSIONS ARE IN INCHES		S. LINDSAY	3/18/2010
INTERPRET GEOMETRIC TOLERANCING PER:			
MATERIAL			
FINISH			
NEXT ASSY			
LEED ON			
DOWNS SCALE DRAWING			

# Rotational Shaft

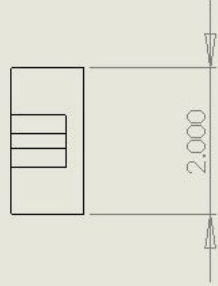
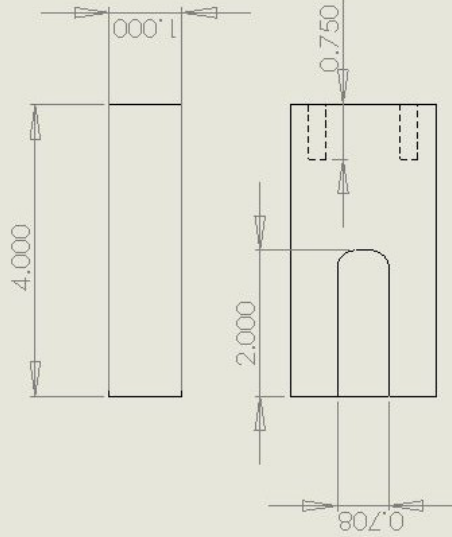
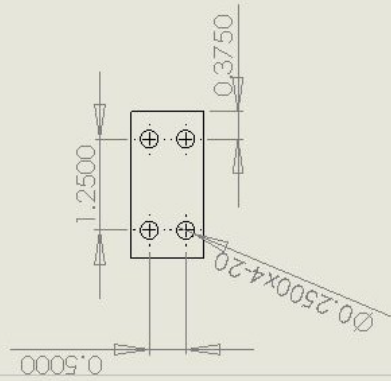
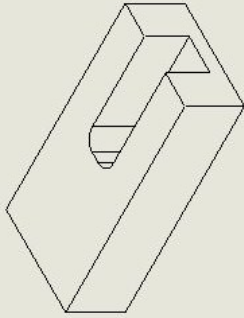
SIZE DWG. NO. **A** **R2** REV

SCALE: 1:2

5	4	3	2	1
---	---	---	---	---



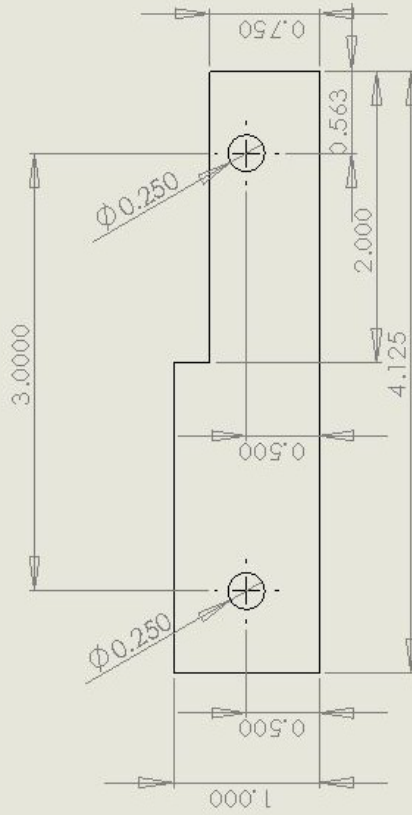
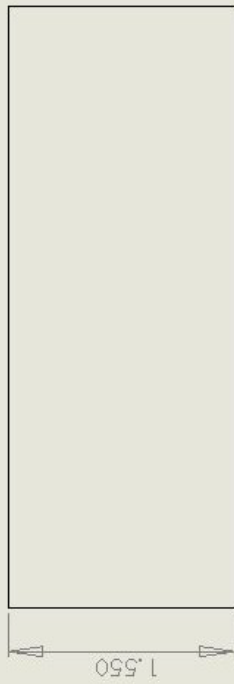
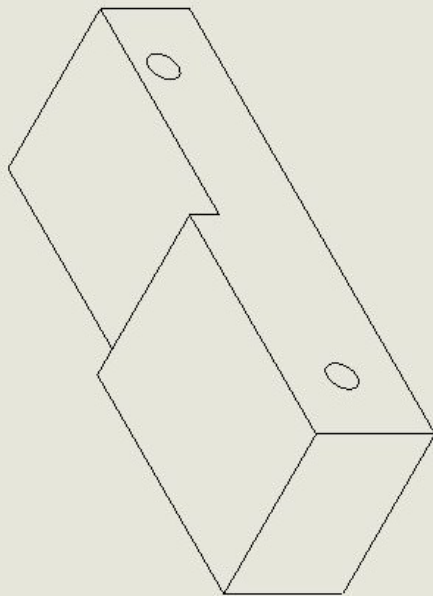




UNLESS OTHERWISE SPECIFIED:		NAME	DATE
DIMENSIONS ARE IN INCHES		S. LINDSAY	3/18/2010
INTERPRET GEOMETRIC TOLERANCING PER:			
MATERIAL			
FINISH			
USED ON			
NEXT ASSY			
APPLICATION			
DO NOT SCALE DRAWING			
TITLE:		Bottom Idler Mount	
SIZE		DWG. NO.	REV
A		L_2	
SCALE: 1:2			

PROPRIETARY AND CONFIDENTIAL  
 THE INFORMATION CONTAINED IN THIS DRAWING IS THE SOLE PROPERTY OF BOSTON ELECTRIC COMPANY. ALL RIGHTS ARE RESERVED. WITHOUT THE WRITTEN PERMISSION OF BOSTON ELECTRIC COMPANY, REPRODUCTION OR TRANSMISSION IS PROHIBITED.

5 4 3 2 1



UNLESS OTHERWISE SPECIFIED:		NAME	DATE
DRAWN	CHECKED	S. LINDSAY	9/18/2010
ENG APPR.	MEG A PPR.		
Q.A.	COMMENTS:		
INTERPRET GEOMETRIC TOLERANCING PER:			
MATERIAL:	ALUMINUM 6061		
FINISH:	NONE		
NEXT ASSY	USED ON		
APPLICATION			

PROPRIETARY AND CONFIDENTIAL  
 THE INFORMATION CONTAINED IN THIS  
 DRAWING IS THE SOLE PROPERTY OF  
 INTERNATIONAL S. AN  
 THIS DOCUMENT IS TO BE USED AS A GUIDE  
 WITH ALL NECESSARY PRECAUTIONS  
 INTERNATIONAL S. IS  
 PROHIBITED.

### Top Gap Spacer

SIZE	DWG. NO.	REV
<b>A</b>	<b>L3</b>	
SCALE: 1:1		

1 2 3 4 5



## APPENDIX I: FABRICATION DETAILS

### I.1 Manufacturing Plan

<b>Part ID</b>	C1 - Idler Side Wall	<b>QTY:</b>	1		
<b>Material</b>	6061 T4 Aluminum				
<b>Step</b>	<b>Operation</b>	<b>Machine</b>	<b>Cutting Tool</b>	<b>Cutting Speed</b>	<b>Notes</b>
1	Cut to size (rough)	Band saw		high	
2	Clamp to mill	Mill			clamp
3	Mill Edges to final dimensions	Mill	.5" edge mill	800 rpm	
4	zero	Mill	edge finder	500 rpm	
5	Mill slots	Mill	3/8" end mill	350 fpm, 800 rpm	
6	Mill thru slots	Mill	3/4" end mill	350 fpm, 800 rpm	
7	drill rail holes	Mill	39/64" drill	1000 rpm	
8	ream rail holes	Mill	5/8" ream	rpm	
9	drill bolt holes	Mill	D drill	1000 rpm	
10	ream holes	Mill	1/4" ream	rpm	
<b>Part ID</b>	Wall Ribs	<b>QTY:</b>	4		
<b>Material</b>	6061 T4 Aluminum				
<b>Step</b>	<b>Operation</b>	<b>Machine</b>	<b>Cutting Tool</b>	<b>Cutting Speed</b>	<b>Notes</b>
1	Rough cut	band saw	band saw	High	
2	Secure in mill	mill			clamp
3	Zero	mill	edge finder	500 rpm	
4	Mill edges	mill	1/2" end mill	350 fpm, 800 rpm	
<b>Part ID:</b>	C3 - Base Plate	<b>Qty</b>	1		
<b>Material:</b>	6061-T4 Aluminum				
<b>Step</b>	<b>Operation</b>	<b>Machine</b>	<b>Cutting Tool</b>	<b>Cutting Speed</b>	<b>Notes</b>
1	Secure in mill	CNC mill			clamp
2	Zero	CNC mill			(modifying
3	Cut bearing mount	CNC mill	1/2" end mill	350 fpm, 800 rpm	existing
4	Drill ball transfer holes (3)	CNC mill	ISO 6.75 mm drill	1000 rpm	part)
5	Drill motor mount holes	CNC mill	T drill	1000 rpm	
6	Tap b.t. holes	by hand	M8x1.25 tap		
<b>Part ID:</b>	C4 - Motor Connector	<b>Qty</b>	1		
<b>Material:</b>	6061-T4 Aluminum				
<b>Step</b>	<b>Operation</b>	<b>Machine</b>	<b>Cutting Tool</b>	<b>Cutting Speed</b>	<b>Notes</b>
1	Cut stock to length	band saw		high	
2	secure in mill	mill			

3 Plane faces	mill	1/2" end mill	350 fpm, 800 rpm
4 Zero			
5 Drill holes	mill	ISO 8.9 drill	
6 Ream holes	mill	ISO 9 mm ream	

**Part ID:** G1 Linear Stage

**Qty** 1

**Material:** 6061-T4 Aluminum

Step	Operation	Machine	Cutting Tool	Cutting Speed	Notes
1	Rough cut	band saw	band saw	high	
2	secure in mill	cnc mill			
3	Mill top faces	CNC mill	0.5" end mill	350 fpm, 800 rpm	
4	rotate and secure	cnc mill			
5	Mill bottom faces	CNC mill	0.5" end mill	350 fpm, 800 rpm	
6	rotate and secure	cnc mill			
7	Mill front faces	CNC mill	0.5" end mill	350 fpm, 800 rpm	
8	rotate and secure	cnc mill			
9	Mill back faces	CNC mill	0.5" end mill	350 fpm, 800 rpm	
10	rotate and secure	cnc mill			
11	Mill left faces	CNC mill	0.5" end mill	350 fpm, 800 rpm	
12	rotate and secure	cnc mill			
13	mill right faces	CNC mill	0.5" end mill	350 fpm, 800 rpm	
	Back side features				
14	secure in mill	CNC mill			
15	Mill stepped hole	CNC mill	1/4" end mill	350 fpm, 800 rpm	
16	drill screw holes(6)	CNC mill	1/4" drill	1000 rpm	
	front side features				
17	secure in mill	CNC mill			
18	Mill stepped hole	CNC mill	1/4" end mill	350 fpm, 800 rpm	
19	drill screw holes (4)	CNC mill	1/4" drill	1000 rpm	
	right side features				
20	drill screw holes (2)	CNC mill	1/4" drill	1000 rpm	
	top side features				
21	mill slot	CNC mill	1/4" end mill	350 fpm, 800 rpm	
	bottom side features				
22	mill slot	CNC mill	1/4" end mill	350 fpm, 800 rpm	
23	tap holes (10)	by hand	1/4-20 tap		

**Part ID:** G4 Motor Mount

**Qty** 1

**Material:** 6061-T4 Aluminum

Step	Operation	Machine	Cutting Tool	Cutting Speed	Notes
1	rough cut	band saw	band saw	high	begin with

2 secure in mill	mill			L shaped
3 cut edges	mill	1/2" end mill	350 fpm, 800 rpm	stock
3 drill holes (4)	mill	ANSI 40 drill	1000 rpm	
4 rotate and secure	mill			
5 drill holes (4)	mill	1/4" drill	1000 rpm	
6 Countersink holes	mill	ANSI 62 mill	1000 rpm	

**Part ID:** G5 Screw End Cap

**Qty** 1

**Material:** 6061-T4 Aluminum

Step	Operation	Machine	Cutting Tool	Cutting Speed	Notes
1	mount in lathe	lathe			begin with
2	cut to diameter	lathe	cutter		1.25" stock
3	drill center hole	lathe	3/8" drill	1000 rpm	
4	cut to length	lathe	cutter	1000 rpm	
5	tap	by hand	3/8" -20		

**Part ID:** G6 Damper End Cap

**Qty** 1

**Material:** 6061-T4 Aluminum

Step	Operation	Machine	Cutting Tool	Cutting Speed	Notes
1	mount in lathe	lathe			begin with
2	cut to diameter	lathe	cutter		1.25" stock
3	drill center hole	lathe	3/8" drill	1000 rpm	
4	cut to length	lathe	cutter	1000 rpm	
5	tap	by hand	3/8" -20		

**Part ID:** R1 Fork Clamp

**Qty** 4

**Material:** 6061-T4 Aluminum

Step	Operation	Machine	Cutting Tool	Cutting Speed	Notes
1	rough cut	band saw	band saw		
2	cut profile	waterjet	abrasive water jet		
3	sand/file	hand	file		

**Part ID:** R2 Rotational shaft

**Qty** 1

**Material:** Alloy steel

Step	Operation	Machine	Cutting Tool	Cutting Speed	Notes
1	cut	band saw	band saw	low	3/4" drive
2	file ends	hand	file		shaft stock

**Part ID:** L1 top Idler mount

**Qty** 1

**Material:** 6061-T4 Aluminum

Step	Operation	Machine	Cutting Tool	Cutting Speed	Notes
------	-----------	---------	--------------	---------------	-------

1 rough cut	band saw	band saw	high
2 secure in mill	mill		
3 cut edges	mill	1/2" end mill	350 fpm, 800 rpm
4 cut slit	mill	1/2" end mill	350 fpm, 800 rpm
5 rotate and secure	mill		
6 drill holes (4)	mill	1/4" drill	1000 rpm
7 tap holes (4)	by hand	1/4"-20 tap	

**Part ID:** L2 bottom Idler mount

**Qty** 1

**Material:** 6061-T4 Aluminum

**Notes**

Step	Operation	Machine	Cutting Tool	Cutting Speed
1	rough cut	band saw	band saw	high
2	secure in mill	mill		
3	cut edges	mill	1/2" end mill	350 fpm, 800 rpm
4	cut slit	mill	1/2" end mill	350 fpm, 800 rpm
5	rotate and secure	mill		
6	drill holes (4)	mill	1/4" drill	1000 rpm
7	tap holes (4)	by hand	1/4"-20 tap	

**Part ID:** L3 Top Gap Spacer

**Qty** 1

**Material:** 6061-T4 Aluminum

**Notes**

Step	Operation	Machine	Cutting Tool	Cutting Speed
1	rough cut	band saw	band saw	high
2	secure in mill	mill		
3	cut edges	mill	1/2" end mill	350 fpm, 800 rpm
4	drill holes	mill	1/4" drill	1000 rpm

## I.2: Detailed Assembly

### Chassis Sub Assembly

The Chassis sub system consists of the base plate and wall structure which serves as a rigid structure for all other subsystems and assemblies to be mounted to. Figure 6.1 below shows a CAD model of the Chassis sub assembly.

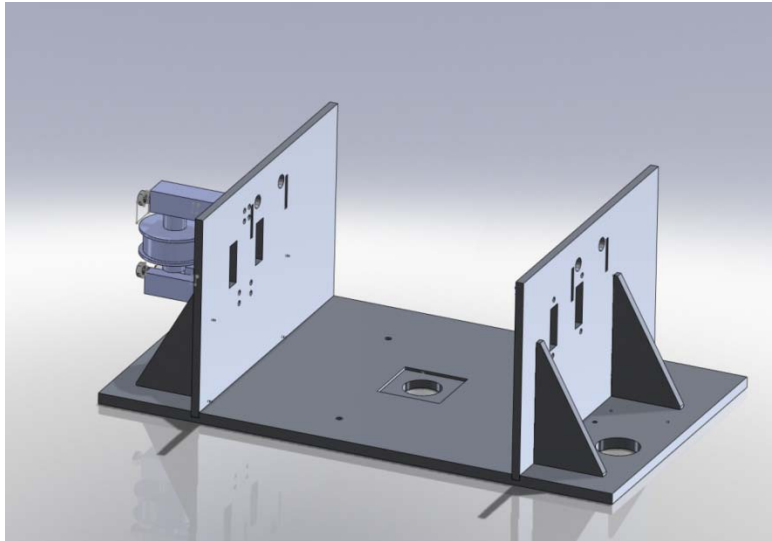


**Figure 6.1:** Chassis Sub Assembly

This sub assembly will be put together in the following steps:

1. Lower the idler side wall onto the base plate and align bolt holes from base plate to lower surface of side wall as seen in Figure 6.2 below. Once aligned, bolt in place with 4 ¼- 20 bolts.

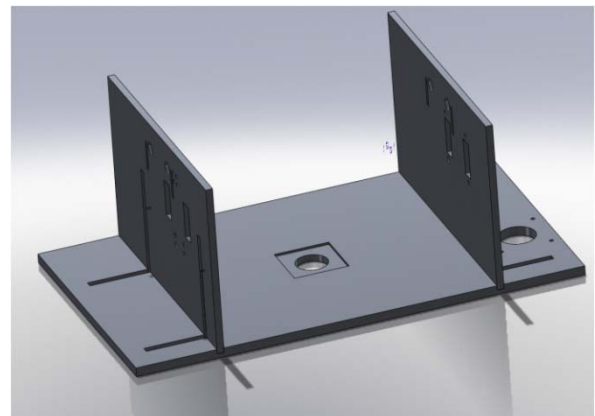
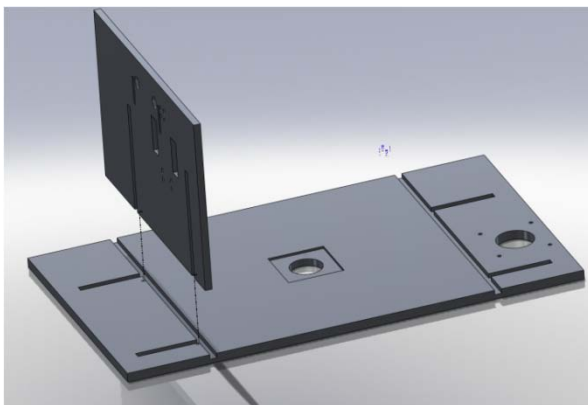


**Figure 6.2:** Side wall assembly for left and right walls

2. Fit both side rib attachments in the grooves that are manufactured into both the base plate and side wall as seen in Figure 6.3 below. Once in place, align both the bolt holes on the bottom and side faces of the attachment rib. Put all bolts in place and slowly tighten each one twist at a time until tight.





**Figure 6.3:** Side Reinforcement Assembly

3. With the main structure for the chassis in place, bolt on the upper and lower idler pulley mounts. Align the ¼” holes on the chassis wall to the corresponding holes on both idler pulley mounts and insert all 4 1/4” bolts into the threaded holes on the mounts as seen in Figure X below. Once the top and bottom mounts are bolted to the side wall slide the idler pulley wheel onto the 1” pulley shaft and place the belt over the pulley before sliding it into the pulley mount as seen in Figure 6.4 below.

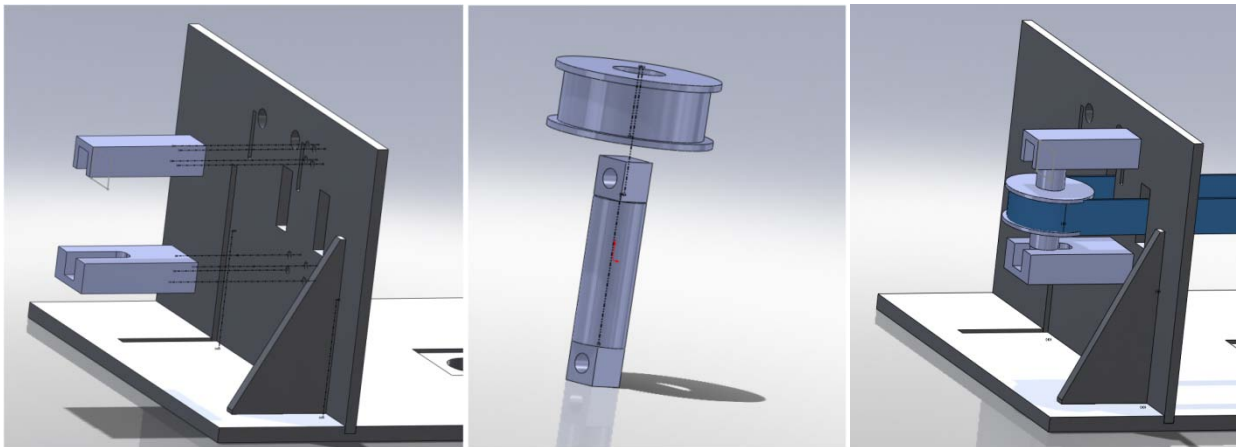


**Figure 6.4:** Idler Mount Assembly

4. Once the pulley and mounts are in place, place a nut on each of the tensioner bolts and thread onto the pulley shaft. Once both bolts have threaded onto the shaft enough to be touching the back wall of the mount, slowly tighten each bolt in unison to the desired torque. The full assembly for the belt tensioner system can be seen on the next page in Figure 6.5.

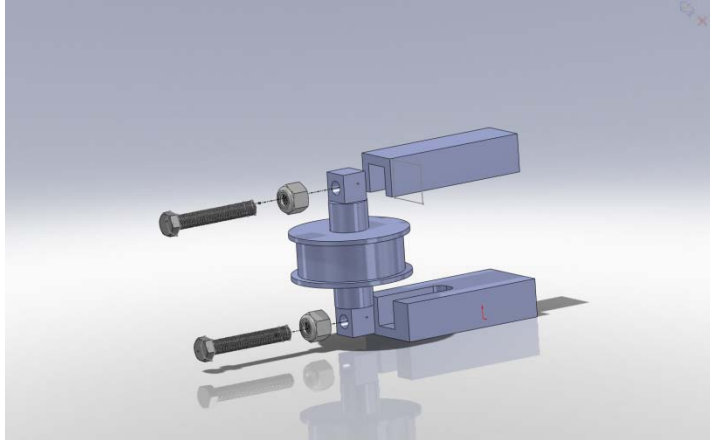


**Figure 6.5:** Assembly of bolt tensioners onto pulley shaft

### **Rotation System Sub Assembly**

The rotation system sub assembly is made up of the rotational motor/ gear system and rotation plate/ bearing system and sample holding system. Figure 6.6 below shows the full rotation sub assembly.

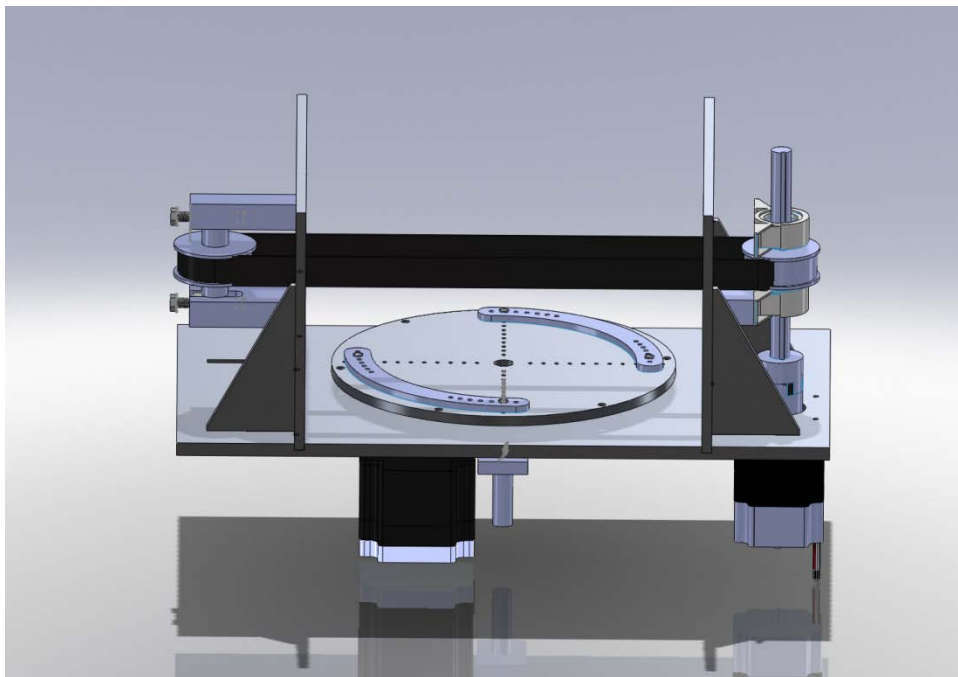


**Figure 6.6:** Rotation system sub assembly

This sub assembly will be put together in the following steps:

1. Mount the drive gear onto the motor shaft. Align the keyway of the gear with that of the motor shaft and insert the keyway as shown in Figure 6.7 on the next page.

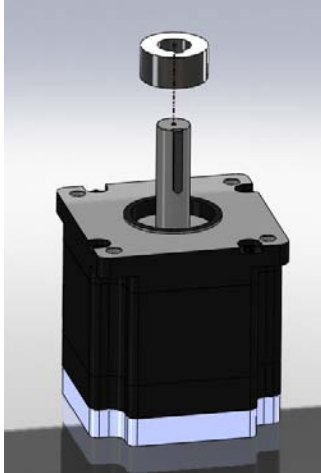


**Figure 6.7:** Drive gear mounting onto Rotational Motor with keyway alignment

2. Mount the motor to the base plate with four ¼” bolts and secure with ¼” nuts on top of base plate.
3. Press fit each ball transfer into the three base plate holes as shown in Figure 6.8. Also press fit the radial bearing into the hole located in the center of the base plate as shown.

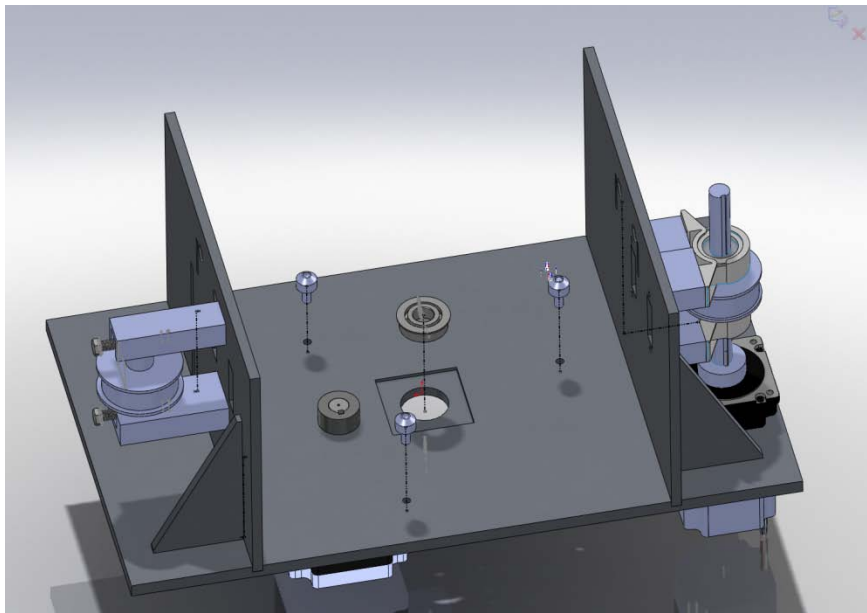


**Figure 6.8:** Ball transfer and radial bearing assembly

4. Press fit the steel rotational shaft into the center hole of the gear/ rotational plate assembly. The gear and rotational plate have already been assembled so no assembly is needed for these two parts. Once the shaft has been press fit into the follower gear on the underside of the rotating plate, insert it into the center shaft hole as shown in Figure 6.9 on the next page.

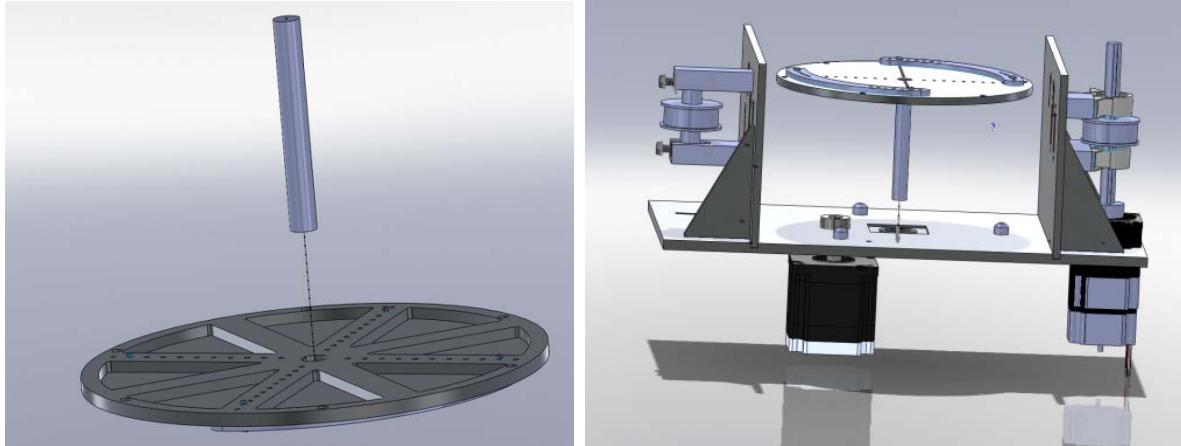


**Figure 6.9:** Rotational Shaft and Plate Assembly

### Gantry Subassembly

The gantry subassembly consists of the normal force application system and the linear sliding system. These are all housed in the linear stage. The following steps outline the assembly of this subassembly and the overall final assembly is shown in Figure 6.10.

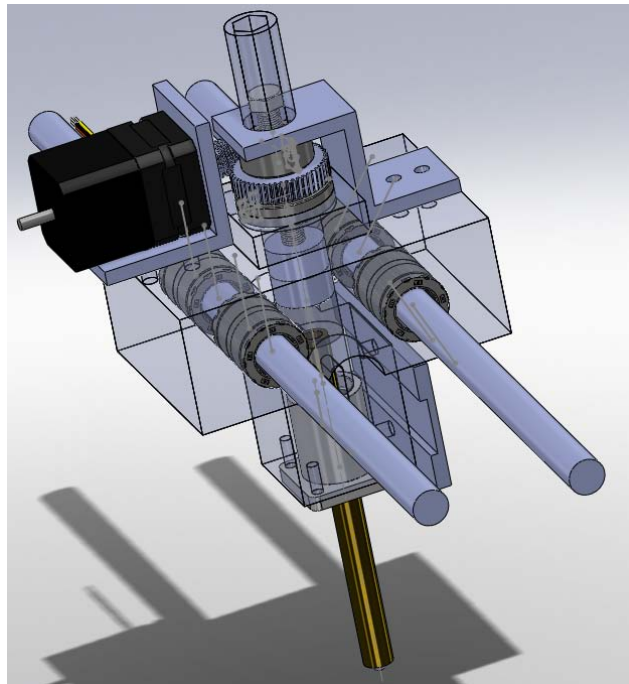


**Figure 6.10:** Full assembly of the gantry system

This sub assembly will be put together in the following steps.

1. Press fit the four linear bearings into the linear stage. Two bearings are inserted into each face. Align flush with face of the linear stage. The outer diameter of the bearings is 1.125". The location of the bearings is shown in Figure 6.11.

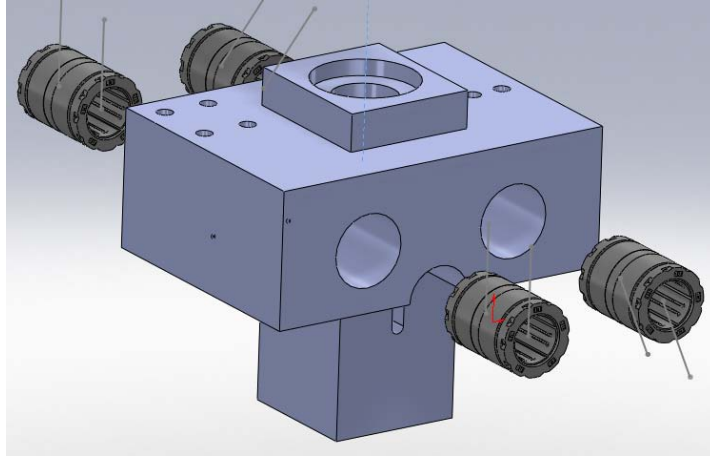


**Figure 6.11:** Press fit linear bearings into stage

2. Press fit the 1" diameter worm wheel into the radial bearing and press the spacer, 3/8" ID, into the upper race of the thrust bearing, 1/2" diameter. This is shown below in Figure 6.12.

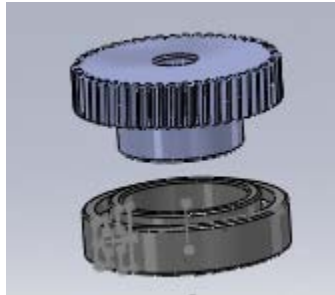


**Figure 6.12:** Press fit worm wheel and radial bearing

3. Slide the 3/8" diameter bolt through the thrust bearing with spacer (3/8" ID), thread through the worm wheel (and through the radial bearing connected in step 2) until about 0.75" of threads are exposed. Next thread on the cap to the bolt, 1" OD. This is shown in Figure 6.13.

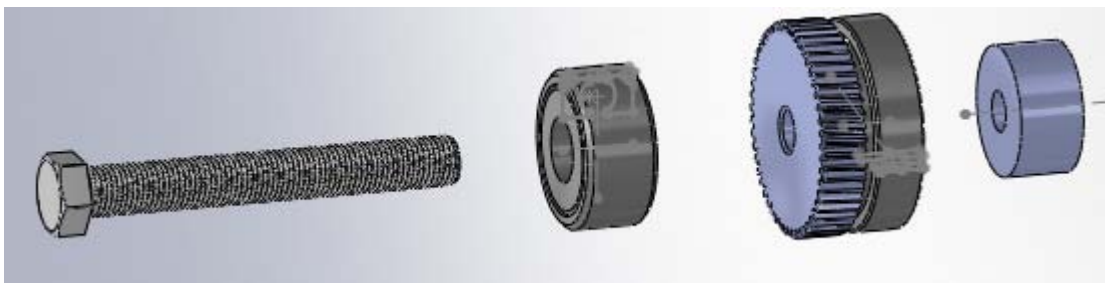


**Figure 6.13:** Bolt, gear, and bearing connection

4. Press fit the 1.625" OD radial bearing into the housing in the linear stage. It will sit on a flat surface in the housing with a depth of 0.25" which is half the height of the bearing. The cap and tip of the bolt will fit through the inner diameter in the linear stage. This is shown in Figure 6.14.

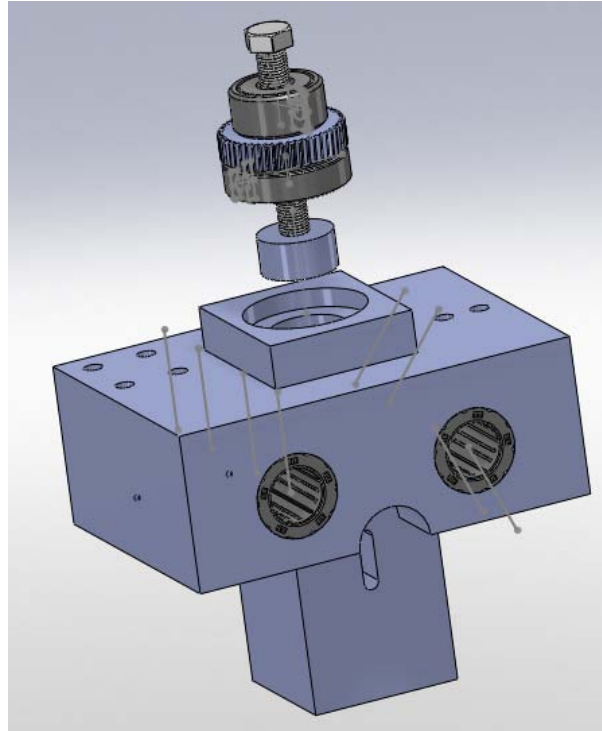


**Figure 6.14:** Securing the radial bearing into the linear stage

5. Slide 0.5" diameter pin through the bottom linear bearing. Then screw in appropriate rubber insert to the top of the pin. Screw on cap to the rubber insert. Make sure all connections are tight and secure. All threads are 1/4-20. Attach pin tip with appropriate ball sample inserted. This is shown in Figure 6.15.

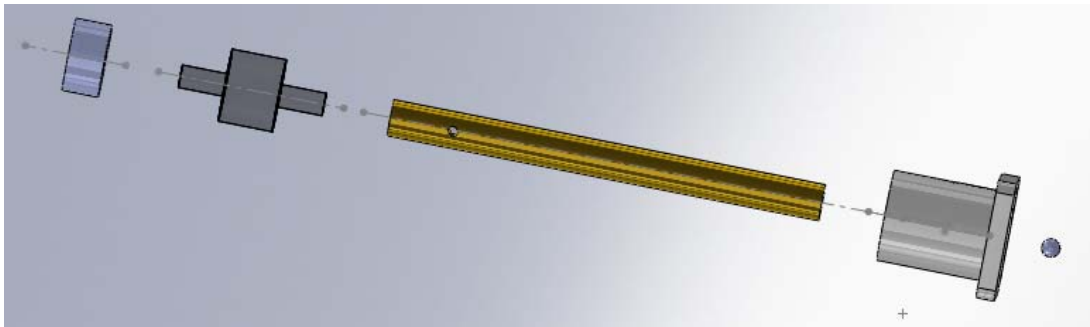


**Figure 6.15:** Pin connections

6. Slide pin and linear bearing, 1.25" OD, into the linear stage and secure the linear bearing to the bottom of the linear stage using 3/16" diameter bolts. The rubber insert and cap will fit into the inner through hole. This is shown in Figure 6.16.

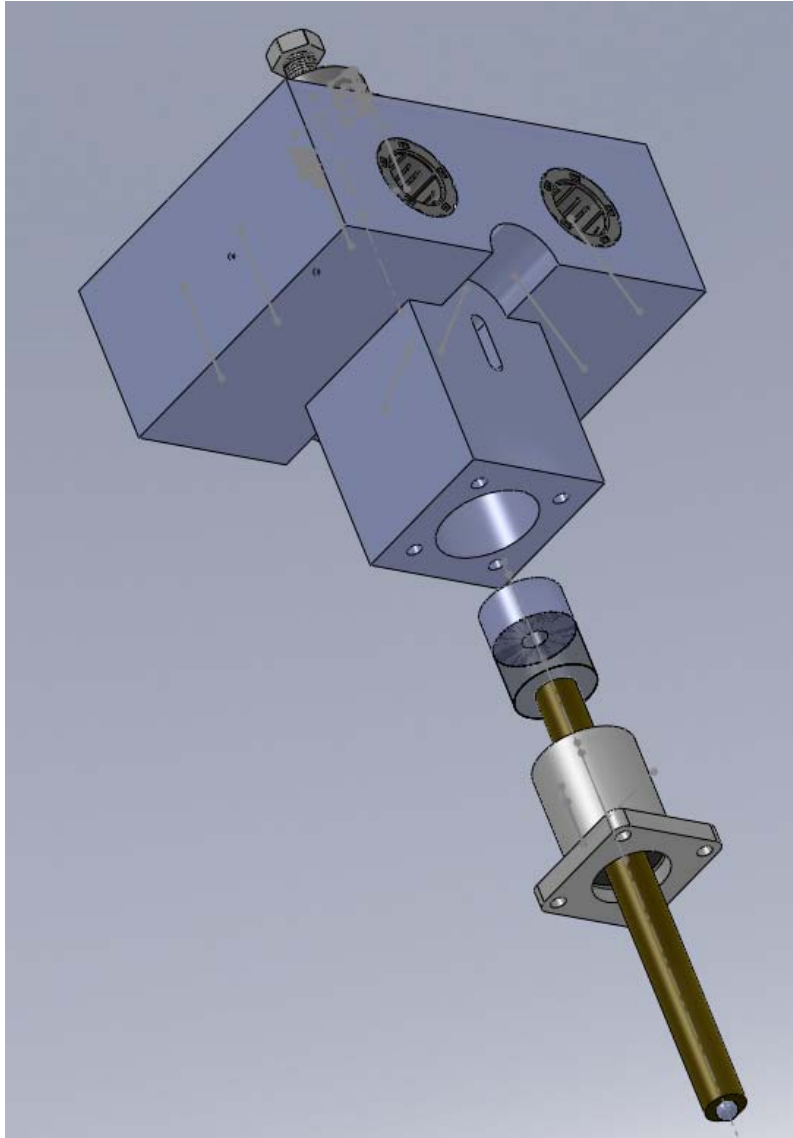


**Figure 6.16:** Connection of pin and linear bearing into linear stage

7. Use hand to rotate the pin until shoulder bolt holes are exposed. Thread shoulder bolts into the pin, through the groove in the side of the linear stage, to prevent rotation of the pin.
8. Bolt motor mount to the top of the linear stage using bolts using  $\frac{1}{4}$ -20, 0.5" bolts. The bolt heads will be recessed into the mount giving clearance for the motor to be on top of the bolted area. This is shown in Figure 6.17.

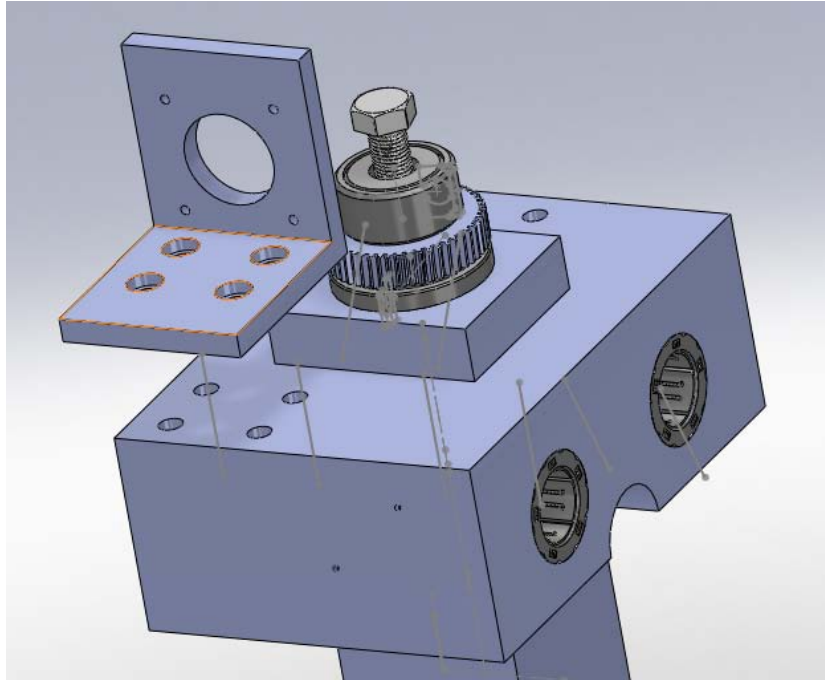


**Figure 6.17:** Connection of the motor mount

- Slide 0.5" OD guide rails through linear bearings that were press fit into the linear stage in step 1 and then through corresponding mount holes in the side walls. First slide the rails through one of the side walls, then through the linear stage, and finally through the other wall. Secure the guide rails on both walls with the provided shaft collars. These should be flush with the walls to prevent translation. This is shown in Figure 6.18.

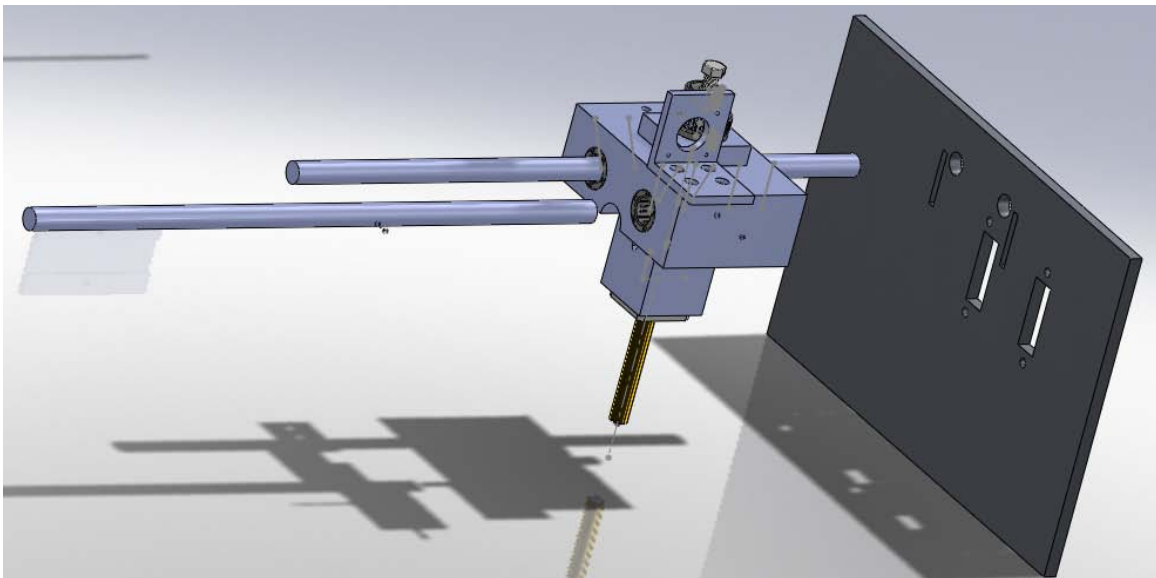


**Figure 6.18:** Secure gantry to guide rails and side walls

- Bolt motor to the motor mount aligning with the bolt holes and then secure the worm gear to the motor shaft using the set screw. Align the worm gear so there is a good connection between the gear and the worm wheel. This is shown in Figure 6.19.



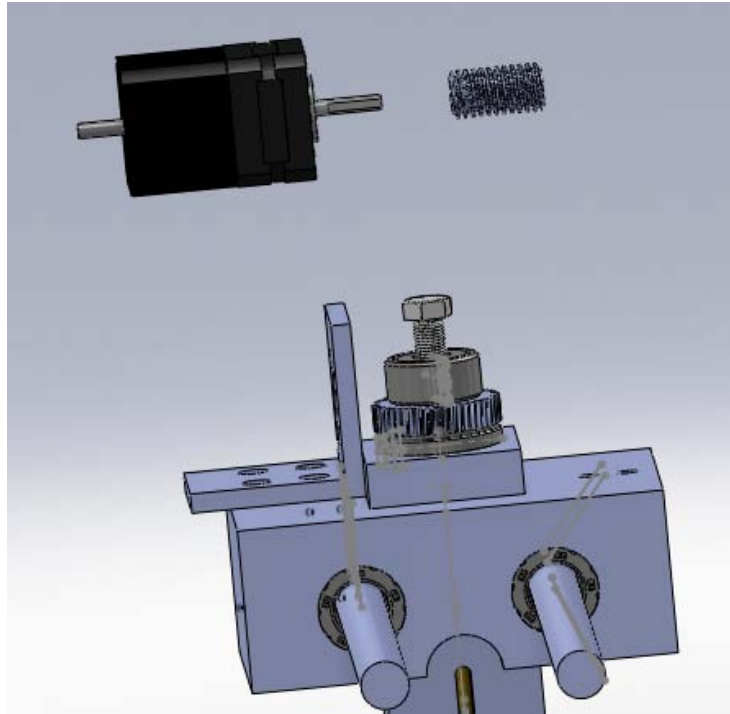


**Figure 6.19:** Connection of the motor and worm gear

11. Weld hex socket cap to Z-clamp connector using the welding tools in the machine shop.
12. Turn the application bolt so it slides smoothly into the 9/16" hex socket. Secure the z-clamp and hex socket weld to the top of the linear stage using 1/4-20, 0.5" long bolts. This will complete the assembly of the gantry system. This is shown in Figure 6.20.

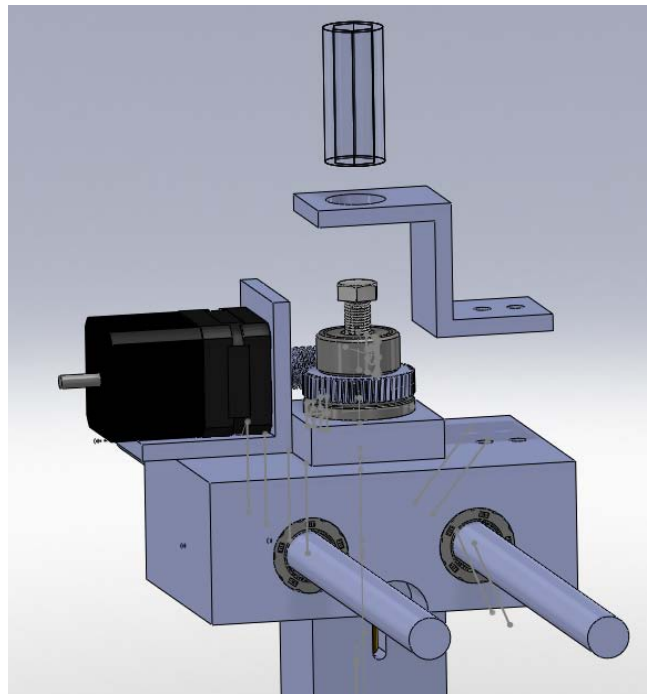


**Figure 6.20:** Connection of the hex socket and z-clamp  
**Linear Drive Shaft Sub-Assembly**

The linear drive shaft assembly consists of a DC servo motor and all of the components needed to transmit power from the shaft of the motor to the drive belt. This assembly is shown in Figure 6.21.

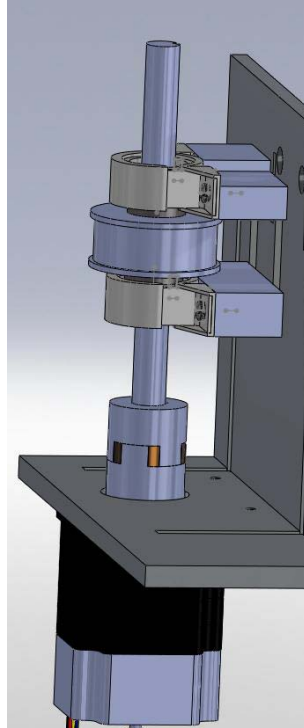


**Figure 6.21:** Linear drive shaft sub-assembly

This sub assembly will be put together in the following steps.

1. Mount one of the coupling hubs to the motor shaft (Figure 6.22) by inserting a key into the keyway of each the hub and shaft. This is the first portion of the flexible shaft coupling, which protects the motor shaft from bending moments. The connection should be snug.

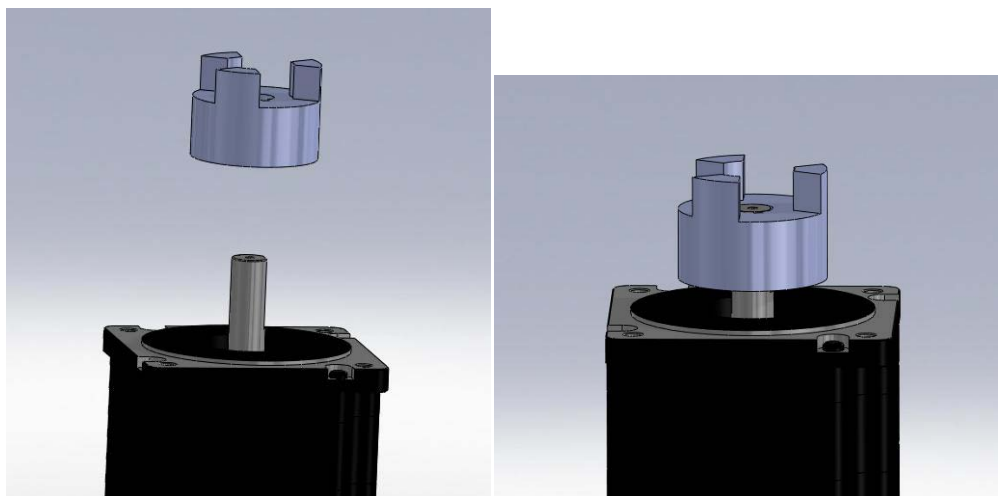


**Figure 6.22:** Flexible coupling hub mounting onto DC motor with keyway alignment

2. Bolt the motor to the base plate as shown in Figure 6.23 with  $\frac{1}{4}$ " bolts and secure with  $\frac{1}{4}$ " nuts.

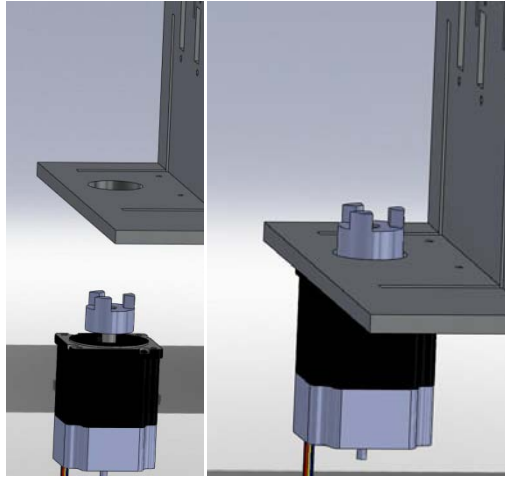


**Figure 6.23:** Motor mounting onto the base plate

3. Bolt the bearing spacer blocks to the side wall with  $\frac{1}{4}$ "-20 bolts as shown in Figure 6.24.

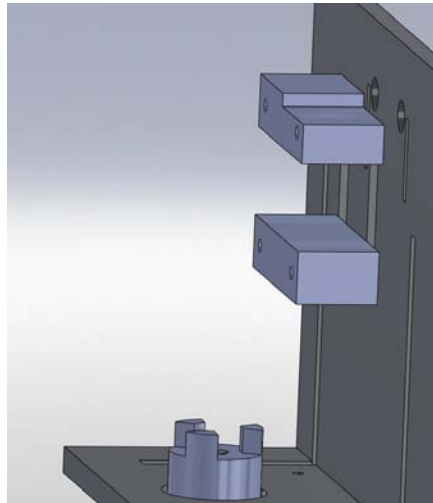


**Figure 6.24:** Mounting the spacers to the side wall

4. Mount the remaining coupling hub to the end of the  $\frac{3}{4}$ " shaft in the same way that the first coupling hub was mounted to the motor shaft.
5. Slide the first radial bearing onto the  $\frac{3}{4}$ " shaft. Then mount the drive pulley to the  $\frac{3}{4}$ " shaft so that the bottom of the pulley is 3.1 inches from the top of the flex coupling hub. The pulley should be rigidly fixed to the  $\frac{3}{4}$ " shaft by inserting a key into the keyways. Then slide the second radial bearing onto the  $\frac{3}{4}$ " shaft. This process is illustrated in Figure 6.25.

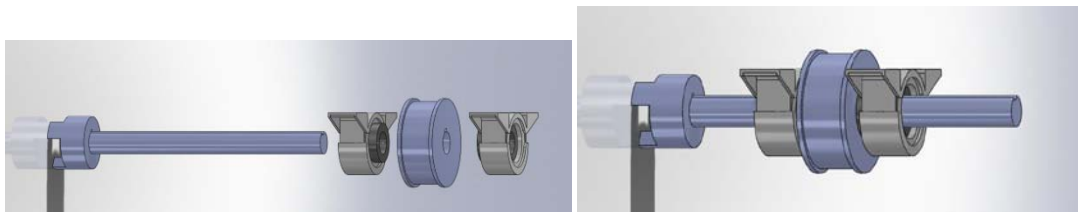


**Figure 6.25:** Mounting the drive pulley and bearings to the drive shaft

6. Place the spider gear in the coupling hub on the motor. Then place the shaft assembled in the previous two steps on the spider gear so that the two halves of the coupling mesh. This is shown in Figure 6.26. Start bolting the radial bearings to the spacer blocks, but do not tighten them yet.

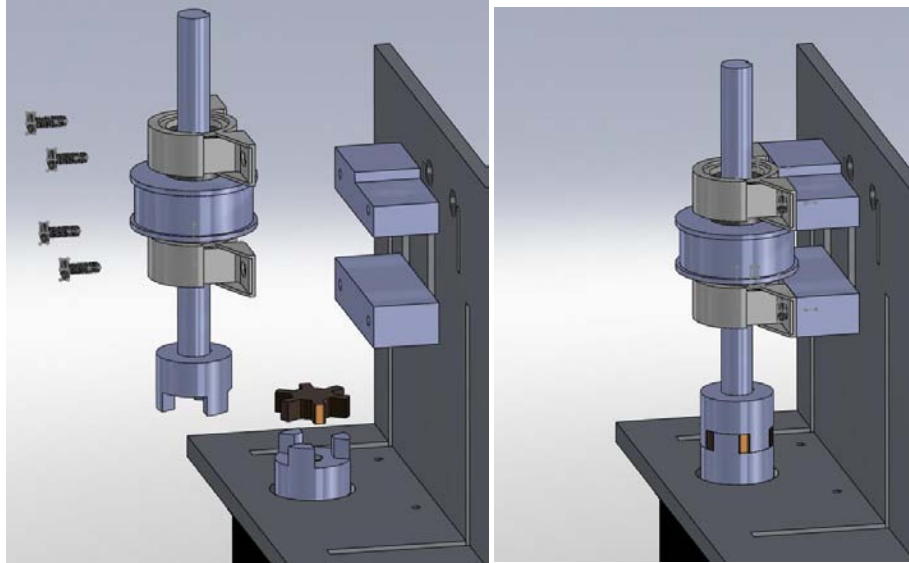


**Figure 6.26:** Mounting assembled drive shaft to motor and chassis

7. While ensuring that the radial bearings remain aligned with the  $\frac{3}{4}$ " shaft, tighten the bolts connecting the bearings to the spacer blocks. The bolts should not be tightened all at once. Rather, tighten one bolt one half turn, then tighten the next bolt one half turn, and so on until the bolts are securing the radial bearings snugly to the spacer blocks.

### Motor Setup

All of the motors used will have to be wired to their respective drivers. To do this we have included the wiring diagrams for the motors we will purchase. The following Figures 6.27 and 6.28 show the wiring diagrams of the Rotational Stepper Motor and the DC Linear Motion Motor, respectively.

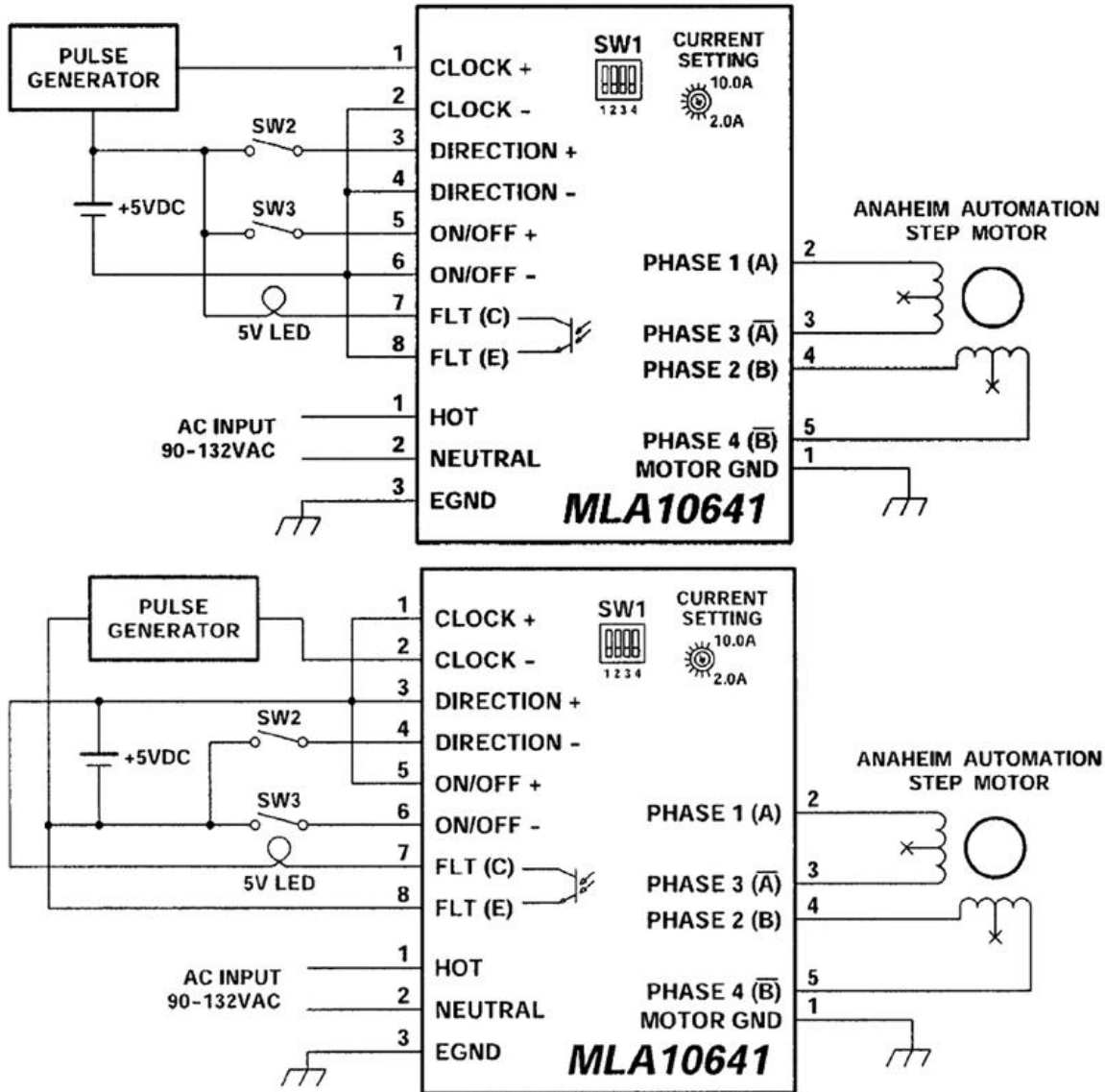
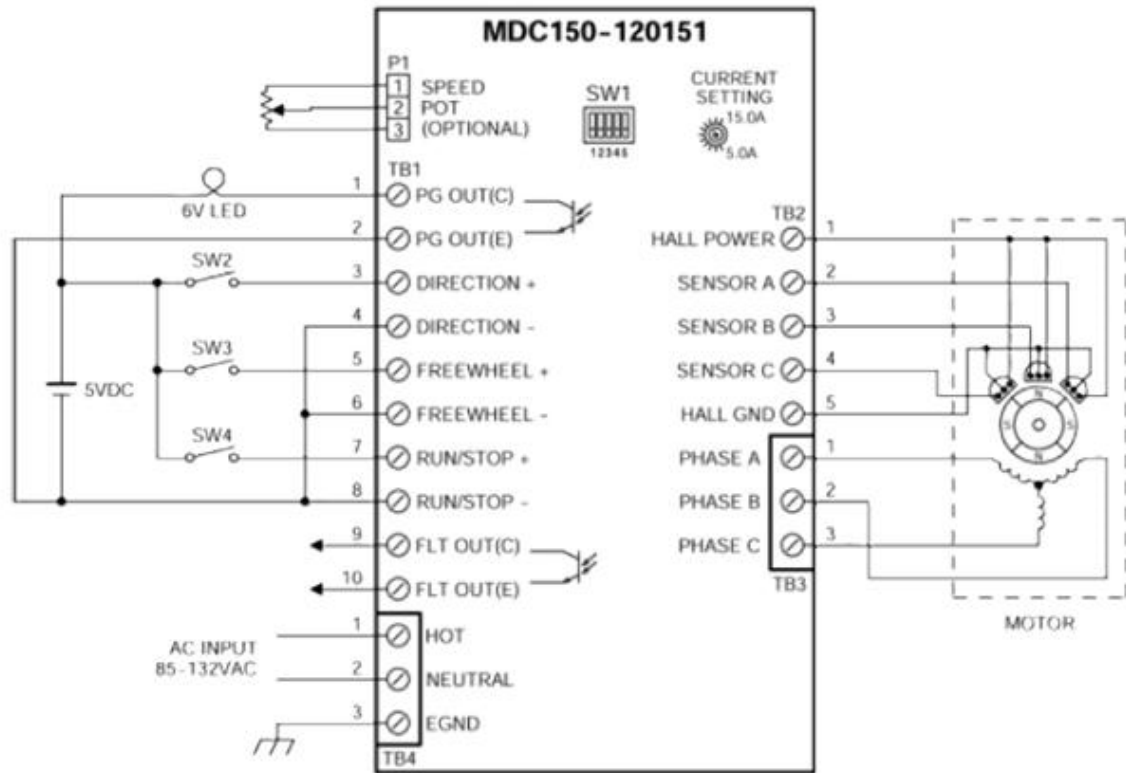
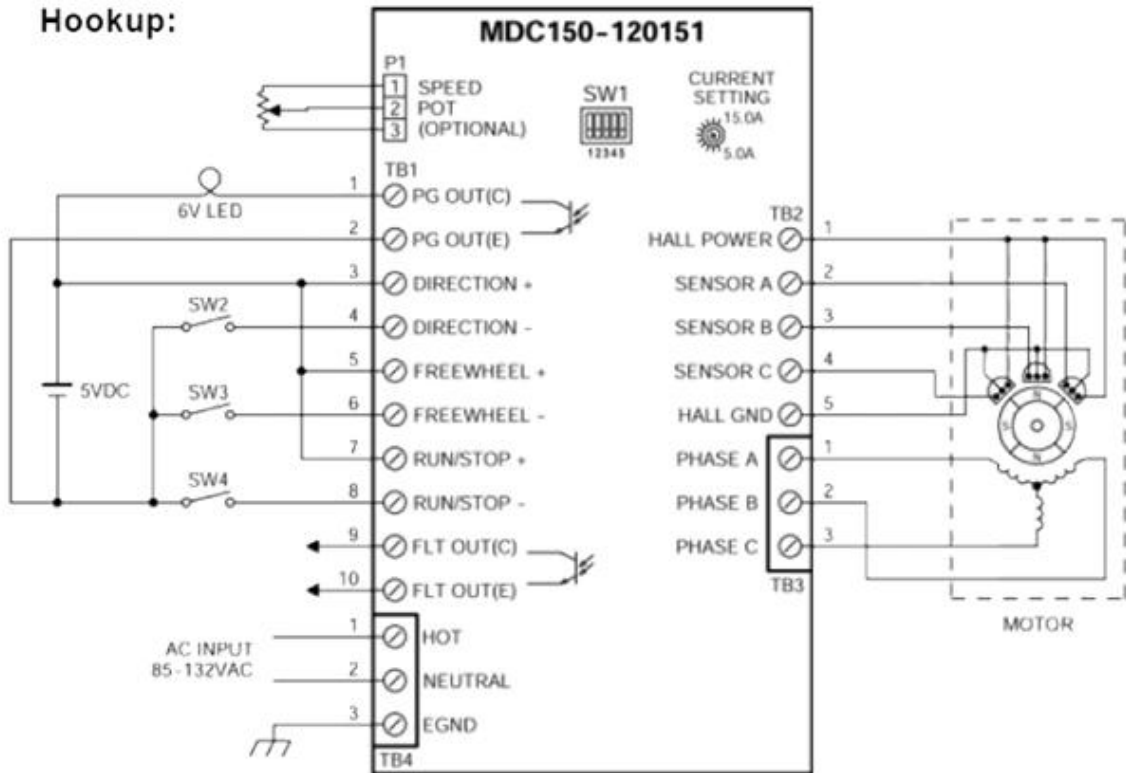


Figure 6.27: Stepper motor wiring diagram

# Hookup:



## APPENDIX J: BILL OF MATERIALS

Name	Description	Vendor	Vendor part no.	Qty	Cost	Total Cost
Controls/DAQ	Control Processor DAQ	SparkFun	DEV-09152	1	\$ 64.95	\$ 64.95
		National Instruments	779026-01	1	\$ 279.00	\$ 279.00
Motors	DC Motor	Anaheim Automation	BLZ482S-160V-3500	1	\$ 556.90	\$ 556.90
	DC Motor Driver	Anaheim Automation	MDC150-120151	1	\$ 296.00	\$ 296.00
	Stepper Motor	Anaheim Automation	42Y112S-LW8	1	\$ 252.00	\$ 252.00
	Microstepper	Anaheim Automation	MLA10641	1	\$ 495.00	\$ 495.00
Linear Stage Drive Shaft	Coupling Hub	McMaster-Carr	6408K139	2	\$ 4.17	\$ 8.34
	Spider Gear	McMaster-Carr	6408K74	1	\$ 3.67	\$ 3.67
	Radial Bearing	McMaster-Carr	5913K63	2	\$ 11.78	\$ 23.56
	Drive shaft	McMaster-Carr	1497K161	1	\$ 20.75	\$ 20.75
Normal Force Application	Worm Gear	Quality Transmission Components	K3W0.8-R1	1	\$ 64.97	\$ 64.97
	Worm Wheel	Quality Transmission Components	KBG0.8-50R1	1	\$ 37.94	\$ 37.94
	Radial Bearing	McMaster-Carr	6455K88	1	\$ 5.55	\$ 5.55
	Thrust Bearing	McMaster-Carr	60715K11	1	\$ 14.84	\$ 14.84
	Application Bolt	McMaster-Carr	92865A225	1	\$ 2.89	\$ 2.89
	Hex Socket	McMaster-Carr	5544A45	1	\$ 6.78	\$ 6.78
	Damper	Advanced Antivibration Mounts	V10Z 2-305B	1	\$ 2.40	\$ 2.40
	Damper	Advanced Antivibration Mounts	V10Z 2-307A	1	\$ 2.12	\$ 2.12
	Damper	Advanced Antivibration Mounts	V10Z60-MM3U2552	1	\$ 7.57	\$ 7.57
	Linear Bearing	McMaster-Carr	64825K111	1	\$ 59.51	\$ 59.51
	Sleeve Bearing	McMaster-Carr	7095K44	1	\$ 0.40	\$ 0.40
	Guide Rails	McMaster-Carr	6253K57	2	\$ 34.11	\$ 68.22
	Linear Bearing	McMaster-Carr	6489K51	4	\$ 24.78	\$ 99.12
Shaft Collar	McMaster-Carr	6436K15	5	\$ 3.66	\$ 18.30	
Quick Release SC	McMaster-Carr	1511K13	1	\$ 16.00	\$ 16.00	
Aluminum stock	Alfo		1	\$ 100.00	\$ 100.00	
Belt Pre-tensioner	Bolt	Home Depot	07716	2	\$ 0.78	\$ 1.56
	Lock Nut	Home Depot		2	\$ 0.50	\$ 1.00
Rotational Motion	Drive Shaft	McMaster-Carr	1346K31	1	\$ 10.22	\$ 10.22
	Top Bearing	McMaster-Carr	6383K251	1	\$ 8.71	\$ 8.71
	Bottom Bearing	McMaster-Carr	5908K190	1	\$ 36.78	\$ 36.78
	Ball Rollers	SKF	11 MI-08-13	3	\$ 35.49	\$ 106.47
Strain Gauges/Pin	Backed half-bridge strain gauge	Micron Instrument	SS-080-050-1000PB-SSGH	2	\$ 46.49	\$ 92.98
Environment sensors	Temp./Humid. Sensor	Omega	RH-USB	1	\$ 145.00	\$ 145.00
	Humidity/temperature sensor w/ USB					\$ 2,909.50





